TECHNICAL UNIVERSITY OF LIBEREC

Faculty of Science, Humanities and Education

Department of Chemistry

Field

Textile Technology and Material Engineering

Hybrid organosilane materials and its application in material engineering

Hybridní organosilanové materiály a jejich aplikace v materiálovém inženýrství

Habilitation Thesis

MSc. Veronika Máková, Ph.D.

2021

ACKNOWLEDGMENT

This work is dedicated to my great colleagues without whose support and the cooperation of the whole team such unique results could never have originated. I would especially like to thank my colleagues Dr. Bára Holubová, for her valuable advice, ideas, and strong support during the writing of this thesis and MEng. Johanka Kulhánková for her support during the implementation of this work.

I would also like to thank my family for the support they provided me throughout the implementation of this habilitation thesis.

Special thanks belong to my wonderful husband Zdeněk and beloved son Zdeněček!

"I've learned that the way to progress is neither quick nor easy."

Marie-Curie-Sklodowska

LIST OF ABBREVIATIONS

Å	Ångström unit
AFM	Atomic force microscope
APTES	(3-Aminopropyl)trimethoxysilane
BiTSAB	1,4-bis(3-(triethoxysilyl)propylamide)benzene
BTEB	1,4-bis(triethoxysilyl)benzene
BTEPDA	bis(3-(triethoxysilyl)propyl)pyridine-2,6-dicarboxamide
CP/MAS NMR	Cross Polarization/Magic Angle Spinning Nuclear Magnetic Resonance
CSPTC	(2-(4-(chlorosulfonyl)phenyl)ethyl)trichlorosilane
DCM	Dichloromethane
DMDMOS	Dimethyldimethoxysilane
DMF	Dimethylformamide
DMSO-d_6	Deuterated dimethylsulfoxide
BTEBP	4,4'-bis(triethoxysilyl)-1,1'-biphenyl
EtOH	Ethanol
eV	Electronvolt
FESEM	Field Emission Scanning Electron Microscopy
FTIR	Fourier transform infrared spectroscopy
GPTMS	(3-Glycidyloxypropyl)trimethoxysilane
HV	High voltage
HRTEM	High-resolution transmission electron microscopy
ICPTMS	3-(triethoxysilyl)propyl isocyanate
IPA	Isopropyl alcohol
LMWGs	Low molecular weight gelators
MTMS	Methyltrimethoxysilane
MPTMS	(3-Mercaptopropyl)trimethoxysilane
MTEOS	Methyltriethoxysilane
NPs	Nanoparticles
ssNMR	Solid state nuclear magnetic resonance
OBA	*N,N′*-bis(3-(triethoxysilyl)propyl)oxamide

ORMOSIL	Organically modified silica
ORMOCER	Organically modified ceramics
PAN	Polyacrylonitrile
PCL	Polycaprolactone
PDMS	Polydimethylsiloxane
PEI	Poly(ethylene imine)
PEO	Polyethylenoxide
PFS	Polyferrocenylsilane
PFMVS	Polyferrocenylmethylvinylsilane
PMMA	Poly(methylmethacrylate)
PTMS	Phenyltrimethoxysilane
PVA	Polyvinylalcohol
PVDF-HFP	Polyvinylidenefluoride-hexafluoropropylene
PVP	Polyvinylpyrrolidone
PS	Polystyrene
RT	Room temperature
SEM	Scanning electron microscopy
SPME	Solid-phase microextraction
STM	Scanning tunneling microscope
XRD	X-Ray diffraction
TEA	Triethylamine
TEOS	Tetraethylorthosilicate
TEPS	Triethoxyphenyl silane
TESP-SA	(3-triethoxysilylpropyl)succinic anhydride
Tg	Glass transition temperature
TGA	Thermogravimetric analysis
THF	Tetrahydrofuran
TMO	Transition metal oxides
TMOS	Tetramethylorthosilicate
TMSPMA	3-(trimethoxysilyl)propyl methacrylate

TPOS	Tetra(isopropoxy)silane
VTMS	Vinyltrimethoxysilane

CONTENT

ANNOTATION

Nanomaterials together with nanotechnologies bring everyday challenges to modern material science and allow scientists worldwide to develop completely new types of unique materials having extraordinary properties. Although interest in hybrid organic-inorganic organosilane fibrous nanomaterials is rising, there is no complete review and/or literature covering and completing the knowledge regarding this highly promissive research area. To-date, only a few solitary research papers have been published regarding this topic. Herein, organo-mono-silylated and organo-bis-silylated precursors were studied in detail. In addition, the proposed synthetic strategies together with their outcomes were successfully applied for the formation of organosilane fibers made of the above-mentioned hybrid precursors. The techniques of self-assembly, drawing, and in particular electrospinning, are widely discussed in the theoretical part of this thesis. The electrospinning technique was then directly used for the formation of organosilane fibers. The results related to this topic are present in the second part of this thesis. Moreover, they are supported by recently published articles, which are added to and described in the supplementary part of this habilitation thesis.

The presented findings are closely connected to the application potential and show the unique and promising prospects of these hybrid organosilane fibers in various fields of modern material science covering a wide range of industries, including the textile industry, and particularly everyday life.

KEYWORDS: Organic-inorganic Hybrids; Organosilanes; Sol-gel process; One-Pot Synthesis; Electrospinning; Fibers; Applications

ANOTACE

Nanomateriály společně s nanotechnologiemi přinášejí každodenní výzvy moderní vědě o materiálech a umožňují tak vědcům po celém světě vyvinout zcela nové typy jedinečných materiálů s mimořádnými vlastnostmi. I když zájem o hybridní organicko-anorganické organosilanové vlákenné nanomateriály roste, doposud neexistuje řádný ucelený přehled pokrývající a doplňující znalosti týkající se zde uváděné problematiky, vykazující tak obrovský potenciál.

V rámci této práce byly podrobně studovány vlastnosti a povaha organo-mono-silylovaných a organo-bis-silylovaných prekurzorů z hlediska jejich aplikačního potenciálu v oblasti přípravy čistě hybridních organosilanových (nano)vláken, dále byly úspěšně vyvinuty, využity a ověřeny různé syntetické strategie, s podporou kysele katalyzovaného sol-gel procesu, vedoucího k tvorbě organosilanových vláken za použití různých technik přípravy vlákenných materiálů, zejména pak techniky elektrostatického zvlákňování s využitím jehly i průmyslového zařízení Nanospider z nízko molekulárního koloidního roztoku (solu). Konkrétní výsledky práce jsou jednak uvedeny ve druhé části této habilitační práce, dále pak také v příloze této práce v podobě nedávno publikovaných článků.

Zjištění a výsledky prezentované v této předkládané habilitační práci přináší unikátní a ucelené poznatky týkající se problematiky přípravy čistě hybridních organosilanových (nano; submikro a mikro)vláken a zároveň úzce souvisí s jejich aplikačním potenciálem. Získané výsledky dále poukazují na slibné vyhlídky připravovaných hybridních organosilanových (nano; submikro a mikro)vláken v různých oblastech moderní materiálové vědy zahrnující celou řadu průmyslových odvětví včetně textilního průmyslu a především pak každodenního života.

KLÍČOVÁ SLOVA: Organicko-anorganické hybridy; organosilany; sol-gel proces; jednokroková syntéza; elektrostatické zvlákňování; vlákna; aplikace

1. Introduction

When we look back into history, we may see that Liberec (historically called Reichenberg) held a strong position in the worldwide textile industry for the whole of the 19th century. Due to this, Liberec became part of the so-called industrial heart of the Austro-Hungarian Empire. During the 20th century until the early 1990s, the modern textile industry together with research and development of textile materials and technologies were the main sources of income for the population living in this part of the Czech Republic. Then, due to the political and particularly economical changes in the early 1990s, activities relating to the textile industry decreased sharply, but thanks to the discovery of the Nanospider industrial technology used for mass production of various types of nanofibers at the beginning of the 21st century by a group led by Prof. Oldřich Jirsák from the Technical University of Liberec, Liberec began to regain its former glory in the field of modern textile technologies and materials, something which continues to the present time. Thanks to the above-mentioned discovery, nanofibers and their applications are considered by world experts to be materials of the third millennium. In this context, scientists and specialists working at the Technical University of Liberec continue in the research and development of new types of textile technologies, modern textile materials, electrospinning and/or non-electrospinning devices and the associated development of nanofibers. Many researchers from various fields of science, working together at the Technical University of Liberec, are focused on the preparation of new types of nanofibers having unique properties and, therefore, help to spread knowledge of this scientific domain all around the world. The preparation of completely unique, purely hybrid organic-inorganic organosilane (nano)fibers is one of the results of the cooperation of scientists in this field.

Hybrid organic-inorganic materials are unique materials that are able to offer properties that pure inorganic and/or organic materials cannot independently offer. Inorganic and/or organic materials are only able to offer specific properties, which are typically based on their nature, see **Table 1**. The growing interest in hybrid organic-inorganic materials in both academic and industrial fields is due to the convergence of diverse expertise and is driven by the curiosity of open-minded scientists using a combination of different approaches [1]. This multilateralism of perspectives has led to one of the greatest advantages of hybrid materials – their "multifunctionality". However, as hybrid materials are always in competition with other materials (inorganic and organic), it is necessary to demonstrate their real added value. Therefore, the current development of modern hybrid materials is subjected to general rules

taking into account the cost and efficiency of their production. The family of organosilanes is just the type of hybrid material to fulfil such demanding requirements [1,2].

Many hybrid organosilane materials in different forms (primarily coatings [3], particles [4] and composites [5]) have been successfully transferred to the market and further commercialized [1,6]. Moreover, the number of publications on such materials has continuously increased over the last 20 years (**Figure 1a**). Recently, excellent reviews related to this topic have been published [1,7,8]. Nevertheless, the primary scientific literature is surprisingly uninterested in the preparation of hybrid organosilane fibrous materials (**Figure 1b**) [9,10]. Yet, they are easily prepared from quite inexpensive precursors available on an industrial scale and, in addition, the way they are processed is compatible with proven industrial processes. Therefore, the newly prepared organosilane fibrous materials may offer unique added value compared in particular to purely organic polymer fibers. Likewise, the environmental benefits should also be considered, as hybrid organosilane fibers may be prepared under the mild conditions of the sol-gel process with no harmful solvents or organic polymer additives, whereby avoiding the problems with nanoplastics [1,6,11–14].

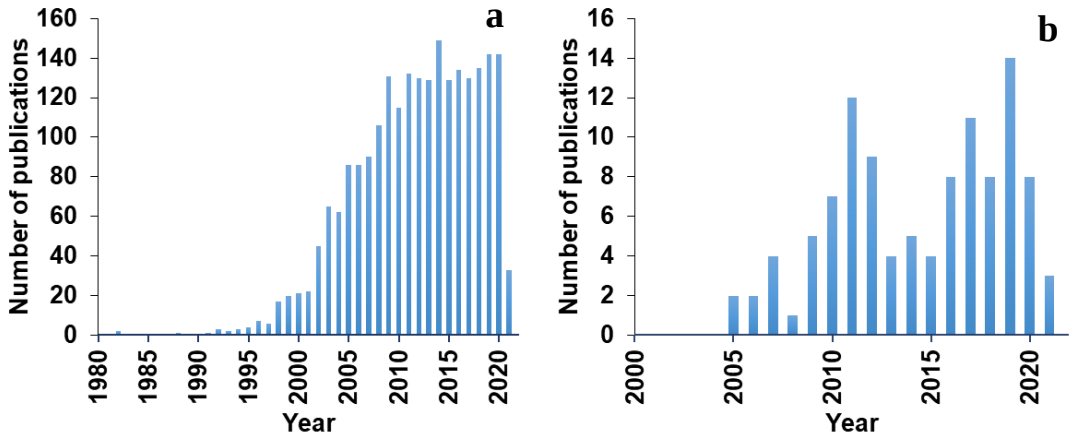

Figure 1. Development in the number of publications related to hybrid organo-alkoxysilane materials **a)**; keywords hybrid AND organo*sil*) and nanofibrous materials containing organo-alkoxysilanes **b)**; keywords nanofib* AND organo*sil*). (Data source: WoS, up to May 2021).

Table 1. An overview of the general properties of typical organic and inorganic materials and their comparison [12].

Properties	Organics (polymers)	Inorganics (SiO_2; transition metal oxides (TMO))
Nature of bonds	covalent, van der Waals, H-bonds	ionic or iono-covalent (M-O)
Tg	low (-120 °C to 200 °C)	high (> 200 °C)
Thermal stability	low (<350 °C – 450 °C)	high (> 100 °C)
Density	0.9 – 1.2	2.0 – 4.0
Refractive index	1.2 – 1.6	1.15 – 2.7
Mechanical properties	elasticity, plasticity	hardness, strength, fragility
Hydrophobicity	hydrophilic	hydrophilic
Permeability	hydrophobic permeable ±to gases	low permeability to gases
Electronic properties	insulating to conductive redox properties	insulating to semiconductors (SiO_2, TMO), redox properties (TMO), magnetic properties
Processability	high (molding, casting, film formation), control of viscosity	low for powders, high for sol-gel coatings

In this context, research of the different ways of preparing organosilane (nano)fibers, their prospects and contribution to modern and currently growing scientific fields such as optoelectronics [14], sensors [15], catalysis [16], energetics [17], and medicine [18] among others should be highlighted. Due to the above-mentioned reasons, a comprehensive overview of the use of organosilane (nano)fibers prepared from organo-mono-silylated and organo-bis-silylated precursors is presented here. Firstly, the origins of organosilane fiber-making chemistry are briefly described in **Chapter 1.1**. Moreover, a historical overview together with important milestones related to this topic are given in **Table 2**. Subsequently, there is an extensive discussion on the properties of organo-mono-silylated and organo-bis-silylated precursors, together with the related process leading to the preparation of convenient spinning solutions and the main fiber-making techniques. Finally, the potential of these hybrid organosilane nanofibers are outlined, together with their benefits and contribution to modern science and different areas of human activity.

The presented habilitation thesis is divided into a theoretical part and a part describing the latest completely new results obtained by the author and her colleagues. The theoretical part is mainly composed of a review that was published by the author of this thesis together with co-authors in 2021 [19].

In detail, the theoretical part provides a comprehensive overview of the use of various types of organosilane (nano)fibers prepared from organo-mono-silylated and/or organo-bis-silylated precursors, including their characteristics and application potential in various fields of modern material sciences. The theoretical part is followed by the part describing the latest results related to the above-mentioned topic together with a wide discussion devoted to these results, which is supported by the reprints of the articles successfully published in 2020. The published results point out the strong potential that these types of fibrous materials may achieve in different fields of industries, including support for the further development of modern textile technologies and the textile industry.

2. Hybrid organosilane materials

2.1 A way leading from silica gel to silica fibers and beyond

The beginnings of the silica, silicate, silane and organosilane chemistries belong to a period between the 17th century and the beginning of the 1940s. Between 1940 and 1980, mixed organic-inorganic materials were developed by various different weakly- or non-interacting scientific communities. In 1976, Yajima et al.[20], and later on Ishikawa et al. [21], published studies describing polymeric networks, without siloxane bonds, based on polycarbosilanes and their conversion to ceramic fibers obtained by sintering an amorphous Si–Al–C–O fiber precursor at different temperatures. A similar study was also published by Baldus et al. in 1999 [22], where the formation of ceramic fibers made of preceramic *N*-methylpolyborosilazane via the melt-spinning technique was described. All of the above-mentioned types of ceramic fibers have found application in tough fiber-reinforced composites. The latter years were marked by the appearance of the first omnibus publications defining and establishing the "sol-gel community". A historical overview of the evolution of silica and its derivative chemistries is included in **Table 2.**

Table 2. A historical overview of the developments leading to hybrid organosilane materials [19].

Year	Scientist(s)	Discovery	References
1640	J. B. van Helmont (Belgium)	The first contribution regarding silicon chemistry.	
1779	T. Berman (Sweden)	Description of the first silica "gel" formation.	
1824	J. J. Berzelius (Sweden)	New molecular silicon and organosilicon precursors	
1843	J. J. Berzelius (Sweden)	Synthesis of $SiCl_4$	
1844	J. J. Ebelmen (France)	"Grandfather of sol-gel chemistry". Description of the formation of silicic ethers Silicon tetrahydride (SiH_4)	[1]
1857	Friedrich Wöhler (Germany)	Hypothesis regarding the existence of an alternative organic chemistry based on silicon	
1863	C. Friedel (France) and J. M. Crafts (USA)	Synthesis of the first organosilicon compound, tetraethylsilane (TEOS)	
1871	A. Ladenburg (Germany)	Hydrolysis of Et_3SiOEt to form triethylsilanol (Et_3SiOH), the first "silanol"	
1904	F. S. Kipping (United Kingdom)	Application of the newly discovered Grignard's reagents to synthetize a wide range of new organo- and chlorosilanes starting from $SiCl_4$	[23]
1952	H. J. Deuel (Germany)	The first organic derivatives of silicates formed through covalent bonds of organic groups and the silicate network	[24]
1964	A. N. Lentz (Germany)	Firstly reported preparation of organic derivatives of silicates	[25]
1978	K. Andrianov (Russia)	The first syntheses of organoalkoxysilanes containing the Si-C covalent bond.	[26]
1980	W. Mahler & M. F. Bechtold (USA)	The first freeze-formed silica fibers	[27]
1980s	Sakka S. (Japan); W. C. LaCourse, H. G. Sowman (USA)	The first preparation of silica and silicate fibers by drawing directly from viscous sols at room temperature	[28]

Probably given the difficulties of the low-temperature fiber-making process, it was not until the 1980s that silica fibers were prepared directly via sol-gel processing. Even though this decade was marked by the first appearance of organoalkoxysilane precursors [29,31,32], the first sol-gel derived fibers were purely inorganic, prepared from various metal alkoxides either by drawing directly from viscous sols at room temperature or by unidirectional freezing of gels [28]. Amorphous or polycrystalline, these first sol-gel fibers were structurally based not only on silica and silicates (SiO_2, SiO_2-TiO_2 (10-50%), SiO_2-AI_2O_3 (30%), SiO_2-ZrO_2 (7-48%), SiO_2-ZrO_2-Na_2O), but also on diverse aluminates, zirconates, titanates, nitrates, and even cuprates or niobates [33]. However, as they displayed unsuitable microstructures for achieving ultrahigh purity and non-circular cross-sections, their potential applications were narrowed down to reinforcement, refractory textiles and high-temperature superconductors [11].

These first sol-gel silica fibers were prepared independently by the scientific groups of Sakka (Japan), W. C. LaCourse and H. G. Sowman (both USA) [33–37]. The group of Sakka et al. [28,33] was particularly interested in the course of sol-to-gel conversion and its influence on fiber-making potential. They were the first to describe the link between the presence of long-shaped particles in the sol and the spinnability, as will be discussed further in this thesis.

As these silica and silicate fibers are well known on both an academic and industrial scale [11,33], this thesis focuses on hybrid organosilane fibers that have still managed to evade the eye of principal hybrid material reviewers [1,6,12]. It was not until the late 2000s that hybrid organosilane fiber-manufacturing came to the forefront of scientific interest (**Figure 1b**). Its methods and strategies will be described further in the present habilitation thesis.

3. Properties of hybrid organosilane precursors

It is essential to understand the hybrid nature of organosilane precursors in order to tailor the structure of the resulting fibrous materials on a molecular level. Generally, hybrid materials are defined as multicomponent materials having at least one of their organic and/or inorganic components blended on a nanometer scale. Commonly, one of these components is inorganic and the other is organic [1,2,12]. The properties of such hybrid materials are then achieved due to the strong synergy of these organic and inorganic components depending on the presence of a large hybrid interface [38].

Therefore, the nature of the interactions, energy, and linkability of the interfacial boundaries play an important role in modulating the properties of the final material. From this point of

view, hybrid materials can be divided into two main classes: Class I where the organic and inorganic components interact via weak bonds, e.g. van der Waals, hydrogen bonds, or electrostatic bonds; and Class II where the organic and inorganic components are linked by rather strong chemical interactions as covalent or iono-covalent bonds [5]. In addition, there is still no clear borderline between hybrid organic-inorganic materials and organic-inorganic nanocomposites, as the large molecular building blocks of hybrid materials can be of a nanometer scale [12]. Common knowledge states that there is a gradual transition between both of them. Nanocomposites come with discrete structural units ranging from 1 to 100 nm (nanoparticles/rods/tubes usually incorporated in organic polymers), while hybrid materials are more often defined by the use of organic or inorganic units formed in situ by molecular precursors (e.g., the sol-gel process) [12]. Organosilane fibrous materials belong mostly to the Class II hybrid materials, and they are often used to prepare a wide range of hybrid (nano) composites. The organosilane hybrid structure is well assured by a strong covalent Si–C bond, stable enough to provide a homogeneous material in which the organic moieties bound to two $SiO_{1.5}$ units are uniformly distributed as elementary building blocks [12,39].

The chemistry related to organo-alkoxysilanes has been well described and there is a wide range of commercially available organosilane precursors. The properties and the synthesis of molecules having the formula $Si(OR')_x–R_{4-x}$ (x = 1–3) containing stable Si–R groups (R = alkyl, aryl, acryl, epoxy, amino group etc.) and hydrolysable alkoxy Si–OR' units have also been widely described. These kinds of organosilane precursors are known as organo-mono-silylated precursors, while organo-bridged trialkoxysilanes $[(R'O)_3Si–R–Si(OR')_3]$ may be referred to as organo-bis-silylated precursors having the same well explored background [40]. The R group is, as in the case of organo-mono-silylated precursors, an organic unit, but in this case directly linked to two Si atoms through Si–C covalent bonds. Arylenes, alkylenes, cyclams, crown ethers, porphyrins, polymers, and many others have been used as the organic component. This diversity of organic moieties enables variation of porosity, thermal stability, optical clarity, refractive index, chemical resistance, hydrophobicity, and dielectric constant [38,41].

Hydrolysis and the subsequent condensation of such silylated organo-trialkoxides (T) (**Figure 2**) result in a formation having the above-mentioned basic repeating unit $[RSiO_{1.5}]$. Moreover, as the number of various alkoxy groups on Si determinates the potential for forming multiple bonds with other silica atoms, the resulting level of crosslinking may differ drastically from the structure of silsesquioxanes. The final hybrid material may be controlled using a whole variety of functional organo-alkoxysilanes from difunctional dialkoxysilanes (D) forming linear oligo or polysiloxane structures to monofunctional trialkoxysilanes (T) or tetraalkoxysilanes

(Q) having a tendency to form highly crosslinked polymers depending on a number of sol-gel parameters. In addition, as the organosilane precursors may possess many different geometries (aryl rigid rod spacers, alkylic flexible spacers), they may be used to precisely control the parameters that govern the structures of the targeted hybrid materials [39].

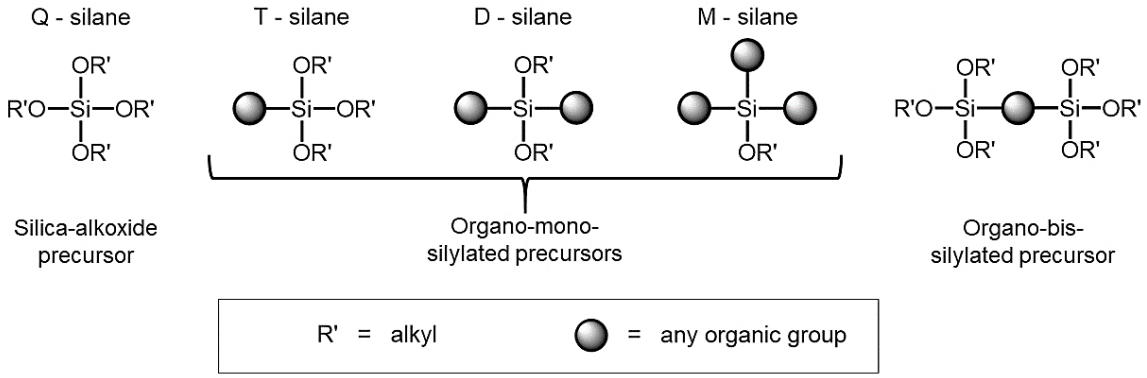

Figure 2. Scheme showing the different types of organosilanes [19].

Furthermore, it is necessary to take into consideration that the organo-bis-silylated precursors have a higher ability for self-organization than organo-mono-silylated precursors. This property is a great advantage in the formation of highly organized structures such as crystal-like structures in non-mesoporous organosilane materials [39]. In the silicon-based sol-gel process, the network behavior of organo-trialkoxysilanes (T) with various types of attachment of the organic moiety to silicon may manifest itself in three networking ways (**Figure 3**).

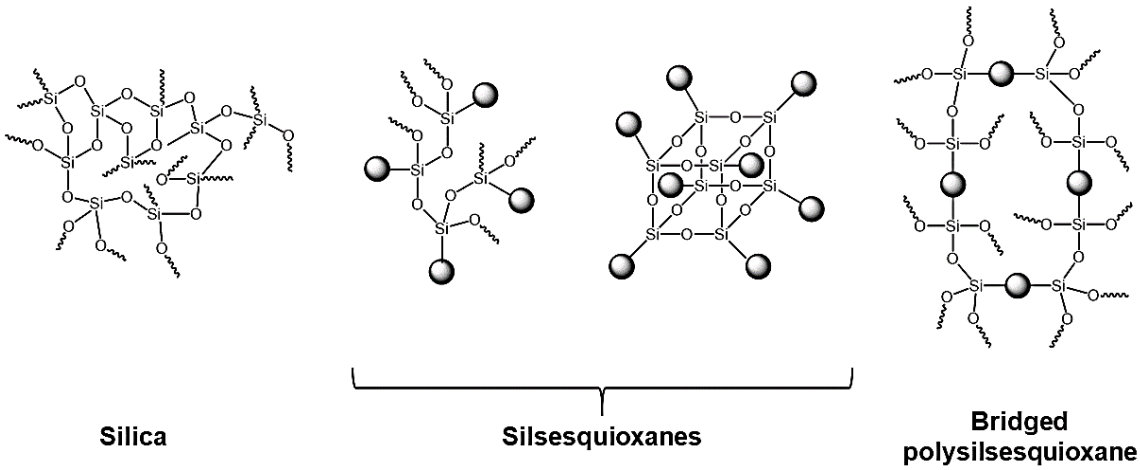

Figure 3. Selected organosilane precursors transforming into nets during polycondensation processes. Pure silica is included for comparison [19].

Bridged bis-silylated organosilane precursors are referred to as "network builders" – their co-polycondensation with or without a tetraalkoxysilane precursor leads to the creation of materials in which the organic segment is an integral part of the hybrid network. By contrast, mono-silylated organosilane precursors act in the final structure as so-called "network modifiers", ultimately modifying a discrete area of the homogeneous silica network. In addition, if the organic moiety is intended to undergo further chemical reaction (as a sort of surface anchor), then organo-trialkoxysilane (e.g., amino-functionalized silanes) serves as a so-called "network functionalizer" [12].

As may be seen, concise use of mono-silylated or bis-silylated organo-alkoxysilanes in sol-gel processing is a fascinating bottom-up approach to fabricating new functional hybrid materials with numerous applications.

3.1 Silicon and carbon as elements; the covalent bond between them

To understand the behavior of the covalent bond between silicon and carbon (Si–C), firstly it is necessary to understand several parameters describing these elements, such as their size, coordination number, electronegativity, bond energy, and ability to form multiple bonds [42]. In terms of the size of these elements, silicon is larger than carbon due to the presence of a third shell: silicon (Si) has $1s^2\ 2s^2\ 2p^6\ 3s^2\ 3p^2$ while carbon (C) has $1s^2\ 2s^2\ 2p^2$. The properties of both elements are compared in detail in **Table 3**.

Table 3. Properties of silicon and carbon elements and their comparison [43].

Property	Si	C
Atomic radius (Bragg-Slater; Å)	1.10	0.70
Covalent radius (Å)	1.17	0.77
Van der Waals radius (Å)	2.17	1.70
Ionization energies (eV)		
E_1	8.15	11.26
E_2	16.34	24.38
E_3	34.49	47.89
Electron affinity (eV)	1.39	1.12
Electronegativity	1.9	2.55
Dipol polarizability (a.u.)	36.3	11.8

The electronegativity of both elements is another important parameter. Carbon is well known to be more electronegative than hydrogen (**Figure 4**). For this reason, the C–H bond is

polarized towards carbon resulting in more protic hydrogen. In contrast, silicon has lower electronegativity, which results in more hydridic hydrogen [42].

Figure 4. Scheme describing the relative polarization of C–H and Si–H bonds [44].

Bond energies are the third important factor influencing the behavior of compounds containing the Si–C covalent bond in their molecules. In the beginning, the energetic parameters for bond energies between the C–C and Si–Si bonds should be mentioned. The E–E bond energies for carbon–carbon and silicon–silicon are the levels of 346 kJ/mol and 226 kJ/mol, respectively, while the E–O energies reach values of 359 kJ/mol for carbon–oxygen and 466 kJ/ mol for silicon–oxygen. The bond energy of the C–C bond is slightly higher than the C–O bond, while the Si–O bond is significantly stronger than the Si–Si bond [45].

This difference is reflected in the chemistry of both elements. The chemistry of carbon is dominated by catenation: the ability of a chemical element to form a long chain-like structure via a series of covalent bonds among the atoms of the same element. Although silicon is able to form Si–Si bonds, these bonds are far more reactive than their C–C analogues. In general, silicon polymers are predominantly composed of Si–O chains due to an ability to form very strong bonds between silicon and oxygen, or further with carbon.

A covalent bond between silicon and carbon (Si–C) usually has a bond energy of around 360 kJ/mol; however, it may reach up to 435 kJ/mol. Overall, this bond has a low polarity and ranks among the strong chemical interactions [43]. It typical exists between the organic and inorganic building blocks in the case of hybrid organosilane materials, particularly in the hybrids of Class II, which can find applications e.g., in fuel cells. This topic is discussed in more detail in **Chapter 6.1.2.** [12].

Most organosilicon compounds containing bonds between the silicon and carbon atom can be well described with the help of structural chemistry, where the Si–C single bond is examined in detail. The Si–C bond is markedly polarized and an increase in the bond ionicity by attaching different substituents to either the silicon or the carbon atoms may affect its length. The Si–C bond may take various forms, typically Si–C(sp) bonds; Si–C(sp^2) bonds; Si–C(sp^3) bonds; and Si–C(aryl) bonds [43].

The Si–C(sp) bond is described as a single bond between a silicon and dicoordinate carbon atom. The average bond length (1.839 Å) was calculated from 226 values via X-Ray Diffraction

(XRD). Si–C(sp^2) bonds affected the lengthening of the Si–C bond by only 0.04 Å. The average length of the bond was calculated from 633 individual values obtained from XRD to be 1.878 Å. The average bond length of Si–C(sp^3) was calculated from 19,169 individual XRD values to be 1.860 Å. The average bond length of Si–C(aryl) bonds was calculated from 3371 individual values to be 1.879 Å [43].

The Si–C bond generally represents a stable link in the sol-gel process, as the Si–C (sp^3/sp^2)-linkage has proven to be stable under sol-gel processing conditions [12]. Advantages of this bond include high resistance to hydrolysis and oxidation.

Organosilicon chemistry has been widely developed due to this bond, providing many chemical ways of introducing silicon-containing groups into an organic molecule in order to synthesize molecular building blocks [43].

3.2 Sol-gel process and its parameters focusing on the fiber formation

The sol-gel process can be generally defined as a method allowing the transition from a mostly colloidal liquid "sol" into a solid "gel" [46] as shown in **Figure 5**. The main advantages of this method include the possibility to prepare various different materials with novel, fine-tuned properties using a simple and versatile process, which is commonly used to synthesize ORMOCER and ORMOSIL materials (hybrid organic-inorganic materials based on organosilanes) at low temperatures. The purity of the products and the possibility of incorporating thermolabile molecules are possibly the most important advantages of the sol-gel process [47].

Generally, the thermal stability of fragile organics is limited to a high temperature, meaning that high temperatures cannot be used during the hybrid formation process. Thanks to soft sol-gel processing, it is possible to overcome this limitation during the preparation of hybrid organosilane materials. These types of materials have undergone tremendous development over the past few years and even fiber-making research has benefited greatly from mild sol-gel processing [1,5,6,37,55–57].

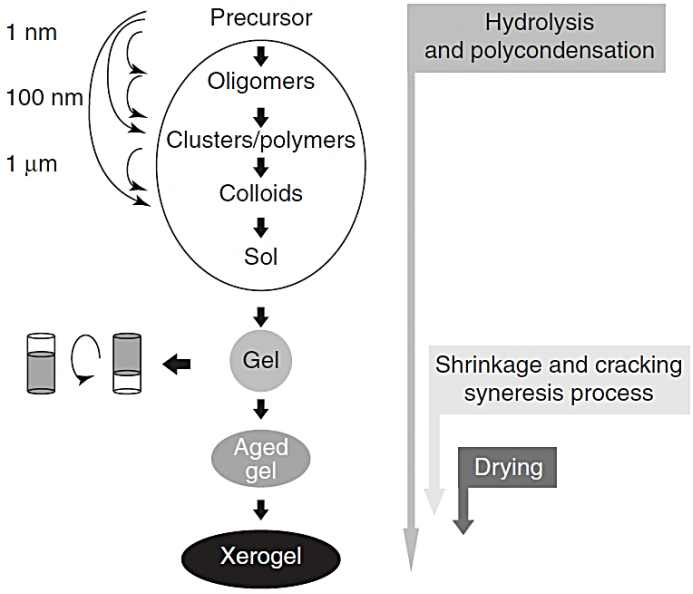

Figure 5. An overview of the transformations ongoing during the sol-gel process [43].

In order to obtain materials with controlled structures and properties, the conditions of the sol-gel process have to be adjusted. Various parameters lead to the different forms of sol-gel products mentioned in **Figure 6**. Bulk gels, films, powders, fibers and nanoparticles are synthesized using the "organic route" of sol-gel processing, where the formation of a sol is achieved via the addition of an alkoxy-organosilane precursor to a solvent (mostly alcohol) [47,48].

The solvent is commonly used as a homogenizing agent due to the fact that the water and organosilane precursors are practically non-miscible. Both transformation reactions (hydrolysis and condensation) are affected by the molar ratios of the reactants, by the chemical nature of the precursors used and other processing parameters (pH, polycondensation time, temperature, etc.). All of the parameters strongly influence either the gelation time, the degree of aggregation and condensation, final structure and form, or the dimensions of the pores. In fact, the higher the degree of aggregation and condensation, the higher the viscosity of the sol to work with [47].

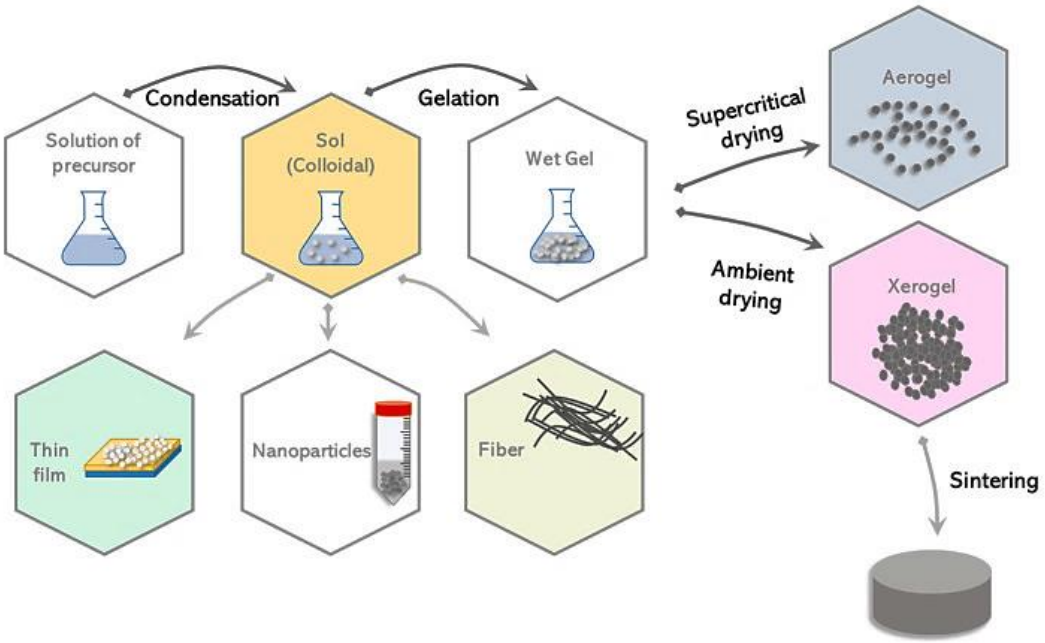

Figure 6. Various products, including fibers, that may be obtained using the sol-gel process [47].

In general, the sol-gel process focusing on the formation of fibers should be conducted under acidic conditions, as the transformation reactions (**Equations 1** to **3; Figure 7**) lead to the formation of linear, low-branched organosilane macromolecular structures, ideal for fiber formation. The process itself may be described by the following hydrolysis and polycondensation reactions. In the first phase, the alkoxy (≡Si–OR) groups contained in the structure of the alkoxy-organosilane precursors are hydrolyzed to silanol groups (≡Si–OH) (**Equation 1** in **Figure 7**). These silanol groups then polycondensate to form a three-dimensional organosilane matrix (polysiloxane bond ≡Si–O–Si≡) (**Equations 2** and **3** below, **Figure 7**), whose structure is filled with molecules of used polar solvent based on alcohol, water, and inorganic mineral acid, which should evaporate during the subsequent electrospinning process.

$$\equiv Si\text{-}OR + H_2O \xrightarrow{\textbf{hydrolysis}} \equiv Si\text{-}OH + ROH \qquad \textbf{(1)}$$

$$\equiv Si\text{-}OR + HO\text{-}Si\equiv \xrightarrow[\textbf{condensation}]{\textbf{alcohol}} \equiv Si\text{-}O\text{-}Si\equiv + ROH \qquad \textbf{(2)}$$

$$\equiv Si\text{-}OR + HO\text{-}Si\equiv \xrightarrow[\textbf{condensation}]{\textbf{water}} \equiv Si\text{-}O\text{-}Si\equiv + H_2O \qquad \textbf{(3)}$$

Figure 7. General equations 1-3 describing the hydrolysis and condensation steps leading to the various sol-gel products [9].

In more detail, the hydrolytic reaction takes place under acidic conditions via the S_N2–Si mechanism, i.e., bimolecular nucleophilic substitution on the silicon atom. **Equation 1** may be described in more detail as follows (**Equation 4; Figure 8**): under acidic conditions, an alkoxy group (–OR) of precursor(s) is protonated in a rapid first step (H^+ access), thereby withdrawing the electron density on the central atom of silicon. This process makes the silicon atom more electrophilic and at the same time more susceptible to attack by a water molecule. As a result, the pentacovalent intermediate is formed **(Figure 8**) and the positive charge on the first protonated alkoxy group is reduced becoming the so-called "leaving group" (leaving in the form of the alcohol molecule ROH). Thus, the hydrolysis results in the transformation of the alkoxy groups (≡Si–OR) to silanol groups (≡Si–OH) (**Equations 1 in Figure 7** and **4 in Figure 8**) [47,49,50].

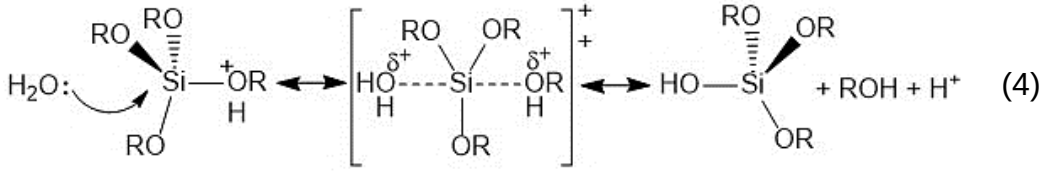

(4)

Figure 8. Scheme showing the formation of the pentacovalent intermediate on the silicon atom.

After the beginning of the hydrolysis, the remaining transformation reactions take place (**Equations 2** and **3; Figure 7**), i.e., polycondensation with the product of water or alcohol. The formed silanol groups (Si–OH) immediately polycondensate (≡Si–O–Si≡, polysiloxane bond) and repeat to form an organosilane matrix (**Equations 2** and **3 in Figure 7**). In more detail (**Equation 5; Figure 9**), this step may also be described based on the type of S_N2–Si reaction, i.e., the nucleophilic attack of the neutral silanol on the acid-protonated silanol gives the pentacoordinated intermediate. The leaving group in this case is a protonated hydroxyl group. After the exit of the water molecule, a Si–O–Si bond is formed, which further elongates and grows into a macromolecular structure, whereby forming the mostly liner or low-branched polysiloxane matrix of the resulting sol [45,47,50,51].

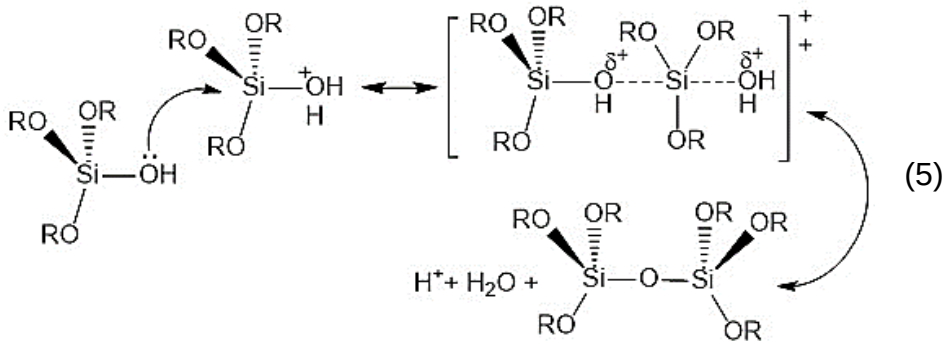

Figure 9. Scheme showing the nucleophilic attack of the neutral silanol on the acid-protonated silanol to again give the pentacoordinated intermediate.

We should keep in mind that, although acidic conditions accelerate the hydrolysis and enhance the silanol entities stability at the beginning of the process, the same conditions slow down the rate of the self-condensation reactions, as can be seen from in situ ^{1}H and ^{13}C NMR [52]. That is why the water/silane ratio should be kept low in order to suppress the process and to further reduce the branching. Likewise, the sol-gel reaction rate of organo-mono-silylated and organo-bis-silylated precursors and their outcomes are strongly affected by steric and inductive effects. It should be taken into consideration that the hydrolysis will be rather enhanced with polar and electron-providing organic moiety, due to the improvement of the solubility in the water by the formation of hydrogen bonds and the stabilization of the positively charged intermediates of the sol-gel reactions. On the other hand, the steric hindrance of the organic species significantly slows down the hydrolysis rates [11,50,51,53–57].

In order for the as-described sol to be electrospun, it is absolutely necessary to set all the above-mentioned sol-gel parameters appropriately in order to form linear or low-branched organosilane macromolecular units (so-called “non-bridging oxygens” are formed as a consequence), so the resulting structure does not show crosslinking in greater volume [9,58].

It is necessary to mention that such a procedure based on the above-mentioned parameters and conditions was successfully designed and the first silica fibers were prepared in the early 1980s by Sakka et al. [33,36]. Tetraethoxysilane (TEOS) and tetramethoxysilane (TMOS) were the main components used for the preparation of these fibers. Sakka et al. [33,36] also introduced the issue of sol spinnability, which may be achieved as a combination of acid-catalyzed sol-gel conditions having an r = water/silane ratio of less than 2, to the wide scientific community [33,36]. Therefore, a structurally convenient polymerization in an acidic medium is the most important factor influencing the preparation of spinnable sols [11,50,53–55].

Nevertheless, the primary academic literature struggles with the above-described suitable polymerization of organosilanes in long spinnable polymeric chains. Therefore, most research groups enhance the sol formulas with various types of surfactants, low-molecular-weight polymeric gelators or spinnable polymers in order to facilitate the fiber making process. However, our research clearly shows that with a concise choice of sol-gel processing parameters, spinnable sols and organosilane fibers made purely on the basis of organo-mono-silylated and/or organo-bis-silylated analogues may be obtained (**Figure 10**) via sol-gel "one-pot synthesis" [9,10].

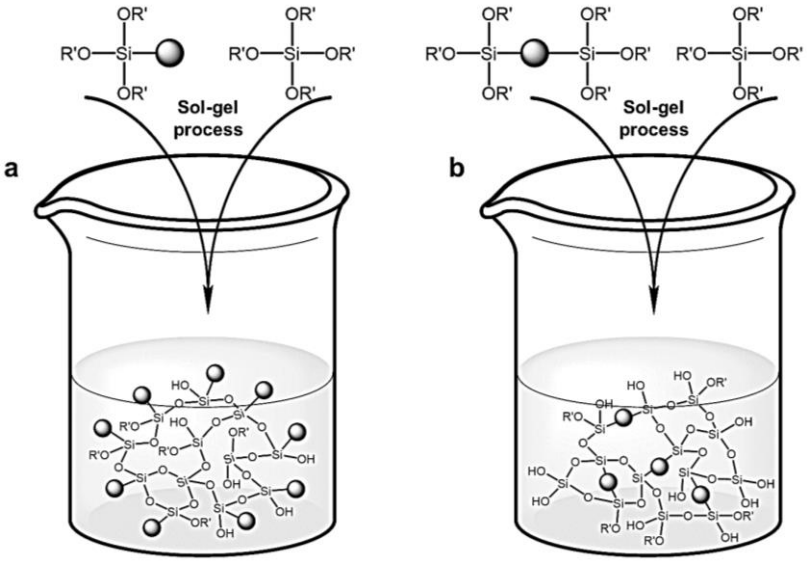

Figure 10. Scheme describing the polycondensation processes of **a**) organo-mono-silylated and **b**) organo-bis-silylated precursors [19].

To summarize, these basic factors strongly influence not only fiber formation on the basis of organo-mono-silylated and organo-bis-silylated precursors, but sol-gel processing in general may be divided into two main groups: The primary factors such as the types of catalysts, water/silane ratio, pH, and organo-functional groups, strongly influence the polymerization outcomes, while the secondary factors, such as temperature, solvent, ionic strength, leaving group, and silane concentration, influence the reaction rates [50]. In addition, the viscosity of spinnable sols should be carefully observed throughout the process of hydrolysis-polycondensation as a concentration dependence is characteristic for the presence of linear (organo) siloxane polymers. Hence, the conditions suitable for various fiber formation techniques may be determined [9,10,33,59].

3.3 Common fiber-making techniques - their prospects and consequences

Fibers have been a fundamental part of human life since the dawn of civilization [60]. A vast number of papers have reported the preparation, characterization and applications of different types of nanofibers via various techniques (**Figure 11**) mainly allowing the inclusion of electrospinning, drawing and self-assembly [61,62].

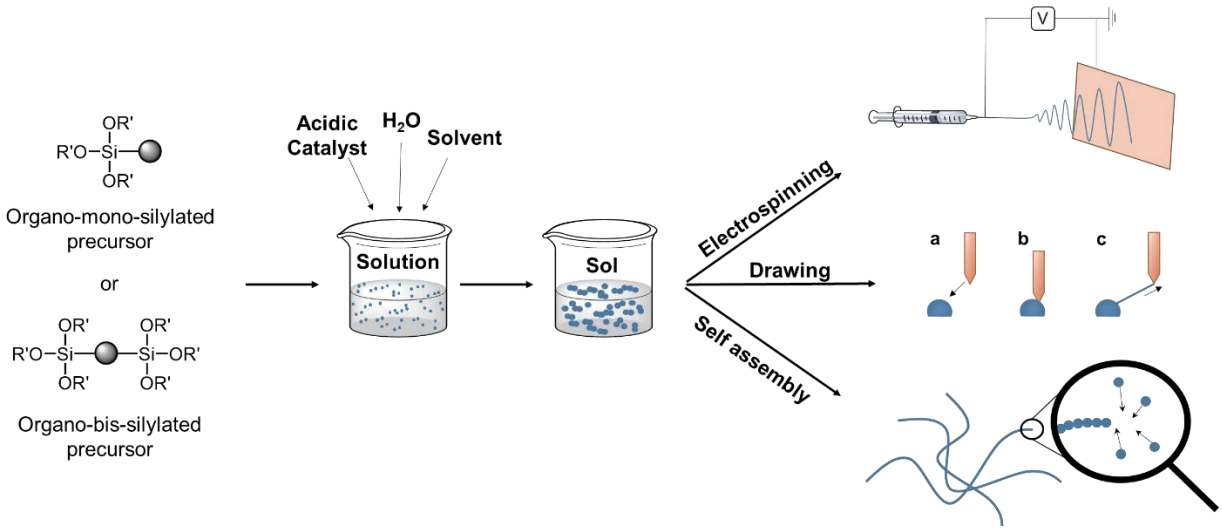

Figure 11. Preparation of nanofibers from organo-mono-silylated and/or organo-bis-silylated precursors using various fiber making techniques [19].

3.3.1 The electrospinning technique

Polymer nanofibers fabricated with the help of electrospinning have attracted much attention recently because of their unique thermodynamic and mechanical properties compared to bulk materials. The history of the electrospinning process resulting in the fabrication of polymer fibers of sub-micron diameters spans more than 100 years [63]. Looking back into history, the beginnings of electrospinning techniques started in the year 1887 when Charles Vernon Boys suggested the process of nanofiber manufacture, which may be regarded as the first time a prototype for electrospinning was ever mentioned [63]. In 1902, the first patent for an electrospinning device was filed by John Francis Cooley [64] **(Figure 12**).

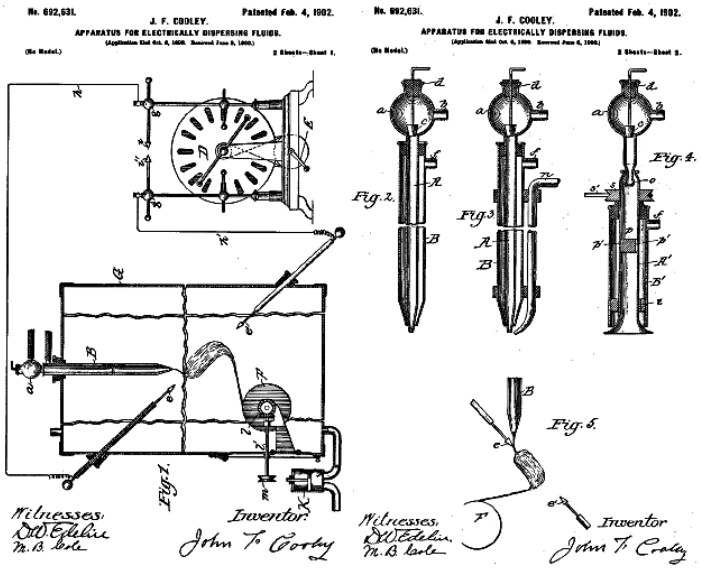

Figure 12. US Patent #692631 filed by John Francis Cooley in 1902 describing his electrospinning device [64].

Another important period occurred between 1931 and 1944 when the scientist Anton Formhals took out at least 22 patents relating to electrospinning. This was followed by a very important time period between 1964 and 1969, during which Sir Geoffrey Ingram Taylor first described the shape of the (Taylor) cone formed by the fluid droplet under the effect of an electric field using mathematical modeling [65]. Later on in the 1990s, a group led by Darrell Reneker popularized the name "electrospinning" [66].

Electrospinning is known as a versatile and viable technique for generating ultrathin fibers made of polymeric, metal oxide materials, as well as their combinations. Remarkable progress has been made with regard to the development of electrospinning methods and engineering of electrospun nanofibers to suit or enable various applications [60,67]. According to the data released by "Research and Markets", the global market for nanofibers can reach 1 billion USA dollars by the end of 2021 [60]. Although electrospun nanofibers have unique applications, they still encounter several challenges in the production stage, such as large volume processing, reproducibility; and safety [61].

Electrospinning equipment consists of four major components: a high-voltage power supply, a syringe pump, a spinneret, and a collector (**Figure 13** on the left). The main principle is based on a small amount of viscoelastic fluid, which is pumped out through the spinneret and has a tendency to form a spherical droplet as a result of the confinement of surface tension. Thanks to the interconnection of the droplet with the high-voltage power supply, its surface is quickly covered by charges of the same sign. The repulsion among these charges counteracts

the surface tension and destabilizes the spherical shape. If the repulsion is strong enough to overcome the surface tension, the droplet is deformed into a conical shape and a jet emanates from the apex of the cone. As a result, fibers are formed together with the evaporation of the solvent [60].

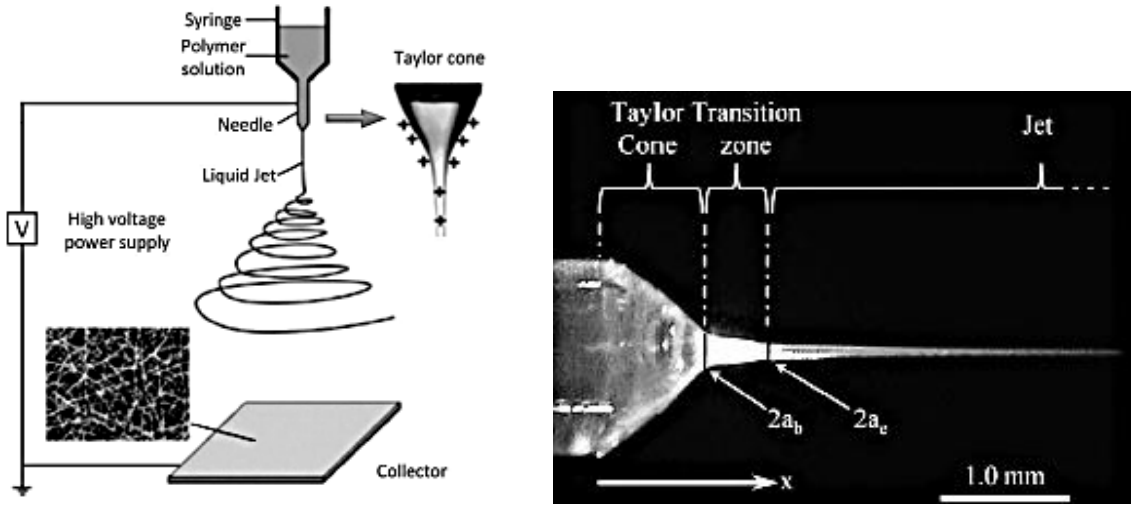

Figure 13. Scheme showing the electrospinning process with the Taylor cone on the left, and detail of the Taylor cone zone and the transition zone supporting the fiber formation on the right [63].

The electrospinning process is influenced by various different factors and parameters, which are essential for the successful formation of fibers [68]: (**I**) environmental parameters, such as solution temperature, humidity and air velocity in the electrospinning chamber; (**II**) solution properties, such as elasticity, viscosity, conductivity and surface tension; and (**III**) governing variables, such as distance between the tip and counter electrode, electrical potential, flow rate, the molecular weight of the selected polymers, and the geometry of the collector [67].

The viscosity of the spinning solution is a critical aspect of the fiber-forming technology, which may be determined by varying the concentration of the polymer solution. Solutions with an optimum viscosity only yield the respective fibers in micro to nanoscale diameters [9]. During the electrospinning process, the applied voltage needs to be high enough to overcome the surface tension of the spinning solution to produce fibers. Yang et al. [69] reported that by reducing the surface tension of the solution without changing the concentration, beaded fibers may be converted into smooth fibers. Likewise, the conductivity of the solution may play a key role in the fiber formation process [68]. Similarly, the diameter and shape of the gauge may change the diameter and morphology of the fiber, respectively. The distance from the tip of the needle to the collector gives ample opportunity for the solvent to evaporate. A lesser distance

results in thicker/ beaded fibers being formed, whereas a greater distance results in discontinuous fibers [60].

From this point of view, there have been two strategies of electrospinning, known as "far-field" and "near-field". The main principle of these methods lies in the distance between the tip of the spinneret and the collector (**H**) determining the stages at which the fibers will be deposited on the collector. Conventional electrospinning is typically conducted in the far-field mode (**H** = 5−15 cm; high voltage 10−20 kV) [60].

Near-field electrospinning is attained when the distance is reduced to 500 μm−5 cm [70]. The distance may be predicted using the critical length (**L**) calculated according to the following equation:

$$L = \frac{4kQ^3}{\pi\rho^2 I^2}\left(\frac{1}{R_0^2} - \frac{1}{r_0^2}\right)$$

where $R_0 = (2\sigma Q/\pi k\rho E)^{1/3}$, **σ** – surface charge; **Q** – flow rate; **k** – electrical conductivity of the fluid; **ρ** – the fluid density; **E** – the strength of the electric field; **I** – the current passing through the jet; and r_0 is the initial radius of the jet [71].

In this case, the electric field is highly concentrated between the spinneret and the collector [72] and the applied voltage may be decreased between 0.6−3 kV. The flow rate of the liquid must be significantly reduced to 0.01−1 mL/h in order to support a stable jet.

Compared to far-field electrospinning, near-field electrospinning offers a number of advantages: (**I**) substantial reduction in the applied voltage, (**II**) the ability to precisely arrange the fibers over a relatively large area with minimum material consumption, and (**III**) the ability to manipulate the spatial positions of the fibers along all three directions of X, Y, and Z for the printing of fibers [73]. However, the flow rate of the liquid in a near-field electrospinning process is relatively low, leading to substantial reduction in the production volume. Moreover, the fibers are usually much thicker than those obtained through far-field electrospinning, and the complexity of the apparatus also limits its use for mass production [73].

The alignment/orientation of the fibers primarily depends on the type of collector used, such as pin, plate, cross bar, rotating rods or wheels, drum, liquid bath, or disk etc. In general, the fiber diameter and the pore diameter increase with an increase in the polymer concentration and flow rate. The geometry of the collector influences the arrangement of the fibers [61]. Through optimization of the above-mentioned parameters, fibers may be obtained randomly or in an ordered way. The choice of determining parameters is made on the basis of the polymer solution and the applicability of the formed fibers.

3.3.2 The drawing technique

The first attempt to draw a fiber was described in the 19th century. The experiment involved shooting an arrow from a droplet of a melted polymer using a crossbow [74]. In 1998, Ondarcuhu and Joachim published a drawing experiment, whereby a single fiber was formed from a droplet of a polymer solution using the tip of a scanning tunneling microscope (STM) [75]. Nowadays, the mechanical drawing of fibers is divided into two main categories: drawing from a solution [69,76] or from a melt [77]. Drawing as a method is particularly used for the production of fibers for optical devices [78,79], optical sensing, or nanophotonic fibers [69,77,80,81].

The principle of the drawing method is based on the mechanical pulling of a polymer solution out of its base droplet, resulting in evaporation of the solvent and fiber solidification in real-time [58]. Polymeric micro or nanofibers may be fabricated using two different ways of drawing, through glass micro-pipettes and/or with help of atomic force microscope (AFM) or scanning tunneling microscope (STM) probe tips (**Figure 14)**. This method is suitable for the formation of fibers having determined geometrical characteristics [76].

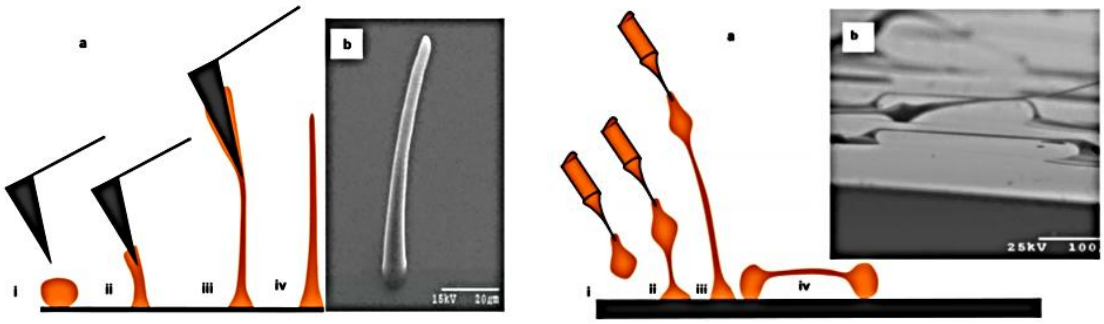

Figure 14. Fiber drawing based on the AFM/STM probe **a)**; SEM image of a drawn vertical fiber **b)** – left image. Process of micro-pipette probe fiber drawing **a)**; SEM image of a suspended fiber **b)** – right image [76].

Drawing has several drawbacks compared to the other methods used for nanofiber formation [82]. These include process control, a limited time of the process influenced by polymer droplet solidification, changes in the viscosity of the droplet with time, and speed of the solvent evaporating from the deposited droplet [76]. On the other hand, one of the greatest advantages of the drawing process is the ability to prepare oriented fibers in a range from nanometers to micrometers, compared to electrospun fibers, which are randomly oriented at similar scales [83].

The literature focused on the preparation of fibers made of organosilane precursors includes a publication from 1998 describing the preparation of mesoporous silica fibers by drawing [84]. However, the overwhelming majority of papers dealing with this method are focused on drawing from purely organic polymers [74,76,80].

3.3.3 The self-assembly technique

The principle of the self-assembly technique may be described as the spontaneous and reversible process in which a disordered system of pre-existing components (molecules, polymers, colloids, or macroscopic particles) are organized into ordered and/or functional structures or patterns via non-covalent interactions without external direction [85].

In general, these are spontaneous processes tending towards an equilibrium resulting in various shapes and forms [86]. In chemistry, self-assembly is typically associated with energy minimization processes and thermodynamic equilibrium [87]. Whitesides and Grzybowski divide self-assembly into two categories: static and dynamic. Static self-assembly corresponds to "molecular self-assembly", while dynamic self-assembly corresponds more to "self-organization" [88]. In polymer chemistry, Yamaguchi et al. consider self-assembly and dissipative structures as equilibrium and none-equilibrium forms of pattern formation, regarding them as two complementary manifestations of self-organization [86,89].

Despite the firm attention of academic literature [90–96], organosilane fibers prepared in this way and the technique itself have a number of disadvantages including the stability of self-assembly solutions, fiber length usually being only 100–200 nanometers, and fiber fragility with low mechanical resistance [91,92,97]. In most cases, self-assembled organosilane fibers have a tendency to form into short helical structures with a highly rough surface. Moreover, compared to electrospun fibers, manipulation is very demanding as they are not able to form a continuous layer within a solution.

Numerous studies have been devoted to the self-organization of organo-mono-silylated and organo-bis-silylated precursors and mesoporous materials made of them obtained via supramolecular self-assembly [39]. One example may be observed in **Figure 15**, where the helical mesoporous silica fibers containing various organic linkers were prepared by sol−gel polymerization together with self-assembly.

A large amount of literature regarding the self-assembly organization of organo-mono-silylated and organo-bis-silylated precursors into different shapes including nanofibers already exists and will be described further in the **Chapter 5.1.**

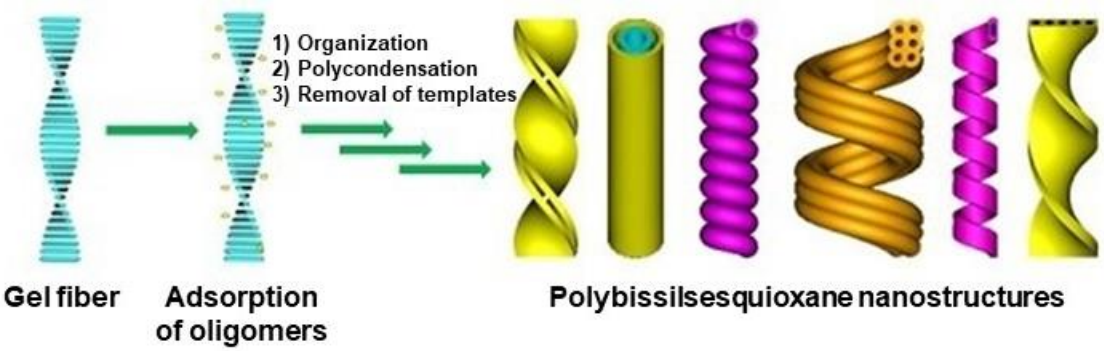

Figure 15. Scheme demonstrating the formation of single-handed helical polybissilsesquioxane nanostructures in the form of mesoporous nanofibers by self-assembly [98].

4. Hybrid organosilane fibers based on organo-mono-silylated precursors

In the moderate literature dealing with the preparation of hybrid organosilane fibrous materials based on organo-mono-silylated precursors, three principal strategies emerge in relation to their preparation. Firstly, and most easily, a wide range of organo-mono-silylated precursors are mixed together with various organic polymers functioning as a spinnable mediator. Likewise, organo-mono-silylated precursors may also be used in the second step to functionalize the prepared inorganic silica or organic polymer fibers. In both cases, the used spinnable mediator (organic polymer) may not bring any added value or may even be toxic in later use. Finally, organo-mono-silylated precursors either on their own or in a mixture with tetraalkoxysilanes may be combined to form a spinnable sol resulting in a purely organosilane composition of fibers. Therefore, the organic moiety is linked to inorganics entirely through Si-C bonds.

Either way, after sufficient networking these organo-mono-silylated mixtures undergo the above-mentioned fiber-making methods (electrospinning, drawing) or directly self-assemble into fibrous forms. Whichever method is used, the resulting fibrous materials should be a Class II organosilane hybrid displaying Si-C bonds in its structure. Nevertheless, depending on the other components, the structural variety may show a complex of hybrid links oscillating between Class I and II hybrids and even nanocomposites. The following chapter is dedicated to hybrid fibers based on organo-mono-silylated precursors, demonstrates the variety of synthetic approaches, and presents some of the most intriguing applications.

4.1 Hybrid organosilane fibers containing organic polymers

As already outlined, the spinnability of organo-alkoxysilanes appears to be the largest obstacle in the subsequent electrospinning and drawing processes of organosilane fiber manufacturing. The difficult search for suitable sol-gel parameters achieving ladder-like spinnable organosiloxane polymer chains may be avoided by using a wide selection of surfactants, low-molecular-weight polymeric gelators or spinnable polymers. Organic polymers used as a so-called "spinnability carrier" in combination with organo-alkoxysilanes or alkoxysilanes seem to be a prolific source of hybrid organosilane or silica/polymer fibers. The most commonly used organic polymers are poly(methylmethacrylate) (PMMA), polyvinylpyrrolidone (PVP), polycaprolactone (PCL), polyvinylalcohol (PVA), polystyrene (PS), and polyacrylonitrile (PAN).

Electrospinning is the most widely used technique for fiber-manufacturing of organo-alkoxysilane and organic polymer solution mixtures. Nevertheless, mixtures of organic polymers with tetraalkoxysilanes (TEOS at most) prevail and are also commonly referred to as organosilane hybrid fibers. However, the resulting structure does not contain Si-C bonds, but Si-O-C links connecting the inorganics with organic polymers (which is not quite in the scope of this review). There are many examples, such as the research of Li, J. et al. [99] who studied the tensile performance of TEOS/PMMA fibrous mats or the preparation of polyhydroxybutyrate (PHB)/PCL/TEOS fibrous scaffolds with a drug releasing function [100] to support bone tissue recovery. Organic polymers are often combined with tetraalkoxysilanes to create pore-forming (structure-directing) agents and are subsequently fired out to leave pure mesoporous silica fibers as a result [101].

Nevertheless, such examples of hybrid organosilane fibers from organo-mono-silylated precursors and organic polymers are not numerous. Ma et al. [102] reported the formation of superhydrophobic fibers (**Figure 16**) by the electrospinning of poly(styrene-*b*-dimethylsiloxane) block copolymers blended with 23.4 wt% homopolymer polystyrene - polydimethylsiloxane - polystyrene (PS-PDMS/PS) from a solution in a mixed solvent of tetrahydrofuran (THF) and dimethylformamide (DMF). The resulting fibrous mats (fiber diameters ranging from 150 to 400 nm) showed a water contact angle of 163° attributed to the combined effect of surface enrichment with PDMS and increased surface roughness.

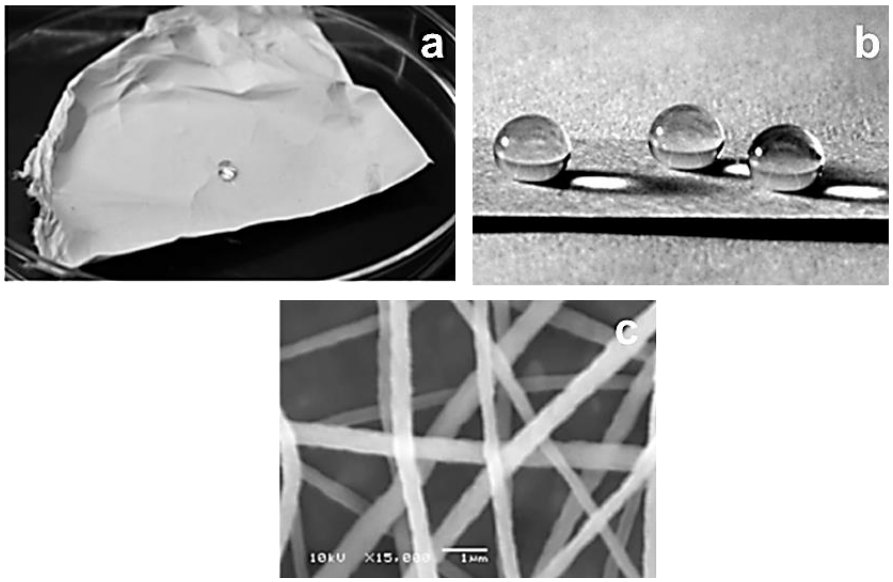

Figure 16. Free-standing mat composed of PS-PDMS/PS electrospun fibers **a**); several 20 μL water droplets on the mat, showing a superhydrophobic surface **b**); SEM image of the prepared fibers at 6000x magnification (scale bar = 2 μm) **c**); [102].

Another PDMS hybrid was prepared by Wei, Z. et al. [103] together with polyethylene oxide (PEO). The organic polymer was used only as an electrospinning carrier in a small ratio of approximately 0.3 – 0.5 wt% together with silica sol. Interestingly, the resulting hydrophobic silica/PDMS/PEO hybrid fibrous mats displayed good thermal stability (>600 °C) promising in related applications. Likewise, the hydrophobicity of PVA fibers was enhanced by Mustafa H. Ugur et al. [104] by adding a whole range of organo-mono-silylated precursors to an electrospinning PVA solution. Cross-linked PVA/organosilica electrospun mats (**Figure 17**) with reticulated structures (average fiber diameter of approximately 70 nm) were obtained with varying percentages of organosilane sol produced through the acetic acid catalyzed reaction of dimethyldimethoxysilane (DMDMOS), methyltrimethoxysilane (MTMS), tridecafluoro-1,1,2,2-tetrahydrooctyltriethoxysilane (FAS1313; Dynasylan® F 8261) and phenyltrimethoxysilane (PTMS; Dynasylan® 9165) in an isopropyl alcohol (IPA)–water mixture.

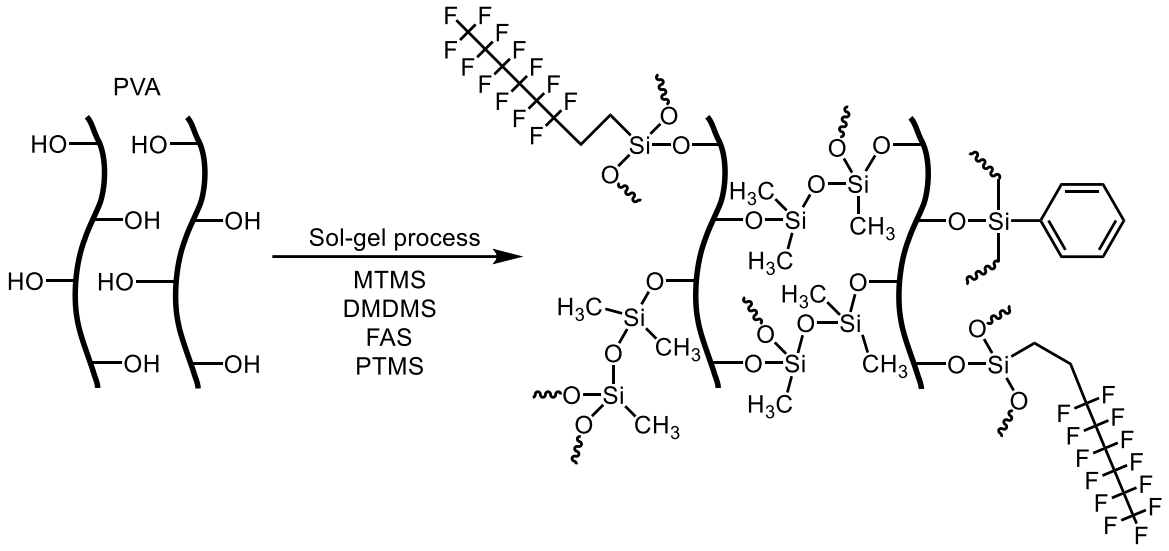

Figure 17. Scheme of PVA/silica nanofibrous mats [104].

Likewise, Arslan et al. [105] used the −OH groups available on the cellulose acetate (CA) structure to proceed with basic sol-gel reactions initiated by a mixture with reactive fluoro-alkoxysilane (FS) (Dynasilan F8261; FS). Perfluoro groups consequently modified the hydrophilic CA nanofibers (NF) to display superhydrophobic properties. Therefore, FS/CA-NF may be quite practical for future application in oil-water separators, as well as self-cleaning or water resistant nanofibrous structures [105].

Finally, an interesting combined method of in situ reduction and sol-gel processing was used to prepare novel fibrous membranes made of Ag@gelatin–silica hybrid nanofibers from gelatin, 3-glycidoxypropyltrimethoxysilane, and Ag@gelatin nanoparticles (NPs) [106]. The resulting fibrous mats showed strong photo-catalytic and antibacterial activity and may be easily recycled with a high recovery efficiency making them ideal adepts for removal of both organic pollutants and microbial contaminants from wastewater.

In rare cases, drawing and self-assembly techniques use a combination of organo-mono-silylated precursors with organic polymers. Drawing processes have been used to fabricate vinyltrimethoxysilane (VTMS) grafted polyethylene (PE)/SiO_2 nanocomposite fiber ropes [107]. The VTMS-g-PE/SiO_2 fibrous hybrid displayed remarkably improved breaking load and breaking strength compared to pure PE fiber ropes and decreased elongation at break. Mixtures of organic polymers with organo-alkoxysilanes are not commonly used in self-assembly techniques.

4.2 Functionalized hybrid organosilane fibers

The functionalization of previously prepared fibers is a commonly used method mainly due to its simplicity. Typically, organic or inorganic fibers are simply dip-coated in a sol based on an organosilane precursor often in combination with TEOS or TMOS. In any case, the resulting material is layered as the first fiber becomes the core and the dipped organosilane makes an external topcoat (a method referred to as "functionalizing"), which may be even multiplied.

The core fiber may be any kind of hydrolysable organic, inorganic, or composite material, so the principle of sol-gel processing may be applied. Hence, this procedure is well known in industrial conditions and the functionalization with various organosilanes is securely performed on glass or silica fibers (SiO_2) modified via 3-mercaptopropyltrimethoxysilane (MPTMS) (**Figure 18**) marked as -SH and silver nanoparticles [108–110], various organic polymers [111–113], cellulose acetate [105,114,115] or even wool [116] and composite materials [117,118]. Nevertheless, there are also very specific strategies of silanization for more demanding materials, such as (nano) cellulose fibers representing so-called "never-dried" materials. Beaumont et al. [119] proposed a two-step silanization protocol for nanostructured celluloses under aqueous conditions using catalytic amounts of hydrogen chloride and then sodium hydroxide. The developed protocol enables the incorporation of vinyl, thiol, and azido groups onto cellulose fibers and cellulose nanofibrils without curing or solvent-exchange. Hence, the functionalized celluloses remain never-dried, and no agglomeration or hornification occurs in the process.

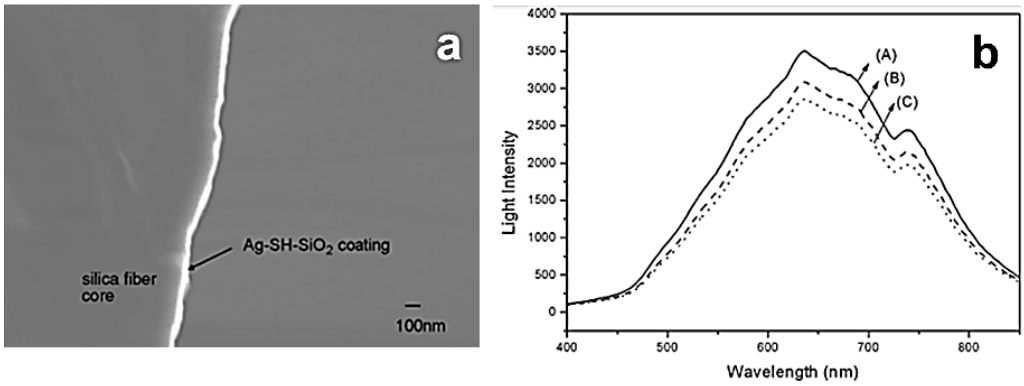

Figure 18. A SEM image of the cross-section of an optical fiber coated via MPTMS containing Ag nanoparticles and its changes in light intensity guided through the coated fiber probe [108].

The most commonly used organo-mono-silylated precursors include fluoro-alkoxysilanes often in combination with TEOS, employed to increase the hydrophobicity of the core fibers [105,111,113,115]. Likewise, the popularity of 3-aminopropyltriethoxysilane (APTES), 3-glycidyloxypropyltrimethoxysilane (GPTMS) and 3-mercaptopropyltrimethoxysilane (MPTMS) will be illustrated in the following section dedicated to applications using fibers based on organo-mono-silylated precursors.

4.3 Purely organosilane fibers

Probably due to the above-mentioned difficulty in achieving spinnable solutions, there are only a few research groups investigating organosilane fibers based purely on organo-mono-silanes (with or without tetraalkoxysilanes).

Groups led by Schramm [59] and Aytan [120] prepared polyimide-silane fibers (**Figure 19**) as new kinds of conductive electrolytes. Even if the starting sol-gel solution was based on organo-mono-silylated precursors, the first step consisted in the synthesis of a silylated polyamic acid precursor (sil-PAA). The silanization proceeded with the help of GPTMS or APTES, and in order to enhance the final properties of the resulting fibers, the sol-gel process was subsequently enriched [120] by other alkoxysilanes (PDMS, 3-(trimethoxysilyl)propyl methacrylate (TMSPMA), 3-(triethoxysilyl)propyl isocyanate (ICPTMS)). The water-soluble electrospun fibers were then subjected to a thermal imidization treatment at various temperatures. As a result, these water-insoluble organosilane materials with a nanoscale fibrous structure were stable at relatively high temperatures and showed electrolyte absorption and sufficient conductivity at room temperature [59,120,121].

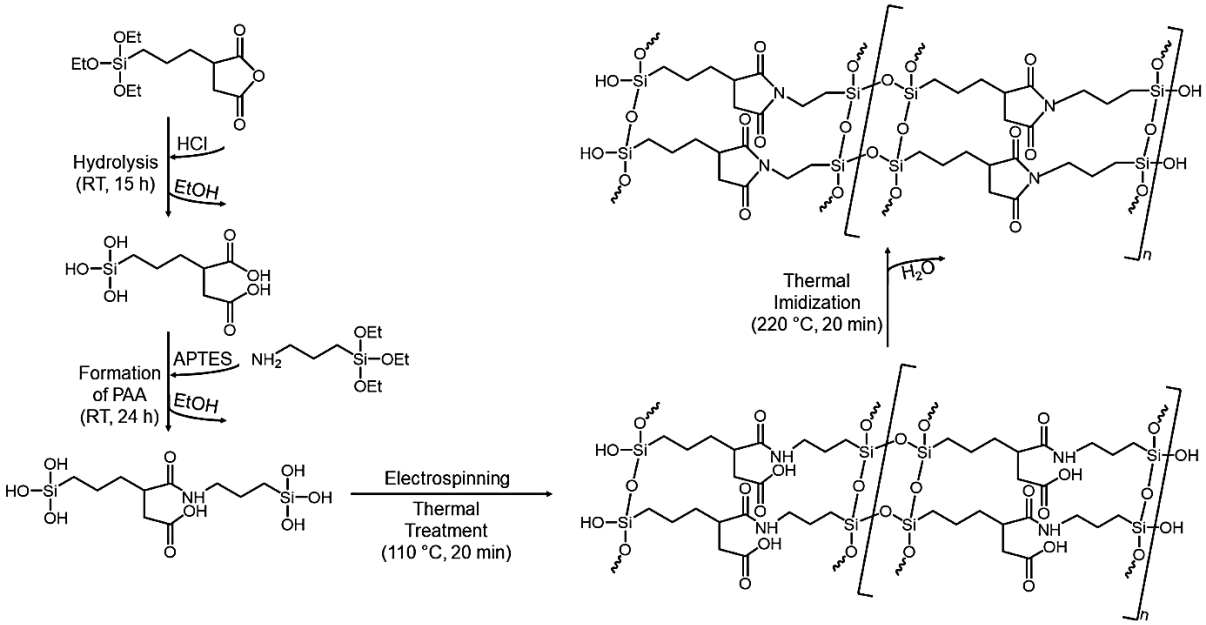

Figure 19. Schematic representation of the preparation of polyimide-silane fibers [121].

Another research group of McDowell [122] synthesized the starting organosilane precursor. In this case, high molecular weight polyferrocenylmethylvinylsilane (PFMVS) was synthesized by anionic ring-opening polymerization and further functionalized through Pt-catalyzed hydrosilylation using ethoxysilane to afford a polyferrocenylsilane (PFS) precursor. Electrospun electroactive microfibers from this gelable PFS cross-linkable alkoxysilane displayed interesting strain-induced buckling behavior on electroactuation at low voltages and, hence, could potentially rival existing bilayer actuators (**Figure 20)** [122].

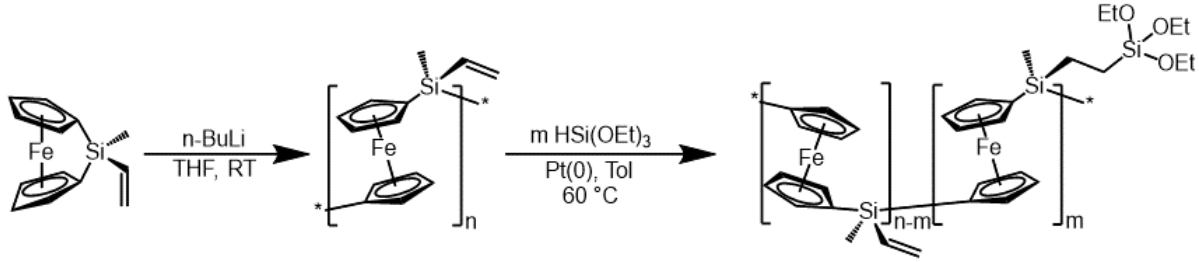

Figure 20. Scheme showing the formation of an organo-mono-silylated precursor [122].

The simplest synthesis in terms of the starting sol-gel solution may be found in the research of He et al. [123]. They prepared a range of electrospun mesoporous (organo)silica nanofibers. The silica sols with the surfactant Pluronic F127 were prepared with the addition of a MPTMS precursor and its influence on the fiber internal structure was evaluated. With the reduced

F127/TEOS mass ratio, the diameter of the (organo)silica nanofibers decreased, but the size and the orientation of the internal mesopores were remarkably regulated (**Figure 21**). Such a fibrous hierarchical hybrid material may be of great interest for modern optical and biomedical applications [123].

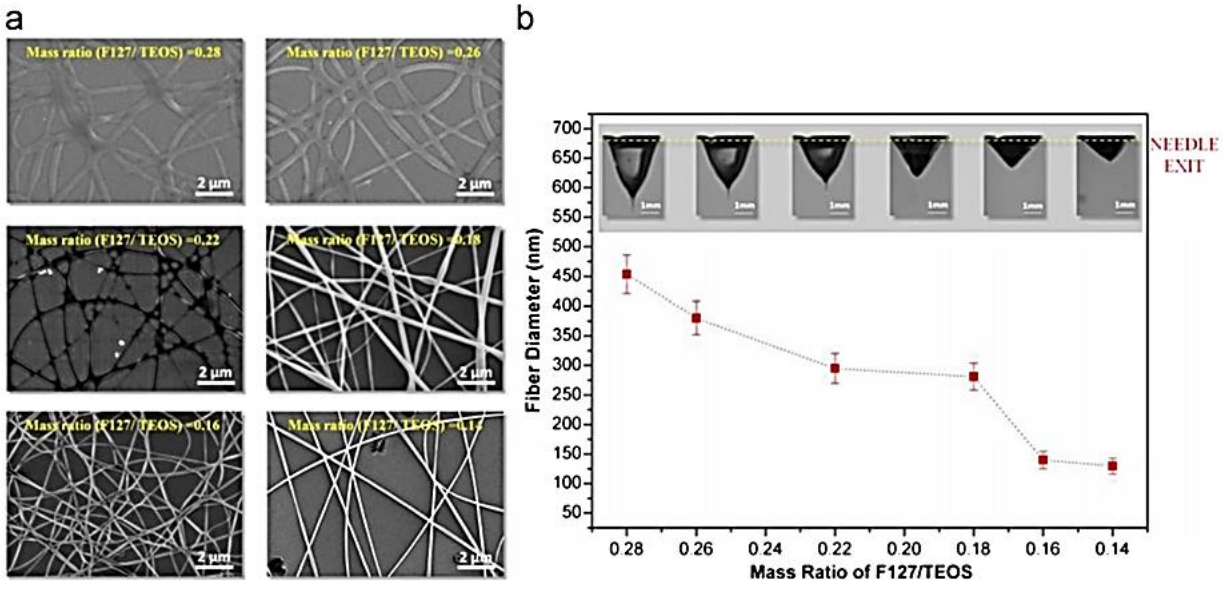

Figure 21. SEM images of silica nanofibers prepared using sols with different F127/TEOS mass ratios **a**); and the relationship between the fiber diameter and the F127/TEOS mass ratios **b**); [123].

5. Hybrid fibrous materials based on organo-bis-silylated precursors

The development of sophisticated organized hybrid materials, made of organo-bis-silylated precursors, exhibiting enhanced properties, plays an important role in tacking the challenging topics of the current scientific domains [124,125]. The first bridged organo-bis-silylated monomers, having arylene and acetylene bridging groups, were firstly used for sol-gel polymerization to form bridged polysilsesquioxanes coatings deposited on glass in the 1950s [40]. However, it was not until the start of the 1990s that bis(trimethoxysilyl)organometallic precursors with different structural features were first synthesized [31].

Nowadays, the number of organo-bis-silylated precursors with a wide variety of organic molecules is continuously increasing and they may finally be incorporated into the targeted materials [124,126,127].

5.1 Hybrid organo-bis-silylated materials: Powders prevail over fibers

Several synthetic approaches leading to the preparation of monomers for bridged polysilsesquioxanes currently exist, these include metalation, hydrosilylation, and organotrialkoxysilane functionalization [40]. From the "fiber-formation" point of view, a very promising class of organo-bis-silylated precursors is shown in **Figure 22**. These precursors are well described in the synthesis and formation of periodic mesoporous organosilica (PMO) materials [128]. Shea et al. reported the process of sol-gel synthesis regarding monolithic bridged silsesquioxane using 15 different alkane-, alkene-, alkyne-, aromatic-, functionalized- and organometallic-bridged precursors [40,126].

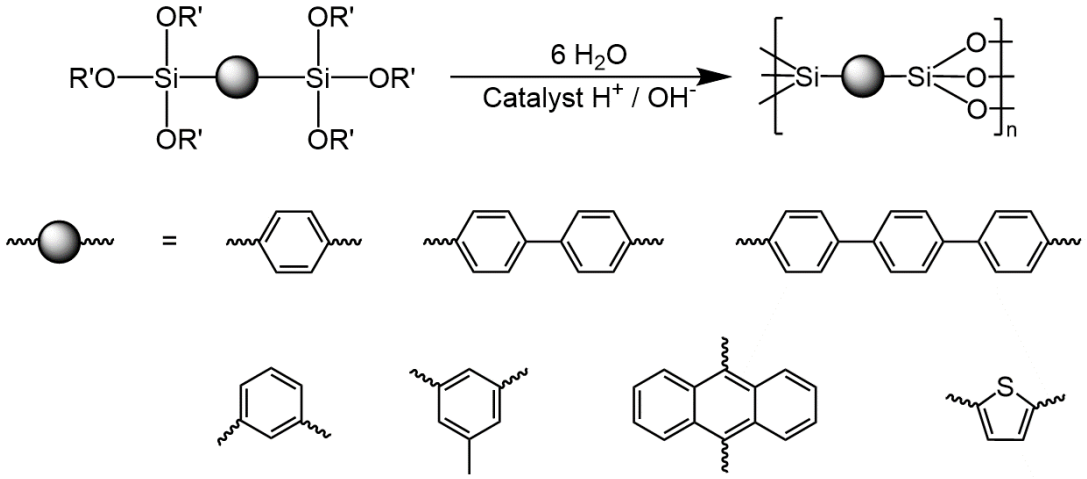

Figure 22. Representatives of arylene bridged polysilsesquioxanes [19].

Many bridged polysilsesquioxanes exhibit excellent thermal stability in inert atmospheres and in air. Phenylene-bridged polysilsesquioxanes are stable up to 500 °C. Alkylene-bridged polysilsesquioxanes are stable to over 400 °C. However, there is a lack of experiments describing the mechanical properties of bridged polysilsesquioxanes [40]. The most distinguishing features of arylene bridged polysilsesquioxanes are that they are porous and have extremely high surface areas, which may also be observed in the case of the fibrous form, which has promising potential for filtration, catalysis or adsorption [9]. Although conventional silica-based materials are generally regarded as biocompatible and suitable for *in vivo* use, the bio-safety of organo-bridged materials is still not entirely clear because of the lack of extensive and detailed *in vitro* and *in vivo* research and evaluations [129].

Interestingly, in the research or review literature, there are very few papers focused on the preparation of purely organosilane fibrous materials using organo-bis-silylated precursors [9,10,121,130]. The greatest obstacles seem to lay in the supposed difficulty of the

polymerization process of organo-bridged silanes, their conversion into a spinnable polymeric solution, and the choice of a suitable electrospinning technique.

Until 2020, only two solitary research papers regarding these types of nanofibers were published [121,130]. Tao et al. [130] dealt with the fabrication of purely organosilane electrospun nanofibrous mats containing porphyrin unit bridged organosilanes; however, the final material contained a very low amount of these organo-bridged silanes (10^{-4} mol.%) compared to TEOS (i.e. the result was mainly silica fibers). The second group [121] used the co-polycondensation process of two organosilanes combined with the sol-gel process and electrospinning to form ultra-thin polyimide fibers, also known as poly(amic)acid (PAA) fibers. These fibers are made of a combination of (3-triethoxysilylpropyl)succinic anhydride (TESP-SA) with either TEOS or methyltriethoxysilane (MTEOS), which were hydrolyzed and reacted subsequently with APTES, leading to the formation of an electrospinnable PAA solution. However, the solution had to be adjusted before electrospinning with a non-ionic surfactant Triton X-100 to improve the spinnability, but this reagent inevitably remained in the hybrid structure [121,131].

Nevertheless, the proof that all of the above-mentioned sol-gel parameters may be effectively linked to obtain spinnable sols may be found in the following research papers [9,10]. Both papers describe the one-pot synthesis of purely organosilane fibers without the addition of any kinds of surfactants, low-molecular-weight polymeric gelators or spinnable polymers (**Figure 23**), which were successfully produced on an industrial electrospinning device, paving the way for possible fabrication on a large scale. Moreover, the use of mono and bis-silylated model benzene functionalized organoalkoxysilanes [9] or a custom-made bis-silylated 1,2-diaminocyclohexane derivative [10] demonstrates the possibility of designing a molecularly engineered material tailored to specific applications such as reusable catalysts, adsorption agents, conducting membranes, or as novel types of biomaterials with additional properties.

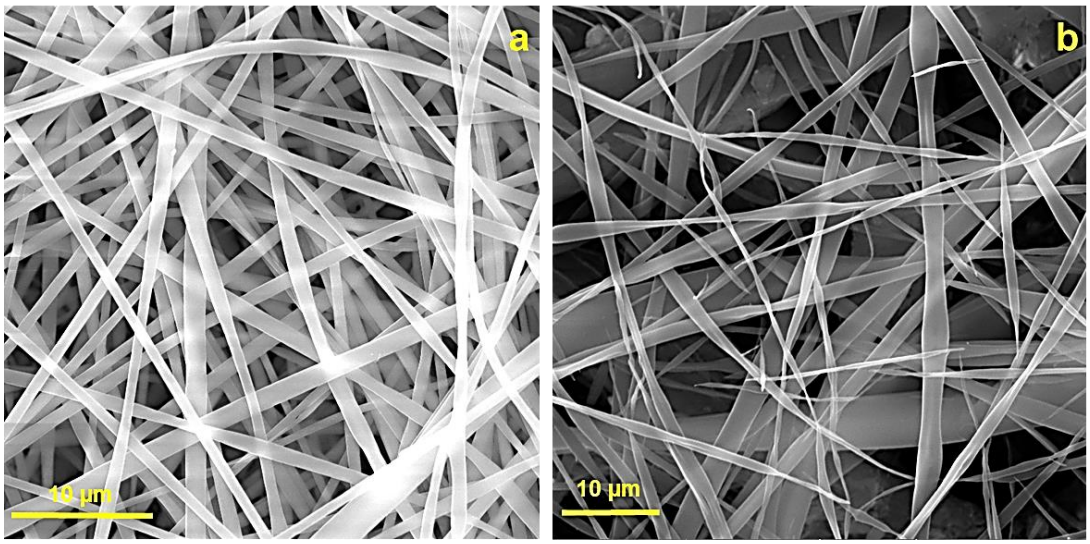

Figure 23. Electron microscopy images showing organosilane nanofibers prepared from a combination of 1,4-bis(triethoxysilyl)benzene with TEOS - sample **a**), and nanofibers prepared from a (1*S*,2*S*)-cyclohexane-1,2-diamine – bis – silylated precursor in combination with TEOS - sample **b**) [19,132].

If organo-bis-silylated precursors are not used in fiber-making via electrospinning and drawing techniques, the self-assembly procedure counterweights this lack of interest. Helical hybrid nanofibers have attracted the attention of many research groups due to their potential application for chiral catalysis and separations [91,92,133]. Although many approaches to the preparation of helical mesoporous silica nanofibers have been developed, those for the preparation of helical organic–inorganic mesoporous hybrid organosilane nanofibers are rare [92]. They may be prepared using chiral low-molecular weight amphiphiles [134] or mixtures of a cationic and fluorinated surfactant. Moreover, the reduction of surface free energy was proposed as the driving force of helix formation in the fiber structure [92].

A wide range of helical fibers has been prepared using various synthetic methods including self-assembled bridged silsesquioxane helical fibers formed through hydrogen bonds promoted by the urea groups within the organic bridged fragment [135]; periodic mesoporous ethene-1,2-diyl-silica nanorods (**Figure 24**) prepared using cetyltrimethylammonium bromide (CTAB) in concentrated aqueous ammonia solutions, applicable in fields such as chiral separation and catalysis [133]; mesoporous silica nanofibers using co-structure-directing agents e.g. chiral anionic surfactants [136,137]; screw-like hierarchical chiral fibers constructed by co-templating two building blocks, DNA and porphyrin with using cationic organosilane precursor as a formation support [138]; single-handed helical mesoporous poly-bis-silsesquioxane

(methylene, ethane-1,2-diyl, ethene-1,2-diyl, benzene-1,4-diyl, biphenyl-4,4′-diyl bridged) nanofibers prepared by sol-gel polymerization using chiral cationic low molecular weight gelators (LMWGs) and different types of catalysts e.g. HCl, NaOH, and ammonium hydroxide [98]; organosilane fibers obtained from acidic catalyzed syntheses using either TEOS or tetra(isopropoxy)silane (TPOS) in the presence of various oils [90]; mesoporous hybrid silica nanofibers made of 1,4-bis(trimethoxysilyl) benzene with a high surface area [91,95]; mesoporous ethane-1,2-diyl–silica nanofibers prepared using CTAB and (*S*)-2-methyl-1-butanol (MB) as a co-structure-directing agent, whose helical pitch is controllable by changing the MB/CTAB 0.5–10 molar ratio [93,139]; and mesoporous methylene, ethane-1,2-diyl, ethene-1,2-diyl, benzene-1,4-diyl silica nanofibers prepared using CTAB and (*S*)-β-citronellol as a co-structure-directing agent under basic pH with a range of 0.2–2.0 μm in length and 100–200 nm in diameter with helical pitches of approximately 1.0 μm [92,96].

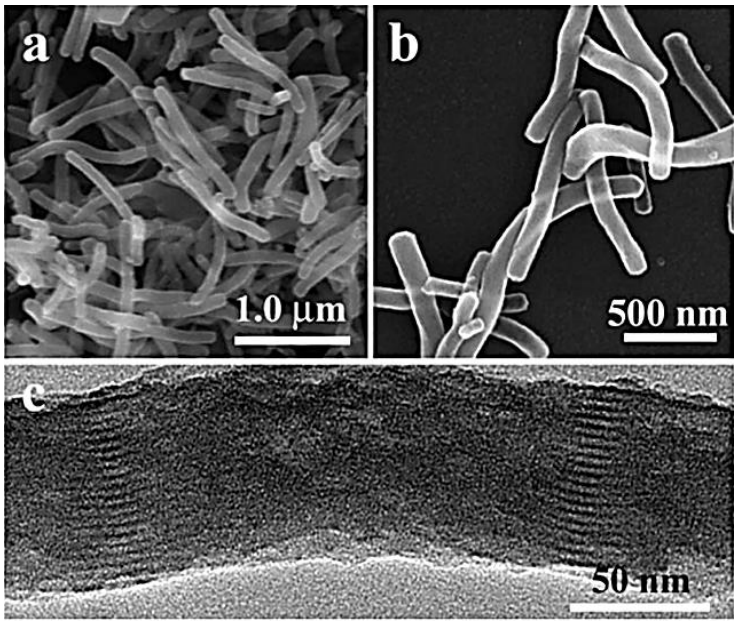

Figure 24. Electron microscopy images of the formation of mesoporous ethane-1,2-diyl – silica nanorods via the self-assembly process. FESEM microscopy **a)**; **b**) and TEM microscopy **c**) [133].

Hierarchically organized functionalized periodic mesoporous organosilica (PMO) fibers with longitudinal pore architectures have been prepared via a simple one-pot synthesis procedure from the co-condensation of 1,2-bis(triethoxysilyl)ethane with either ICPTMS or 1-[3-(trimethoxysilyl)propyl] urea in basic pH. The diameters of the fibers range from 50 to 300 nm, and the lengths are up to 7 μm [140]. Single-handed helical benzene-1,4-diyl bridged

polysilsesquioxane nanofibers have been prepared through a different supramolecular templating approach [94,141].

Helical mesoporous silica, methylene, ethane-1,2-diyl, ethene-1,2-diyl, benzene-1,4-diyl, octane-1,8-diyl nanofibers have been prepared by sol-gel polymerization using a chiral cationic gelator under a shear flow. The morphologies of the silica nanofibers were sensitive to preparation conditions. In acidic conditions, right-handed helical nanofibers were observed (**Figure 25**), and in basic conditions, rod-like mesoporous nanofibers were formed [95].

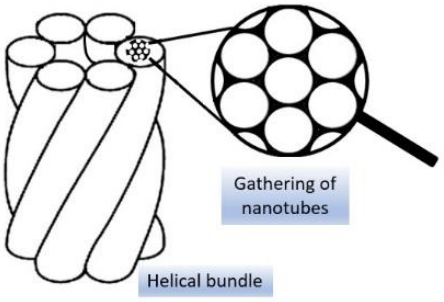

Figure 25. Schematic representation of right-handed helical nanofibers[19].

6. Application potential and prospective of the reviewed fibrous materials

6.1 (Nano)fibers prepared from organo-mono-silylated precursors

Taking account of the availability of raw materials, easy maneuverability, and outstanding chemical, physical, optical and mechanical properties, organo-alkoxysilanes in the form of fibers may find a wide range of potential applications in various different fields of current interest [117,118,142,143]. Examples include ternary nanofibers having remarkable solvent and temperature resistance (e.g. in DMF at 200 °C) [116] and nanofibrous PVA/PAA/SiO_2 mats having unique malleability and high breaking elongation [97]. This versatility is typical for all of the discussed materials; nevertheless, others will be discussed in the appropriate sections according to their target design, i.e., optoelectronics and sensors, energetics, filtration and adsorption, catalysis and biomedicine.

6.1.1 Optoelectronics and sensors

Organo-mono-silylated precursors are especially useful in optoelectronic devices and sensor applications due to their wide range of functional groups, which may be selected to

facilitate the covalent attachment of indicator molecules directly to the targeted areas. These precursors may be used various different forms e.g., organo-alkoxysilane coatings deposited on organic fibers, directly prepared organic-inorganic fibers from convenient organo-mono-silylated precursors, inorganic fibers modified with the above-mentioned precursors, and many other possibilities bringing additional properties to these fibrous materials [110]. According to the literature, APTES is one of the most frequently used organo-mono-silylated precursors and is known as a coupling agent for sensors. It is usually used to bond organic probe molecules to glass, silica sol-gel surfaces, optical glass fibers and other types of organic, inorganic and or hybrid organic-inorganic fibers [110,144,145]. Some of the newest environmentally-friendly and low-cost applications for optoelectronic devices include two types of high-performance polyimide (PI) fibers, which are modified with APTES (KH-550) and applied in light-weight composite devices possessing a high strength modulus, higher temperature resistance and lower density [146]. The morphology of these modified fibers is shown in **Figures 26** and **27**.

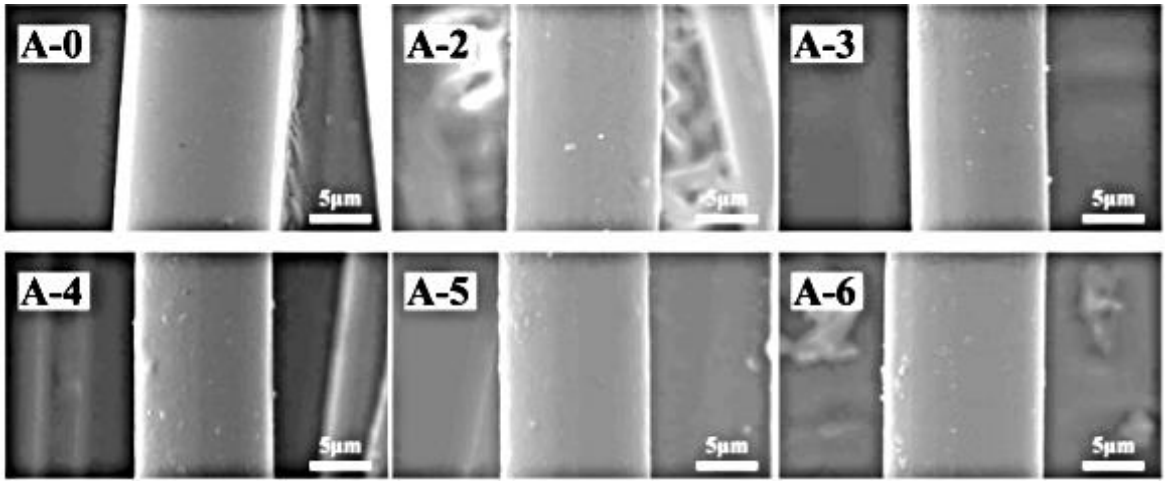

Figure 26. SEM images of PI fibers treated with 0, 2, 3, 4, 5 and 6 wt% of APTES (KH-550) [146].

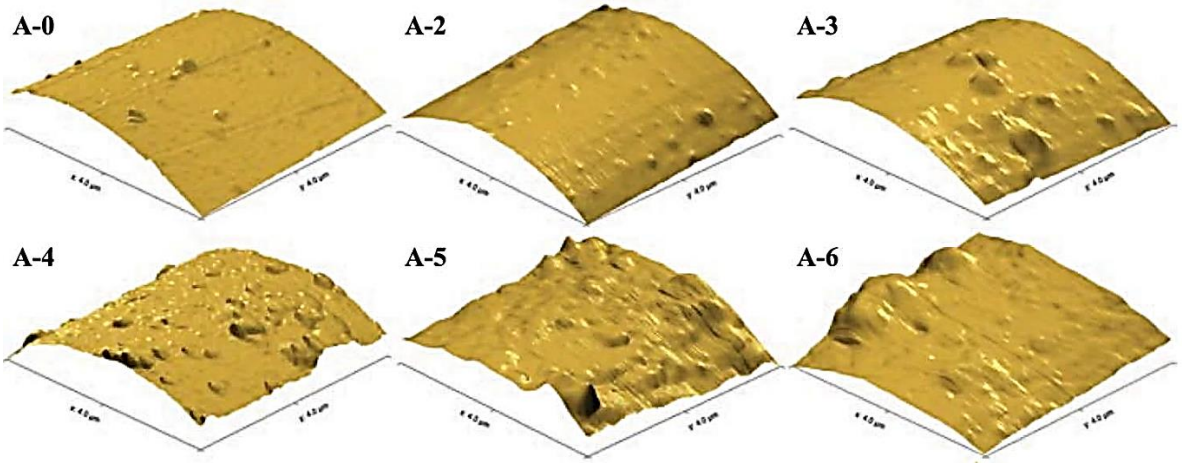

Figure 27. AFM images representing PI fiber surface roughness treated with 0, 2, 3, 4, 5 and 6 wt% of APTES (KH-550) [146].

Typical representatives of hybrid organic-inorganic fibers are organically modified silica (ORMOSIL) fibers used in microchip couplers for optoelectronic applications [109], or electroactive electrospun PFS fibers functionalized by pendant alkoxysilane groups, which have been successfully incorporated into miniature electrochemical cells containing lithium triflate/γ-butyrolactone electrolyte [122]. Other examples include optical fibers coated with different types of organo-monosilylated precursors such as APTES, GPTMS, PDMS with or without TEOS used for sensor applications [110], optical fibers coated with an Ag-doped silica nanocomposite used as sensors for trace ammonia in gas samples [108], or optical PMMA fibers coated with a mixture of TEOS and methyltriethoxysilane (MTES) or phenyltriethoxysilane (PTES) doped with bromophenol blue, which have been successfully applied as low-cost pH sensors for monitoring biological fluids for the diagnosis and evaluation of therapies in wound healing applications [112].

6.1.2 Energetics

Nano-structured fibrous materials consisting of organic and inorganic components are an interesting alternative to the pure polymeric materials used in energetics. The new types of hybrid fibrous materials offer higher mechanical, chemical and physical resistance, which is necessary for stable performance in all modern energetics devices such as new types of fuel cells and/or lithium-ion batteries [147–149].

Silicon oxide (SiO_x) is one of the most promissive anode materials suitable for lithium-ion batteries with the advantages of high theoretical capacity, low platform (<0.5 V) and environmental friendliness. However, SiO_x is known to have low electronic conductivity and

the degradation of the structure upon cycling limits the electrochemical performance of SiO_x. For this reason, a conductive carbon fiber network was covered by a SiO_x/C composite by a combination of two methods, electrospinning and carbonization (**Figure 28**). The amount of SiO_x in the composite may be adjusted by changing the amounts of organosilane nanospheres used during the electrospinning process (**Figure 29**). These new anode material exhibits good cycling stability, rate capabilities and superior electrochemical performance, which guarantees enhanced overall ion and electron transportation and structural integrity suitable for advanced lithium-ion batteries [149].

Figure 28. A scheme showing the design of the pea-pod structure of SiO_x/C nanofibers [149].

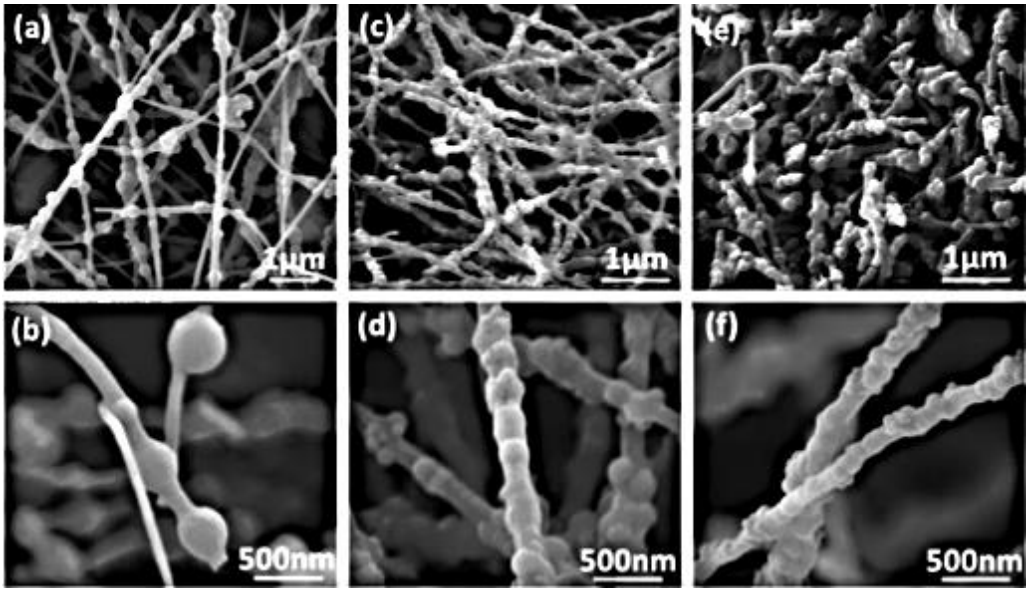

Figure 29. SEM images showing the pea-pod structure of SiOx/C nanofibers with different amounts of SiOx (SiO_x/C-0.3g (**a,b**); SiO_x/C-0.4g (**c,d**) and SiO_x/C-0.5g (**e,f**)) [149].

Hybrid organic-inorganic electrospun fibrous membranes made of (2-(4-(chlorosulfonyl)phenyl)ethyl)trichlorosilane (CSPTC) with TEOS, polyvinylidenefluoride-hexafluoropropylene (PVDF-HFP) in DMF are typical representatives of hybrid power devices used for proton exchange membrane fuel cells working at a high temperature. The inorganic parts allow the more effective transport of protons and water management, and the organic materials bring softness, tightness, processability to the overall system [150]. Other examples include hybrid 1,4-bis(triethoxysilyl)benzene/GPTMS fibrous membranes with sulfonated aromatic rings providing proton conductivity [147].

Electrospun fibers based on a combination of GPTMS modified polyamic acid and alkoxysilane functional poly(dimethylsiloxane), subsequently soaked with 0.5 M $LiFP_6$ solution, and used as a hybrid gel electrolyte for lithium-ion batteries are an example of the latest research work in this area [120], as well as reinforced nanofiber composites prepared with a combination of PVA and nanosilica modified with mercaptopropionic acid and MPTMS [151]. Mullite fibers (MF) functionalized via APTES used as a filament in wound epoxy nanocomposites [152] or aramid fibers functionalized with APTES [153,154] also show promising potential in energetics.

6.1.3 Filtration and adsorption

Hybrid fibrous membranes used in water [155] or air filtration systems, which are made of or modified via organo-mono-silylated precursors, offer additional properties such as durability, good tensile properties, chemical stability, catalytic properties, or sufficient porosity compared to the conventional systems already used [156,157].

Most of the currently used filtration membranes are made of organic polymers, which are subsequently functionalized via different types of organo-mono-silylated precursors. These include electrospun cellulose acetate nanofibers (CA-NF) modified with perfluoro alkoxysilanes (FS/CA-NF) for oil–water separation purposes [105], omniphobic fibrous cellulose acetate membranes containing silica nanoparticles modified via APTES used for desalinating the wastewaters with low-surface-tension contaminants [115], other types of organic fibrous membranes modified via APTES [158–160], composite PVA/TEOS/APTES fiber membranes used to remove cadmium from aqueous solution [161], or polyacrylonitrile fibers functionalized via APTES in PDMS membranes used for air filtration systems [162].

Surprisingly, when focusing on the literature related to the preparation of purely organoalkoxysilane fibrous membranes, most of the filtration systems are based on the combination of organic fibrous membranes modified via organo-alkoxysilane nanoparticles and

nanocoatings. There are only a few solitary research papers describing the preparation of purely organosilane fibrous membranes used in filtration applications [121,130].

In the first of them, Tao et al. [130] describe the preparation of porphyrin-doped nanocomposite fibers (**Figure 30**) in the form of nanofibrous membranes, which were prepared by combining sol-gel chemistry and the electrospinning technique, without the addition or help of organic polymers. The membrane was successfully tested as a novel fluorescence-based chemosensor for the rapid detection of the trace vapor (10 ppb) of explosives, and has exhibited remarkable sensitivity to trace (2,4,6-trinitrotoluene) TNT vapor.

In the second, Schramm et al. [121] prepared ultra-thin polyimide fibers, which were thermally treated at 220 °C. This temperature supports the rise of the formation of polyimide (PI) groups in the final polysiloxane network and the resulting fibers have a ladder-like structure. Moreover, the authors incorporated various organo-trialkoxysilanes with different functional groups enabling the production of ultra-fine fiber mats with tailor-made properties. The fibers may be applied in filtration, sensor systems, or drug release processes.

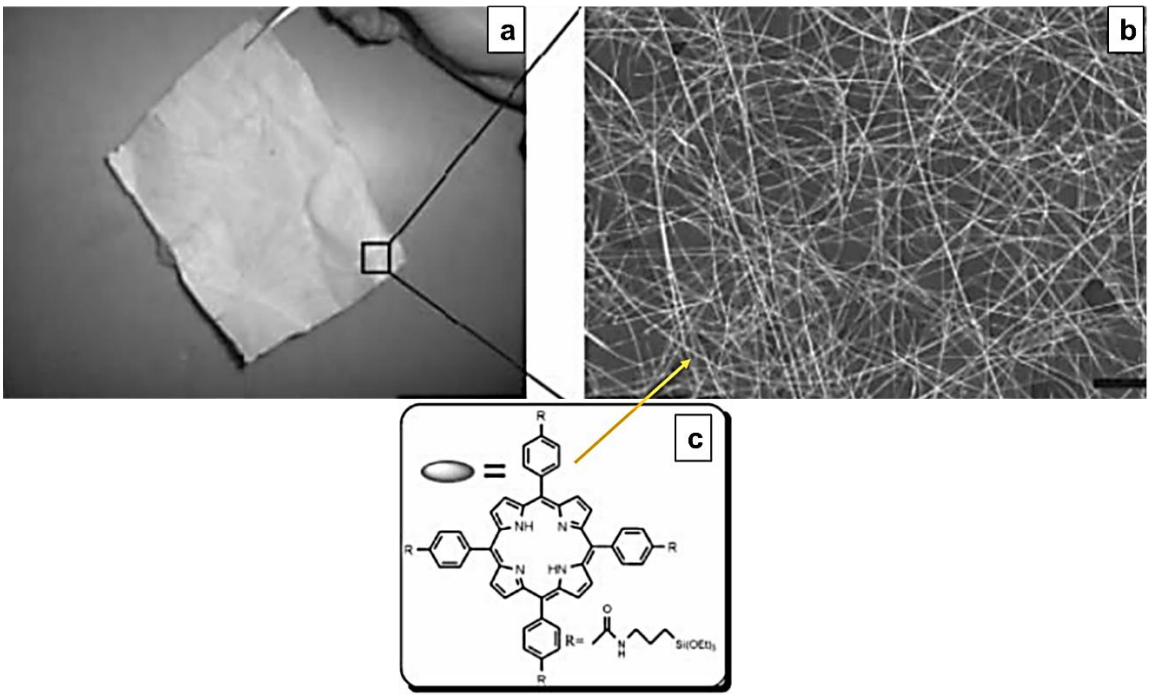

Figure 30. Photo of an electrospun porphyrin-doped freestanding nanofibrous membrane **a**); SEM image of this membrane, scale bar = 20 μm **b**); structure of the porphyrin-silane precursor used in the silica matrix with a content of (10^{-4} mol.%) **c**)[130].

6.1.4 Catalysis

According to a literature search of the application of organo-mono-silylated precursors strictly in the form of (nano)fibers in catalysis, there are only a very small number of research papers compared to the same precursors used in the form of nanoparticles or nanocoatings on different substrates [163,164]. Most of the published literature describes organic fibers functionalized via different types of alkoxides, or organo-mono-silylated precursors. Specific examples of fibrous systems used for catalytic applications include linear poly(ethylene imine) (PEI) fibrous aggregates modified via TEOS or TMOS, which are able to reduce $PtCl_4^{2-}$ [165], or nanoporous silica fibers functionalized with MPTMS used for solid-phase microextraction (SPME) of phenolic compounds (**Figure 31**) [166], mesoporous silica nanofibers made of a combination of TEOS, and MPTMS, whose mesostructure corresponds to MCM-41 nanoparticle systems [167].

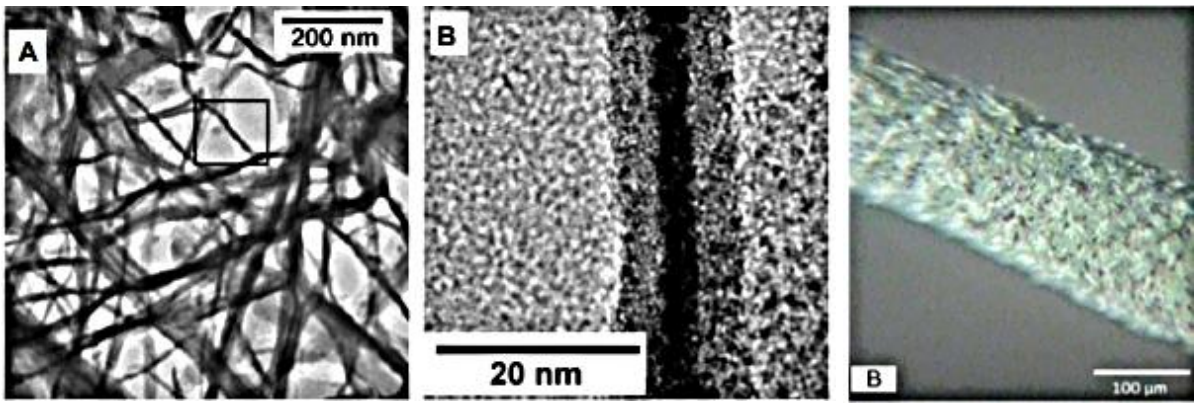

Figure 31. Si2-Pt nanofibers containing Pt nanocrystals **a)**; HRTEM image of the boxed region in Figure 32a **b**) - center [165]; optical microscopic image of a proposed SPME fiber **b**) - right [166].

6.1.5 Organosilane fibrous materials in medicine

Hybrid fibrous materials made of organo-mono-silylated precursors find their widest application in the field of medicine, and particularly in various types of scaffolds applicable in tissue engineering supporting cell growth, and/or in wound care therapy. They are typically used in a combination of organic polymers, alkoxides and organo-mono-silylated precursors [62] e.g., mixtures of poly(γ-glutamic acid) (γ-PGA)/TEOS and GPTMS providing an excellent extracellular matrix in bone tissue regeneration (**Figure 32**) [168], silica/poly(L-lactic acid) (PLLA) for skeletal defect regeneration [169], protein-encapsulated fiber mats using a combination of poly(γ-glutamate) (PGA)/(GPTMS) offering an effective method of

encapsulating bioactive molecules (**Figure 33**) while maintaining their structure and function [170], drug delivery systems based on PCL/PLA) with Halloysite nanotubes (HNT) [171], regenerated cellulose nanofibers (RC-NF) with PCL, modified via APTES with the aim of increasing the mechanical properties of the prepared scaffolds [172], APTES functionalized electrospun poly(*N*-vinyl-2-pyrrolidone) fibers (NH_2-PVP) capping gold nanoparticles for drug delivery systems working at different pH (5.0, 6.0, 7.4) supporting cell growth [173,174], or fibrous materials used in wound-healing applications with antibacterial effects composed of mesoporous silica nanoparticles in PVP nanofiber mats [175,176].

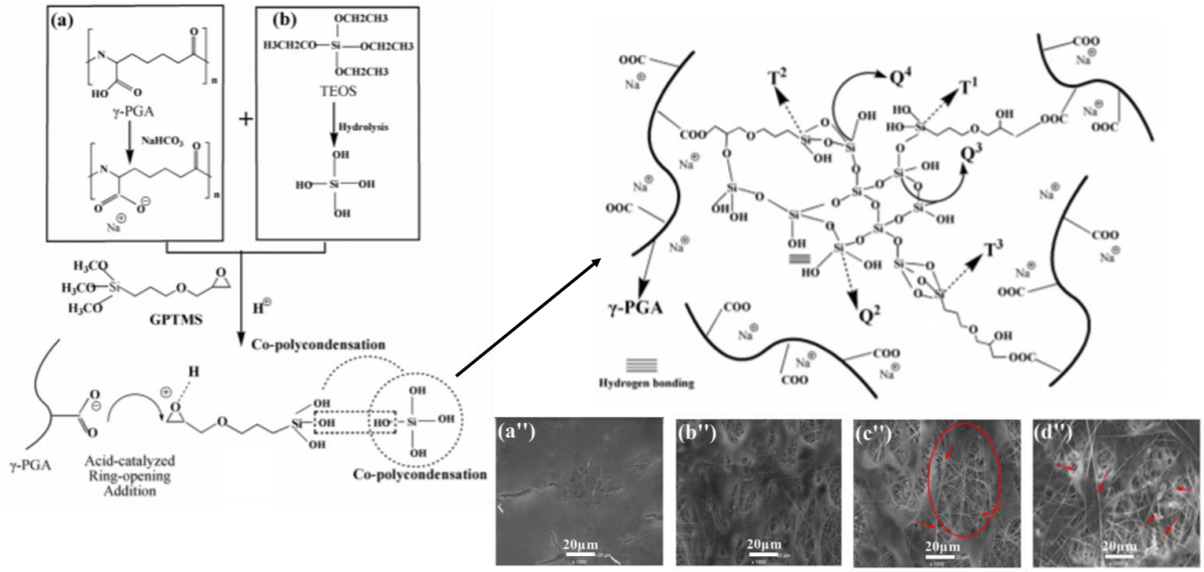

Figure 32. Scheme showing the formation of electrospun γ-NaPGA-silica hybrid scaffolds using GPTMS as a cross-linking agent and SEM images of MC3T3-E1 cells present on these hybrid scaffolds containing different molar ratios of γ -PGA/TEOS: (a) 1:0, (b) 5:3, (c) 1:1 and (d) 3:5 after 7 days of incubation [168].

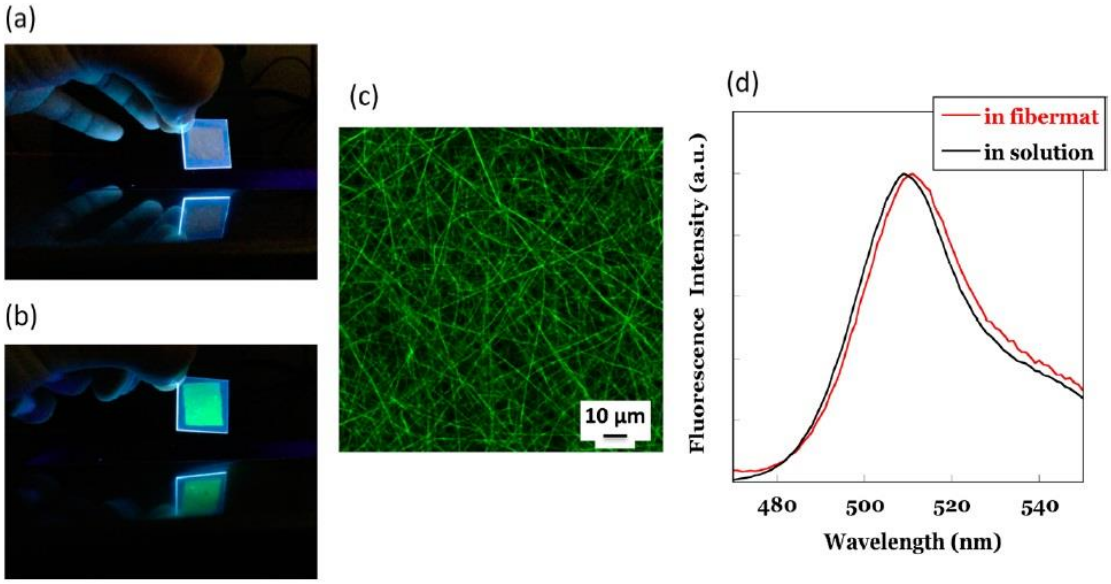

Figure 33. Fluorescence emission (excited at 312 nm) of silica/PGA fiber mats without encapsulated green fluorescent protein (GFP) wetted with a 20 mM phosphate buffer (pH 7) **a**); fluorescence emission (excited at 312 nm) of silica/PGA fiber mats with encapsulated GFP wetted with a 20 mM phosphate buffer (pH 7) **b**); fluorescence image of GFP-encapsulated silica/PGA fiber mats wetted with a 20 mM phosphate buffer (pH 7) using a laser scanning confocal microscope (excited at 405 nm) **c**); fluorescence spectra (excited at 460 nm) of GFP encapsulated in a silica/PGA fiber mat (red line) or in a 20 mM phosphate buffer (pH 7, black line) **d**); [170].

6.2 Hybrid materials based on organo-bis-silylated precursors

Hybrid organosilane materials based on organo-bis-silylated precursors in various different forms (mainly nanoparticles) seem to be a very promising class of materials having extraordinary properties applicable in separation methods, e.g., chromatographies [177]. Earlier, ethane-1,2-diyl and benzene-1,4-diyl bridged polysilsesquioxanes functionalized with amino and thiol groups in the form of nanoparticles were used as adsorbents of volatile organic compounds (*n*-hexane, *n*-heptane, cyclohexane, benzene, triethanolamine, acetonitrile) from gas phase chromatography [178]. Another application of these materials may be found in catalysis [126,179–183] and/or in optics [125,126,184,185]. Another example in this field are carbon/silica superstructures made of perylenediimide-bridged silsesquioxane (PDBS) with controllable morphologies (tubes, fibers or spheres), sizes, and excellent electrical properties, which are very promising candidates for optoelectronics and sensing devices [186]. In general,

organosilanes with various different forms containing aromatic rings (**Figure 34**) have a significant potential for use in modern batteries [127].

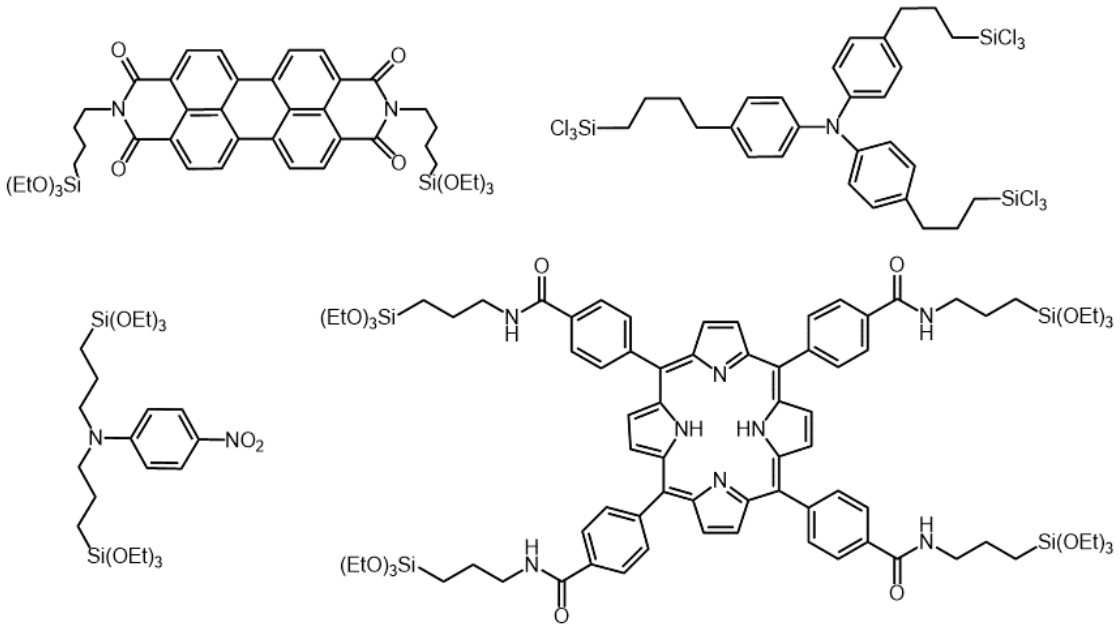

Figure 34. Examples of bridged polysilsesquioxanes with chromophore bridging groups, adapted according to the reference [40].

The above-mentioned findings prove that novel hybrid pure organosilane materials based on bridged alkoxysilane precursors and in a fibrous form belong to a promising class of materials offering additional value and aiming at a wide range of end-applications [9,10] particularly catalysis, separations [91,92,133] and/or modern biomaterials having additional value [138].

7. The knowledge obtained and the results providing the novelty of this work

The results of this work were obtained based on knowledge of long-term problematics relating to silicon alkoxides together with organo-mono-silylated and organo-bis-silylated precursors (also known as bridged silsesquioxanes). By combining three different and independent fields of science (organic and organometallic chemistry, sol-gel chemistry, and electrospinning technology), it was possible to obtain completely unique results in the preparation of purely organosilane (nano, sub-micro and micro) fibers. To prepare such fibrous materials, it is not necessary to use the support of organic polymers, various types of surfactants,

or non-polar organic solvents, which are in many cases highly toxic and economically inconvenient.

Various spinning facilitators, such as organic surfactants and/ or organic polymers, are currently used, without which these organosilane sols are generally considered to be non-electrospinnable [12,187]. Examples of organic surfactants used for this purpose are cetyltrimethylammonium bromide (CTAB), poly (ethylene glycol)-block-poly (propylene glycol)-block-poly(ethylene glycol) (P123), Pluronic F127 hydrogel, sodium dodecyl sulphate (SDS), or Triton X-100. Organic polymers such as polyvinylpyrrolidone (PVP), polycaprolactone (PCL), polyvinyl alcohol (PVA), or polyhydroxybutyrate (PHB), in the form of supports for electrospinning, are often used. The main disadvantage of these surfactants and/or organic polymers is that in many cases they are toxic substances, which may be difficult to remove by washing or burning from the prepared fibrous structures [188] due to the fact that their residues may remain in the structure of the prepared fibers [189,190] and act as undesirable impurities in them. The removal of these substances not only prolongs and complicates the preparation of fibers, but also impairs their physical and chemical, and/ or mechanical properties, and may lead to the embrittlement of the fiber material, etching of their surface, or thermal degradation of their organic part.

On the other hand, the fibrous materials developed using our research method are prepared with a high content of hybrid organosilane precursors inside the hybrid matrix, reaching almost or entirely 100 mol.% compared to pure inorganic nanofibers made of TEOS. During the preparation of these organosilane fibers, great emphasis is placed on ecological aspects such as the use of polar solvents based on alcohols, particularly ethanol, water, and acid catalysts in the form of mineral acids such as hydrochloric acid, nitric acid and/or sulfuric acid.

The novelty and topicality of the whole issue may also be documented by the recently filed **national patent application, PV 2021-160, and international patent application EP21172710.2** entitled: "*A process for preparing a sol for the preparation of hybrid organosilane fibers by electrospinning technique, a sol thus prepared and hybrid organosilane fibers prepared by electrospinning of this sol"*.

The completely unique properties of the prepared hybrid, purely organosilane (nano, sub-micro and micro) fibers were successfully published in the prestigious journals Polymer [9] and Polymers [10] in 2020 by the author of this thesis.

The results of this work, focusing on the preparation of (nano, sub-micro and micro)fibers from commercially available organo-mono-silylated and organo-bis-silylated precursors based on phenyltriethoxysilane and 1,4-bis (triethoxysilyl) benzene, their characterization using

various techniques, including nuclear magnetic resonance (NMR) together with their application potential, are partly presented in the form of a published article in the supplements (**Chapter 11.5**), as well as in the case of (nano)fibers prepared from a synthesized organo-bis-silylated precursor ((1*S*,2*S*)-1,2-bis{*N*′-[3 (triethoxysilyl)propyl]ureido}cyclohexane). A specific example describing the whole preparation process of this type of (nano)fibers is demonstrated on use a hybrid organo-bis-silylated precursor based on 4,4'-bis(triethoxysilyl)-1,1'-biphenyl. Moreover, 3 other types of organo-bis-silylated precursors were synthesized and two of them are already tested in the fiber formation process using the jet needle-electrospinning technique.

All the above mentioned commercially available and/or synthesized precursors were chosen with the aim to primarily test them in biomedical applications, but according to their characteristics, they may find more application potential particularly in the fields of optoelectronics, energetics, catalysis and/ or filtration processes.

7.1 Nanomaterials including (nano)fibers made of 4,4'-bis(triethoxysilyl)-1,1'-biphenyl

Hybrid organo-bis-silylated precursor entitled 4,4'-bis(triethoxysilyl)-1,1'-biphenyl (BTEBP) has several advantages. First of all, it is a commercially available precursor which is moreover well known in many applications described in patents (CN110723738(A), 24.1.2020; CN106610397(A) and CN106610394 (A), 3.5.2017; CN106353389(A), 25.1.2017, as well as in the research papers [98,191–193]. Patents regarding refer to this precursor in various forms such as aerogel for the fields of heat preservation materials, heat insulation materials, waste gas treatment materials, wastewater treatment materials and catalysts, or in the form of the sensor for electrochemical detection of dopamine, and/or ascorbic acid by using biphenyl organic mesoporous material-doped carbon paste electrode.

The above-mentioned research papers present 4,4'-bis(triethoxysilyl)-1,1'-biphenyl in various forms including nanoparticles used as drug delivery systems for doxorubicin [191], composites showing fluorescence due to the existence of biphenyl chromophores in the stable organosilica framework [192], thin films exhibiting very smooth surface without cracks and excellent mechanical behavior determined for applications as acoustic wave sensors and biosensors, [193], or mesoporous nanofibers and/ or nanotubes (**Figure 35**) prepared with a help of chiral low molecular weight gelators (LMWGs) [98], which are sensitive to pH value, temperature, and polarity of solvents. The optical activity of these fibers is attributed to the π–

π stacking and the chiral conformation of present aromatic groups, thus they can potentially be used as a chiral stationary phase for enantioseparation [98]. However, the preparation of such types of nanofibers based on the 4,4'-bis(triethoxysilyl)-1,1'-biphenyl by sol-gel process together with electrospinning technique has not been described yet.

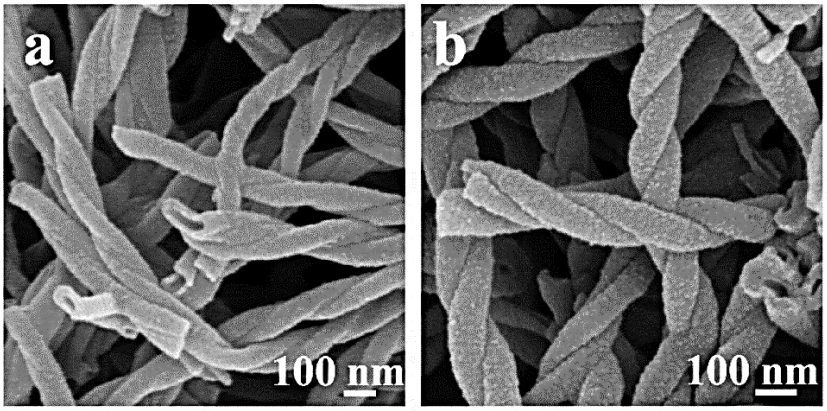

Figure 35. FESEM images of (**a,b**) showing formation of 4,4′-biphenylene bridged polybissilsesquioxane nanotubes via self-assembly [98].

7.1.1 Characterization and performance of these (nano)fibers

The fibers were prepared according to the above-mentioned general sol-gel principles. The detailed description is now legally patented and thus confidential. However, the parameters that can be stated with respect to the filed patent application are closely specified in the following chapters but are not given in detail with respect to the filed patent and its possible future licensing.

When combining 4,4'-bis(triethoxysilyl)-1,1'-biphenyl (BTEBP) and TEOS, these precursors may be homogeneously mixed at room temperature in any molar ratio as required in the range of hybrid precursor : alkoxide 100 mol.% : 0 mol.% with a polar alcohol-based solvent. Molar ratio *Alc*, i.e., the molar ratio of the polar alcohol-based solvent to the mixture of the organo-bis-silylated precursor : alkoxide precursor can be used up to 90.

It should be noted that when the sol contains more than 70 mol.% of suitable organo-bis-silylated precursor and above, and unexpected abrupt changes occur in the physical and chemical properties of these fibers, especially their electrical conductivity, optical activity, or biocompatibility. This phenomenon may be attributed to the reduced effect of the inorganic component (TEOS).

Distilled or demineralized water is required for the subsequent hydrolysis of the silane mixture. The molar ratio ***k***, i.e., the molar ratio of water to the mixture of hybrid precursor and

alkoxide, may be used up to a value of 2.4. At least one strong inorganic mineral acid, has to be added to the mixture. The addition of acid is small in volume and its purpose is to acidify the mixture to a suitable pH.

After mixing and homogenization, the mixture is heated to a reflux, which depends on the precursors and alcohol used, and the sol remains heated for a determined period of time. This promotes and accelerates the transformation reactions already initiated by the addition of acid to the mixture.

The appropriate values of electrospinnable sols prepared using 4,4'-bis(triethoxysilyl)-1,1'-biphenyl with/without the addition of TEOS are shown in **Table 4**.

Table 4. Values of electrospinnable sols prepared from BTEBP and TEOS in various molar ratios.

Molar ratio BTEBP : TEOS (mol.%)	**25 : 75**	**50 : 50**	**75 : 25**	**100 : 0**
BTEBP : TEOS (vol. %)	45 : 55	71 : 29	85 : 15	100 : 0
BTEBP : TEOS (wt. %)	48 : 52	73 : 27	86 : 14	100 : 0

Polycondensation time, mixing and temperature of the sol

These values were experimentally determined to be optimal for the formation of the desired sol structure described above. The qualitative evaluation of polycondensation was checked by FTIR analysis (**Figure 36** in the **Chapter 7.1.3**). The suitable (poly)condensation time is obtained when no significant changes in the siloxane network occur in the set time interval.

In general, the (poly)condensation is responsible for the formation of siloxane bridges (Si–O–Si) by removing a water or alcohol molecule from two alkoxysilane molecules. Its kinetics are more complicated, and it many has individual reaction rates, including the formation of silsesquioxanes $(RSiO_{1.5})_n$. The kinetics of (poly)condensation mainly depend on factors such as water/Si ratio (***r***), catalyst, nature of the silane, the temperature, pH, solvent, ionic strength (IS), and silane/solvent ratio [50].

Mixing and temperature are another two important factors influencing the suitable sol formation. Mixing is closely related to the Brown motion of the molecules and their collisions during the formation of the sols. In the beginning, when the precursors are mixed with the solvent, it is enough to use slow mixing, but after the addition of water and acid catalyst, when the hydrolysis starts, the rotations should be increased due to the better access of H^+ protons to the ethoxy ($–OCH_2–CH_3$) functional groups. The temperature depends on the properties and thermal stability of the precursors used as well as on the solvent.

Sol concentration

It is important to stop the growth of the organosilane matrix at the appropriate time and to process the sol rapidly before the structure grows further in the 3D network or the sol enters the gel phase. At the same time, from the point of view of spinning techniques, it is necessary to bring the sol to a state of suitable viscosity or surface tension so that it may be entrained by electric forces during electrostatic spinning. However, in the case of thickening of the sol by freezing or prolonging the polycondensation time with/without access to air, the organosilane structure increases (compacts) further and becomes non-fibrous. Therefore, the addition of various surfactants, low molecular weight additives or viscous polymers, which adjust the viscosity or surface tension of the spinning liquid, is often used for electrospinning. However, a disadvantage is that these components remain in the resulting structure and alter the resulting properties. For these reasons, the viscosity of sols has to be properly adjusted and measured after the set time of polycondensation.

The final electrospinnable sol

The final concentrated sol consists of the linear, low-branched macromolecular organosilane matrix described above, which, despite the concentration, is filled with polar solvent molecules based on alcohol, water, and inorganic mineral acid, which evaporate during the subsequent electrospinning process.

7.1.2 Characterization of the spinnable sols as evaluated by FTIR spectroscopy

The sols containing the above-mentioned molar ratios (**Table 4**) were further characterized by Fourier transform infrared spectroscopy (**Figure 36**). This confirmed that the sols have the same chemical structure with the typical structural units corresponding to the composition of the organosilane matrix containing conjugated aromatic nuclei. This is very evident in the area known as the “fingerprint region”, i.e., the area of characteristic single bonds, in which no two molecules have exactly the same spectrum. In the case of organosilane materials, the areas of 950 to 1000 cm^{-1} and 1050 to 1100 cm^{-1}, which correspond to the characteristic vibrations of silanol (Si–OH) and siloxane (Si–O–Si) structural units of the organosilane matrix are carefully studied as well as the organic part of the hybrid organosilane structure visible in the area of characteristic vibrations of aromatic nuclei, i.e. 1400 to 1600 cm^{-1} (a series of valence vibrations of C=C and C–H structural units). These examples differ only in the signal intensity corresponding to the amount of the given component in the analyzed sols.

The most intensive band, at about 1100 cm^{-1}, is related to asymmetric stretching vibrations of the Si–O–Si bridges. In the case of hybrid structures, this band becomes clearly split into two separate bands at about 1050 and 1100 cm^{-1}. Vibrations of the silicon–oxygen (O–Si–O) bridges are also responsible for the bands at about 800 cm^{-1} (symmetric stretching vibrations, bending vibrations) and also bending vibrations visible at about 450 cm^{-1}. A band related to vibrations of the Si–OH groups is observed at about 950 cm^{-1} – 1000 cm^{-1}. Bands contributing to the vibrations of the organic groups are usually very sharp and are situated in the ranges of 1400 – 3070 and 540 – 740 cm^{-1}. These bands are usually connected to vibrations of C–H, Si–C bonds as well as ring structures [194]. Additionally in the spectra, the peaks appearing at 1600 cm^{-1} are assigned to the in-plane stretching vibrations of phenyl groups C=C bonds, and a peak attributed to the value of 1450 cm^{-1} confirms the presence of the Si–C covalent bond [195]. Moreover, the molecularly adsorbed water may be seen in the range of 3100 $^{-1}$ – 3600 cm^{-1} together with the silanol groups Si–OH, among which terminal silanol groups may also be identified, particularly in the region of 3600 $^{-1}$ – 3700 cm^{-1} [194][195].

The FTIR spectra confirm that both organic and inorganic structural units are present and interconnected in the prepared sols. The siloxane matrix is evidently well built as the successful creation of the polysiloxane matrix is demonstrated by the increase in the intensity of the absorption peaks assigned to the siloxane groups at the expense of the absorption peaks of the silanol groups. The strongest increment may be found at 1050 cm^{-1} belonging to the bridging TO phonon mode of Si–O–Si antisymmetric stretching, together with a distinct shoulder on the side of the higher wavenumber points belonging to the LO mode of Si–O–Si antisymmetric stretching. These are very important for the qualification of polysiloxane densification processes as they refer to the disorder-induced modes to be found in more porous and humid gels [196]. These observations support the above-mentioned idea that a spinnable linear structure was created dominated by incompletely condensed silica species. Likewise, the FTIR spectra indirectly prove that no Si–C cleavage occurred, and the volume and nature of the organic part remained the same throughout the whole sol-gel processing.

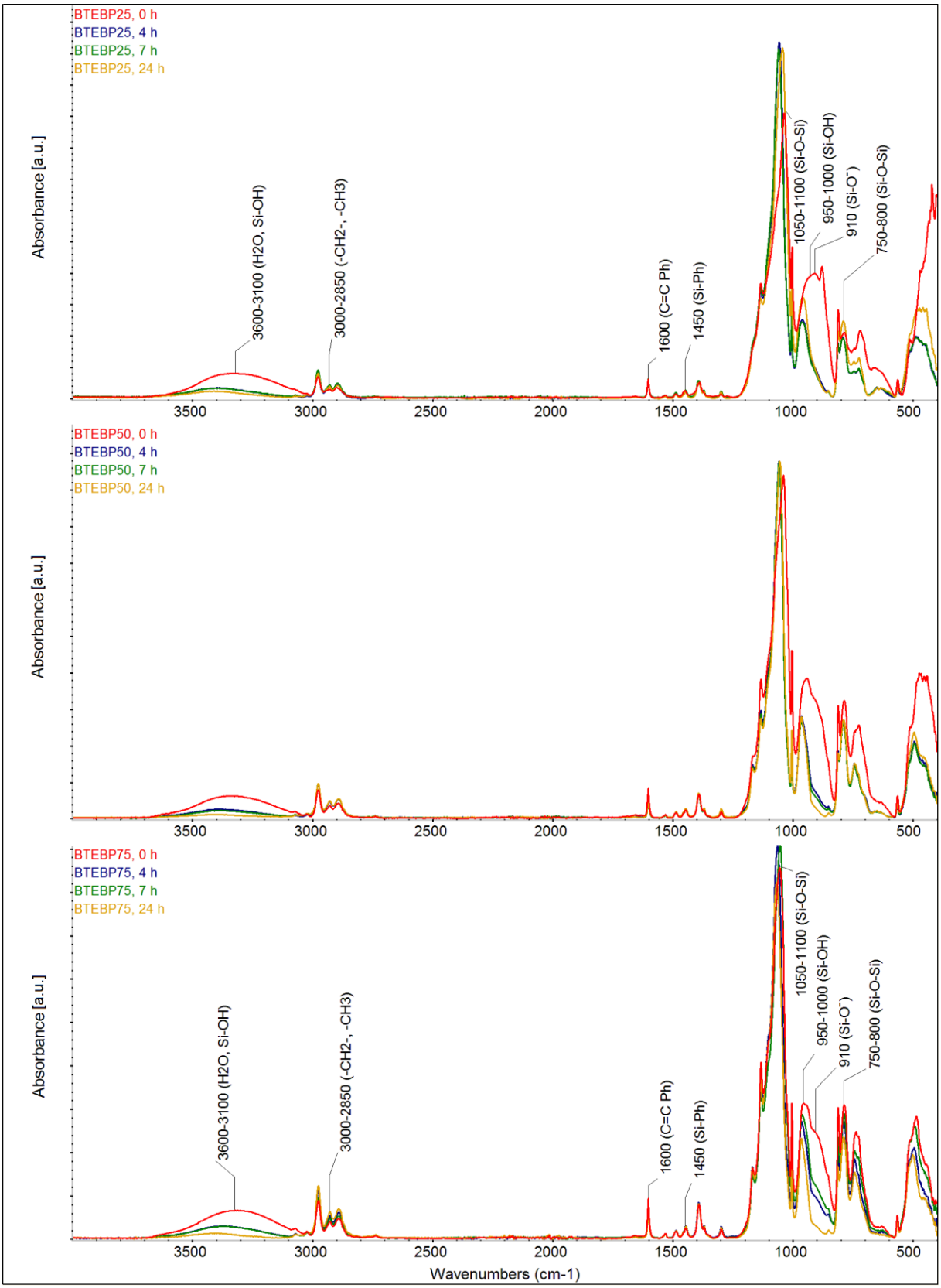

Figure 36. FTIR spectra describing the kinetics of the sols containing BTEBP in different molar ratios, which were specified as suitable for the formation of fibers after the established time interval.

7.1.3 Fiber formation via the electrospinning technique

To spin the sol prepared in this way, it is possible to use electrospinning technology from a hollow needle with a constant supply of sol, electrospinning technology from the front of the rod, or the so-called needleless electrospinning technology, which uses a spinning electrode consisting of a moving body (e.g., cylinder CZ 274294), or a static or moving string (e.g., according to CZ 300345), which is applied, for example, in the Nanospider technology of Elmarco and enables the preparation of submicron fibers and microfibers on an industrial scale. The prepared organosilane (nano)fibers have diameters in the range of 140 to 5100 nm, depending on the composition of the sol, the conditions, and the spinning technology.

Preferably, the fibers prepared by electrospinning are further thermally stabilized, depending on the type of alkoxide precursor(s) used and the molar ratio of bridged organosilane precursor(s) and alkoxide precursor(s).

Suitable parameters supporting the formation of the fibers based on 4,4'-bis(triethoxysilyl)-1,1'-biphenyl in the above-mentioned molar ratios with/without TEOS are described in **Table 5** below.

Table 5. An overview of the parameters suitable for BTEBP fiber formation.

Parameters	**Conditions for electrospinning**
BTEBP : TEOS 25 : 75 mol.%	
Viscosity (mPa.s)	>29
High voltage (kV)	<30
Distance between needle and collector (cm)	<25
Polymer extrusion rate (ml/h)	>2
BTEBP : TEOS 50 : 50 mol.%	
Viscosity (mPa.s)	>29
High voltage (kV)	<25
Distance between needle and collector (cm)	<25
Polymer extrusion rate (ml/h)	>2
BTEBP : TEOS 75 : 25 mol.%	
Viscosity (mPa.s)	>29
High voltage (kV)	<25
Distance between stick and collector (cm)	<25
Polymer extrusion rate (ml/h)	<5
BTEBP : TEOS 100 : 0 mol.%	
Viscosity (mPa.s)	>29
High voltage (kV)	suitable
Nanospider NS 1W500U (Elmarco s.r.o.)	string diameter 0.2 mm
Distance between electrodes (cm)	<20
Polymer extrusion rate (ml/h)	<10

7.2 Characterization of the prepared BTEBP (nano)fibers

All of the prepared (nano)fibers were characterized via the various different techniques mentioned below, with the aim to determine their properties. The (nanofibers) based on BTEBP : TEOS with the following molar ratio of BTEBP in the sol mixture (25 mol.%; 50 mol.% and 75 mol.%) are mainly presented in this part of the thesis.

7.2.1 Solid-state NMR analysis of the prepared fibers

Solid-state ^{29}Si and ^{13}C NMR spectra of different fibrous samples obtained by reaction of 4,4'-bis(triethoxysilyl)-1,1'-biphenyl (BTEBP) and tetraethoxysilane (TEOS) were recorded and the formation of siloxane network was confirmed (**Figure 37**). The complex of the hybrid structure contains various siloxane units such as T^n and Q^n units [9,194,197], which were confirmed by ^{29}Si ssNMR experiments (additional results are shown in the supplement, **Figures S1** and **S2**). The ^{29}Si CP/MAS NMR spectra indicated the presence of T^1 (-65 ppm), T^2 (-72 ppm), T^3 (-79 ppm), Q^1 (-89 ppm), Q^2 (-95 ppm), and Q^3 (-102 ppm) structural units in all of the fibrous samples. A sample of 25 mol.% BTEBP also contained Q^4 (-109 ppm) moieties. The molar content of each unit in the samples and the condensation degree were calculated based on the integral intensity of the respective signals, and the results are listed in **Table 6.**

The ^{13}C MAS NMR spectra of all of the investigated systems confirmed the presence of aromatic carbons of BTEBP. Moreover, signals around 59 ppm (–OCH_2– groups) and 18 pmm (–CH_3 groups) were detected in the spectra. These signals revealed the presence of residual ethoxy groups (**Figure 37-** right column). The relative molar percentages of non-reacted ethoxy groups for each sample are summarized in **Table 7** as an average value of $I(–CH_3)_{exp}/I(–CH_3)_{Theor}$ and $I(–OCH_2–)_{expt}/I(–OCH_2–)_{Theor}$ ratios, where $I(–CH_3)_{exp}$ and $I(–OCH_2-)_{expt}$ are derived as the integral intensity from the experimental ^{13}C MAS NMR spectra of the corresponding signals, and $I(-CH_3)_{Theor}$, $I(–OCH_2–)_{Theor}$ are theoretical integral intensities in a non-reacted mixture. The different molar ratios of the components in the individual samples were considered.

From the obtained results (**Tables 6** and **7**) it follows that an increase in the content of BTEBP in the initial mixture leads to an increase in the amount of T^n units in the final product. In particular, an increase in the content of T^1 and $Q^{2,3}$ units was observed, which indicates the formation of a less branched siloxane network. This is consistent with decreases in the amount of condensation, which was also confirmed by ^{13}C MAS NMR spectra where an increase in the amount of unreacted ethoxy groups was detected.

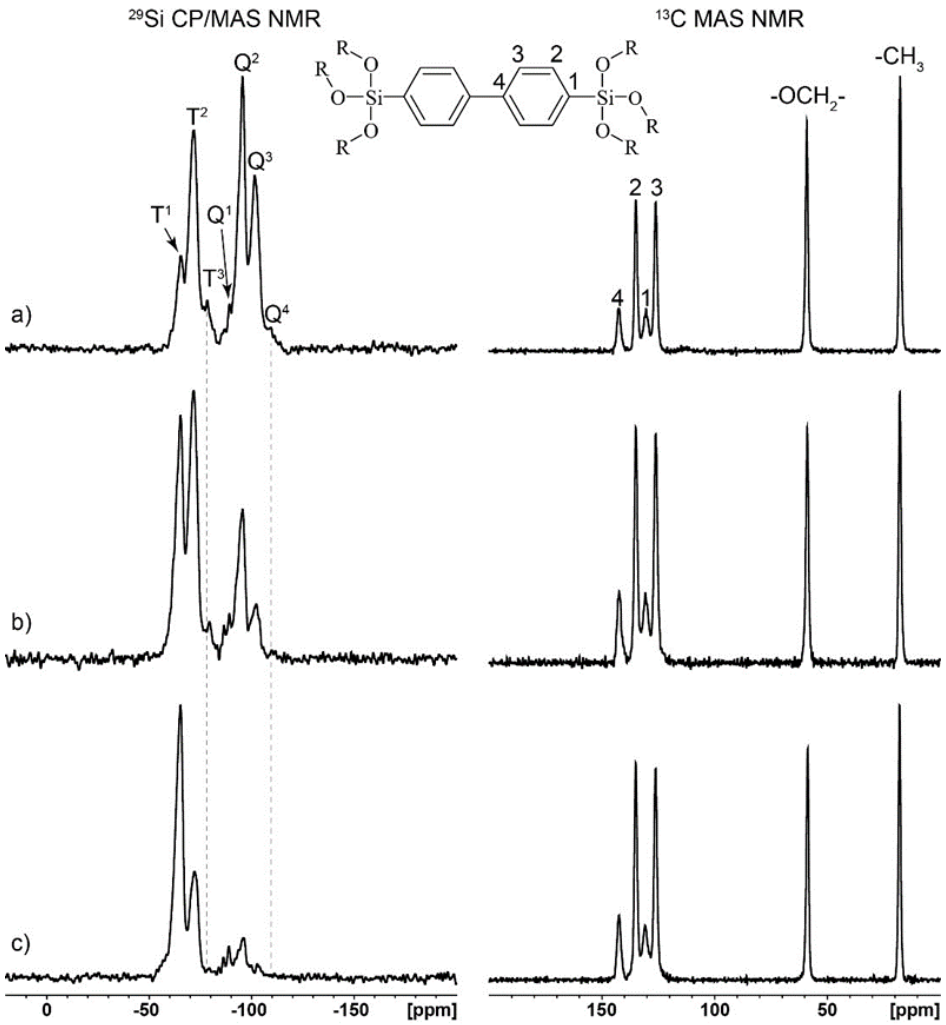

Figure 37. ssNMR spectra of the fibers: **a)** variant with a molar ratio of BTEBP:TEOS 25 mol.%:75 mol.%; **b)** variant with a molar ratio of BTEBP:TEOS 50 mol.%:50 mol.%; **c)** variant with a molar ratio of BTEBP:TEOS in the sol of 75 mol.%:25 mol.%.

Table 6. The molar percentages of siloxane units determined from ^{29}Si CP/MAS NMR, the ratios between total amounts of T^n and Q^n structure units, and the calculated condensation degrees q_i

Sample	Molar content of silicon units, %							Ratio	q_i^*
	T^1	T^2	T^3	Q^1	Q^2	Q^3	Q^4	$\sum T^n$:Q^n	
BTEBP : TEOS 25	10.2	29.5	4.4	3.5	29.1	21.2	2.1	44.1:55.9	0.609
BTEBP : TEOS 50	31.4	35.3	3.7	5.1	17.9	6.6	-	70.4:29.6	0.529
BTEBP : TEOS 75	62.5	19.9	1.3	5.5	7.9	2.9	-	83.7:16.3	0.429

*Condensation degree was calculated using the formula [198,199]: $q_i = \sum_{n=1}^{3}\left(\frac{nT^n}{3}\right) + \sum_{n=1}^{4}\left(\frac{nQ^n}{4}\right)$, where T^n and Q^n is a molar fraction of T^n and Q^n units, respectively; n is a number of bridged Oxygen atoms attached to the unit.

An interesting result may be seen in **Table 6**, in the column regarding the ratio of T^n and Q^n units. More organosilane units remain in the fibers than in the initial sol. This may be attributed to TEOS, which is probably not built into the hybrid matrix and, therefore, it is not further built into the fibers during the electrospinning process. We assume that unreacted TEOS, which has a boiling point of 168 °C, may evaporate during the reflux or spinning process. Therefore, resulting fibers are predominantly hybrid. We are currently intensively working to clarify this theory.

Table 7. The relative amount of non-reacted ethoxy groups (relative to the initial mixture) determined from ^{13}C MAS NMR spectra.

Sample	Relative amount of non-reacted ethoxy groups, %
BTEBP : TEOS 25	31.4
BTEBP : TEOS 50	35.0
BTEBP : TEOS 75	48.1

7.2.2 Thermal stability of the prepared hybrid fibers determined by the TGA method

The thermal stability test of the submicron fibers produced from the 25 mol.% sol mixture of BTEBP in the temperature range of 20 to 650 °C was performed by thermogravimetric measurement (TGA) (**Figure 38**), which shows the TGA spectrum of their thermal decomposition. During the TGA analysis, the gaseous products formed during the heating and thermal decomposition of these fibers were analyzed simultaneously by infrared spectroscopy (FTIR).

Moreover, three weight losses were recorded during the analysis: two smaller ones with a size of 0.06 wt.% and 6.26 wt.% in the temperature range of 20 to 350 °C, which corresponds to the evaporation of water and the evaporation or dissociation of residual ethanol and residual ethoxy groups from the imperfectly polycondensed organosilane matrix; a larger one of 28.38 wt.%, which was recorded in the temperature range of 350 to 650 °C with a maximum at 531.92 °C. This decrease was attributed based on the FTIR analysis to the decomposition of the organic component of the organosilane matrix. From these results it is clear that the prepared organosilane fibers show thermal stability up to temperatures of around 350 to 400 °C.

During the TGA-FTIR analysis, the fibers from the 50 mol.% sol mixture of BTEBP showed a more significant weight loss of 30.9 wt.% in the temperature range of 350 to 650 °C with a maximum at a temperature of 518.27 °C (**Figure 39**), which confirms the thermal stability of the submicron organosilane fibers up to a temperature of around 400 °C.

The fibers from 75 mol.% sol mixture of BTEBP showed similar values during the TGA-FTIR analysis (**Figure 40**). Three weight losses were recorded: two smaller, 0.05 wt.% and 7.03 wt. %, in the temperature range of 50 to 260 °C, which correspond to the evaporation of water and the evaporation or dissociation of residual ethanol and residual ethoxy groups from the imperfectly polycondensed organosilane matrix; and a greater weight loss of 31.66 wt.% recorded in the temperature range 375 to 650 °C, with a maximum at 526.74 °C. This decrease was attributed to the decomposition of the organic component of the organosilane matrix based on the FTIR analysis. From these results, it is clear that the prepared organosilane fibers show thermal stability up to a temperature of around 400 °C.

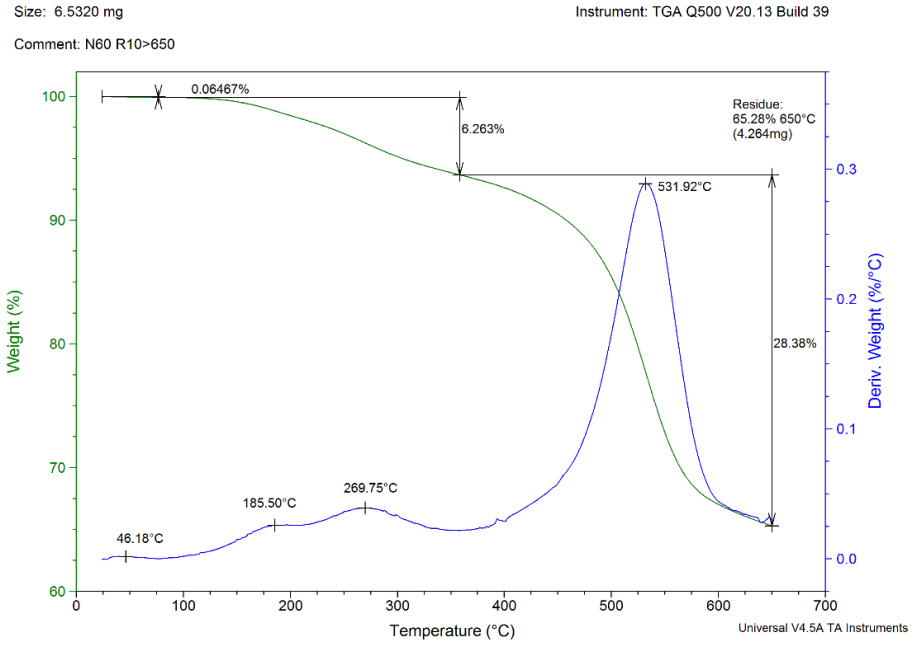

Figure 38. TGA spectrum of the thermal decomposition of the organosilane fibers containing BTEBP (25 mol.%) in the hybrid network. The temperature range moves between 25 and 650 °C.

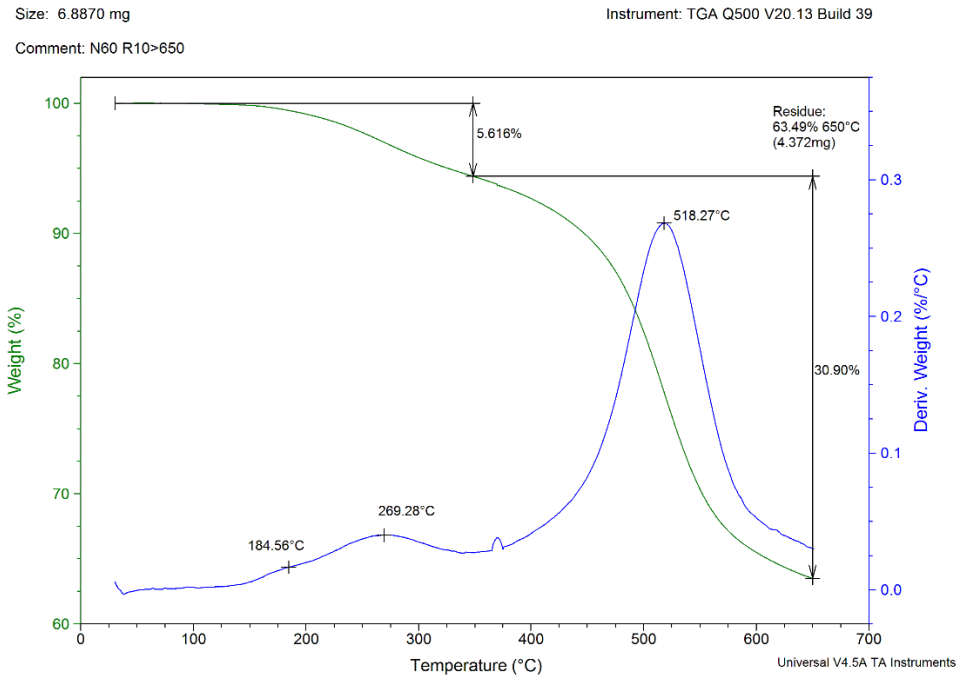

Figure 39. TGA spectrum of the thermal decomposition of the organosilane fibers containing BTEBP (50 mol.%) in the hybrid network. The temperature range moves between 25 and 650 °C.

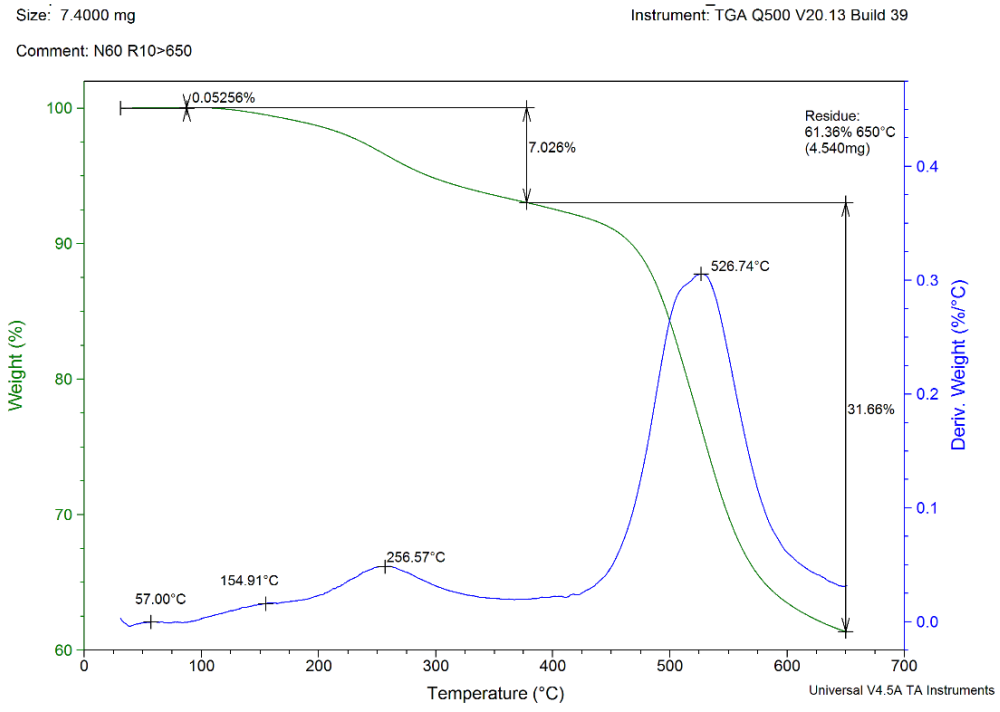

Figure 40. TGA spectrum of the thermal decomposition of the organosilane fibers containing BTEBP (75 mol.%) in the hybrid network. The temperature range moves between 25 and 650 °C.

7.2.3 Morphology of the fibers determined by scanning electron microscopy

The organosilane fibers made of combination BTEBP and TEOS in various molar ratios were examined using scanning electron microscopy, their overall morphology, and the average size of the organosilane fibers were determined. According to the obtained results (**Figure 41**), morphologically compact and homogeneous fibers were obtained using both electrospinning techniques (jet needle-electrospinning, and/or Nanospider). The fibers were oval in cross-section, i.e., flattened, probably due to the presence of bulky bridged organosilane, which has a tendency to form a linear ladder-like structure.

The prepared organosilane fibers were quite long and were continuously deposited onto the collector depending on several of the parameters regarding the electrospinning process. The diameters of the fibers may be seen in **Figure 42**, and their average size ranges from hundreds of nanometers to units of micrometers. Even though they are quite thin, they do not have a tendency to crack during manipulation. As may be seen in **Figure 41**, very similar organosilane fibrous structures were obtained although different molar ratios of the precursors were used in the sols and various electrospinning conditions were tested.

Figure 42 depicts fibrous sample BTEBP50 were bead inhomogeneities are distributed on the surface of the fibers. These structural defects are most probably related to the sol viscosity, due to which the network size exceeded the electrostatic force needed to create the jet. As is mentioned in the literature [200], the optimal viscosity and sol network, where linear chains of macromolecules predominate, support the production of smooth and continuous fibers, as may be seen in samples BTEBP25 and BTEBP75 in **Figure 42**. Fibrous samples having a greater thickness/diameter (**Table 8**) presumably contain hyper-branched or a larger network of organosilanes. These samples are electrospun with a greater viscosity due to the use of the more sterically bulky organo-bis-silylated precursor. The calculated fiber diameters are shown in **Table 8**. It is generally stated that the values of the average diameter decrease as the high voltage (HV) increases [59,200]. However, this phenomenon also brings an increase in the diameter distribution of the fibers [59,200]. The measured thicknesses of the prepared fibrous layers are also included in **Figure 43**.

Table 8. Calculated fiber diameters for the different molar ratios of BTEBP:TEOS present in the hybrid matrix.

Sample	Fiber diameter range interval (nm)	Fiber mean value (nm)	Fibrous layer thickness (µm)
BTEBP:TEOS 25	400 - 1300	812	88.91
BTEBP:TEOS 50	580 - 1510	952	21.12
BTEBP:TEOS 75	580 - 2100	1040	21.96
BTEBP:TEOS 100	658 - 5100	2040	16.87

To conclude this part, it may be said that various different structural morphologies of fibers (homogeneity, inhomogeneity, average diameter, and their distributions) may be reached independently of the type and amount of the organosilane precursor used in the initial mixture. The important parameters are mainly the degree of polycondensation together with the viscosity of the polymer solution related to the sol-gel processing parameter, which is followed by the suitable conditions of the electrospinning process. If the above-mentioned parameters are observed and controlled, it is possible to produce different organosilane fibers, tailored according to the specific application.

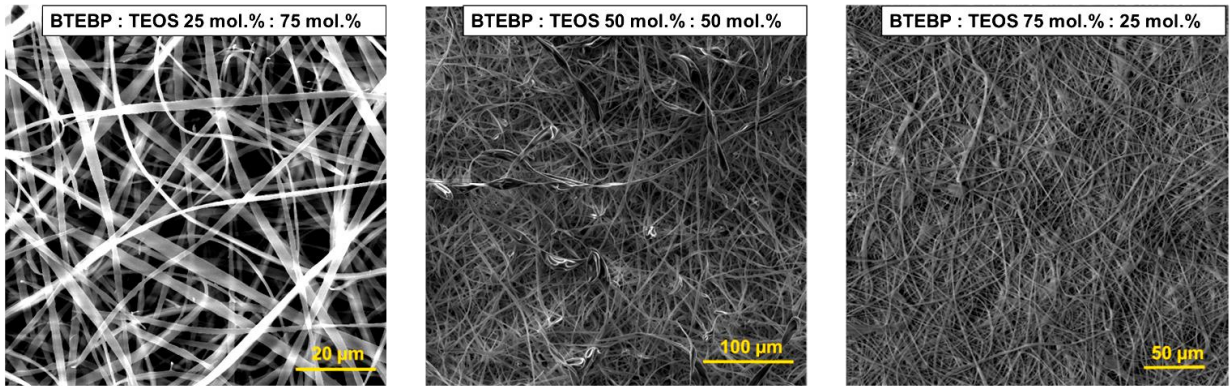

Figure 41. SEM images of the prepared BTEBP fibers at different molar ratios.

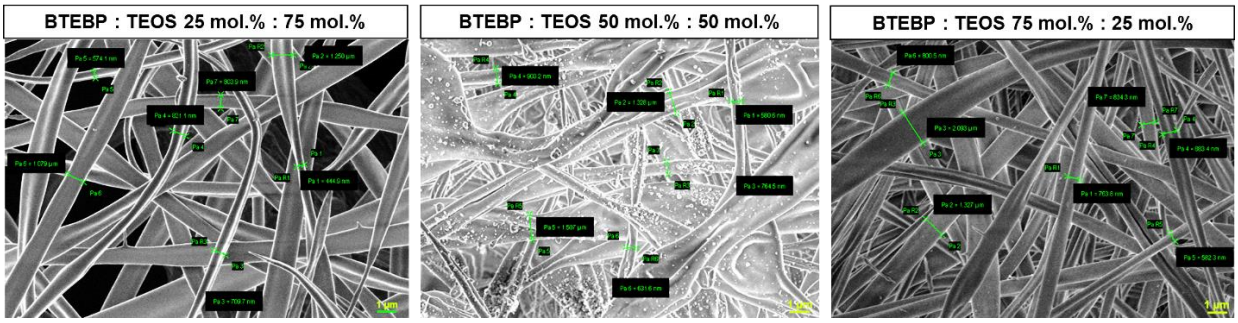

Figure 42. SEM images showing the diameters of the prepared hybrid organosilane BTEBP fibers.

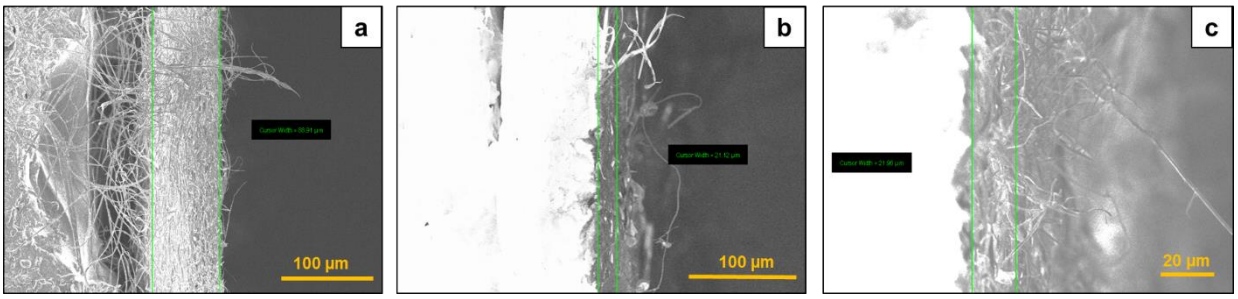

Figure 43. SEM images showing the layer thickness (µm) of the prepared hybrid organosilane BTEBP fibers at various molar ratios (BTEBP 25 mol.% **a)**; BTEBP 50 mol.% **b)**; BTEBP 75 mol.% **c)**.

7.2.4 Conductivity of the prepared BTEBP fibers

The electrical conductivity of fibers made of organo-bis-silylated precursors based on 4,4'-bis(triethoxysilyl)-1,1'-biphenyl and/ or 1,4-bis(triethoxysilyl)benzene and starting at a 25 mol.% content in a hybrid silica sol mixture exceeds the semiconductor limit – i.e., 10^{-10} S/cm (**Figure 44**), which significantly increases their application possibilities. In general, when the precursors containing aromatic functional groups or conjugated multiple bonds are used (see **Figure S3**, **Chapter 11.4** in the supplements), then the new localized levels are formed in the "forbidden band" of the electronic structure, reducing the energy gap of the electron moving from the valence to the conduction band.

Using these new levels, the electron then travels from the valence band to the conduction band with the insertion of lower energy, which results in a further increase in conductivity, up to the band of semiconductors or conductors (1st order). With a higher proportion of such organosilanes at a content of above 70 mol.%, the influence of the predominant inorganic siloxane network is significantly suppressed in favor of the conductive effect of organic molecules [45].

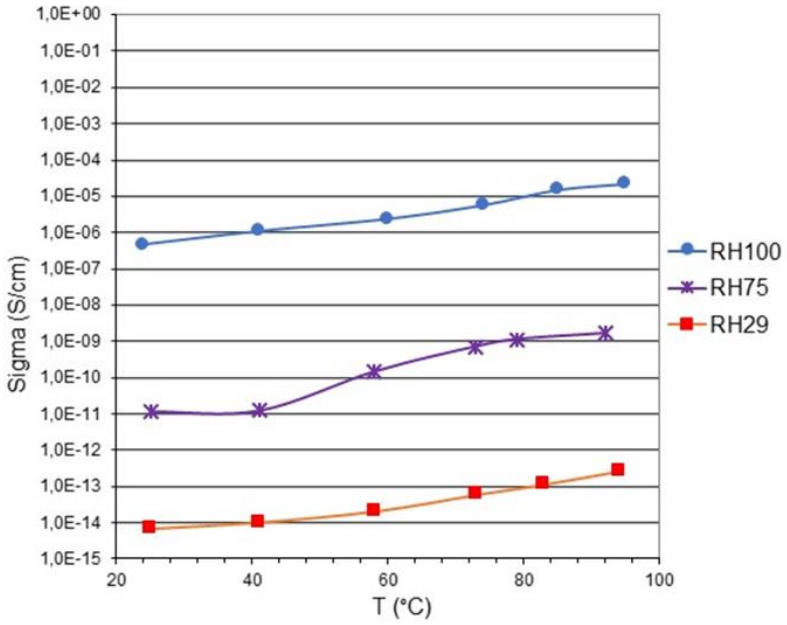

Figure 44. Dependence of the specific electrical conductivity on the temperature and relative humidity (RH = 29; 75 and 100) of the environment of hybrid pure organosilane fibers with a BTEBP:TEOS molar ratio of 25 mol.%:75 mol.%.

7.3 The latest results of ongoing research

Based on the previous experiments demonstrated in this thesis as well as in the articles included in the supplementary part (**Chapter 11.5**), structures were and are further designed with regard to the planned applications into the fields of medicine, optoelectronics and energetic devices. From this point of view, the following organo-bis-silylated precursors have been proposed as suitable candidates with respect to fulfilling the set aims.

Table 9. Synthesized organo-bis-silylated precursors planned to be used for the formation of fibers.

Names of the proposed organo-bis-silylated precursors	**Molecular structure**
N,N'-bis(3-(triethoxysilyl)propyl)oxamide (**OBA** precursor) [201]	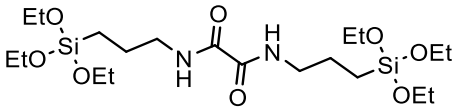

1,4-bis(3-(triethoxysilyl)propylamide)benzene (**BiTSAB** precursor)	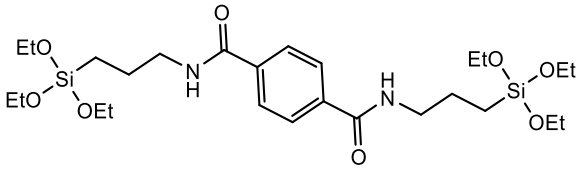
bis(3-(triethoxysilyl)propyl)pyridine-2,6-dicarboxamide (**BTEPDA** precursor) [16]	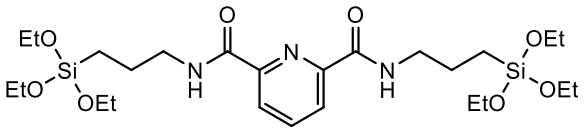

7.3.1 Syntheses of the proposed organo-bis-silylated precursors

OBA precursor

The whole procedure was undertaken under argon: Into 100 mL anhydrous dichloromethane (DCM), 60.0 mmoles of triethylamine (TEA) and 40.0 mmoles of TEA were added, followed by cooling to 0 (±5) °C. The Reaction flask was continuously stirred at 350 rpm. Subsequently, into 20 mL of anhydrous DCM, 20.1 mmoles of oxalyl chloride were added and mixed very slowly. After that, the diluted oxalyl chloride was added drop-wise into the reaction flask and the reaction was stirred at 350 rpm/ 3 h. Then the reaction was diluted with 30 mL of DCM and 300 mL of distilled water was added, followed by vigorous mixing and separation of phases. The organic phase (with precursor) was mixed with Na_2SO_4/ 2 h, followed by filtering, with the filtrate put on Roto-Vap. The sample thus obtained was then mixed with toluene, following by filtering through a syringe filter, and the filtrate was placed on Roto-Vap. Finally, the product was 2x more re-dissolved in toluene and evaporated on Roto-Vap with conditions (~2 h/ 0 mbar). The final product is of yellowish semi-viscous liquid. The yield is 61.2 % [201].

BiTSAB precursor

This type of organo-bis-silylated precursor has been designed according to the author´s proposal based on the following literature [201,202] where similar structures may be found. The following procedure was undertaken under argon: Into 50 mL anhydrous toluene, 10.02 mmoles terephthaloyl chloride was added (not completely soluble), followed by cooling to 0 (±5) °C. The reaction flask was continuously stirred at 350 rpm, then 45 mmoles of TEA was added into the reaction flask together with 19.5 mmoles of APTES. The reaction was left to react for 2 h/ 400 rpm. After this time, 200 mL of water was added, followed by vigorous mixing and separation of phases. The product was washed 2x more times with water and the organic phase (with precursor) was mixed with Na_2SO_4, for 2 h, followed by filtering, with the filtrate

put on Roto-Vap to remove solvents. The sample thus obtained was then mixed with toluene, following by filtering through a syringe filter, and filtrate placed on Roto-Vap again. After that, the sample was 2x more re-dissolved in toluene and evaporated on Roto-Vap (~2 h/ 0 mbar). The final product is of yellow-orange solid at RT. The yield is 81.8 % [16,201].

BTEPDA precursor

The following compounds sodium ethoxide (0.1 mmol), diethyl pyridine-2,6-dicarboxylate (10 mmol), and 3-(triethoxysilyl)propyl amine (20.5 mmol,) were mixed together and subsequently were heated in a sealed tube at 170 °C under stirring in argon atmosphere for 5 h. After cooling down to RT, chloroform was poured into the reaction tube to extract the reaction product. Subsequently, the suspension was filtered and the solvent was removed under vacuum on the Roto-Vap (~2 h/ 0 mbar)), obtaining pure bis(3-(triethoxysilyl)propyl)pyridine-2,6-dicarboxamide as a white solid in 92% yield [16].

7.3.2 Characterization of the two synthesized precursors

All of the above-prepared precursors were characterized with the aim of confirming their purity, before the preparation of the sols. The methods used were ^{1}H liquid-state NMR spectroscopy (**Figures 45, 46**) and the TGA method (**Figures 47, 48**) with the aim of stating the decomposition temperatures for the prepared precursors. These characterizations (^{1}H liquid-state NMR spectroscopy and TGA method) are known for the BTEPDA precursor [16], so in this respect they are not stated in this part of the thesis.

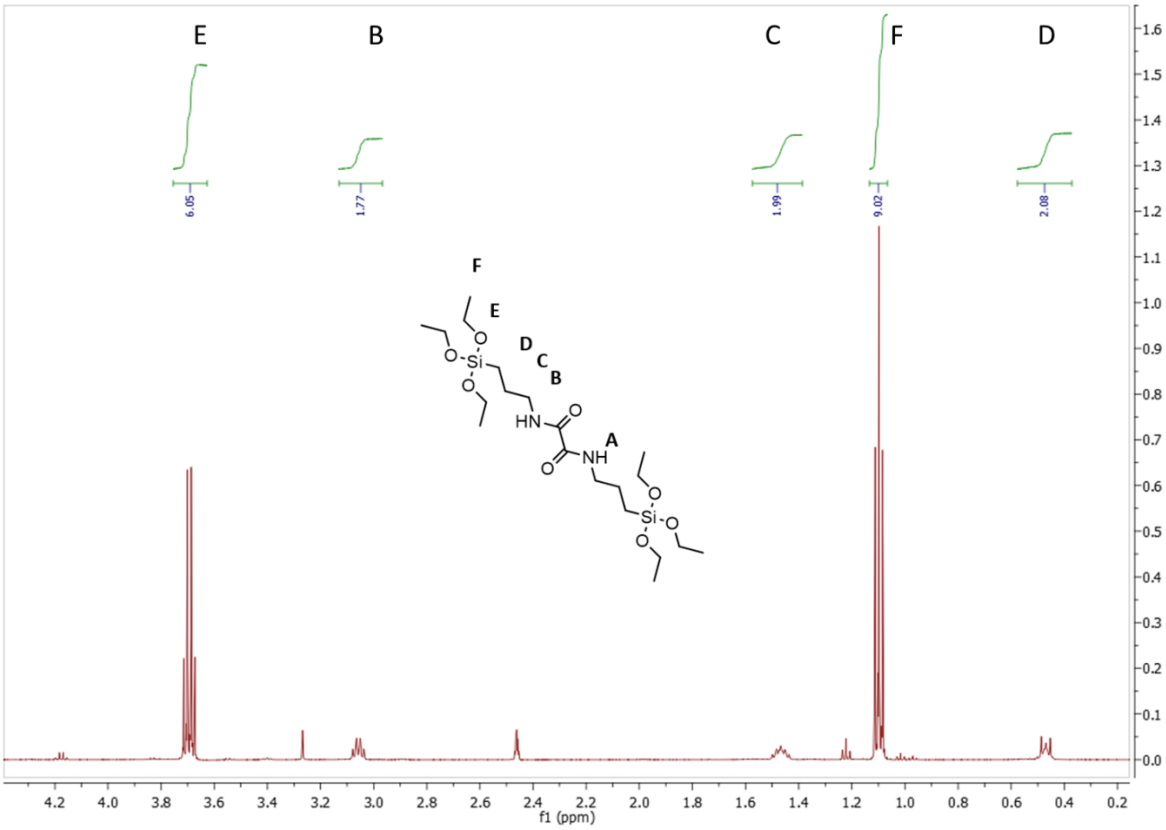

Figure 45. Spectrum of the ^{1}H liquid state NMR of the OBA precursor measured in DMSO-d_6.

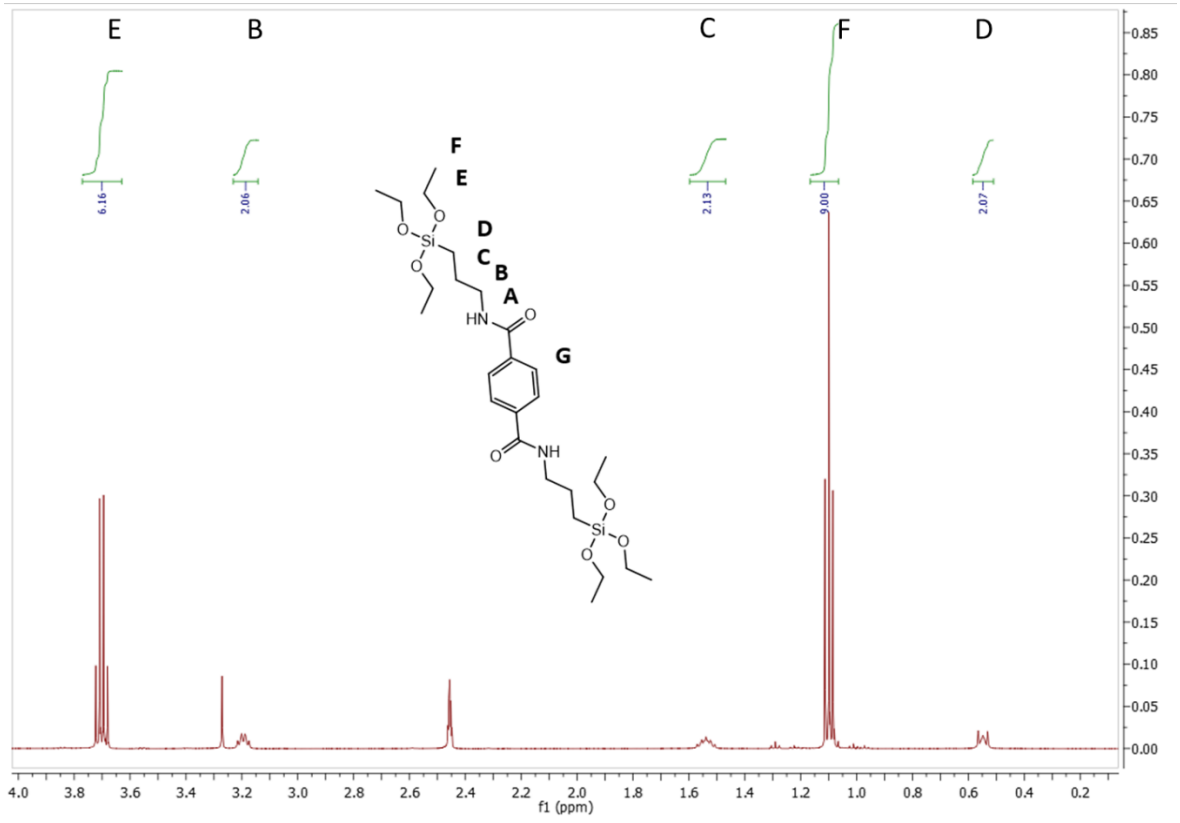

Figure 46. Spectrum of the ^{1}H liquid state NMR of the BiTSAB precursor measured in DMSO-d_6.

TGA results of OBA and BiTSAB precursors

A thermal stability test of the synthesized OBA and BiTSAB precursors in the temperature range of 20 to 800 °C was performed by thermogravimetric measurements (TGA), see **Figures 47 and 48** which show the TGA spectra of their thermal decomposition.

The TGA analysis performed in a nitrogen (N) atmosphere showed that the first leakage occurred at a temperature of 96 °C. This corresponds to the evaporation of water and the evaporation of residual solvents from the OBA precursor. A larger weight loss of 90.12 wt.% most probably assigned to the dissociation of the bond between the carbonyl groups, was then recorded in the temperature range of 100 to 375 °C, with a maximum at 288.48 °C. This decrease is attributed to the decomposition of the organic part present inside the organosilane molecule based on the FTIR analysis. The results indicate that the prepared OBA precursor is thermally stable up to temperatures of around 100 °C.

The second precursor, BiTSAB, showed the following results: during the TGA-IR measurement in a nitrogen (N) atmosphere, the first very low weight loss 1.37 % was visible at a temperature of 121.50 °C. This is primarily attributed to the leakage of the organic solvent residues used during the synthesis of the BiTSAB precursor. On the contrary, a more interesting and significant weight loss of 52.88 wt.% occurred in the temperature range of 250 to 390 °C, with a maximum at a temperature of 336.61 °C (**Figure 48**). The second weight loss of 79.45 wt.% occurred at the temperature range of between 450 and 550 °C, with a maximum at 449.37 °C. The first weight loss may be attributed to the decomposition of amide bonds present next to the aromatic nuclei. The second weight loss is more related to the decomposition of the aromatic ring itself.

This confirms that the thermal stability of the prepared BiTSAB precursor may be used in the sol-gel process up to a temperature of around 240 °C.

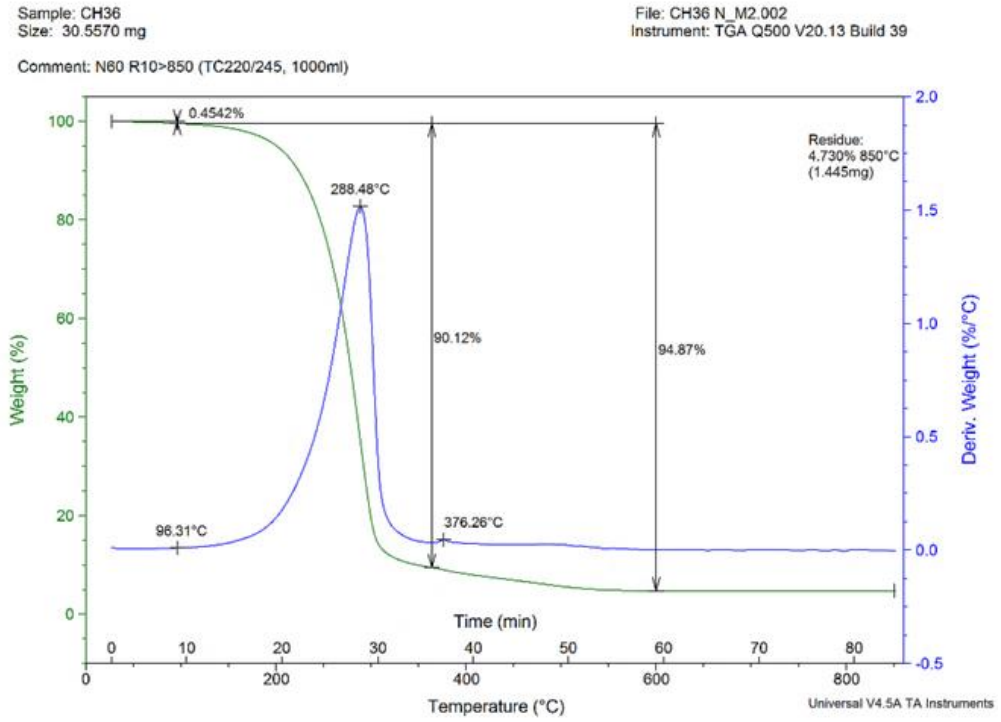

Figure 47. TGA spectrum determining the thermal stability of the OBA precursor in the range of 10 to 800 °C.

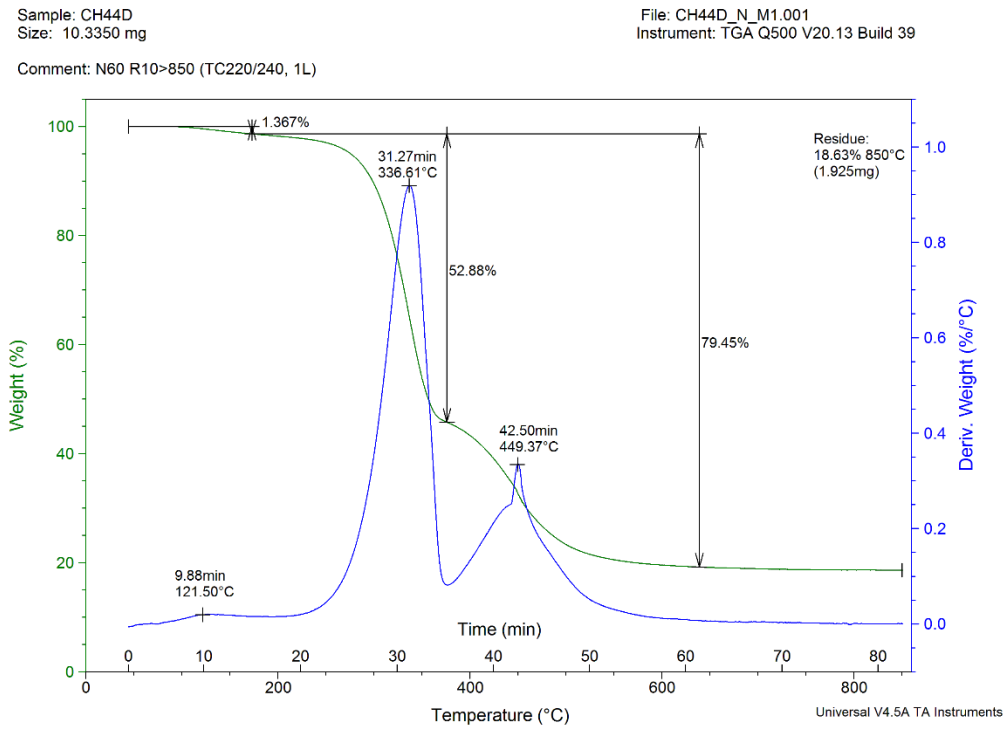

Figure 48. TGA measurement determining the thermal stability of the BiTSAB precursor in the range of 10 to 800 °C

7.3.3 Preparation of the sols OBA and BiTSAB

Certain synthetic steps and details were intentionally omitted from the text to maintain the confidentiality of the patented process.

The standard procedure for the synthesis of a spinnable organosilane sol solution was as follows: the precursors composed of TEOS : OBA and/or BiTSAB (in a molar ratio of 50:50), a suitable polar solvent, deionized water, and mineral acid were added into a Teflon bottle and stirred (**Table 10**). The pH of the sols was adjusted to an appropriate value. Finally, the solutions were heated for a suitable time and mixing speed, the dynamic viscosity was measured before the electrospinning process and appropriately adjusted. Hybrid fibers (marked as OBA and/or BiTSAB) were prepared via jet needle-electrospinning (**Table 10**) and finally dried in a desiccator for subsequent SEM analysis (**Figures 50-52**).

7.3.4 Characterization of both sols measured by FTIR spectroscopy

According to the FTIR spectroscopy evaluation (**Figure 49**), it was found a suitable degree of polycondensation and thus electrospinnable sols occurs after only 6 hours of the set sol-gel process. Between 6 and 24 hours, no significant changes appeared in the area of the polycondensation in either of the sols. The efficient incorporation of both types of organic moieties into the structure of the organo-bis-silylated precursors was confirmed by Fourier-transform infrared spectroscopy (FTIR), which is depicted in **Figure 49**. In this context, the presence of both the silica matrix and the organic moieties was confirmed.

According to the spectrum of the first precursor, BiTSAB (**Figure 49; upper spectrum**), the following bands confirming the stable BiTSAB structure present in the sol may be seen. Firstly, the characteristic vibrations of siloxane (Si–O–Si) structural units belonging to the organosilane matrix may be seen at 690, 750 – 800 ((symmetric stretching vibrations, bending vibrations) and 1050 to 1100 cm^{-1}, as well as silanol (Si–OH) structural units, which are visible at 950 to 1000 cm^{-1}. The most intensive band appears at around 1100 cm^{-1} and is connected with asymmetric stretching vibrations of the Si–O–Si units (known as “bridging oxygens”).

The organic part of the hybrid organosilane precursor (BiTSAB) is then visible in two main areas. One belongs to the characteristic vibrations of aromatic nuclei at 1445 to 1550 cm^{-1} and 3000 - 2800 cm^{-1} (a series of valence and deformation vibrations of C=C and C–H structural units). The second area is dedicated to the absorption sublet of amidic units (NH–CO), which are clearly visible in the peaks at 1650 and 1520 cm^{-1}.

In the case of the second precursor (OBA), the first amide band (NH–CO) was detected at 1650 cm^{-1} together with the carbonyl group (C=O) stretching vibration. The second amide band

(NH–CO) is clearly visible at the value of 1520 cm^{-1} (δ(NH)). Therefore, the presence of the stable amidic structures in the synthesized OBA precursor present in the sol may be confirmed. With this in mind, it is possible to assume that the organic linker present in the structure of the hybrid precursor does not decompose during the sol-gel processes. Furthermore, the amide occurrence in the material may be confirmed by the presence of the N–H stretching vibration together with the occurrence of the molecular water at around 3100 – 3600 cm^{-1}, appearing as a broad band with emerging shoulders. In addition, other bands observable in **Figure 49 (lower spectrum)** are the symmetric and antisymmetric stretching vibrations of $–CH_2$, $–CH_3$ units at the region 2850 – 3000 cm^{-1}. As already mentioned above, the bands found in the region between 500 and 1000 cm^{-1} mostly belong to the silica matrix, where the characteristic stretching vibrations of Si–O–Si structural units appear at approximately 690, 750 – 800 and 1050 – 1100 cm^{-1}, as well as Si–OH structural units, which may be clearly observed in the regions of 950 – 1000 cm^{-1} [1].

According to the obtained results, the following assumptions may be made: both the synthesized hybrid precursors are stable during the sol preparations. The organic linkers stay firmly bonded inside the hybrid silica matrix. In a good accordance to the TGA-FTIR evaluation, the decomposition process for both organic linkers does not occur up to a temperature of 80 °C.

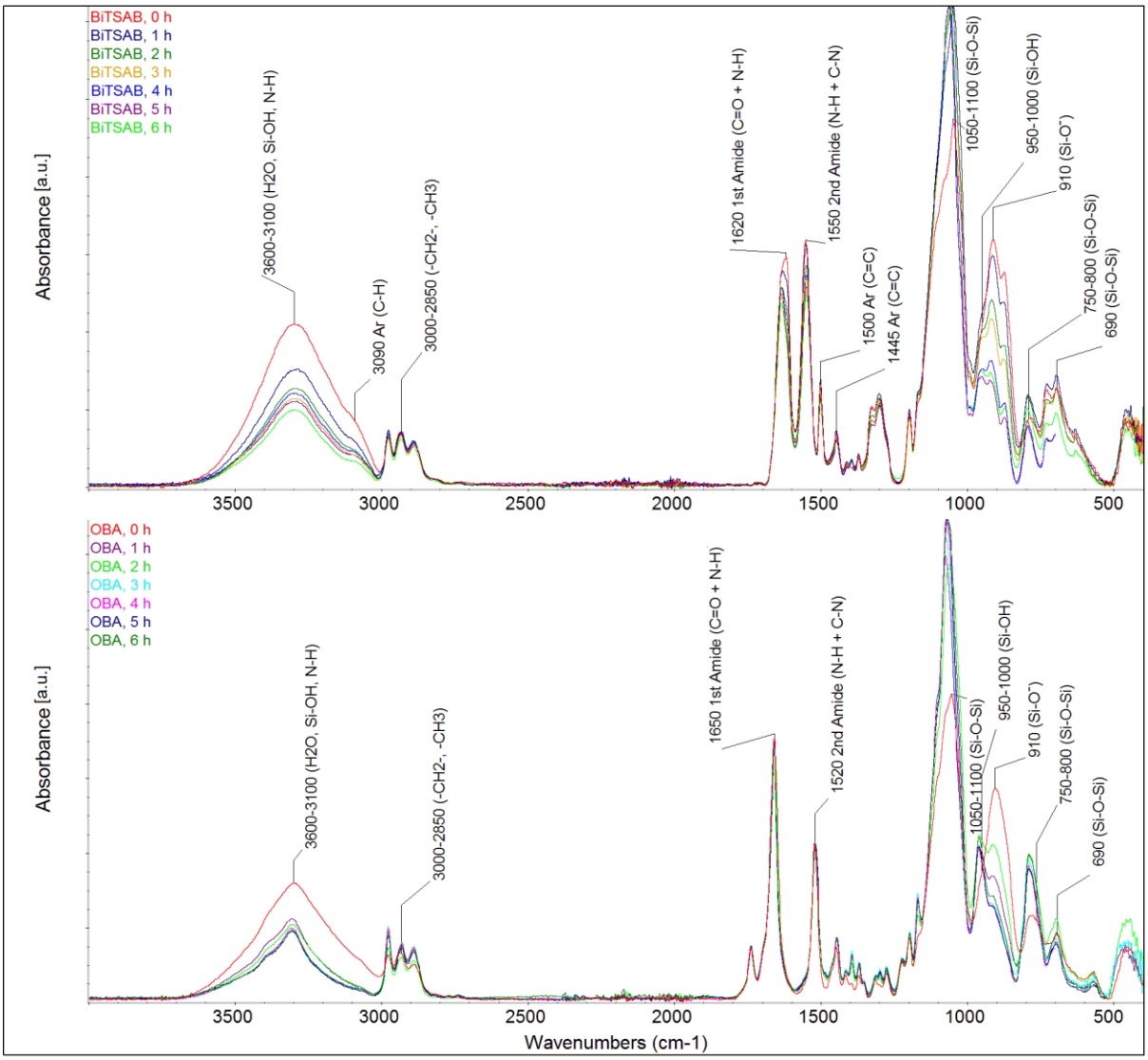

Figure 49. FTIR spectra describing the kinetics of the sols containing 50 mol.% of BiTSAB precursor (**upper spectrum**) and OBA precursor (**lower spectrum**) which were established as being suitable for the formation of fibers after 6 hours of heating at an appropriate temperature.

Table 10. Sols and conditions employed for the jet needle-electrospinning of both of the synthesized precursors (OBA and BiTSAB).

Sol-gel parameters		Parameters of jet needle-electrospinning				
Molar ratio *k* = [H_2O] / [silanes]	**Molar ratio Alc = [EtOH] / [silanes]**	**Viscosity [mPa.s]**	**Feeding rate [$ml.s^{-1}$]**	**Tip-to-collector distance [cm]**	**High Voltage [kV]**	**Temperature/ relative humidity**
<2.0	>60	>39	<1	<20	<23	>18 °C / >32 %

7.3.5 Preliminary results of the formation of OBA and BiTSAB fibers

In this chapter, only an overview of the latest results of (nano)fibrous structures, which were successfully prepared from the synthesized precursors (**Figures 51-53**), is given. Due to the fact that these are currently unpublished and especially in the case of the latest results, which are currently being intensively worked on, there is only an overview of images of the prepared fibers via jet needle-electrospinning, which lead to their formation. **Figure 52**, where the hybrid sub-micron OBA fibers (100 mol.%) prepared without the addition of TEOS may be seen, is completely unique. The diameter of these fibers varies between 443 and 940 nm.

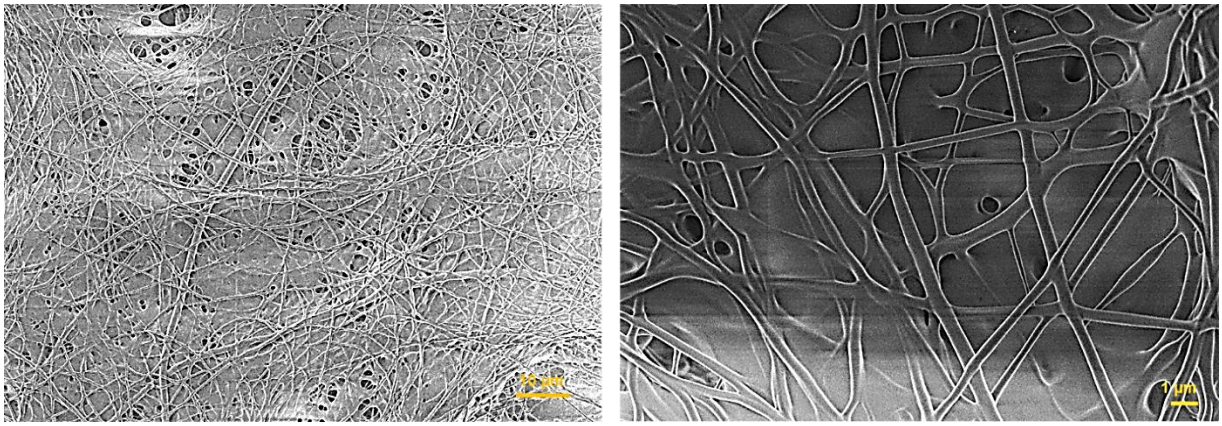

Figure 50. Fibers prepared from a combination of the OBA precursor:TEOS 50 mol.%

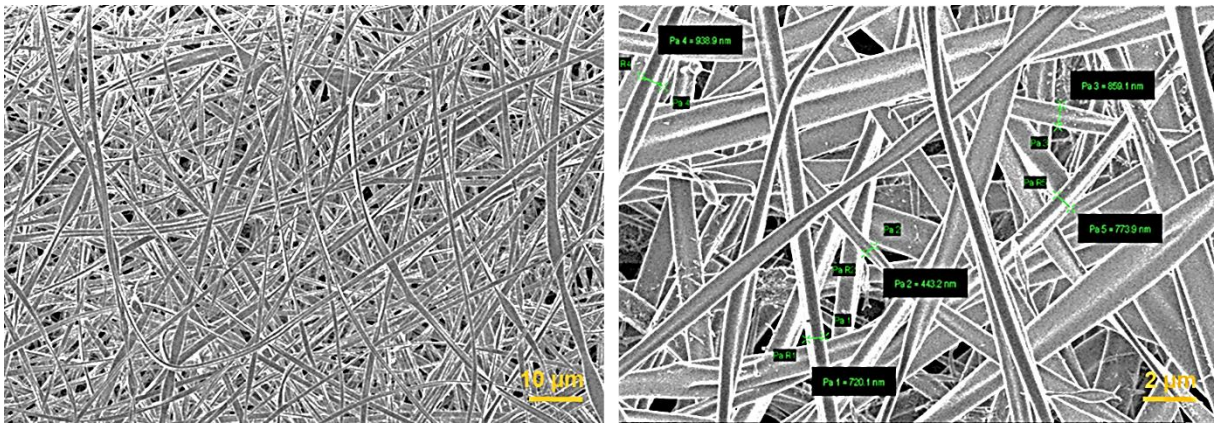

Figure 51. Hybrid organosilane fibers prepared from the OBA precursor at 100 mol.% without the use of TEOS.

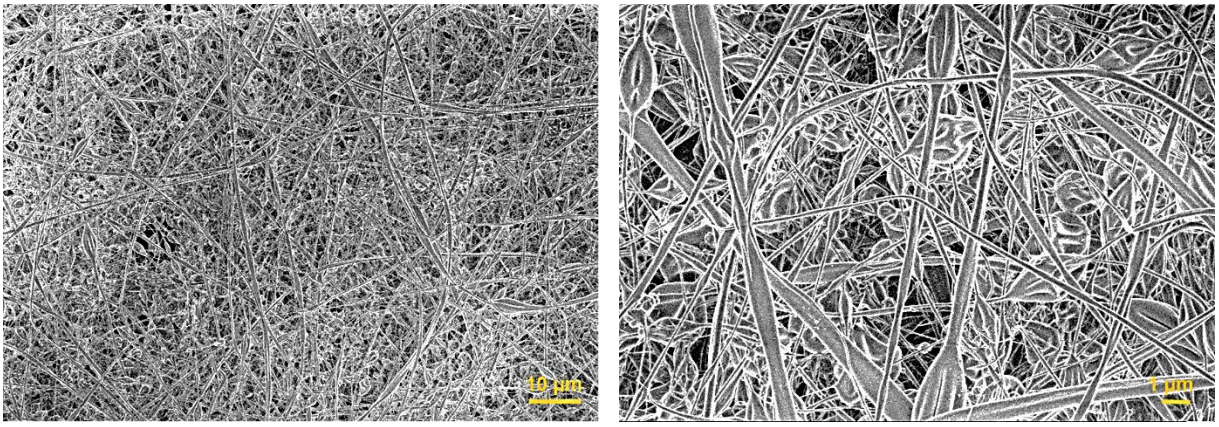

Figure 52. Disrupted hybrid organosilane fibers containing beads prepared from a combination of the BiTSAB precursor:TEOS 50 mol.% under different needle-electrospinning conditions.

8. The potential of these newly prepared organosilane fibrous materials

Today's modern science requires a comprehensive approach and intensive interconnection of a number of scientific disciplines, which used to be developed completely individually. By applying such an approach, completely new and unique results may be achieved, especially in the field of materials science. This is precisely the case of hybrid organic-inorganic materials, which enable and support a multidisciplinary approach of a number of scientific disciplines leading to completely new and unique results, which may be further developed both in basic and applied research. From this point of view, it is possible to say that organosilane-based materials have the potential to fulfil the above-mentioned statements and parameters.

Completely unique materials may be obtained due to the properties that can be achieved by combining organic and inorganic components within the hybrid matrix in these fibrous organosilane materials by the presence of a Si–C covalent bond. These materials show a wide application potential in various fields. However, their development is still in its infancy, so a vast field of activity is open to a wide range of scientific disciplines and scientific groups.

The presented thesis and results humbly compare the past and current research of the preparation of hybrid organosilane fibrous materials with the aim of emphasizing their contribution to modern science. The organo-mono-silylated and organo-bis-silylated precursors were deeply studied stressing the consequent synthetic strategies and outcomes and/or ways leading to the formation of these fibers. The presented findings are complemented with a subsequent survey of their suitable applications highlighting the potential of such hybrid organosilane fibers in various different fields of modern material science.

The various classes of hybrid organosilane (nano)fibers provide additional value compared to the conventional fibrous systems already in use and may be applied to many fields of modern science, such as optoelectronics, energetics, filtration, catalysis, and medicine. Many of the presented hybrid organosilane fibrous materials seem to have a strong potential to open up completely new directions in hybrid material chemistry with an emphasis on the non-toxicity, environmental friendliness and efficiency of their performance.

One of the greatest advantages of these organosilane fibrous materials lies in the very high variability in the choice of organic molecules (linkers) that are firmly anchored by the covalent bonding of Si–C inside the structures of organo-mono or organo-bis-silylated precursors, which form the main components in the subsequent formation of the fibers. Due to this variability, nano/submicron/microfibers of the required properties may be subsequently prepared.

As an example of our ongoing research, the following specific types of organic molecules were presented: an aliphatic type i.e., *N,N'*-bis(3-(triethoxysilyl)-propyl)oxamide; an aromatic type with one nuclei i.e., 1,4-bis(triethosilyl)benzene and/or more nuclei i.e., 4,4-bis(triethoxysilyI)terphenyl; cyclic type i.e., (1*S*,2*S*)-1,2-bis{*N'*-[3-(triethoxysilyl)propyl]ureido}cyclohexane; or heterocyclic type i.e., bis(3-(triethoxysilyl)propyl)pyridine-2,6-dicarboxamide. The selected organic molecule (linker) is then able to impart the desired properties to the hybrid fibrous material. However, when selecting organic linkers, it is necessary to take into account some of their properties, such as thermal stability, flexibility, strength, conductivity, or the steric factors, which include the size, shape, composition and structure of the chosen or proposed molecules. All of the above-mentioned factors may influence and in many cases greatly affect both the sol-gel process and the subsequent ability to form fibers via one or more electrospinning techniques.

The deepest meaning regarding these fibrous organosilane materials lies in their following properties and parameters: **I.** The ability to prepare spinnable sols via a one-pot synthesis with the help of the sol-gel process; **II.** The most common fiber-making techniques such as jet needle-electrospinning, stick electrospinning and or Nanospider technology leading from the laboratory scale to semi-industrial scale may be used; **III.** All hybrid organosilane fibrous materials based on organo-mono-silylated, particularly organo-bis-silylated precursors, may be prepared without the use of further inorganic and/or organic surfactants, polymeric or low-molecular additives; **IV.** The hybrid network leading to the formation of these hybrid organosilane fibers may be composed of a variety of suitable organic molecules, which are covalently bonded inside of the hybrid network via Si–C bonds, according to the planned uses of these fibers.

9. Conclusion

The aim of the presented habilitation thesis

The aim of the presented habilitation thesis and its first part is to acquaint the scientific committee with the completely unique and so far under-researched topic of purely hybrid organosilane (nano)fibers prepared from organo-mono-silylated and particularly organo-bis-silylated precursors using a combination of various different approaches based on organic/organometallic synthesis, which is interconnected with the subsequently applied methods of sol-gel and electrospinning.

These hybrid pure organosilane fibers (nano fibers; submicron fibers; microfibers) may be prepared using a number of electrospinning techniques, including Nanospider technology. Likewise, these fibrous mats show high biocompatibility depending on their composition, which may be used in medical applications, such as tissue engineering and/or regenerative medicine. Furthermore, the above-mentioned fiber systems may exhibit fluorescence at different wavelengths, which may be used in the fields of optoelectronics and sensors. These are materials whose further properties may be classified as semiconductors or conductors, and there is the potential for application of these materials in high-performance energy devices (ion-lithium batteries, solar cells) in the form of new types of (semi) conductive membranes. Due to the variability of organic molecules within hybrid structures, these materials may also be used in the field of air and water filtration, or catalysis. The materials are prepared with an emphasis on current ecological and economic aspects, i.e., environmental protection and reasonable production costs.

Chapters 2 to 6 are devoted to an overview of the whole issue, which covers the origins of silica and (organo)silane fiber-making chemistry leading to the successful preparation of pure organosilane fibers via a one-pot synthesis, followed by a description of the parameters which are necessary for sol-gel processing for the preparation of spinnable sols, such as the molar ratio of the hybrid precursors to tetraethylorthosilicate, acid catalyst and its properties, polar solvent (alcohol), which is necessary for the kinetics (hydrolysis and polycondensation processes) of the whole sol, constant ***k*** determining the level of polycondensation reactions, and viscosity of the sols, which are some of the key parameters for subsequent formation of fibers via electrospinning. **This part of the thesis is based on a review that the author and her colleagues published this year in the journal Polymer entitled: "*Hybrid organosilane fibrous materials and their contribution to modern science*" [19]. The author provided the main contribution to the above-mentioned published review.**

The results providing the novelty of this habilitation thesis

The second part of the thesis is focused on the results providing the novelty of this work, where (nano, submicro, and micro)fibers were successfully prepared from the precursor 4,4'-bis(triethoxysilyl)-1,1'-biphenyl in a high molar ratio in the hybrid matrix. Here, the results related to their preparation and their complete characterization via various techniques, including solid-state NMR, thermogravimetric analysis (TGA), FTIR spectroscopy, and scanning electron microscopy (SEM), were described. These results have not been published yet, and are partly confidential due to the filing of the national patent application **PV 2021-160 submitted on 31 March 2021, and the international patent application EP21172710.2 submitted on 7 May 2021** entitled: "*A process for preparing a sol for the preparation of hybrid organosilane fibers by electrospinning technique, a sol thus prepared and hybrid organosilane fibers prepared by electrospinning of this sol*".

The author's contribution to the topic

The author's contribution stems from an internship at the Institut de Science et d'Ingénierie Supramoléculaires, l'Université de Strasbourg, France, which the author completed between 2014 and 2015. Suring this internship, the author was more deeply acquainted with the preparation of hybrid bridged organosilane precursors in the form of nanoparticle systems intended primarily for the fields of medicine, photophysics, and optoelectronics.

Upon her return, the author applied the knowledge she gained from the internship in the field of hybrid bridged organosilanes and the potential offered by the Technical University of Liberec in preparation of nanofibers and nanofiber devices. Thanks to a GACR project performed between 2018 and 2020, she focused intensively on the preparation of organo-bis-silylated precursors by a combination of the sol-gel process and electrospinning techniques.

Later on, together with her colleagues and also using the knowledge she previously obtained in the fields of organic and organometallic synthesis, she extended the synthesis of selected types of hybrid bridged organosilane precursors, which are prepared according to the required properties together with the considered areas of application.

The whole topic is further described in the reprints of articles (**Chapter 11.5**) published in 2020 and 2021, in which the author provided a major contribution. The results of this research work are further mentioned in the currently filed national patent application **PV2021-160**, which has also been submitted as international patent application **EP21172710.2**.

Contribution of this thesis to the development of the field of textile technology and materials engineering

The habilitation thesis provides a completely new point of view and possibilities to the field of textile technology and materials engineering. As was widely discussed in all parts of this thesis, these new types of hybrid organosilane fibrous materials may strongly support the development, growth, and expansion of fields related to the textile industry and material sciences.

These (nano, submicro, and micro)fibers may find application in almost all fields of the textile industry. Particularly interesting and potentially very promissive are the fields related to the modern textile protective materials used for military purposes, intelligent textiles having incorporated organic molecules as optical sensors, thermo and/or chemo sensors. Furthermore, these fibrous materials may find strong application potential in medicine, particularly in the form of new types of non-woven wound dressings focused on difficult-to-heal wounds including burns and/or scaffolds. This is particularly due to a wide variety of active organic molecules, which may be covalently incorporated into the hybrid matrix without the help of additional components and/or supports such as different types of surfactants and/or organic polymers. The incorporated active molecules may further offer functionalization of other biomolecules such as proteins, enzymes, drugs, antimicrobials, and antifungals, whereby increasing the impact of the prepared hybrid organosilane fibrous materials. Equally important is the field of tissue engineering, where these fibrous organosilane materials may find wide application, especially in the area of nerve tissue regeneration, due to their ability to also covalently incorporate conductive organic molecules (linkers). These fibrous materials may also be applied in the field of fibrous and/or non-fibrous (nano)composites due to their physical and chemical properties and/or in the form of fibrous membranes used for air or water filtration, having an additional effect, which lies not only in the capture of different “toxic” components but also in their effective deactivation, thanks to the presence of suitable covalently bonded active organic molecules (linkers) in the hybrid silica matrix.

It was possible to develop these new and unique fibrous materials due to the combination of specialists from the fields of chemistry, materials science, and textile technology offered to us by the Technical University of Liberec. Last but not least, the uniqueness of this thesis together with its contribution to the field of textile technology and materials engineering lies in the variety of topics related to these new hybrid organosilane fibrous materials. Moreover, each reader may find his or her own focus regarding this topic and help to spread the above-presented knowledge, which may lead to an increase in the significant and highly promissive potential of

this topic within research and development worldwide, not only in the field of textile technology and materials engineering but also in daily life.

10. References

[1] M. Faustini, L. Nicole, E. Ruiz-Hitzky, C. Sanchez, History of Organic–Inorganic Hybrid Materials: Prehistory, Art, Science, and Advanced Applications, Advanced Functional Materials. 28 (2018) 1704158. https://doi.org/10.1002/adfm.201704158.

[2] CRC Concise Encyclopedia of Nanotechnology, CRC Press. (n.d.). https://www.routledge.com/CRC-Concise-Encyclopedia-of-Nanotechnology/Kharisov-Kharissova-Ortiz-Mendez/p/book/9781466580343 (accessed May 6, 2020).

[3] R.B. Figueira, Hybrid Sol-gel Coatings for Corrosion Mitigation: A Critical Review, Polymers. 12 (2020) 689. https://doi.org/10.3390/polym12030689.

[4] A. Bouibed, R. Doufnoune, Synthesis and characterization of hybrid materials based on graphene oxide and silica nanoparticles and their effect on the corrosion protection properties of epoxy resin coatings, Journal of Adhesion Science and Technology. 33 (2019) 834–860. https://doi.org/10.1080/01694243.2019.1571660.

[5] C. Sanchez, B. Julián, P. Belleville, M. Popall, Applications of hybrid organic–inorganic nanocomposites, J. Mater. Chem. 15 (2005) 3559–3592. https://doi.org/10.1039/B509097K.

[6] C. Sanchez, P. Belleville, M. Popall, L. Nicole, Applications of advanced hybrid organic–inorganic nanomaterials: from laboratory to market, Chem. Soc. Rev. 40 (2011) 696–753. https://doi.org/10.1039/C0CS00136H.

[7] V.P. Ananikov, Organic–Inorganic Hybrid Nanomaterials, Nanomaterials (Basel). 9 (2019). https://doi.org/10.3390/nano9091197.

[8] R.S. Andre, R.C. Sanfelice, A. Pavinatto, L.H.C. Mattoso, D.S. Correa, Hybrid nanomaterials designed for volatile organic compounds sensors: A review, Materials & Design. 156 (2018) 154–166. https://doi.org/10.1016/j.matdes.2018.06.041.

[9] B. Holubova, V. Makova, J. Mullerova, J. Brus, K. Havlickova, V. Jencova, A. Michalcova, J. Kulhankova, M. Rezanka, Novel chapter in hybrid materials: One-pot synthesis of purely organosilane fibers, Polymer. 190 (2020) 122234. https://doi.org/10.1016/j.polymer.2020.122234.

[10] V. Máková, B. Holubová, D. Tetour, J. Brus, M. Řezanka, M. Rysová, J. Hodačová, (1S,2S)-Cyclohexane-1,2-diamine-based Organosilane Fibres as a Powerful Tool Against Pathogenic Bacteria, Polymers. 12 (2020) 206. https://doi.org/10.3390/polym12010206.

[11] C.J. Brinker, G.W. Scherer, Sol-Gel Science: The Physics and Chemistry of Sol-Gel Processing, Elsevier Inc., 2013. https://doi.org/10.1016/C2009-0-22386-5.

[12] G. Kickelbick, Hybrid Materials: Synthesis, Characterization, and Applications, John Wiley & Sons, 2007.

[13] G. Schottner, Hybrid Sol−Gel-Derived Polymers: Applications of Multifunctional Materials, Chem. Mater. 13 (2001) 3422–3435. https://doi.org/10.1021/cm011060m.

[14] A. Godet, T. Sylvestre, V. Pecheur, J. Chretien, J.-C. Beugnot, K.P. Huy, Nonlinear elasticity of silica nanofiber, APL Phontonics. 4 (2019) 080804. https://doi.org/10.1063/1.5103239.

[15] M. Gao, J. Zeng, K. Liang, D. Zhao, B. Kong, Interfacial Assembly of Mesoporous Silica-Based Optical Heterostructures for Sensing Applications, Advanced Functional Materials. 30 (2020) 1906950. https://doi.org/10.1002/adfm.201906950.

[16] F. Rajabi, A.Z. Ebrahimi, A. Rabiee, A. Pineda, R. Luque, Synthesis and Characterization of Novel Pyridine Periodic Mesoporous Organosilicas and Its Catalytic Activity in the Knoevenagel Condensation Reaction, Materials (Basel). 13 (2020). https://doi.org/10.3390/ma13051097.

[17] S. Karamikamkar, H.E. Naguib, C.B. Park, Advances in precursor system for silica-based aerogel production toward improved mechanical properties, customized morphology, and

multifunctionality: A review, Adv. Colloid Interface Sci. 276 (2020) 102101. https://doi.org/10.1016/j.cis.2020.102101.
[18] T. Linhares, M.T. Pessoa de Amorim, L. Duraes, Silica aerogel composites with embedded fibres: a review on their preparation, properties and applications, J. Mater. Chem. A. 7 (2019) 22768–22802. https://doi.org/10.1039/c9ta04811a.
[19] V. Máková, B. Holubová, I. Krabicová, J. Kulhánková, M. Řezanka, Hybrid organosilane fibrous materials and their contribution to modern science, Polymer. 228 (2021) 123862. https://doi.org/10.1016/j.polymer.2021.123862.
[20] S. Yajima, J. Hayashi, M. Omori, K. Okamura, Development of a silicon carbide fibre with high tensile strength, Nature. 261 (1976) 683–685. https://doi.org/10.1038/261683a0.
[21] T. Ishikawa, Y. Kohtoku, K. Kumagawa, T. Yamamura, T. Nagasawa, High-strength alkali-resistant sintered SiC fibre stable to 2,200 °C, Nature. 391 (1998) 773–775. https://doi.org/10.1038/35820.
[22] P. Baldus, M. Jansen, D. Sporn, Ceramic Fibers for Matrix Composites in High-Temperature Engine Applications, Science. 285 (1999) 699–703. https://doi.org/10.1126/science.285.5428.699.
[23] N.R. Thomas, Frederic Stanley Kipping—Pioneer in Silicon Chemistry: His Life & Legacy, Silicon. 2 (2010) 187–193. https://doi.org/10.1007/s12633-010-9051-x.
[24] H. Deuel, Organic derivatives of clay minerals*, Clay Minerals Bulletin. 1 (1952) 205–214. https://doi.org/10.1180/claymin.1952.001.7.04.
[25] C.W. Lentz, Silicate Minerals as Sources of Trimethylsilyl Silicates and Silicate Structure Analysis of Sodium Silicate Solutions, Inorg. Chem. 3 (1964) 574–579. https://doi.org/10.1021/ic50014a029.
[26] K.A. Andrianov, A.A. Zhdanov, V.Y. Levin, Some Physical Properties of Organosilicon Ladder Polymers, Annual Review of Materials Science. 8 (1978) 313–326. https://doi.org/10.1146/annurev.ms.08.080178.001525.
[27] W. Mahler, M.F. Bechtold, Freeze-formed silica fibres, Nature. 285 (1980) 27–28. https://doi.org/10.1038/285027a0.
[28] S. Sakka, K. Kamiya, The sol-gel transition in the hydrolysis of metal alkoxides in relation to the formation of glass fibers and films, Journal of Non-Crystalline Solids. 48 (1982) 31–46. https://doi.org/10.1016/0022-3093(82)90244-7.
[29] H.K. Schmidt, New type of non-crystalline solids between inorganic and organic materials, (1985). https://doi.org/10.22028/D291-24311.
[30] Sol-Gel Science, Elsevier, 1990. https://doi.org/10.1016/C2009-0-22386-5.
[31] R.J.P. Corriu, J.J.E. Moreau, P. Thepot, M.W.C. Man, New mixed organic-inorganic polymers: hydrolysis and polycondensation of bis(trimethoxysilyl)organometallic precursors, Chem. Mater. 4 (1992) 1217–1224. https://doi.org/10.1021/cm00024a020.
[32] K.J. Shea, D.A. Loy, O. Webster, Arylsilsesquioxane gels and related materials. New hybrids of organic and inorganic networks, J. Am. Chem. Soc. 114 (1992) 6700–6710. https://doi.org/10.1021/ja00043a014.
[33] S. Sakka, T. Yoko, Fibers from gels, Journal of Non-Crystalline Solids. 147–148 (1992) 394–403. https://doi.org/10.1016/S0022-3093(05)80650-7.
[34] A.E. Comyns, Sol-gel technology for thin films, fibers, preforms, electronics, and specialty shapes Edited by Lisa C. Klein; Noyes Publications, Park Ridge, New Jersey, 1988. pp. xxi + 407, price $72.00 (USA). ISBN 0-8155-1154-X, British Polymer Journal. 21 (1989) 361–362. https://doi.org/10.1002/pi.4980210420.
[35] C.T. Ho, W.C. LaCourse, R.A. Condrate, A. Jillavenkatesa, A Raman spectral investigation of structural variations in thin silicate glass fibers, Materials Letters. 23 (1995) 237–240. https://doi.org/10.1016/0167-577X(95)00037-2.

[36] H. Kozuka, H. Kuroki, S. Sakka, The change of flow characteristics of Si(OC2H5)4 solutions in the course of sol-to-gel conversion, Journal of Non-Crystalline Solids. 101 (1988) 120–122. https://doi.org/10.1016/0022-3093(88)90377-8.
[37] J. Geltmeyer, J. De Roo, F. Van den Broeck, J.C. Martins, K. De Buysser, K. De Clerck, The influence of tetraethoxysilane sol preparation on the electrospinning of silica nanofibers, J Sol-Gel Sci Technol. 77 (2016) 453–462. https://doi.org/10.1007/s10971-015-3875-1.
[38] P. Judeinstein, C. Sanchez, Hybrid organic–inorganic materials: a land of multidisciplinarity, J. Mater. Chem. 6 (1996) 511–525. https://doi.org/10.1039/JM9960600511.
[39] S. Fujita, S. Inagaki, Self-Organization of Organosilica Solids with Molecular-Scale and Mesoscale Periodicities, Chem. Mater. 20 (2008) 891–908. https://doi.org/10.1021/cm702271v.
[40] K.J. Shea, D.A. Loy, Bridged Polysilsesquioxanes. Molecular-Engineered Hybrid Organic−Inorganic Materials, Chem. Mater. 13 (2001) 3306–3319. https://doi.org/10.1021/cm011074s.
[41] S. Fujita, M.P. Kapoor, S. Inagaki, Organic-Inorganic Hybrid Mesoporous Silica, in: A. Muramatsu, T. Miyashita (Eds.), Nanohybridization of Organic-Inorganic Materials, Springer, Berlin, Heidelberg, 2009: pp. 141–169. https://doi.org/10.1007/978-3-540-92233-9_7.
[42] R. West, M.J. Fink, J. Michl, Tetramesityldisilene, a Stable Compound Containing a Silicon-Silicon Double Bond, Science. 214 (1981) 1343–1344. https://doi.org/10.1126/science.214.4527.1343.
[43] The Chemistry of Organic Silicon Compounds. Volume 3 Edited by Zvi Rappoport (The Hebrew University, Jerusalem) and Yitzhak Apeloig (Israel Institute of Technology, Haifa). J. Wiley & Sons: New York. 2001. xviii + 1153 pp. $445.00. ISBN 0-471-62384-9., J. Am. Chem. Soc. 124 (2002) 5602–5602. https://doi.org/10.1021/ja025204p.
[44] 7.9: Comparison Between Silicon and Carbon, Chemistry LibreTexts. (2020). https://chem.libretexts.org/Bookshelves/Inorganic_Chemistry/Book%3A_Chemistry_of_the_Main_Group_Elements_(Barron)/07%3A_Group_14/7.09%3A_Comparison_Between_Silicon_and_Carbon (accessed May 19, 2021).
[45] A.G. Sharpe, C.E. Housecroft, Anorganická chemie, 1st ed., VŠCHT, Praha, 2014.
[46] C.J. Brinker, G. Scherer, Sol-Gel Science: The Physics and Chemistry of Sol-Gel Processing, Elsevier Inc., 2013. https://doi.org/10.1016/C2009-0-22386-5.
[47] M. Catauro, S.V. Ciprioti, Characterization of Hybrid Materials Prepared by Sol-Gel Method for Biomedical Implementations. A Critical Review, Materials (Basel). 14 (2021). https://doi.org/10.3390/ma14071788.
[48] C. Bogatu, THE INFLUENCE OF PARAMETERS IN SILICA SOL-GEL PROCESS, Bull. Transilv. Univ. Bras. 2011 (2011) 53.
[49] C.J. Brinker, Hydrolysis and condensation of silicates: Effects on structure, Journal of Non-Crystalline Solids. 100 (1988) 31–50. https://doi.org/10.1016/0022-3093(88)90005-1.
[50] A.A. Issa, A.S. Luyt, Kinetics of Alkoxysilanes and Organoalkoxysilanes Polymerization: A Review, Polymers. 11 (2019) 537. https://doi.org/10.3390/polym11030537.
[51] A.S. Lee, S.-S. Choi, K.-Y. Baek, S.S. Hwang, Hydrolysis kinetics of a sol-gel equilibrium yielding ladder-like polysilsesquioxanes, Inorganic Chemistry Communications. 73 (2016) 7–11. https://doi.org/10.1016/j.inoche.2016.09.004.
[52] M.-C. Brochier Salon, P.-A. Bayle, M. Abdelmouleh, S. Boufi, M.N. Belgacem, Kinetics of hydrolysis and self condensation reactions of silanes by NMR spectroscopy, Colloids

and Surfaces A: Physicochemical and Engineering Aspects. 312 (2008) 83–91. https://doi.org/10.1016/j.colsurfa.2007.06.028.

[53] G.J. McIntosh, Theoretical investigations into the nucleation of silica growth in basic solution part II – derivation and benchmarking of a first principles kinetic model of solution chemistry, Phys. Chem. Chem. Phys. 15 (2013) 17496–17509. https://doi.org/10.1039/C3CP53223B.

[54] S. Okumoto, N. Fujita, S. Yamabe, Theoretical Study of Hydrolysis and Condensation of Silicon Alkoxides, J. Phys. Chem. A. 102 (1998) 3991–3998. https://doi.org/10.1021/jp980705b.

[55] T.W. Zerda, I. Artaki, J. Jonas, Study of polymerization processes in acid and base catalyzed silica sol-gels, Journal of Non-Crystalline Solids. 81 (1986) 365–379. https://doi.org/10.1016/0022-3093(86)90503-X.

[56] G. Jia, Q.-H. Wan, Separation and identification of oligomeric vinylmethoxysiloxanes by gradient elution chromatography coupled with electrospray ionization mass spectrometry, Journal of Chromatography A. 1395 (2015) 129–135. https://doi.org/10.1016/j.chroma.2015.03.079.

[57] Y. Jiang, Q.-H. Wan, Separation and identification of oligomeric phenylethoxysiloxanols by liquid chromatography-electrospray ionization mass spectrometry, Journal of Chromatography A. 1394 (2015) 95–102. https://doi.org/10.1016/j.chroma.2015.03.043.

[58] S. Sakka, K. Kamiya, The sol-gel transition in the hydrolysis of metal alkoxides in relation to the formation of glass fibers and films, Journal of Non-Crystalline Solids. 48 (1982) 31–46. https://doi.org/10.1016/0022-3093(82)90244-7.

[59] C. Schramm, B. Rinderer, R. Tessadri, Synthesis and characterization of novel ultrathin polyimide fibers via sol-gel process and electrospinning, Journal of Applied Polymer Science. 128 (2013) 1274–1281. https://doi.org/10.1002/app.38543.

[60] J. Xue, T. Wu, Y. Dai, Y. Xia, Electrospinning and Electrospun Nanofibers: Methods, Materials, and Applications, Chemical Reviews. (2019). https://doi.org/10.1021/acs.chemrev.8b00593.

[61] S. Thenmozhi, N. Dharmaraj, K. Kadirvelu, H.Y. Kim, Electrospun nanofibers: New generation materials for advanced applications, Materials Science and Engineering: B. 217 (2017) 36–48. https://doi.org/10.1016/j.mseb.2017.01.001.

[62] R. Sahay, P.S. Kumar, R. Sridhar, J. Sundaramurthy, J. Venugopal, S.G. Mhaisalkar, S. Ramakrishna, Electrospun composite nanofibers and their multifaceted applications, J. Mater. Chem. 22 (2012) 12953–12971. https://doi.org/10.1039/C2JM30966A.

[63] Electrospun Polymer Nanofibers, Routledge & CRC Press. (n.d.). https://www.routledge.com/Electrospun-Polymer-Nanofibers/Arinstein/p/book/9789814745277 (accessed May 1, 2021).

[64] J.F. Cooley, Apparatus for electrically dispersing fluids, US692631A, 1902. https://patents.google.com/patent/US692631A/en (accessed May 1, 2021).

[65] G.I. Taylor, M.D. Van Dyke, Electrically driven jets, Proceedings of the Royal Society of London. A. Mathematical and Physical Sciences. 313 (1969) 453–475. https://doi.org/10.1098/rspa.1969.0205.

[66] D.H. Reneker, I. Chun, Nanometre diameter fibres of polymer, produced by electrospinning, Nanotechnology. 7 (1996) 216–223. https://doi.org/10.1088/0957-4484/7/3/009.

[67] D.I. Braghirolli, D. Steffens, P. Pranke, Electrospinning for regenerative medicine: a review of the main topics, Drug Discovery Today. 19 (2014) 743–753. https://doi.org/10.1016/j.drudis.2014.03.024.

[68] D. Lukáš, A. Sarkar, L. Martinová, K. Vodsed'álková, D. Lubasová, J. Chaloupek, P. Pokorný, P. Mikeš, J. Chvojka, M. Komárek, Physical principles of electrospinning

(Electrospinning as a nano-scale technology of the twenty-first century), Textile Progress. 41 (2009) 59–140. https://doi.org/10.1080/00405160902904641.
[69] Q. Yang, X. Jiang, F. Gu, Z. Ma, J. Zhang, L. Tong, Polymer micro or nanofibers for optical device applications, Journal of Applied Polymer Science. 110 (2008) 1080–1084. https://doi.org/10.1002/app.28716.
[70] Y. Huang, N. Bu, Y. Duan, Y. Pan, H. Liu, Z. Yin, Y. Xiong, Electrohydrodynamic direct-writing, Nanoscale. 5 (2013) 12007–12017. https://doi.org/10.1039/C3NR04329K.
[71] X.-X. He, J. Zheng, G.-F. Yu, M.-H. You, M. Yu, X. Ning, Y.-Z. Long, Near-Field Electrospinning: Progress and Applications, J. Phys. Chem. C. 121 (2017) 8663–8678. https://doi.org/10.1021/acs.jpcc.6b12783.
[72] T.P. Lei, X.Z. Lu, F. Yang, Fabrication of various micro/nano structures by modified near-field electrospinning, AIP Advances. 5 (2014) 041301. https://doi.org/10.1063/1.4901879.
[73] Production Scale Up of Nanofibers. A Review | Nanotechnology | Materials Science, Scribd. (n.d.). https://www.scribd.com/document/498303541/2017-Production-Scale-Up-of-Nanofibers-A-review (accessed April 26, 2021).
[74] K. Strnadová, L. Stanislav, I. Krabicová, F. Sabol, J. Lukášek, M. Řezanka, D. Lukáš, V. Jenčová, Drawn aligned polymer microfibres for tissue engineering, Journal of Industrial Textiles. (2019) 1528083718825318. https://doi.org/10.1177/1528083718825318.
[75] T. Ondarçuhu, C. Joachim, Drawing a single nanofibre over hundreds of microns, EPL. 42 (1998) 215. https://doi.org/10.1209/epl/i1998-00233-9.
[76] A.S. Nain, J.C. Wong, C. Amon, M. Sitti, Drawing suspended polymer micro-/nanofibers using glass micropipettes, Appl. Phys. Lett. 89 (2006) 183105. https://doi.org/10.1063/1.2372694.
[77] X. Xing, Y. Wang, B. Li, Nanofiber drawing and nanodevice assembly in poly(trimethylene terephthalate), Opt. Express, OE. 16 (2008) 10815–10822. https://doi.org/10.1364/OE.16.010815.
[78] D. Liu, J. Li, W. Huang, S. Yang, Progress in Polymer Complex Fibers, Acta Polym. Sin. (2018) 445–455. https://doi.org/10.11777/j.issn1000-3304.2017.17285.
[79] Z. Wang, N. Li, W. Lu, W. Chen, Highly-efficient Fabrication and Crystallinity and Orientation of Polyacrylonitrile Nanofibers, Acta Polym. Sin. (2018) 755–764. https://doi.org/10.11777/j.issn1000-3304.2017.17226.
[80] C. Meng, Y. Xiao, P. Wang, L. Zhang, Y. Liu, L. Tong, Quantum-dot-doped polymer nanofibers for optical sensing, Adv. Mater. Weinheim. 23 (2011) 3770–3774. https://doi.org/10.1002/adma.201101392.
[81] A.C.A. Wan, M.F. Leong, J.K.C. Toh, Y. Zheng, J.Y. Ying, Multicomponent Fibers by Multi-interfacial Polyelectrolyte Complexation, Advanced Healthcare Materials. 1 (2012) 101–105. https://doi.org/10.1002/adhm.201100020.
[82] S.A. Harfenist, S.D. Cambron, E.W. Nelson, S.M. Berry, A.W. Isham, M.M. Crain, K.M. Walsh, R.S. Keynton, R.W. Cohn, Direct Drawing of Suspended Filamentary Micro- and Nanostructures from Liquid Polymers, Nano Lett. 4 (2004) 1931–1937. https://doi.org/10.1021/nl048919u.
[83] Z. Xie, H. Niu, T. Lin, Continuous polyacrylonitrile nanofiber yarns: preparation and dry-drawing treatment for carbon nanofiber production, RSC Adv. 5 (2015) 15147–15153. https://doi.org/10.1039/c4ra16247a.
[84] P. Yang, D. Zhao, B.F. Chmelka, G.D. Stucky, Triblock-Copolymer-Directed Syntheses of Large-Pore Mesoporous Silica Fibers, Chem. Mater. 10 (1998) 2033–2036. https://doi.org/10.1021/cm980201q.
[85] K.S. Mali, S. De Feyter, Principles of molecular assemblies leading to molecular nanostructures, Philosophical Transactions of the Royal Society A: Mathematical,

Physical and Engineering Sciences. 371 (2013) 20120304. https://doi.org/10.1098/rsta.2012.0304.
[86] J.D. Halley, D.A. Winkler, Consistent concepts of self-organization and self-assembly, Complexity. 14 (2008) 10–17. https://doi.org/10.1002/cplx.20235.
[87] K.F. Bohringer, U. Srinivasan, R.T. Howe, Modeling of capillary forces and binding sites for fluidic self-assembly, Technical Digest. MEMS 2001. 14th IEEE International Conference on Micro Electro Mechanical Systems (Cat. No.01CH37090). (2001). https://doi.org/10.1109/MEMSYS.2001.906555.
[88] G.M. Whitesides, B. Grzybowski, Self-Assembly at All Scales, Science. 295 (2002) 2418–2421. https://doi.org/10.1126/science.1070821.
[89] T. Yamaguchi, N. Suematsu, H. Mahara, Self-organization of hierarchy: Dissipative-structure assisted self-assembly of metal nanoparticles in polymer matrices, Nonlinear Dynamics in Polymeric Systems. (2004) 16–27.
[90] F. Kleitz, F. Marlow, G.D. Stucky, F. Schüth, Mesoporous Silica Fibers: Synthesis, Internal Structure, and Growth Kinetics, Chem. Mater. 13 (2001) 3587–3595. https://doi.org/10.1021/cm0110324.
[91] H. Li, B. Li, Y. Chen, X. Wu, J. Zhang, Y. Li, K. Hanabusa, Y. Yang, Transfer helix and chirality to 1,4-phenylene silica nanostructures, Materials Chemistry and Physics. 118 (2009) 135–141. https://doi.org/10.1016/j.matchemphys.2009.07.018.
[92] Y. Li, L. Bi, S. Wang, Y. Chen, B. Li, X. Zhu, Yonggang. Yang, Preparation of helical mesoporous ethylene-silica nanofibers with lamellar mesopores on the surfaces., Chem. Commun. (Cambridge, U. K.). 46 (2010) 2680–2682. https://doi.org/10.1039/b926593g.
[93] S. Wang, B. Li, L. Bi, M. Zhang, Y. Chen, Y. Li, Yonggang. Yang, Preparation of helical mesoporous ethylene-silica nanofibers using CTAB and (S)-2-methyl-1-butanol., Mater. Lett. 65 (2011) 2261–2264. https://doi.org/10.1016/j.matlet.2011.04.079.
[94] Z. Xiao, Y. Guo, B. Li, Yi. Li, Preparation and characterization of single-handed helical carbonaceous nanofibers using 1,4-phenylene bridged polybissilsesquioxanes., J. Wuhan Univ. Technol., Mater. Sci. Ed. 31 (2016) 1149–1154. https://doi.org/10.1007/s11595-016-1504-7.
[95] Y. Yang, M. Suzuki, H. Fukui, H. Shirai, Kenji. Hanabusa, Preparation of Helical Mesoporous Silica and Hybrid Silica Nanofibers Using Hydrogelator., Chem. Mater. 18 (2006) 1324–1329. https://doi.org/10.1021/cm0519030.
[96] M. Zhang, Y. Li, L. Bi, W. Zhuang, S. Wang, Y. Chen, B. Li, Yonggang. Yang, Preparation of helical mesoporous ethenylene-silica nanofibers with lamellar mesopores on their surface., Chin. J. Chem. 29 (2011) 933–941. https://doi.org/10.1002/cjoc.201190191.
[97] D. Liu, B. Li, Y. Guo, Y. Li, Y. Yang, Inner Surface Chirality of Single-Handed Twisted Carbonaceous Tubular Nanoribbons, Chirality. 27 (2015) 809–815. https://doi.org/10.1002/chir.22496.
[98] J. Hu, Y. Yang, Single-Handed Helical Polybissilsesquioxane Nanotubes and Mesoporous Nanofibers Prepared by an External Templating Approach Using Low-Molecular-Weight Gelators, Gels. 3 (2017) 2. https://doi.org/10.3390/gels3010002.
[99] J. Li, C. Nie, B. Duan, X. Zhao, H. Lu, W. Yin, Y. Li, X. He, Tensile performance of silica-based electrospun fibrous mats, J. Non-Cryst. Solids. 470 (2017) 184–188. https://doi.org/10.1016/j.jnoncrysol.2017.05.016.
[100] Y. Ding, W. Li, A. Correia, Y. Yang, K. Zheng, D. Liu, D.W. Schubert, A.R. Boccaccini, H.A. Santos, J.A. Roether, Electrospun Polyhydroxybutyrate/Poly(epsilon-caprolactone)/Sol-Gel-Derived Silica Hybrid Scaffolds with Drug Releasing Function for Bone Tissue Engineering Applications, ACS Appl. Mater. Interfaces. 10 (2018) 14540–14548. https://doi.org/10.1021/acsami.8b02656.

[101] C. Wu, W. Yuan, S.S. Al-Deyab, K.-Q. Zhang, Tuning porous silica nanofibers by colloid electrospinning for dye adsorption, Applied Surface Science. 313 (2014) 389–395. https://doi.org/10.1016/j.apsusc.2014.06.002.

[102] M. Ma, R.M. Hill, J.L. Lowery, S.V. Fridrikh, G.C. Rutledge, Electrospun Poly(Styrene- *block* -dimethylsiloxane) Block Copolymer Fibers Exhibiting Superhydrophobicity, Langmuir. 21 (2005) 5549–5554. https://doi.org/10.1021/la047064y.

[103] Z. Wei, J. Li, C. Wang, J. Cao, Y. Yao, H. Lu, Y. Li, X. He, Thermally stable hydrophobicity in electrospun silica/polydimethylsiloxane hybrid fibers, Appl. Surf. Sci. 392 (2017) 260–267. https://doi.org/10.1016/j.apsusc.2016.09.057.

[104] M.H. Ugur, B. Oktay, A. Gungor, N. Kayaman-Apohan, Highly thermally resistant, hydrophobic poly(vinyl alcohol)-silica hybrid nanofibers, J. Serb. Chem. Soc. 83 (2018) 885–897. https://doi.org/10.2298/JSC171121032H.

[105] O. Arslan, Z. Aytac, T. Uyar, Superhydrophobic, Hybrid, Electrospun Cellulose Acetate Nanofibrous Mats for Oil/Water Separation by Tailored Surface Modification, ACS Appl. Mater. Interfaces. 8 (2016) 19747–19754. https://doi.org/10.1021/acsami.6b05429.

[106] Y. Yao, L. Shen, A. Wei, T. Wang, S. Chen, Facile synthesis, microstructure, photo-catalytic activity, and anti-bacterial property of the novel Ag@gelatin-silica hybrid nanofiber membranes, J. Sol-Gel Sci. Technol. 89 (2019) 651–662. https://doi.org/10.1007/s10971-018-04914-z.

[107] W. Yu, J. Shi, L. Wang, X. Chen, M. Min, L. Wang, Y. Liu, The structure and mechanical property of silane-grafted-polyethylene/SiO 2 nanocomposite fiber rope, Aquaculture and Fisheries. 2 (2017) 34–38. https://doi.org/10.1016/j.aaf.2017.01.003.

[108] H. Guo, S. Tao, Silver nanoparticles doped silica nanocomposites coated on an optical fiber for ammonia sensing, Sens. Actuator B-Chem. 123 (2007) 578–582. https://doi.org/10.1016/j.snb.2006.09.055.

[109] K.W.K. Li, E.J. Salley, P. Melman, M.J. Tabasky, J. Zhao, C.Y. Li, Self-aligned ormosil waveguide devices, in: L.G. HubertPfalzgraf, S.I. Najafi (Eds.), Organic-Inorganic Hybrid Materials for Photonics, Spie-Int Soc Optical Engineering, Bellingham, 1998: pp. 58–64. https://doi.org/10.1117/12.312920.

[110] D.A. Nivens, Y.K. Zhang, S.M. Angel, A fiber-optic pH sensor prepared using a base-catalyzed organo-silica sol-gel, Anal. Chim. Acta. 376 (1998) 235–245. https://doi.org/10.1016/S0003-2670(98)00505-4.

[111] M. Ma, R.M. Hill, G.C. Rutledge, A Review of Recent Results on Superhydrophobic Materials Based on Micro- and Nanofibers, J. Adhes. Sci. Technol. 22 (2008) 1799–1817. https://doi.org/10.1163/156856108X319980.

[112] B. Schyrr, S. Pasche, E. Scolan, R. Ischer, D. Ferrario, J.-A. Porchet, G. Voirin, Development of a polymer optical fiber pH sensor for on-body monitoring application, Sens. Actuator B-Chem. 194 (2014) 238–248. https://doi.org/10.1016/j.snb.2013.12.032.

[113] N.E. Zander, Hierarchically Structured Electrospun Fibers, Polymers. 5 (2013) 19–44. https://doi.org/10.3390/polym5010019.

[114] R. Bel-Hassen, S. Boufi, M.-C.B. Salon, M. Abdelmouleh, M.N. Belgacem, Adsorption of silane onto cellulose fibers. II. The effect of pH on silane hydrolysis, condensation, and adsorption behavior, J. Appl. Polym. Sci. 108 (2008) 1958–1968. https://doi.org/10.1002/app.27488.

[115] D. Hou, C. Ding, C. Fu, D. Wang, C. Zhao, J. Wang, Electrospun nanofibrous omniphobic membrane for anti-surfactant-wetting membrane distillation desalination, Desalination. 468 (2019) UNSP 114068. https://doi.org/10.1016/j.desal.2019.07.008.

[116] X.M. He, K.L. Xie, Dyeing Properties of Chitosan-Sulfamic Acid Solution Treated Wool with Silane Coupling Agent, AMR. 331 (2011) 377–381. https://doi.org/10.4028/www.scientific.net/AMR.331.377.
[117] B. Sharma, R. Chhibber, R. Mehta, Seawater ageing of glass fiber reinforced epoxy nanocomposites based on silylated clays, Polymer Degradation and Stability. 147 (2018) 103–114. https://doi.org/10.1016/j.polymdegradstab.2017.11.017.
[118] B. Sharma, R. Chhibber, R. Mehta, Curing studies and mechanical properties of glass fiber reinforced composites based on silanized clay minerals, Applied Clay Science. 138 (2017) 89–99. https://doi.org/10.1016/j.clay.2016.12.038.
[119] M. Beaumont, M. Bacher, M. Opietnik, W. Gindl-Altmutter, A. Potthast, T. Rosenau, A General Aqueous Silanization Protocol to Introduce Vinyl, Mercapto or Azido Functionalities onto Cellulose Fibers and Nanocelluloses, Molecules. 23 (2018) 1427. https://doi.org/10.3390/molecules23061427.
[120] E. Aytan, M.H. Ugur, N. Kayaman-Apohan, Synthesis, characterization, and ionic conductivity of electrospun organic-inorganic hybrid gel electrolytes, Polym. Eng. Sci. 60 (2020) 619–629. https://doi.org/10.1002/pen.25320.
[121] C. Schramm, B. Rinderer, R. Tessadri, Synthesis and characterization of hydrophobic, ultra-fine fibres based on an organic–inorganic nanocomposite containing a polyimide functionality, Polymers and Polymer Composites. 27 (2019) 268–278. https://doi.org/10.1177/0967391119832408.
[122] J.J. McDowell, N.S. Zacharia, D. Puzzo, I. Manners, G.A. Ozin, Electroactuation of Alkoxysilane-Functionalized Polyferrocenylsilane Microfibers, J. Am. Chem. Soc. 132 (2010) 3236-+. https://doi.org/10.1021/ja9089236.
[123] H. He, J. Wang, X. Li, X. Zhang, W. Weng, G. Han, Silica nanofibers with controlled mesoporous structure via electrospinning: From random to orientated, Materials Letters. 94 (2013) 100–103. https://doi.org/10.1016/j.matlet.2012.12.032.
[124] S.C. Nunes, V. de Zea Bermudez, Structuring of Amide Cross-Linked Non-Bridged and Bridged Alkyl-Based Silsesquioxanes, The Chemical Record. 18 (2018) 724–736. https://doi.org/10.1002/tcr.201700096.
[125] S.S. Park, M. Santha Moorthy, C.-S. Ha, Periodic mesoporous organosilicas for advanced applications, NPG Asia Materials. 6 (2014) e96–e96. https://doi.org/10.1038/am.2014.13.
[126] A. Noureddine, C.J. Brinker, Pendant/bridged/mesoporous silsesquioxane nanoparticles: Versatile and biocompatible platforms for smart delivery of therapeutics, Chemical Engineering Journal. 340 (2018) 125–147. https://doi.org/10.1016/j.cej.2018.01.086.
[127] M. Weinberger, P.-H. Su, H. Peterlik, M. Linden, M. Wohlfahrt-Mehrens, Biphenyl-Bridged Organosilica as a Precursor for Mesoporous Silicon Oxycarbide and Its Application in Lithium and Sodium Ion Batteries, Nanomaterials. 9 (2019) 754. https://doi.org/10.3390/nano9050754.
[128] J. Morell, M. Güngerich, G. Wolter, J. Jiao, M. Hunger, P.J. Klar, M. Fröba, Synthesis and characterization of highly ordered bifunctional aromatic periodic mesoporous organosilicas with different pore sizes, J. Mater. Chem. 16 (2006) 2809–2818. https://doi.org/10.1039/B603458F.
[129] X. Du, X. Li, L. Xiong, X. Zhang, F. Kleitz, S.Z. Qiao, Mesoporous silica nanoparticles with organo-bridged silsesquioxane framework as innovative platforms for bioimaging and therapeutic agent delivery, Biomaterials. 91 (2016) 90–127. https://doi.org/10.1016/j.biomaterials.2016.03.019.
[130] S. Tao, G. Li, J. Yin, Fluorescent nanofibrous membranes for trace detection of TNT vapor, J. Mater. Chem. 17 (2007) 2730–2736. https://doi.org/10.1039/B618122H.

[131] S.-Q. Wang, J.-H. He, L. Xu, Non-ionic surfactants for enhancing electrospinability and for the preparation of electrospun nanofibers, Polymer International. 57 (2008) 1079–1082. https://doi.org/10.1002/pi.2447.

[132] V. Makova, B. Holubova, D. Tetour, J. Brus, M. Rezanka, M. Rysova, J. Hodacova, (1S,2S)-Cyclohexane-1,2-diamine-based Organosilane Fibres as a Powerful Tool Against Pathogenic Bacteria, Polymers. 12 (2020) 206. https://doi.org/10.3390/polym12010206.

[133] L. Bi, Y. Li, S. Wang, Z. Zhu, Y. Chen, Y. Chen, B. Li, Yonggang. Yang, Preparation and characterization of twisted periodic mesoporous ethenylene-silica nanorods., J. Sol-Gel Sci. Technol. 53 (2010) 619–625. https://doi.org/10.1007/s10971-009-2140-x.

[134] Y. Yang, M. Suzuki, S. Owa, H. Shirai, K. Hanabusa, Control of Mesoporous Silica Nanostructures and Pore-Architectures Using a Thickener and a Gelator, J. Am. Chem. Soc. 129 (2007) 581–587. https://doi.org/10.1021/ja064240b.

[135] J.J.E. Moreau, B.P. Pichon, M.W.C. Man, C. Bied, H. Pritzkow, J.-L. Bantignies, P. Dieudonné, J.-L. Sauvajol, A Better Understanding of the Self-Structuration of Bridged Silsesquioxanes, Angewandte Chemie International Edition. 43 (2004) 203–206. https://doi.org/10.1002/anie.200352485.

[136] H. Jin, L. Wang, N. Bing, Mesoporous silica helical ribbon and nanotube-within-a-nanotube synthesized by sol-gel self-assembly, Mater. Lett. 65 (2011) 233–235. https://doi.org/10.1016/j.matlet.2010.09.051.

[137] Y. Zhao, C. Beuchat, Y. Domoto, J. Gajewy, A. Wilson, J. Mareda, N. Sakai, S. Matile, Anion−π Catalysis, J. Am. Chem. Soc. 136 (2014) 2101–2111. https://doi.org/10.1021/ja412290r.

[138] Y. Cao, Y. Duan, L. Han, S. Che, Hierarchical chirality transfer in the formation of chiral silica fibres with DNA-porphyrin co-templates, Chem. Commun. 53 (2017) 5641–5644. https://doi.org/10.1039/c7cc02382k.

[139] W. Zhu, B. Li, L. Bi, S. Wang, W. Zhuang, Y. Li, Yonggang. Yang, Preparation of mesoporous 1,4-phenylene-silica nanorings through a dual-templating approach., Chin. J. Chem. 30 (2012) 144–150. https://doi.org/10.1002/cjoc.201180464.

[140] M.A. Wahab, I. Imae, Y. Kawakami, I. Kim, C.-S. Ha, Functionalized periodic mesoporous organosilica fibers with longitudinal pore architectures under basic conditions, Microporous and Mesoporous Materials. 92 (2006) 201–211. https://doi.org/10.1016/j.micromeso.2005.12.016.

[141] W. Zhuang, L. Bi, M. Zhang, S. Wang, Y. Li, B. Li, Yonggang. Yang, Structural control of mesoporous 1,4-phenylene-silica using the mixture of CTAB/SDS., Chin. J. Chem. 29 (2011) 883–887. https://doi.org/10.1002/cjoc.201190183.

[142] J. Muthu, J. Priscilla, A. Odeshi, N. Kuppen, Characterisation of coir fibre hybrid composites reinforced with clay particles and glass spheres, J. Compos Mater. 52 (2018) 593–607. https://doi.org/10.1177/0021998317712568.

[143] J. Park, R. Subramanian, Interfacial Shear-Strength and Durability Improvement by Monomeric and Polymeric Silanes in Basalt Fiber Epoxy Single-Filament Composite Specimens, J. Adhes. Sci. Technol. 5 (1991) 459–477. https://doi.org/10.1163/156856191X00602.

[144] M. Jimenez, J. Gonzalez-Benito, A.J. Aznar, J. Baselga, Hydrolytic degradation of polysiloxanic coatings on glass fibers, Bol. Soc. Esp. Ceram. Vidr. 39 (2000) 425–430. https://doi.org/10.3989/cyv.2000.v39.i4.791.

[145] X.-C. Zhang, X. Xiong, J. Yu, Z.-X. Guo, Amine-functionalized thermoplastic polyurethane electrospun fibers prepared by co-electrospinning with 3-aminopropyltriethoxysilane and preparation of conductive fiber mats, Polymer. 53 (2012) 5190–5196. https://doi.org/10.1016/j.polymer.2012.09.015.

[146] J. Zhou, F. Liu, X. Dai, L. Jiao, H. Yao, Z. Du, H. Wang, X. Qiu, Surface modification of high-performance polyimide fibres by using a silane coupling agent, Compos. Interfaces. 26 (2019) 687–698. https://doi.org/10.1080/09276440.2018.1526607.

[147] M. Aparicio, J. Mosa, F. Sánchez, A. Durán, Synthesis and characterization of proton-conducting sol-gel membranes produced from 1,4-bis(triethoxysilyl)benzene and (3-glycidoxypropyl)trimethoxysilane, Journal of Power Sources. 151 (2005) 57–62. https://doi.org/10.1016/j.jpowsour.2005.03.042.

[148] F. Si, N. Zhao, L. Chen, J. Xu, Q. Tao, J. Li, C. Ran, A superhydrophobic surface with high performance derived from STA-APTES organic-inorganic molecular hybrid, J Colloid Interface Sci. 407 (2013) 482–487. https://doi.org/10.1016/j.jcis.2013.06.068.

[149] Y. Zheng, X. Kong, I. Usman, X. Xie, S. Liang, G. Cao, A. Pan, Rational design of the pea-pod structure of SiOx/C nanofibers as a high-performance anode for lithium ion batteries, Inorg. Chem. Front. 7 (2020) 1762–1769. https://doi.org/10.1039/D0QI00069H.

[150] V. Maneeratana, J.D. Bass, T. Azais, A. Patissier, K. Valle, M. Marechal, G. Gebel, C. Laberty-Robert, C. Sanchez, Fractal Inorganic-Organic Interfaces in Hybrid Membranes for Efficient Proton Transport, Adv. Funct. Mater. 23 (2013) 2872–2880. https://doi.org/10.1002/adfm.201202701.

[151] B. Oktay, E. Basturk, M.V. Kahraman, N.K. Apohan, Thiol-yne photo-clickable electrospun phase change materials for thermal energy storage, React. Funct. Polym. 127 (2018) 10–19. https://doi.org/10.1016/j.reactfunctpolym.2018.03.018.

[152] D. Dhanapal, A. Muthukaruppan, A.K. Srinivasan, Tetraglycidyl Epoxy Reinforced with Surface Functionalized Mullite Fiber for Substantial Enhancement in Thermal and Mechanical Properties of Epoxy Nanocomposites, Silicon. 10 (2018) 585–594. https://doi.org/10.1007/s12633-016-9496-7.

[153] C. Jia, R. Zhang, C. Yuan, Z. Ma, Y. Du, L. Liu, Y. Huang, Surface modification of aramid fibers by amino functionalized silane grafting to improve interfacial property of aramid fibers reinforced composite, Polymer Composites. 41 (2020) 2046–2053. https://doi.org/10.1002/pc.25519.

[154] X. Zhang, G. Wu, Grafting Halloysite Nanotubes with Amino or Carboxyl Groups onto Carbon Fiber Surface for Excellent Interfacial Properties of Silicone Resin Composites, Polymers. 10 (2018) 1171. https://doi.org/10.3390/polym10101171.

[155] F. Yalcinkaya, A review on advanced nanofiber technology for membrane distillation, Journal of Engineered Fibers and Fabrics. 14 (2019) 1558925018824901. https://doi.org/10.1177/1558925018824901.

[156] R. Rajan, E. Rainosalo, S.P. Thomas, S.K. Ramamoorthy, J. Zavasnik, J. Vuorinen, M. Skrifvars, Modification of epoxy resin by silane-coupling agent to improve tensile properties of viscose fabric composites, Polym. Bull. 75 (2018) 167–195. https://doi.org/10.1007/s00289-017-2022-2.

[157] A.V. Rajulu, L.G. Devi, R.R. Devi, Effect of orientation of fibers and coupling agent on tensile properties of phenolic/silica composites, J. Reinf. Plast. Compos. 27 (2008) 599–603. https://doi.org/10.1177/0731684407079092.

[158] T.A. Otitoju, B.S. Ooi, A.L. Ahmad, Synthesis of 3-aminopropyltriethoxysilane-silica modified polyethersulfone hollow fiber membrane for oil-in-water emulsion separation, React. Funct. Polym. 136 (2019) 107–121. https://doi.org/10.1016/j.reactfunctpolym.2018.12.018.

[159] Z. Yu, X. Min, F. Li, Q. Chen, Synthesis of Ag-SiO2-APTES Nanocomposites by Blending Poly(Vinylidene Fluoride) Membrane with Potential Applications on Dye Wastewater Treatment, Nano. 13 (2018) 1850034. https://doi.org/10.1142/S1793292018500340.

[160] Y. Zhao, J. Qiu, H. Feng, M. Zhang, The interfacial modification of rice straw fiber reinforced poly(butylene succinate) composites: Effect of aminosilane with different alkoxy groups, J. Appl. Polym. Sci. 125 (2012) 3211–3220. https://doi.org/10.1002/app.36502.

[161] M. Irani, A.R. Keshtkar, M.A. Moosavian, Removal of cadmium from aqueous solution using mesoporous PVA/TEOS/APTES composite nanofiber prepared by sol-gel/electrospinning, Chemical Engineering Journal. 200–202 (2012) 192–201. https://doi.org/10.1016/j.cej.2012.06.054.

[162] L. Hu, J. Cheng, Y. Li, J. Litt, J. Zhou, K. Cen, Amino-functionalized surface modification of polyacrylonitrile hollow fiber-supported polydimethylsiloxane membranes, Appl. Surf. Sci. 413 (2017) 27–34. https://doi.org/10.1016/j.apsusc.2017.04.006.

[163] U. Díaz, D. Brunel, A. Corma, Catalysis using multifunctional organosiliceous hybrid materials, Chem. Soc. Rev. 42 (2013) 4083–4097. https://doi.org/10.1039/C2CS35385G.

[164] S.S. Park, C.-S. Ha, Organic–inorganic hybrid mesoporous silicas: functionalization, pore size, and morphology control, The Chemical Record. 6 (2006) 32–42. https://doi.org/10.1002/tcr.20070.

[165] J.-J. Yuan, P.-X. Zhu, N. Fukazawa, R.-H. Jin, Synthesis of nanofiber-based silica networks mediated by organized poly(ethylene imine): Structure, properties, and mechanism, Adv. Funct. Mater. 16 (2006) 2205–2212. https://doi.org/10.1002/adfm.200500886.

[166] M. Shamizadeh, M.B. Gholivand, M. Shamsipur, P. Hashemi, Mercaptopropyl-functionalized nanoporous silica as a novel coating for solid-phase microextraction fibers, Anal. Methods. 7 (2015) 2505–2513. https://doi.org/10.1039/c4ay02826k.

[167] Synthesis of Novel Mesoporous Silica Twist Nanofibers Through Co-condensation Method--《Chemical Journal of Chinese Universities》2012年08期, (n.d.). http://en.cnki.com.cn/Article_en/CJFDTotal-GDXH201208001.htm (accessed April 24, 2020).

[168] C. Gao, S. Ito, A. Obata, T. Mizuno, J.R. Jones, T. Kasuga, Fabrication and in vitro characterization of electrospun poly (gamma-glutamic acid)-silica hybrid scaffolds for bone regeneration, Polymer. 91 (2016) 106–117. https://doi.org/10.1016/j.polymer.2016.03.056.

[169] G. Poologasundarampillai, B. Yu, J.R. Jones, T. Kasuga, Electrospun silica/PLLA hybrid materials for skeletal regeneration, Soft Matter. 7 (2011) 10241–10251. https://doi.org/10.1039/c1sm06171b.

[170] S. Koeda, K. Ichiki, N. Iwanaga, K. Mizuno, M. Shibata, A. Obata, T. Kasuga, T. Mizuno, Construction and Characterization of Protein-Encapsulated Electrospun Fibermats Prepared from a Silica/Poly(gamma-glutamate) Hybrid, Langmuir. 32 (2016) 221–229. https://doi.org/10.1021/acs.langmuir.5b02862.

[171] H.J. Haroosh, Y. Dong, D.S. Chaudhary, G.D. Ingram, S. Yusa, Electrospun PLA: PCL composites embedded with unmodified and 3-aminopropyltriethoxysilane (ASP) modified halloysite nanotubes (HNT), Appl. Phys. A-Mater. Sci. Process. 110 (2013) 433–442. https://doi.org/10.1007/s00339-012-7233-7.

[172] S. Inukai, N. Kurokawa, A. Hotta, Mechanical properties of poly(epsilon-caprolactone) composites with electrospun cellulose nanofibers surface modified by 3-aminopropyltriethoxysilane, J. Appl. Polym. Sci. 137 (2020) 48599. https://doi.org/10.1002/app.48599.

[173] A. Kurniawan, F. Gunawan, A.T. Nugraha, S. Ismadji, M.-J. Wang, Biocompatibility and drug release behavior of curcumin conjugated gold nanoparticles from aminosilane-

functionalized electrospun poly (N-vinyl-2-pyrrolidone) fibers, Int. J. Pharm. 516 (2017) 158–169. https://doi.org/10.1016/j.ijpharm.2016.10.067.

[174] S. Taokaew, M. Phisalaphong, B.Z. Newby, Modification of bacterial cellulose with organosilanes to improve attachment and spreading of human fibroblasts, Cellulose. 22 (2015) 2311–2324. https://doi.org/10.1007/s10570-015-0651-x.

[175] D. Li, W. Nie, L. Chen, Y. Miao, X. Zhang, F. Chen, B. Yu, R. Ao, B. Yu, C. He, Fabrication of curcumin-loaded mesoporous silica incorporated polyvinyl pyrrolidone nanofibers for rapid hemostasis and antibacterial treatment, RSC Adv. 7 (2017) 7973–7982. https://doi.org/10.1039/c6ra27319j.

[176] Y. Liu, Q. Li, H. Liu, H. Cheng, J. Yu, Z. Guo, Antibacterial thermoplastic polyurethane electrospun fiber mats prepared by 3-aminopropyltriethoxysilane-assisted adsorption of Ag nanoparticles, Chin. J. Polym. Sci. 35 (2017) 713–720. https://doi.org/10.1007/s10118-017-1928-3.

[177] Y. Zhang, Y. Jin, H. Yu, P. Dai, Y. Ke, X. Liang, Pore expansion of highly monodisperse phenylene-bridged organosilica spheres for chromatographic application, Talanta. 81 (2010) 824–830. https://doi.org/10.1016/j.talanta.2010.01.022.

[178] A. Dabrowski, M. Barczak, Bridged Polysilsesquioxanes as a Promising Class of Adsorbents. A Concise Review, Croatica Chemica Acta. 80 (2007) 367–380.

[179] E. Doustkhah, H. Mohtasham, M. Hasani, Y. Ide, S. Rostamnia, N. Tsunoji, M. Hussein N. Assadi, Merging periodic mesoporous organosilica (PMO) with mesoporous aluminosilica (Al/Si-PMO): A catalyst for green oxidation, Molecular Catalysis. 482 (2020) 110676. https://doi.org/10.1016/j.mcat.2019.110676.

[180] Y. Iamamoto, H.C. Sacco, J.C. Biazzotto, K.J. Ciuffi, O.A. Serra, Porphyrinosilica and Metalloporphyrinosilica: Hybrid Organic-Inorganic Materials prepared by Sol-Gel Processing, An. Acad. Bras. Cienc. 72 (2000) 59–66. https://doi.org/10.1590/s0001-37652000000100008.

[181] D. Jiang, Q. Yang, H. Wang, G. Zhu, J. Yang, C. Li, Periodic mesoporous organosilicas with trans-(1R,2R)-diaminocyclohexane in the framework: A potential catalytic material for asymmetric reactions, Journal of Catalysis. 239 (2006) 65–73. https://doi.org/10.1016/j.jcat.2006.01.018.

[182] W. Liu, H. Wei, H. Li, Y. Wang, L. Wu, B. Li, Y. Li, Y. Yang, Structurally coloured organic–inorganic hybrid silica films with a chiral nematic structure prepared through a self-templating approach, Liquid Crystals. 0 (2020) 1–5. https://doi.org/10.1080/02678292.2020.1791984.

[183] S. Shylesh, P.P. Samuel, S. Sisodiya, A.P. Singh, Periodic Mesoporous Silicas and Organosilicas: An Overview Towards Catalysis, Catal Surv Asia. 12 (2008) 266. https://doi.org/10.1007/s10563-008-9056-2.

[184] L. Brigo, V. Auzelyte, K.A. Lister, J. Brugger, G. Brusatin, Phenyl-bridged polysilsesquioxane positive and negative resist for electron beam lithography, Nanotechnology. 23 (2012) 325302. https://doi.org/10.1088/0957-4484/23/32/325302.

[185] D.A. Loy, K.J. Shea, Bridged Polysilsesquioxanes. Highly Porous Hybrid Organic-Inorganic Materials, Chem. Rev. 95 (1995) 1431–1442. https://doi.org/10.1021/cr00037a013.

[186] H. Peng, Y. Zhu, D.E. Peterson, Y. Lu, Nanolayered carbon/silica superstructures via organosilane assembly, Adv. Mater. 20 (2008) 1199-+. https://doi.org/10.1002/adma.200701303.

[187] S. Kalia, Y. Haldorai, Organic-Inorganic Hybrid Nanomaterials, Springer, 2014.

[188] Z. Yang, Z. Niu, X. Cao, Z. Yang, Y. Lu, Z. Hu, C.C. Han, Template synthesis of uniform 1D mesostructured silica materials and their arrays in anodic alumina membranes, Angew Chem Int Ed Engl. 42 (2003) 4201–4203. https://doi.org/10.1002/anie.200250808.

[189] D.S. de Almeida, L.D. Martins, E.C. Muniz, A.P. Rudke, R. Squizzato, A. Beal, P.R. de Souza, D.P.F. Bonfim, M.L. Aguiar, M.L. Gimenes, Biodegradable CA/CPB electrospun nanofibers for efficient retention of airborne nanoparticles, Process Saf Environ Prot. 144 (2020) 177–185. https://doi.org/10.1016/j.psep.2020.07.024.

[190] Z. Zhang, Synthesis of Dendritic Polyaniline Nanofibers in a Surfactant Gel, (2004). https://doi.org/10.1021/ma035891k.

[191] J. Lin, C. Peng, S. Ravi, A.K.M.N.A. Siddiki, J. Zheng, K.J. Balkus, Biphenyl Wrinkled Mesoporous Silica Nanoparticles for pH-Responsive Doxorubicin Drug Delivery, Materials. 13 (2020) 1998. https://doi.org/10.3390/ma13081998.

[192] Y. Li, A. Keilbach, M. Kienle, Y. Goto, S. Inagaki, P. Knochel, T. Bein, Hierarchically structured biphenylene-bridged periodic mesoporous organosilica, J. Mater. Chem. 21 (2011) 17338–17344. https://doi.org/10.1039/c1jm12023a.

[193] P. Masse, L. Vellutini, B. Bennetau, M.A. Ramin, F. Fournel, L. Blanc, C. Dejous, D. Rebiere, P. Weisbecker, J.-P. Pillot, Chimie douce route to novel acoustic waveguides based on biphenylene-bridged silsesquioxanes, J. Mater. Chem. 21 (2011) 14581–14586. https://doi.org/10.1039/c1jm11866h.

[194] Z. Olejniczak, M. Łęczka, K. Cholewa-Kowalska, K. Wojtach, M. Rokita, W. Mozgawa, 29Si MAS NMR and FTIR study of inorganic–organic hybrid gels, Journal of Molecular Structure. Complete (2005) 465–471. https://doi.org/10.1016/j.molstruc.2004.11.069.

[195] R. Al-Oweini, H. El-Rassy, Synthesis and characterization by FTIR spectroscopy of silica aerogels prepared using several Si(OR)4 and R″Si(OR′)3 precursors, Journal of Molecular Structure. 919 (2009) 140–145. https://doi.org/10.1016/j.molstruc.2008.08.025.

[196] R.M. Almeida, C.G. Pantano, Structural investigation of silica gel films by infrared spectroscopy, Journal of Applied Physics. 68 (1990) 4225–4232. https://doi.org/10.1063/1.346213.

[197] P. Massé, L. Vellutini, B. Bennetau, M.A. Ramin, F. Fournel, L. Blanc, C. Dejous, D. Rebière, P. Weisbecker, J.-P. Pillot, Chimie douce route to novel acoustic waveguides based on biphenylene-bridged silsesquioxanes, J. Mater. Chem. 21 (2011) 14581–14586. https://doi.org/10.1039/C1JM11866H.

[198] H. Dong, Z. Zhang, M.H. Lee, D.W. Mueller, R.F. Reidy, Sol-gel polycondensation of methyltrimethoxysilane in ethanol studied by 29Si NMR spectroscopy using a two-step acid/base procedure, Journal of Sol-Gel Science and Technology. 41 (2007) 11–17. https://doi.org/10.1007/s10971-006-0115-8.

[199] J. Brus, J. Karhan, P. Kotlík, 29Si NMR study of distribution of oligomers in polycondensation of tetraethoxysilane, Collection of Czechoslovak Chemical Communications. 61 (1996) 691–703. https://doi.org/10.1135/cccc19960691.

[200] F. Huang, B. Motealleh, W. Zheng, M.T. Janish, C.B. Carter, C.J. Cornelius, Electrospinning amorphous SiO2-TiO2 and TiO2 nanofibers using sol-gel chemistry and its thermal conversion into anatase and rutile, Ceramics International. 44 (2018) 4577–4585. https://doi.org/10.1016/j.ceramint.2017.10.134.

[201] Y. Fatieiev, J.G. Croissant, K. Julfakyan, L. Deng, D.H. Anjum, A. Gurinov, N.M. Khashab, Enzymatically degradable hybrid organic–inorganic bridged silsesquioxane nanoparticles for in vitro imaging, Nanoscale. 7 (2015) 15046–15050. https://doi.org/10.1039/C5NR03065J.

[202] C.R. Morcombe, K.W. Zilm, Chemical shift referencing in MAS solid state NMR, Journal of Magnetic Resonance. 162 (2003) 479–486. https://doi.org/10.1016/S1090-7807(03)00082-X.

11. SUPPLEMENTARY MATERIALS

11.1 Solid-state NMR experimental conditions

All solid-state NMR spectra were recorded at 11.7 T using a Bruker AVANCE III HD spectrometer. The 3.2-mm and 4-mm probes were used for ^{13}C (Larmor frequency of 125.783 MHz) and ^{29}Si (Larmor frequency of 99.367 MHz) experiments, respectively. The ^{13}C NMR chemical shift was calibrated using α-glycine (^{13}C: 176.03 ppm; carbonyl signal) as an external standard [200] and ^{29}Si NMR spectra were referenced to the external standard M_8Q_8 (^{29}Si: -109.8 ppm). The ^{13}C MAS NMR spectra were acquired at the speed of the sample rotation of 20 kHz using a 10 s recycle delay and a number of scans of 4096. The ^{29}Si CP/MAS NMR spectra were recorded at the magic angle spinning (MAS) rate of 7 kHz with a number of scans of 4096. For the recording of ^{29}Si CP/MAS NMR spectra, a 5 s recycle delay and 5 ms cross-polarization (CP) contact time were used. In all cases, high-power ^{1}H decoupling (SPINAL64) was used for the removal of heteronuclear coupling.

The samples were placed into ZrO_2 rotors and subsequently kept at room temperature. All NMR experiments were measured under active cooling in order to compensate for the frictional heating caused by the spinning of the samples. All experiments were performed at a temperature of 298 K. For the processing and deconvolution of the spectra, the Bruker TopSpin 3.2 pl5 software package was used.

All liquid state ^{1}H NMR spectra were measured using a JEOL JNM-ECZR 500 MHz spectrometer at the Chemical Technology Institute in Prague. Deuterated solvent dimethylsulfoxide (DMSO-d_6) was used as a solvent for both of the analyzed hybrid organosilane precursors (OBA and BiTSAB).

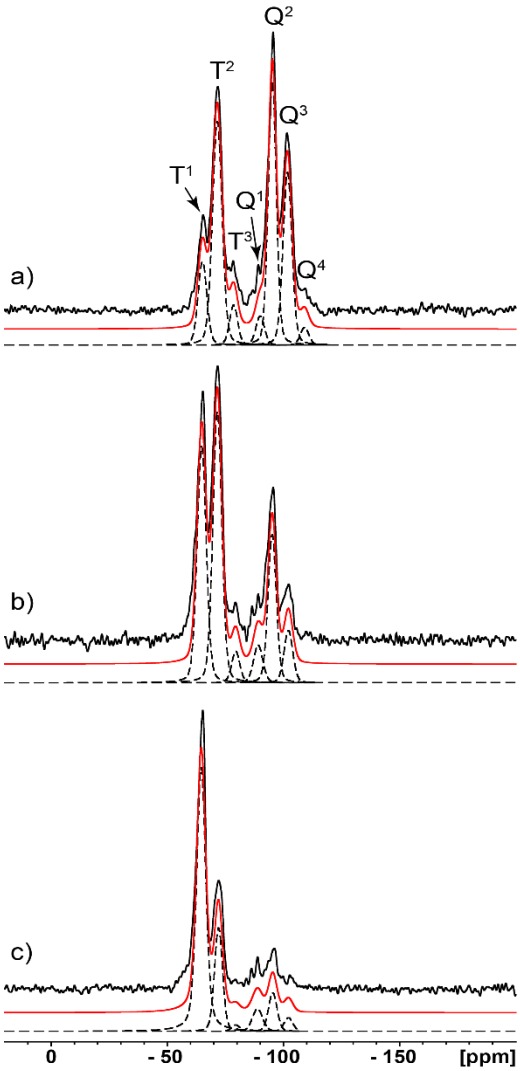

Figure S1. Experimental ^{29}Si CP/MAS NMR spectra (black solid line), simulations of the individual Si atoms (black dashed lines), and their sum (red solid line) of fibrous samples BTEBP 25 mol.% (a); BTEBP 50 mol.% (b), BTEBP 75 mol.% (c).

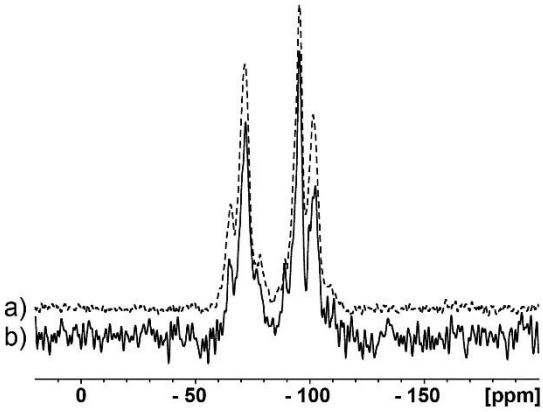

Figure S2. Comparison of ^{29}Si CP/MAS (a) and ^{29}Si MAS (b) NMR spectra of the BTEBP 25 mol.% fibrous sample.

11.2 Conditions of the TGA-IR process

The samples were analyzed via a Q500 thermogravimetric analyzer (TA Instruments, New Castle, USA). Each sample was placed on a platinum pan and analyzed in a non-reactive atmosphere of nitrogen and/or synthetic air (SA) with a flow rate of 60 ml/ min. The samples were heated at 10 °C/min, the range was from 20 °C to 650 °C and 20 °C to 800 °C. The thermal decompose products were analyzed by a FT-IR spectrometer (Nicolet iS10, Thermo Scientific, USA). The spectra were taken every 10 s with a resolution of 2 cm^{-1} in the spectral range of 4000–650 cm^{-1} [9].

11.3 Conditions of the scanning electron microscopy analyses

The samples and their morphologies were studied by SEM (ZEISS, Sigma Family, DE). All of the samples were sputtered with a 2-nm platinum layer and were subsequently viewed as secondary electron images (1 kV). The NIS Elements software (LIM s.r.o., CZ) was used to determine the fiber diameters. The diameters were assessed from a total of 100 measurements per material, taken from five independent images.

11.4 Conductivity of the other tested organosilane fibrous samples

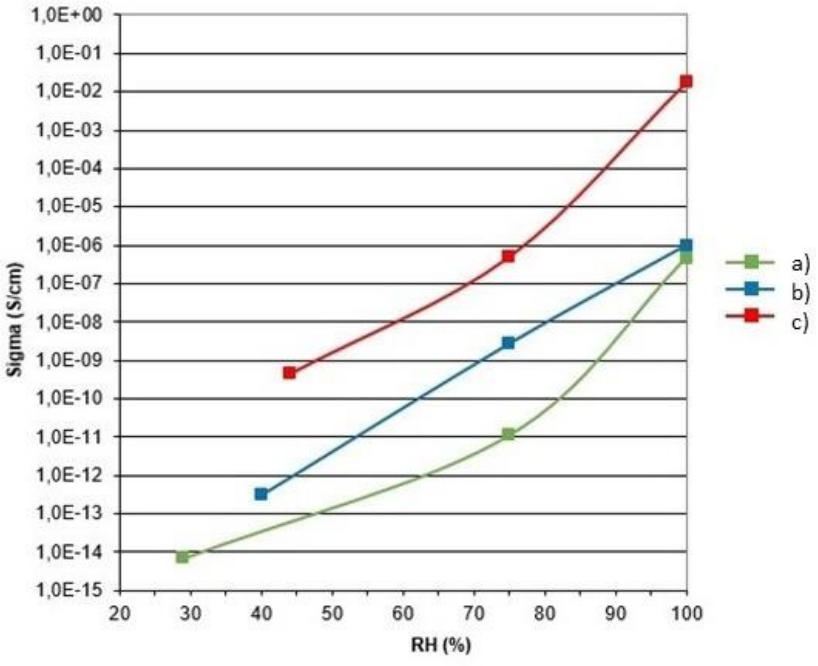

Figure S3. The dependence of specific electrical conductivity on the relative humidity of the environment of hybrid pure organosilane fibers **a)** with molar ratio of BTEBP:TEOS 25 mol.% : 75 mol.%; **b)** with a molar ratio of triethoxyphenyl silane (TEPS):TEOS in the sol of 75

mol.%:25 mol.%; **c)** with a molar ratio of 1,4-bis(triethoxysilyl) benzene (BTEB):TEOS in the sol of 75 mol.%:25 mol.%.

11.5 Reprints of articles

The scientific articles below fully describe the process leading to the preparation of purely organosilane fibers including their characterization and potential applications, which the author together with her colleagues published during 2020. These are the first studies describing the preparation of such types of organosilane fibers, containing hybrid precursors covalently bonded via Si-C bonds inside the silica matrix in a relatively high molar ratio achieving up to 50 mol.%.

The first article entitled: ***"Novel chapter in hybrid materials One-pot synthesis of purely organosilane fibers"***, deals in detail with the whole process of preparing pure organosilane nanofibers using sol-gel and electrospinning. The two types of organosilane precursors (organo-mono-silylated precursor phenyltriethoxysilane and organo-bis-silylated precursor 1,4-bis(triethoxysilyl) benzene were intensively studied from the point of view of the ability to form fibers. In both cases, the hybrid precursors are commercially available and are usually used for the formation of catalytic systems based on periodic mesoporous organosilica (PMOs), or they are prepared in the form of thin films for use in optical devices.

This article brings a completely new point of view and knowledge to the preparation of purely organosilane fibers. Furthermore, the article describes the significant differences between the fibers formed from commercially available organo-mono-silylated and/or organo-bis-silylated precursors and proposes their application potential.

The second article entitled: *"*(***1S,2S)-Cyclohexane-1,2-diamine-based organosilane fibres as a powerful tool against pathogenic bacteria"*** provides new knowledge related to the formation of organosilane fibers from a synthesized organosilane precursor. The article widely discusses the issues related to health-care-associated infections caused by pathogenic bacteria, particularly *Staphylococcus aureus* and *Pseudomonas aeruginosa*. The fibers formed from (1*S*,2*S*)-1,2-Bis{*N'*-[3-(triethoxysilyl)propyl]ureido}cyclohexane at a high molar ratio (43 mol.%) were fully characterized by various techniques including solid state NMR. Moreover, according to results the obtained from the biomedical field, these organosilane fibers may find a strong potential in the area of tissue engineering/regenerative medicine and wound care therapy due to their properties.

The third article entitled: ***"Hybrid organosilane fibrous materials and their contribution to modern science"*** provides an overview of the preparation of the various types of hybrid

organosilane fibers via various techniques including electrospinning. The theoretical part of this habilitation thesis is mainly based on the below-presented review article, which is extended in detail in this part of the thesis.

11.6 National and international patent application forms (Czech Republic, Europe)

Both patent application forms are presented following the reprints of the above-mentioned articles.

Polymer 190 (2020) 122234

Contents lists available at ScienceDirect

Polymer

journal homepage: http://www.elsevier.com/locate/polymer

Novel chapter in hybrid materials: One-pot synthesis of purely organosilane fibers

Barbora Holubová [a], Veronika Máková [a,*], Jana Müllerová [a], Jiří Brus [b], Kristýna Havlíčková [c], Věra Jenčová [d], Alena Michalcová [e], Johana Kulhánková [a], Michal Řezanka [a]

[a] Department of Nanomaterials in Natural Science, Institute for Nanomaterials, Advanced Technologies and Innovation, Technical University of Liberec, Studentská 1402/2, 461 17, Liberec, Czech Republic
[b] Institute of Macromolecular Chemistry, Academy of Sciences of the Czech Republic, Heyrovsky Sq. 2, 162 06, Prague, Czech Republic
[c] Department of Nonwovens and Nanofibrous Materials, Faculty of Textile Engineering, Technical University of Liberec, Studentská 1402/2, 461 17, Liberec, Czech Republic
[d] Department of Chemistry, Faculty of Science, Humanities and Education, Technical University of Liberec, Studentská 1402/2, 461 17, Liberec, Czech Republic
[e] Department of Metals and Corrosion Engineering, University of Chemistry and Technology, Prague, Technická 5, 166 28, Praha, Czech Republic

ARTICLE INFO

Keywords:
Organosilane fibers
Sol-gel process
One-pot synthesis
Electrospinning
Organic-inorganic hybrids

ABSTRACT

Despite the extensive literature on organosilane hybrid materials, there are very few reports on the preparation of purely organosilane non-woven fibrous mats. Nevertheless, their use in various application fields may be of great importance regarding the global issue of polymer fibers and the toxicity of other compounds used so far in the composite polymer-organosilane fiber-manufacturing process. The greatest obstacle seems to be the supposed difficulty in the polymerization of organosilanes in a spinnable polymeric solution. In this work, we report the one-pot synthesis of electrospun organosilane fibers without any kinds of surfactants, low-molecular-weight polymeric gelators or spinnable polymers. The purely organosilane fibrous mats were prepared only via a suitable adjustment of the sol-gel processing parameters and were successfully produced an industrial electrospinning device, promising possible fabrication on a large scale. Moreover, the use of two differently-structured model benzene functionalized organoalkoxysilanes proves the possibility of designing a molecularly engineered material tailored to specific applications. These organosilane fibrous mats seem to be promising in various application fields, such as reusable catalysts, adsorption or conducting membranes or as novel biomaterials. This latter of these areas was preliminarily studied herein.

1. Introduction

Novel hybrid materials currently play a major role in the development of advanced functional materials in many fields of human activity. In particular, the possibilities of nanoscale molecular engineering of organosilane hybrids are becoming one of the most intriguing challenges of scientific research [1–5]. The family of organosilane hybrids is already well known to academics and has been successfully commercialized on an industrial level since the end of the 1950s, but its potential still remains undepleted [1,5]. The reason for such interest undoubtedly resides in the molecular versatility of the organosilane structure, maneuverable with many synthetic strategies to produce a waste range of chemical arrangements, mixed composites, and geometries with a variety of end-products [1–5].

The inorganic skeleton of the organosilanes, consisting of a polysiloxane backbone (Si–O–Si), is modified through a strong covalent Si–C bond with various organic moieties by starting from a variety of organoalkoxysilane precursors. The already well-established synthetic route leading to nanocrystalline or nanoscaled amorphous organosilane materials is one of the wet chemical methods – the sol-gel process [1–5]. Its mild processing conditions ensure the formation of an organic-inorganic polymeric network, which combines the most important properties of their constituents: low processing temperatures (polymer-like) and sufficient thermal stability (silicone-like) [6]. Altogether with the unique

* Corresponding author.
E-mail addresses: barbora.holubova@tul.cz (B. Holubová), veronika.makova@tul.cz (V. Máková), jana.mullerova@tul.cz (J. Müllerová), brus@imc.cas.cz (J. Brus), kristyna.havlickova@tul.cz (K. Havlíčková), vera.jencova@tul.cz (V. Jenčová), alena.michalcova@vscht.cz (A. Michalcová), johana.kulhankova@tul.cz (J. Kulhánková), michal.rezanka@tul.cz (M. Řezanka).

https://doi.org/10.1016/j.polymer.2020.122234
Received 18 November 2019; Received in revised form 21 January 2020; Accepted 26 January 2020
Available online 30 January 2020
0032-3861/

availability of the respective organoalkoxysilane precursors, a fine engineering control over structural and physical and chemical properties such as porosity, surface tension, chemical resistance and opto-electronic properties in the resulting organosilane material can be provided. Due to stable Si–C bonds, no phase segregation at longer length scales can occur, assuring the stability of the above-mentioned properties. Nowadays, the relative safety and ecological non-toxicity of organosilane precursors and organosilane end-products should also be taken into consideration [1–6].

1.1. In search of purely organosilane fibers

Many outstanding reviews have summarized the state of the art in the field of organosilane materials [1,3,5,7–9]. Those materials are found particularly in the form of nanoparticles or thin coatings on various substrates. Surprisingly, the preparation of purely organosilane fibers and their further applications are rarely reported [10,11]. Moreover, in most cases, composite organosilane fibers were prepared via a combination of organosilanes mixed with organic polymers [7,9,12,13]. However, these composite materials are less ecological and may have a negative effect on the overall performance of such a material (e.g. in the biomedicine application field) as for its fabrication, various inappropriate solvents and precursors are necessary [7,9,12–15].

Most studies related to electrospun polymer-organosilane composite nanofibers and their application in biomedicine are focused on tissue engineering and regenerative medicine [7,9,12,14,15]; e.g. nanofibrous composite polymer-organosilane scaffolds [16–20]. The fibrous organosilane materials designed for other purposes are again only modestly reported and refer mainly to polymer-organosilane composites. Fibrous organosilane hybrids have been prepared via the self-assembly process, e.g. in combination with low-molecular-weight polymeric gelators (LMWGs template) [21–23], but they failed to display good stability after their removal. Other self-assembled organosilane mesoporous fibers were reported by Wahab et al. [24]. However, this material is not fibrous in the sense of a non-woven textile, but rather in the sense of relatively short fiber-like structures growing up from the nanoparticles. The composite polymer-organosilane fibers were also prepared via the drawing technique [25,26] or electrospinning, where many scientific groups reported either the preparation of purely silica fibers or again polymer composites with different organosilane coupling agents [7,9,12,14,27,28]. As an example, electrospun polymer-organosilane fibrous mats were prepared via the sol-gel process for catalytic and separation applications [29,30] or via free-radical polymerization [31]. Likewise, highly porous electrospun organosilane fibers for electrochemical sensing applications were prepared with an organic polymer used as a fiber-forming agent template subsequently removed by ethanol washing [32].

The closest formulas to our objective are described in two solitary research papers by Tao et al. [10] and Schramm et al. [11]. The first group [10] dealt with the fabrication of electrospun purely organosilane fluorescent nanofibrous membranes for trace detection of TNT vapor. However, their final materials contained very low amounts of organosilanes (10^{-4} mol %) to TEOS (i.e. the result was mainly silica fibers). The second group [11] prepared organosilane fibers based on the copolycondensation of two organosilanes via the sol-gel process. In this case, the solution had to be adjusted before electrospinning with a non-ionic surfactant Triton X-100 to improve the spinnability, which inevitably remained in the hybrid structure [11,33].

To summarize, the most problematic issue in the fiber formation of organosilane hybrid materials appears to be the spinnability of the organosilane sol solution due to the difficulties with the suitable polymerization of organosilanes in long spinnable polymeric chains.

1.2. Molecular engineering concept

Organosilane nanofibers are prepared from organo-mono-silylated precursors (Fig. 1a) or with their bridged organo-bis-silylated analogues (Fig. 1b). This choice is made because of the assumption that each type of organosilane precursor will have a different impact on the resulted final properties of the prepared fibers (see in Fig. 1) [1,3,4]. While mono-silylated organosilane precursors are supposed to behave in the final structure as so-called network modifiers, bridged bis-silylated organosilane precursors are known to be so-called network builders [1,3–6,34].

Hence, this project deals with the preparation of fibers with a purely organosilane composition, where particular interest is placed on a suitable choice of sol-gel processing parameters in regard to the spinnability of the electrospun solution and the possibilities of nanoscale molecular engineering of organosilane hybrid materials. Benzene functionalized organo-mono-silylated and bridged organo-bis-silylated precursors were chosen as model organosilane precursors in combination with a tetraethoxysilane (TEOS) precursor at different ratios. No surfactants, low-molecular-weight polymeric gelators or spinnable polymers were used during the subsequent electrospinning process, and the whole one-pot synthesis is based on one solvent solution to minimize the toxicity during fiber formation or the application of fibers. Moreover, two electrospinning methods were employed. Beside the lab-scale needle-electrospinning technique, a Nanospider industrial roller electrospinning machine was also used to prove that organosilane fibers have the potential to be produced at industrial scales. To our knowledge, we are the first to fabricate a purely organosilane nanofibrous material based on functionalized polysilsesquioxanes with no polymeric or spinnability-enhancing additives.

2. Experimental part

2.1. Materials

Tetraethylorthosilicate – TEOS (98%, Merck, DE), triethoxyphenylsilane (marked as MONO, 98%, Merck, DE), 1,4-bis(triethoxysilyl)benzene (marked as BIS, 96%, Merck, DE), ethanol – EtOH (99.9%, Penta, CZ), hydrochloric acid – HCl (35%, Penta, CZ), deionized water – H_2O (Milli-Q, CZ). Aluminum foil with a thickness of 12 μm was supplied from Rotilabo, DE.

2.2. General sol synthesis

The standard procedure for the synthesis of organosilane sol solution in ethanol was as follows. A silica precursor composed of TEOS, various molar ratios of organosilane modifiers: either organo-mono-silylated or bridged organo-bis-silylated precursor (MONO and BIS; in 25, 50, and 75% molar ratio to TEOS) ethanol, deionized water and HCl were add into a 50 ml round bottom flask and stirred at 450 rpm for 30 min at r.t. (Table 1 and Fig. 2). The pH of the sols was adjusted to 2. Finally, the sols were heated up to 90 °C in an oil bath at 450 rpm and refluxed. The sols containing the triethoxyphenylsilane were heated for 48 h. On the contrary, the sols containing 1,4-bis(triethoxysilyl)benzene were heated only for 4 h. The dynamic viscosity was measured before the electrospinning and appropriately adjusted. Hybrid fibers were electrospun according to the conditions mentioned in Table 2 and finally dried for 24 h in a desiccator for further use.

2.3. Electrospinning apparatus for organosilane fiber processing

Hybrid fibers were prepared via two different electrospinning techniques. In the case of jet needle electrospinning, the sol was fed into a syringe (5 ml; needle thickness 1.2 mm) by infusion (ONE Syringe Pump (Darwin Microfluidics, FR)) at a feeding rate interval (0.5–0.9 ml/h). For the other parameters see Table 2. Likewise, a Nanospider (Elmarco s.r.o., CZ) industrial roller electrospinning machine was used to examine the fabrication of the nanofibers on an industrial scale (for the parameters see Table A1 - Supplement).

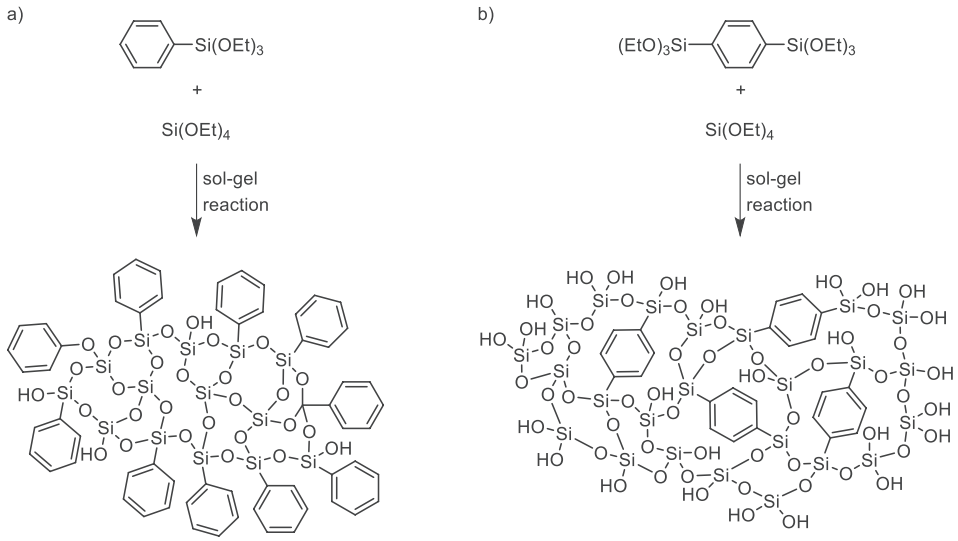

Fig. 1. The role of organically functionalized trialkoxysilanes in the silicon-based sol-gel process [1]: a) use of organo-mono-silylated precursors; b) use of bridged organo-bis-silylated precursors.

Table 1
Sols tested in electrospinning.

Sol	Marked as	Molar ratio r = [H_2O]/[silanes]	Molar ratio Alc = [EtOH]/[silanes]	Sol	Marked as	Molar ratio k = [H_2O]/[silanes]	Molar ratio Alc = [EtOH]/[silanes]
Sol 1	MONO25	2.0	3.2	Sol 4	BIS25	2.0	6.4
Sol 2	MONO50	2.0	3.4	Sol 5	BIS50	2.0	9.6
Sol 3	MONO75	2.0	3.8	Sol 6	BIS75	2.0	13.0

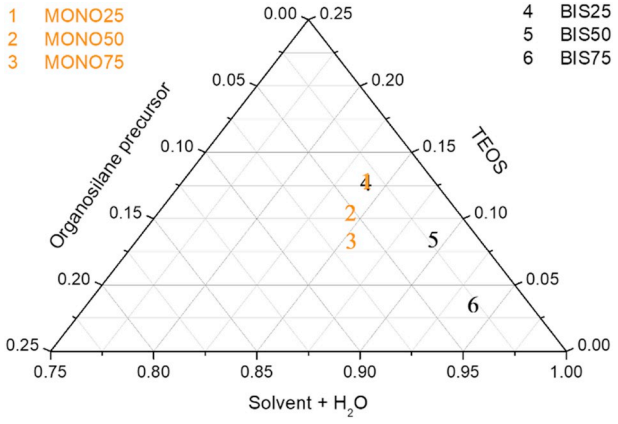

Fig. 2. Organosilane precursor, TEOS, and solvent + H_2O molar compositional relationship of the presented organosilane fibers.

Table 2
Conditions employed for the jet needle-electrospinning.

Viscosity [mPa.s]	Feeding rate [ml. h^{-1}]	Tip-to-collector distance [cm]	High Voltage [kV]	Temperature [°C]	Humidity [Rh %]
40–60	0.5–0.9	15–20	20–40	24	29

2.4. Characterization techniques

2.4.1. FT-IR

A FTIR Spectrometer Nicolet iZ10 (Thermo Fisher Scientific, USA) with an ATR diamond crystal angle of 45° and a spectral range of 4000–700 cm^{-1} was used for the analysis. All of the samples were analyzed after the ethanol evaporation. Number of sample scans: 16, number of the background scans: 32, resolution: 4 cm^{-1}, gain: 4.0, apodization: Happ-Genzel, correction: atmospheric suppression, baseline.

2.4.2. Scanning electron microscopy

The morphologies of the samples were studied by SEM (ZEISS, Sigma Family, DE). All of the samples were sputtered with a 2-nm platinum layer, and were subsequently viewed as secondary electron images (1 kV). The fiber diameter was characterized using NIS Elements software (LIM s.r.o., CZ) and was assessed from a total of 100 measurements per material, taken from five independent images.

2.4.3. Transmission electron microscopy

The microstructure was examined with a transmission electron microscope (EFTEM Jeol 2200 FS) operated at 200 kV. All of the samples were dispersed in an alcoholic solution and measured when placed on the support 300 mesh grid or after preparation of the ultrathin fibrous mats via ion sputtering using Gatan PIPs device. The diffraction pattern and energy-dispersed spectroscopy (EDS) were measured and evaluated for all of the samples.

2.4.4. Solid-state NMR

All solid-state NMR spectra were measured at 11.7 T using a Bruker AVANCE III HD WB/US NMR spectrometer (DE) in a double-resonance 4-mm probe head at spinning frequencies $\omega_r/2\pi = 7$ and 10 kHz. In all cases, finely powdered dry samples were placed into 4-mm ZrO_2 rotors. All of the experiments were conducted at 303 K. The ^{13}C CP/MAS NMR spectra employing cross-polarization (CP) were acquired using the standard pulse scheme at MAS of 10 kHz. The optimized recycle delay was 2 s and the cross-polarization contact time was 1.75 ms. The spectra were referenced to α-glycine (176.03 ppm). The ^{29}Si CP/MAS NMR spectra were recorded at MAS of 7 kHz. The spectra were referenced to

the external standard M_8Q_8 (−109.8 ppm). The number of scans was 0.5 - 5 k depending on the amount of the sample. For quantitative analysis and deconvolution of ^{29}Si CP/MAS NMR spectra, the TopSpin 3.6 program package (Bruker) was used [35].

2.4.5. TGA-FTIR

The samples were analyzed via a Q500 thermogravimetric analyzer (TA Instruments, New Castle, USA). Each sample was placed on a platinum pan and analyzed in the non-reactive atmosphere of nitrogen with a flow rate of 60 ml/min. The samples were heated 10 °C/min, the range was from 20 °C to 650 °C. The thermal decompose products were analyzed by a FT-IR spectrometer (Nicolet iS10, Thermo Scientific, USA). Spectra were taken every 10 s with a resolution of 2 cm^{-1} in the spectral range of 4000–650 cm^{-1}.

2.4.6. Nitrogen adsorption

A gas sorption analyzer (Autosorb® iQ, Quantachrome Instruments, USA) was used to determine the specific surface areas of the prepared fibrous samples. Samples BIS25, BIS50 and BIS75 were degassed in a vacuum at 300 °C/24 h, samples MONO25 and MONO50 were degassed in a vacuum at 200 °C/24 h and sample MONO75 was degassed only at 90 °C/24 h, due to its low thermal stability. The specific surface areas were calculated based on multipoint BET (Brunauer–Emmett–Teller) theory using ASiQwin software.

2.4.7. Analysis of protein (HSA) adsorption

Interactions of human serum albumin (HSA) protein (Merck; CZ) with the prepared materials were tested using HSA solution (5 mg/ml, in PBS with pH 7.4). 10 mg samples (MONO25, MONO50, MONO75, BIS25, BIS50 and BIS75) were incubated in 1 ml of HSA solution at 37 °C/1 h. The samples were then washed in PBS followed by desorption of proteins. The desorption was carried out in 1 ml of PBS solution containing 1% sodium dodecyl sulfate (SDS) (Merck; CZ), and the samples were gently agitated for 1 h at r.t. The protein solutions after desorption were analyzed by electrophoresis (SDS-PAGE, Bio Rad; CZ) and by liquid chromatography. The experiment was carried out in triplicate. For SDS-PAGE, 10 μl of each sample was diluted (1:1) in a loading buffer (0.15 M Tris.HCl, pH 6.8, 30% glycerol (*v/v*)), 15% β-mercaptoethanol (*v/v*), 1% SDS (*w/v*), 0.01% bromophenol blue (*w/v*)). 20 μl of the prepared samples were run using 10% gel (2 h, 110 V) with a wide-range molecular weight marker (protein wide range MW Marker, Amresco, USA). Subsequently, the gels were stained with Coomassie blue solution (2.5% Coomassie brilliant blue R-250 (*w/v*) in 45% methanol (*v/v*) and 10% acetic acid (*v/v*)) and were evaluated after being washed several times in a destaining solution (45% methanol (*v/v*) and 10% acetic acid (*v/v*)). The protein contents in the solutions from the wash step were determined using the Bradford protein assay. 20 μl of samples after washing were mixed in a 96 well plate with 180 μl of Bradford solution (Merck; CZ) and incubated at r.t. for 5 min. The absorbance of the solutions was then measured by a Spark spectrophotometer (TECAN, CZ) at 595 nm. The HSA concentration was calculated using the BSA calibration curve.

3. Results and discussion

3.1. Synthesis and processing of hybrid organosilane fibers

In general, the overall morphology and diameter of electrospun fibers depends on several processing parameters: the polymer solution (chemical nature and average molecular weight, solvent, viscosity and conductivity) and the spinning conditions (high voltage (HV), tip-to-collector distance (TCD), type and diameter of the nozzle, feeding rate, temperature and humidity) [11].

3.1.1. Sol-gel process

To produce an electrospinnable organosilane polymer solution, several processing parameters of the sol-gel process have to be taken into consideration. With standard tetraalkoxysilane precursors ($Si(OR)_4$), the alkoxy group hydrolyzes to particles containing silanol Si–OH groups (sol, eq. (1)), which condensate to a 3D polysiloxane (-Si-O-Si-) polymeric network that is filled with a solvent (gel, eqs. (2) and (3)) [1,4–6,11,34].

$$\equiv Si - OR + H_2O \xrightarrow{hydrolysis} \equiv Si - OH + ROH \quad (1)$$

$$\equiv Si - OR + HO - Si \equiv \xrightarrow[condensation]{alcohol} \equiv Si - O - Si \equiv + ROH \quad (2)$$

$$\equiv Si - OR + HO - Si \equiv \xrightarrow[condensation]{water} \equiv Si - O - Si \equiv + H_2O \quad (3)$$

As a standard starting point to produce organosilane hybrids, mixtures of tetraalkoxysilanes and trialkoxysilanes (organo-mono-silylated R^1-Si-$(OR^2)_3$ or bridged organo-bis-silylated trialkoxides $(R^2O)_3$–Si-(R^1)-Si-$(OR^2)_3$) were used. A dense silicon oxide network is ensured by the hydrolysis/condensation reactions of tetraalkoxides and the incorporation of organic functional groups by trialkoxides leads to the formation of hybrid materials [3]. Hydrolysis and the subsequent condensation of organo-trialkoxides result in the formation of silsesquioxanes having the basic repeating unit [$RSiO_{1.5}$]. However, the resulting material depends on many sol-gel processing parameters, primarily: molar ratio r = [H_2O]/[silanes], catalysis, amount and type of solvents and steric or inductive effects of the used silane precursors [1,3–6,11,34].

The problems with silica fiber sol-gel preparation were reported in several studies [11,27,34,36–39]. In general, the sols appear to be spinnable when hydrolysis is suppressed so the condensation rate and extent of branching are low enough to increase the concentration and viscosity of polymers without premature gelation. In order to achieve the spinnability, a combination of acid-catalyzed conditions with r less than 2 (Table 1) is recommended resulting in the development of a ladder-like crosslinking between the linear polymer chains [11,27,34,36–39]. On the basis of these findings, all of the compositions were adjusted to $r = 2$ and pH 2.

In order to prepare spinnable organosilane sols, several of the sol-gel processing parameters were adjusted. With respect to the mechanism of the acid-catalyzed sol-gel process, we examined different protic solvents [34]. Isopropyl alcohol was used presuming that the sterically more important alcoholic molecule would prevent agglomeration and decelerate the sol to gel reaction due to different molecular weights and steric hindrance of the chosen organosilane precursors. As the solvent also has to be chosen correctly to overcome the immiscibility of water and silane precursors, ethanol was studied for better immiscibility with the intermediates of the ongoing sol-gel reaction. After preliminary experiments, ethanol was chosen for its ability to shorten the time of polycondensation and its better spinnability. In order to further shorten the polycondensation time from weeks to days or hours, the sols were also refluxed at a higher temperature. Regarding the boiling points of all of the compounds, the temperature was set to 90 °C.

In all cases, several polycondensation times were examined until the sol was spinnable without premature gelling, i.e. presumably ladder-like weakly branched organosilane polymer structures were formed [11,34,36]. This study revealed that this parameter is strongly dependent on the type and amount of the organosilane precursor used. Compared to compositions with the organo-mono-silylated precursor, the sol consisting of TEOS + organo-bis-silylated precursor required a shorter polycondensation time, but a greater amount of solvent with an increased molar ratio of the organosilane precursor to TEOS (Fig. 2). The shorter time of polycondensation is presumably related to the twofold number of hydrolysable units within the organo-bis-silylated precursor molecule. Together with a longer molecule, the polymer growth is faster. However, predominantly linear polymer chains (as set by the low pH catalysis and low water content) containing large para-substituted phenylene groups are at some point too bulky, preventing further condensation and the solutions tended to rapidly gel. This behavior is

enhanced with the increasing molar ratio of the bis-organo-silylated precursor in the reaction. An increased amount of solvent could overcome these limitations as the addition of a homogenizing agent most probably works as a prevention against liquid-liquid phase separation and hence promotes network formation. The difference between the compositional impact of the mono and bis-organo-silylated precursors is of great importance as the polycondensation time differs by days. In general, this effect may be influenced by the chemical nature and steric hindrance of the organic functionality attached to the silane monomer [34].

3.1.2. Kinetic studies FT-IR

The adjustment of the sol-gel processing parameters was evaluated using FTIR. The sols with different variables were examined in regular 1-h intervals and the hydrolysis-condensation reactions were assessed on the basis of silica structure evolution in the finger print region primarily from 1150 cm^{-1} to 400 cm^{-1}. In this area, one may observe several strong to moderate absorptions as described in Table 3. If the structures of the silica units progress well towards the interconnected grown network, then the polysiloxane units linked through the Si–O–Si bond (bridging oxygens, BO_x) should prevail over not completely hydrolyzed units such as silanols/alkoxides Si–OH/Si–OEt or defects SiO^- (non-bridging oxygens; NBO_x) [40–43].

Fig. 3 shows the spectra of sol-gel process evolution of MONO75 and BIS75. By comparing the initial and final stage, the increase in intensity and broadening of the strong absorption peaks assigned to BO_x units can be clearly seen. The strongest increment is seen at 1050 cm^{-1} and is linked to bridging the TO phonon mode of Si–O–Si antisymmetric stretching. A distinct shoulder can be seen on the side of the higher wavenumber points in the LO mode of Si–O–Si antisymmetric stretching, which is important for the qualification of polysiloxane densification processes. This belongs to the disorder-induced modes and is more pronounced in more porous and humid gels [42]. These findings support the idea that a spinnable ladder-like structure was created under the set sol-gel conditions dominated by incompletely condensed silica species. The successful evolution of the silica structure is then also demonstrated by the decrease in the intensity of the absorption peaks assigned to the silanol groups. In particular, the strong absorption peaks in the area from 900 to 1000 cm^{-1} are evidence of the ongoing hydrolysis and condensation by structural transformation from Si–OH, SiO^- to Si–O–Si units [34,41–43]. This phenomenon is also accompanied by a decrease in the broad intensity peak above 3500 - 3100 cm^{-1} assigned to the characteristic vibrations of water and Si–OH [40,41,43]. As can be seen, the spectra of BIS75 sol show these structural changes much earlier (already after 4 h) than the spectra of MONO75 sol (after 48 h) due to structural differences in the precursor molecules as stated above.

The assessed FTIR spectra also indirectly prove that no Si–C cleavage occurred. The intensity of the absorption bands assigned to the symmetric and antisymmetric stretching and deformation vibration of $–CH_2$, $–CH_3$ units at 3000 - 2800 cm^{-1} and at around 1380 cm^{-1} are decreasing, indicating the ongoing hydrolysis-condensation and removal of ethoxy groups and the solvent. Likewise, the characteristic vibration of the benzene ring appears unchanged at the interval 1400 - 1600 cm^{-1} (various stretching vibrations of C=C and C–H) [41,43].

Table 3
Assignment of the characteristic vibrations (cm^{-1}) in the FTIR spectra of organosilane sols [40–43].

Peak position	Origin	Structural units
450 cm^{-1}	δ/r O–Si–O	-O-Si-O-
~580 cm^{-1}	ν Si–OH/Si–O^-	SiO_2 defects (NBO_x)
~680 cm^{-1}	νs Si–O–Si	≡Si–O–Si≡ (BO_x)
750 - 800 cm^{-1}	νs Si–O–Si	≡Si–O–Si≡ (BO_x)
~910 cm^{-1}	$\nu\beta$ Si–O	free Si–O^- (NBO_x)
950 - 1000 cm^{-1}	$\nu\beta$/s Si–O	≡Si–OH (NBO_x)
1050 - 1100 cm^{-1}	νas Si–O–Si; transverse optical phonon mode	≡Si–O–Si≡ (BO_x)
1150 - 1200 cm^{-1}	νas Si–O–Si; longitudinal optical phonon mode	≡Si–O–Si≡ (BO_x)

* νs – symmetric stretching vibration, νas – antisymmetric stretching vibration, δ – deformation vibration (bending), $\nu\beta$ – in plane stretching vibration, r – rocking.

3.1.3. Electrospinning process

The two different electrospinning techniques (jet needle electrospinning and the Nanospider industrial machine) successfully provided nonwoven organosilane nanofibrous mats with various diameters. The successful utilization of the Nanospider electrospinning machine opens up the synthesis of hybrid organosilane fibers suggested herein to a wide range of potential industrial scale applications. The morphology and diameter of the electrospun nanofibers depend on the various operational conditions (HV, TCD etc.) of electrospinning process [11].

3.2. Characterization techniques

3.2.1. Morphology and diameter distribution of hybrid organosilane fibers

The overall morphology and average size of the organosilane fibers were examined using scanning electron microscopy. It was confirmed that morphologically compact and homogeneous nonwoven fibrous mats were provided using both of the electrospinning methods. Depending on several of the parameters of the electrospinning process, the prepared organosilane fibers were long and continuously deposited onto the collector. The average size of the fibers observed by SEM ranges around hundreds of nanometers. Although the prepared organosilane fibers are thin, they don't have a tendency to crack during manipulation.

As illustrated in Fig. 4, different organosilane fibrous products were obtained under the different parameters of the polymer solution and spinning conditions. As seen in Fig. 4a, the fibers of BIS25 display spindle-like and bead inhomogeneities distributed along the fibers. These structural defects most probably originated in the sol viscosity and the network size exceeded the electrostatic force needed to create the jet. The optimal viscosity and sol network produced smooth and continuous fibers [44], as in the example of the BIS75 sample in Fig. 4b and the MONO75 sample in Fig. 4c. In the case of BIS75 fibers, thicker homogeneous fibers with a diameter of 1.2 ± 0.32 μm can be seen. The greater thickness is presumably caused by the hyper-branched or larger sol network and greater viscosity due to the use of the more sterically hindering organo-bis-silylated precursor. The values of the average diameter decrease as the HV increases [11,44]. However, this also brings an increase in the diameter distribution [11,44] as in the case of the MONO75 fibers (Fig. 4c), where a wide fiber diameter distribution can be observed, ranging from 0.39 to 1 μm. The calculated fiber diameters are included in Table B.1.1 - Supplement.

To conclude, under the suitable conditions of the electrospinning process and mainly the viscosity of the polymer solution related to the sol-gel processing parameters, various different structural morphologies of fibers (in/homogeneity, average diameter and their distributions) can be reached in dependence of the type and amount of the organosilane precursor in the initial mixture (Fig. 5). By finely controlling these parameters, different organosilane fibrous products, tailored according to the application, can be produced.

According to the TEM measurements, all of the prepared fibers are amorphous. MONO organosilane fibers show very small-sized corrugation on the surface, pointing to possible microporosity (Fig. 6a). On the contrary, BIS organosilane fibers show mesoporosity, which is clearly visible by SEM (Fig. 6b). This could be a consequence of incomplete hydrolysis-condensation of silica structural units, as will be further discussed in the following section.

3.2.2. Structural characterization of hybrid organosilane fibers

Solid-state ^{13}C and ^{29}Si NMR spectroscopies were used to study the surroundings of silicon atoms in the final fibrous materials of presumably cross-linked bridged polysilsesquioxanes structures.

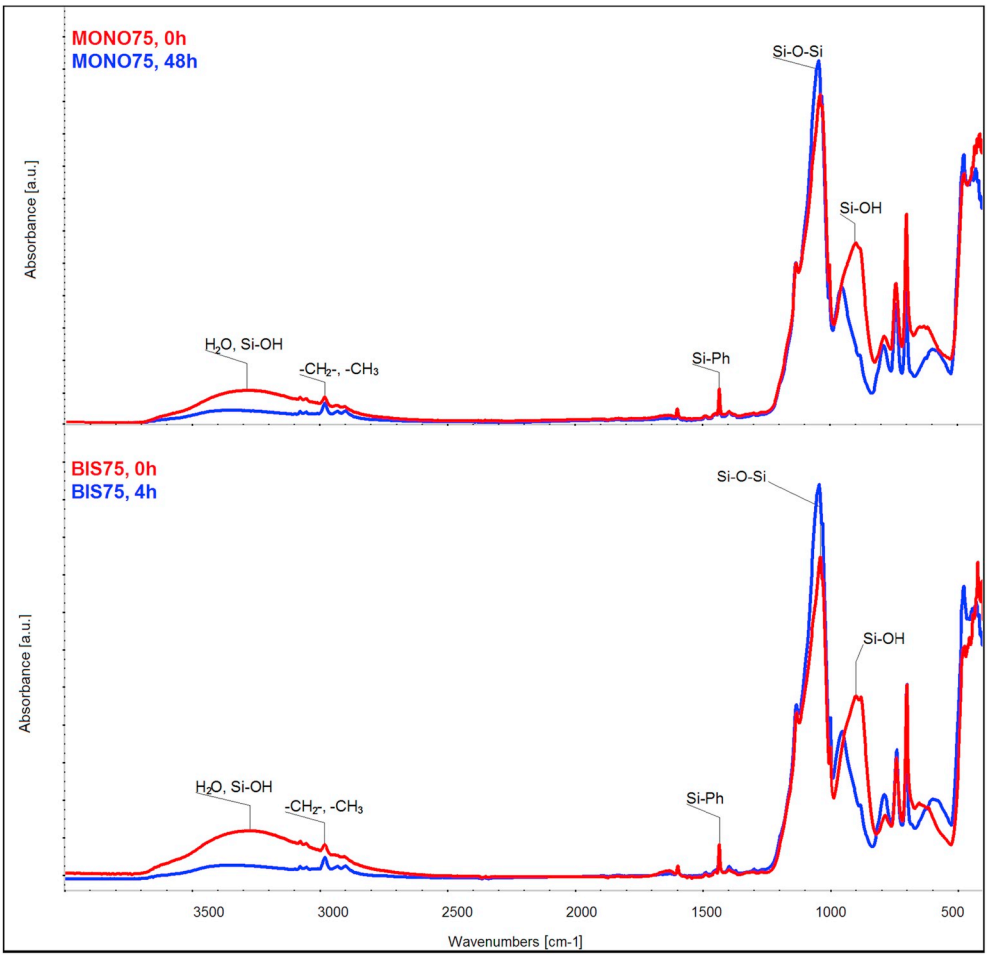

Fig. 3. FTIR spectra of the MONO75 and BIS75 sols at the beginning and at the end of the sol-gel process.

In the recorded ^{29}Si CP/MAS NMR spectra (Fig. 7a and b), seven clearly resolved resonances reflecting the typical structure units of siloxane networks were identified [35,41,45,46]. The spectra of all of the prepared hybrid materials exhibit three T^n and four Q^n signals. The T^n signals origin from Si species covalently bonded to the carbon atoms (organosilane modifiers at different rates of condensation reactions): T^1 [C–Si(OSi) $(OH)_2$, δ −66 ppm], T^2 [C–Si$(OSi)_2$(OH), δ −72 ppm] and T^3 [C–Si$(OSi)_3$, δ −79 ppm]. The Q^n signals (coming from the polysiloxane TEOS matrix at different rates of condensation reactions) resonate at: Q^1 [Si(OSi) $(OH)_3$, δ −88 ppm], Q^2 [Si$(OSi)_2(OH)_2$, δ −95 ppm], Q^3 [Si $(OSi)_3$(OH), δ −101 ppm] and Q^4 [Si$(OSi)_4$, δ −109 ppm]. Asymmetric broadening of some of these signals (shoulders) then indicates incomplete hydrolysis/polycondensation reactions and the presence of both Si–OH and Si–OEt groups. The presence of residual ethoxy groups was confirmed in ^{13}C CP/MAS NMR spectra by the signals at approximately 60 and 18 ppm reflecting –OCH_2- and –CH_3 units, respectively. The high improbability of the cleavage of the strong covalent bond Si–C in organic modifiers even at the low pH of the synthesis [46] is evident in ^{13}C CP/MAS NMR spectra between 120 and 140 ppm, where carbons in the benzene ring resonate.

With the aim of describing the formation of a hybrid material in the course of hydrolysis and the polycondensation reaction of TEOS and organosilane modifiers, quantitative compositions of the siloxane network were calculated from the areas of the individual signals determined by spectral deconvolution of ^{29}Si CP/MAS NMR (Table 4 and Table 5). Olejniczak et al. stated [41] that the effect of the hydrolysis-polycondensation reaction also inevitably leads to the formation of copolymers between the structural units of TEOS (Q) and the organosilane modifier (T). Therefore, it is impossible to separate the two chemical bodies, which further confirms the creation of hybrid material of Class II [47]. However, a clear difference can be seen between the two organosilanes used. In the case of fibers prepared from TEOS + organo-mono-silylated precursor in the initial mixture, the ratio of T^3 and Q^3, Q^4 units derived from the predominantly or completely polymerized units can be clearly distinguished in the overall composition of the siloxane fractions. The ratio of the T^n units increases with the increasing amount of the organo-mono-silylated precursor in the initial mixture (Table 4). However, the distribution of individual T^n and Q^n units in MONO 25, MONO50 and MONO75 (Table 5) does not differ in dependence of the amount of the organo-mono-silylated precursor in the initial mixture. Altogether, this indicates the better ability of the organo-mono-silylated modifier to copolymerize within the newly forming hybrid network. Similarly, the fibers prepared from TEOS + organo-bis-silylated precursor in the initial mixture also display increasing amounts of T^n units compared to Q^n units in the overall composition of the siloxane fractions with an increasing amount of the organic modifier (Table 4), but with a greater ratio of T^1 and Q^1, Q^2 units increasing with an increasing amount of the organo-bis-silylated precursor in the initial mixture. In addition, the distribution of individual T^n and Q^n units (Table 5) points to the fact that the Q^4, Q^3 and T^3 units derived from predominantly or completely polymerized units decrease with the increasing amounts of the organo-bis-silylated precursor in the initial mixture. Presumably, the bulky bridged organo-bis-silylated precursor is not fully polymerized within the hybrid network structure. Nevertheless, as the ratios of the T^2, Q^2 and Q^3 units (predominantly polymerized) still prevail, the prepared organosilane fibers are

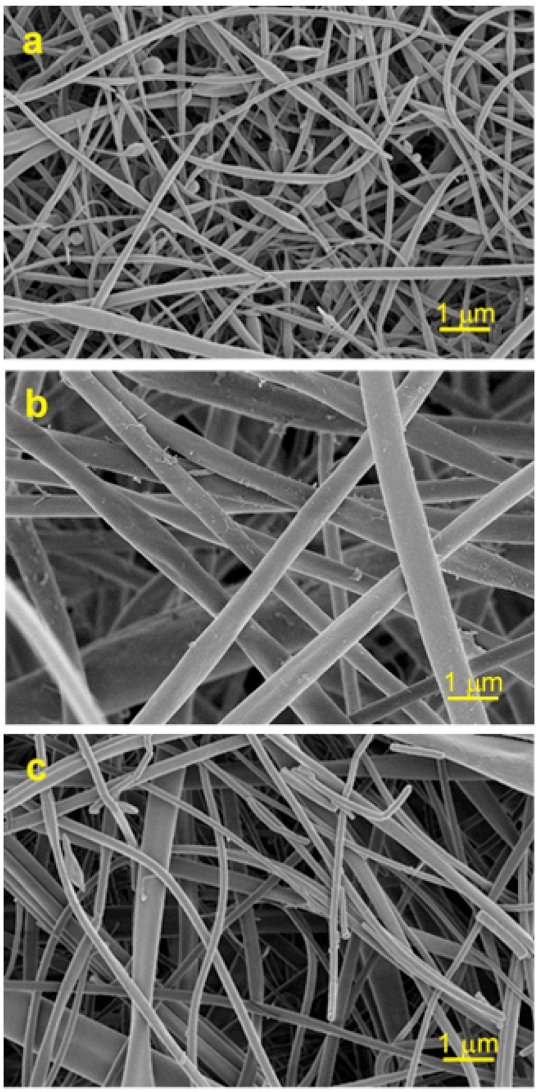

Fig. 4. SEM images of BIS25 (jet needle electrospinning at HV 28 kV, TCD 15 cm) a); BIS75 (Nanospider electrospinning machine at HV 32 kV, TCD 15 cm) b); MONO75 (jet needle electrospinning at HV 36 kV, TCD 15 cm) c); magnification 5 kx.

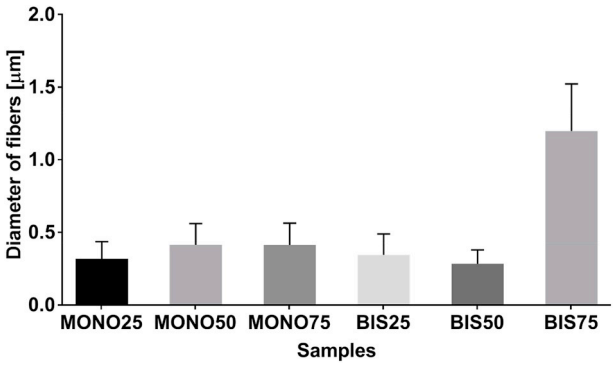

Fig. 5. Fiber diameter with the standard deviation of each material prepared by electrospinning under different operational conditions producing fine smooth fibers: MONO25; MONO50; MONO75; BIS25; BIS50; BIS75.

sufficiently compact and homogeneous. These findings are in good agreement with Brinker and Scherer [34] who stated that spinnable sols are achieved with acid-catalyzed conditions combined with a low *r* ratio, resulting in rather weakly branched, extended polymers. Thus, the average local environment of silicon is then dominated by incompletely condensed Q^2 and Q^3 species. Fully polymerized, mutually grown 3D structures predominated by T^3 and Q^4 units are unsuitable for electrospinning and are typical for bulk materials.

3.2.3. *Thermogravimetric analysis*

TGA analysis coupled with FTIR spectroscopy was used to evaluate the thermal behavior of the prepared hybrid organosilane fibers.

The TGA curves of all of the prepared MONO and BIS organosilane fibers (Fig. B.2.1 - Supplement) behave almost identically and exhibit three weight losses. The smallest weight loss (approximately 0.5 wt %) reaches a maximum at approximately 40 °C and is assigned with the aid of FTIR spectroscopy to the evaporation of adsorbed water. The second weight loss (approximately 5–7 wt %) is assigned to the evaporation or dissociation of ethanol or ethoxy groups present in the not-completely-polymerized network. These findings are in good agreement with the above-mentioned results of NMR spectroscopy.

A major weight loss begins at approximately 340–360 °C, reaches a maximum at around 525 °C and can be attributed to the decomposition of the organic component in the hybrid organosilane network. As expected, the value of weight loss increases with the increment of the organosilane precursor in the initial mixture.

3.2.4. *Solubility*

Dried organosilane fiber mats were carefully removed from aluminum foil and brought into contact with various polar and nonpolar solvents. None of the samples prepared from TEOS + organo-bis-silylated precursor were soluble in any type of solvent, unlike the fibers prepared from TEOS + organo-mono-silylated precursor. Both the fiber types contain differently substituted nonpolar benzene rings, and as a consequence the functional group is differently built into the hybrid structure (see Fig. 1). In the MONO fibers, the phenyl group is oriented in a direction outside the silica matrix and thus presumably more to the surface, which makes the MONO fibers more sensitive to nonpolar solvents. As a consequence, the MONO fibers completely dissolve in nonpolar solvents in a sense of disentanglement of the individual ultrathin fibers and their dispersion in the solvent. This behavior is not observed for the samples of BIS fiber mats. These findings are in good agreement with our assumptions confirming the molecular engineering concept (Fig. 1).

3.2.5. *Nitrogen adsorption*

The results obtained from the nitrogen adsorption analysis closely correspond with the results obtained from the solid-state NMR (Fig. 7a and b), and both electron microscopies (Fig. 6a and b). All of the sample show quite high surface areas, except for sample MONO75 (see Table 6). During the analysis, it was very difficult to determine the porosity of all of the analyzed samples and the measurements took days to assess the isotherms. This effect closely corresponds to the literature [34]. Bringer et al. [34] describe the impossibility of measuring the porosity or surface area by several hypotheses including weak branching combined with limited condensation during the material formation and interpenetration of the precursors due to the decreasing solvent concentration promoting dense packing and possible low or very small-sized porosity (Table 6; Sample MONO75). This could also be the reason for the long degassing times.

4. Up and coming outcomes

The presented preparation of purely organosilane fibers opens up new potential fields of applications. Its attractiveness resides primarily in its non-toxicity, as it is prepared under the mild conditions of the sol-gel process with no harmful solvents. Likewise, the ecological asset should be considered as no organic polymer or other organic low molecular additives are contained. Altogether with the possibility of its

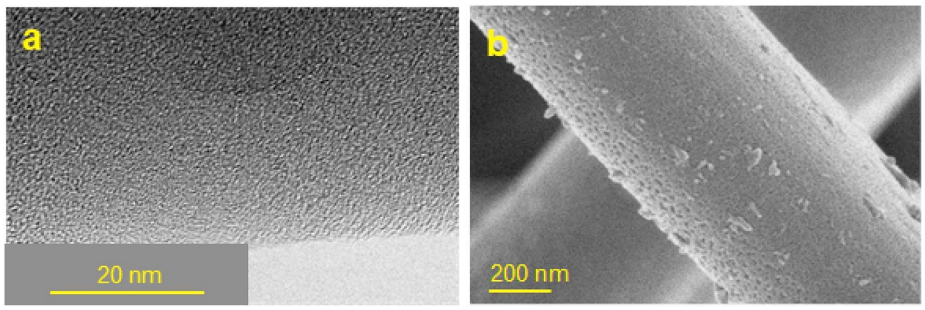

Fig. 6. Sample MONO75 and its microporosity analyzed via TEM a); sample BIS75 showing mesopores in its structure visible by SEM b).

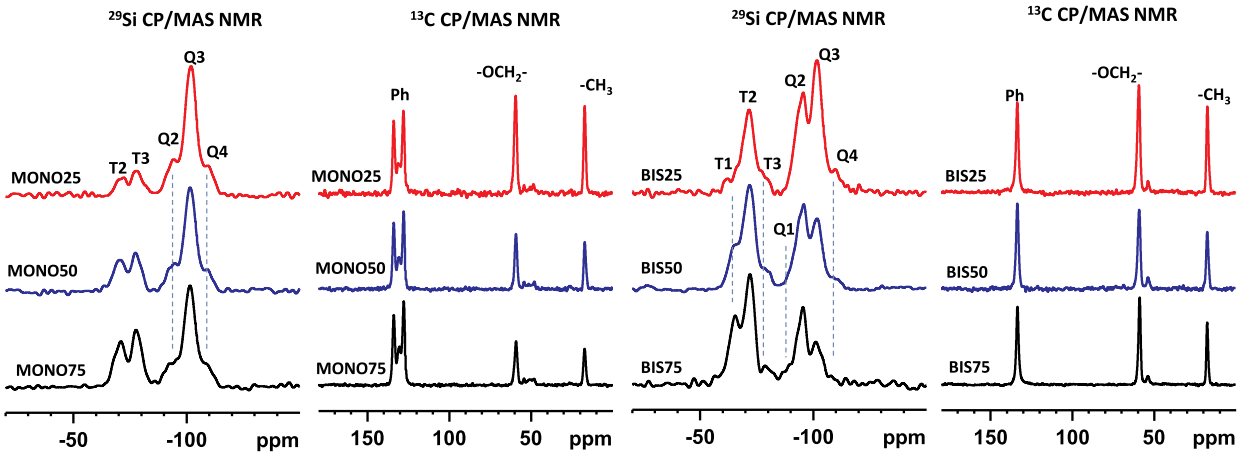

Fig. 7. 29Si CP/MAS and 13C CP/MAS NMR spectra of the investigated samples MONO25, MONO50, MONO75 a); and samples BIS25, BIS50, BIS75 b).

Table 4
Composition of the siloxane fraction defined as the total amount of individual T^n and Q^n structure units in molar %.

Sample	Molar % of silicon units							RATIO Σ T^n: Q^n
	T^1	T^2	T^3	Q^1	Q^2	Q^3	Q^4	
MONO25		6.0	8.2		11.5	58.6	15.7	14.2 : 85.8
MONO50		12.7	13.7		9.8	51.2	12.5	26.4 : 73.6
MONO75		16.3	18.4		9.1	42.9	13.3	34.7 : 65.3
BIS25	4.3	19.4	3.6		23.8	40.4	8.5	27.3 : 72.7
BIS50	11.1	33.1	3.4		25.8	22.4	4.2	47.6 : 52.4
BIS75	20.7	33.8	3.4	4.0	21.9	14.3	2.0	57.9 : 42.2

Table 5
Conversion of individual monomer units calculated separately for T^n and Q^n structure units in molar %.

Sample	Conversion of individual monomer units, %						
	T^1	T^2	T^3	Q^1	Q^2	Q^3	Q^4
MONO25		42.3	57.7		13.4	68.3	18.3
MONO50		48.0	52.0		13.4	69.6	17.0
MONO75		47.0	53.0		14.0	65.7	20.4
BIS25	15.8	70.9	13.3		32.8	55.5	11.7
BIS50	23.2	69.6	7.2		49.2	42.7	8.1
BIS75	35.7	58.5	5.8	9.6	51.9	33.9	4.6

fabrication on an industrial scale, there is a number of potential applications, where such benzene functionalized silane fibrous mats may be applied, such as a stationary reversed phase in HPLC [48,49], removable/reusable mats for acid catalysis [50–52], and also the highly attractive field of new proton-conducting membranes for fuel cells [52,53]. A very promising application seems to be in the field of

Table 6
Surface areas of the fibrous samples measured via nitrogen adsorption analysis.

Sample	Surface area [m^2/g]	Correlation coefficient	Degassing
MONO25	100	0.9999	200 °C/24 h
MONO50	220		
MONO75	N/A		90 °C/24 h
BIS25	310		300 °C/24 h
BIS50	340		
BIS75	250		

biomaterials, which has promoted a steady interest in organosilane materials for over a decade. The use of the prepared organosilane fibers as a new biomaterial will be further discussed in this paper [7.9–13].

4.1. Novel biomaterials

4.1.1. Protein adhesion

The prepared hybrid materials were analyzed for protein adsorption. Protein adsorption changes the properties of a material. If the material is in a protein-containing environment, its adsorption gives it a different biological identity [54,55]. The SDS-PAGE results show that the amount of adsorbed HSA increases with an increasing amount of the benzene functionalized organosilane precursor. This trend is also evident in the analysis of weakly-bounded proteins - the results of the Bradford assay analysis show a greater amount of weakly-bounded proteins on materials with a greater amount of organosilanes (Fig. 8).

5. Conclusions and outlooks

Purely organosilane fibrous mats were prepared in a one-pot synthesis starting from benzene functionalized mono and bis-silylated

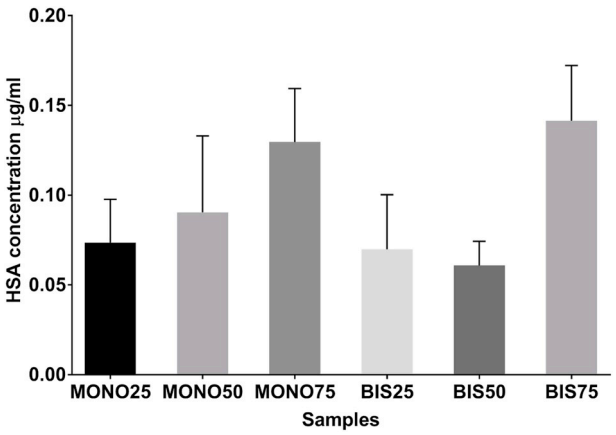

Fig. 8. Concentration of HSA in wash solutions after protein adsorption (weakly-bounded proteins).

organoalkoxy precursors in combination with tetraethoxysilane at various ratios. The suitable setting of sol-gel processing parameters ensured a smooth electrospinning process without the use of any kind of surfactant, polymeric or low-molecular additive remaining in the hybrid structure. The prepared organosilane materials are amorphous, homogeneous fibers with high specific surfaces, good thermal stability and sufficient elasticity to be maneuverable due to the organic part of the hybrid structure. Such fibers are plastic-free and prepared from a non-toxic solvent solution. The molecular engineering concept was proved as two differently benzene functionalized organosilane precursors formed two different structurally behaving fibrous materials. These findings prove that many possible designs of organosilane fibers can be tailored to many specific applications. In addition, industrial-scale fabrication was successfully confirmed with the aid of the Nanospider electrospinning machine.

It is worth mentioning that the sample BIS75 showed excellent biocompatibility. From this point of view, further *in vitro* experiments are planned. The same sample was also preliminarily studied as a new and promising material for fuel cells as it displays proton conductivity over a wide temperature range after a simple additional sulphonation step. The project also continues with other alkoxysilane precursors of various organic functionalities aiming at a wide range of end-applications.

Data availability

The raw/processed data required to reproduce these findings cannot be shared at this time as the data also forms part of an ongoing study.

Declaration of competing interest

The authors declare that they have no known competing financial interests or personal relationships that could have appeared to influence the work reported in this paper.

CRediT authorship contribution statement

Barbora Holubová: Investigation, Conceptualization, Methodology, Writing - original draft. **Veronika Máková:** Investigation, Methodology, Validation, Writing - original draft, Supervision. **Jana Müllerová:** Software, Formal analysis, Data curation. **Jiří Brus:** Software, Formal analysis, Data curation. **Kristýna Havlíčková:** Software, Data curation, Visualization. **Věra Jenčová:** Formal analysis, Data curation. **Alena Michalcová:** Methodology, Software, Data curation, Validation, Visualization. **Johana Kulhánková:** Methodology, Investigation, Formal analysis, Validation. **Michal Řezanka:** Writing - review & editing.

Acknowledgements

This work was supported by the Project 18-09824S of the Czech Science Foundation (GA CR); by the Ministry of Education, Youth and Sports of the Czech Republic and the European Union - European Structural and Investment Funds in the framework of the Operational Programme Research, Development and Education project "Hybrid Materials for Hierarchical Structures (HyHi)", Reg. No. CZ.02.1.01/0.0/0.0/16_019/0000843. The authors would like to thank the Central Laboratories of the University of Chemistry and Technology, Prague, CZ for the possibility to perform the TEM measurements on their EFTEM Jeol 2200 FS instrument within NanoEnviCz, Project no. LM2015073.

Appendix A. Supplementary data

Supplementary data to this article can be found online at https://doi.org/10.1016/j.polymer.2020.122234.

References

[1] G. Kickelbick (Ed.), Hybrid Materials: Synthesis, Characterization, and Applications, Wiley - VCH, Weinheim, 2007.
[2] S. Kalia, Y. Haldorai (Eds.), Organic-Inorganic Hybrid Nanomaterials, Springer International Publishing, Cham, 2015, https://doi.org/10.1007/978-3-319-13593-9.
[3] M. Gugliemli, G. Kickelbick, A. Martucci (Eds.), Sol-gel Nanocomposites, Springer, New York, 2013.
[4] P. Gómez-Romero, C. Sanchez (Eds.), Functional Hybrid Materials, Wiley-VCH, Weinheim, 2004.
[5] C. Sanchez, P. Belleville, M. Popall, L. Nicole, Applications of advanced hybrid organic–inorganic nanomaterials: from laboratory to market, Chem. Soc. Rev. 40 (2011) 696, https://doi.org/10.1039/c0cs00136h.
[6] G. Schottner, Hybrid Sol−Gel-derived polymers: applications of multifunctional materials, Chem. Mater. 13 (2001) 3422–3435, https://doi.org/10.1021/cm011060m.
[7] S. Kaur, M. Gallei, E. Ionescu, Polymer–ceramic nanohybrid materials, in: S. Kalia, Y. Haldorai (Eds.), Org.-Inorg. Hybrid Nanomater, Springer International Publishing, Cham, 2014, pp. 143–185, https://doi.org/10.1007/12_2014_282.
[8] M. Pagliaro, R. Ciriminna, G. Palmisano, Silica-based hybrid coatings, J. Mater. Chem. 19 (2009) 3116, https://doi.org/10.1039/b819615j.
[9] D. Rother, T. Sen, D. East, I.J. Bruce, Silicon, silica and its surface patterning/activation with alkoxy- and amino-silanes for nanomedical applications, Nanomedicine 6 (2011) 281–300, https://doi.org/10.2217/nnm.10.159.
[10] S. Tao, G. Li, J. Yin, Fluorescent nanofibrous membranes for trace detection of TNT vapor, J. Mater. Chem. 17 (2007) 2730, https://doi.org/10.1039/b618122h.
[11] C. Schramm, B. Rinderer, R. Tessadri, Synthesis and characterization of novel ultrathin polyimide fibers via sol-gel process and electrospinning, J. Appl. Polym. Sci. 128 (2013) 1274–1281, https://doi.org/10.1002/app.38543.
[12] C. Gualandi, A. Celli, A. Zucchelli, M.L. Focarete, Nanohybrid materials by electrospinning, in: S. Kalia, Y. Haldorai (Eds.), Org.-Inorg. Hybrid Nanomater, Springer International Publishing, Cham, 2014, pp. 87–142, https://doi.org/10.1007/12_2014_281.
[13] M. Darder, P. Aranda, E. Ruiz-Hitzky, Bionanocomposites: a new concept of ecological, bioinspired, and functional hybrid materials, Adv. Mater. 19 (2007) 1309–1319, https://doi.org/10.1002/adma.200602328.
[14] Y. Li, T. Bou-Akl, Electrospinning in tissue engineering, in: S. Haider, A. Haider (Eds.), Electrospinning - Mater. Tech. Biomed. Appl., InTech, 2016, https://doi.org/10.5772/65836.
[15] S. Thenmozhi, N. Dharmaraj, K. Kadirvelu, H.Y. Kim, Electrospun nanofibers: new generation materials for advanced applications, Mater. Sci. Eng. B 217 (2017) 36–48, https://doi.org/10.1016/j.mseb.2017.01.001.
[16] Y. Ding, Q. Yao, W. Li, D.W. Schubert, A.R. Boccaccini, J.A. Roether, The evaluation of physical properties and in vitro cell behavior of PHB/PCL/sol–gel derived silica hybrid scaffolds and PHB/PCL/fumed silica composite scaffolds, Colloids Surf. B Biointerfaces 136 (2015) 93–98, https://doi.org/10.1016/j.colsurfb.2015.08.023.
[17] Y. Ding, W. Li, A. Correia, Y. Yang, K. Zheng, D. Liu, D.W. Schubert, A. R. Boccaccini, H.A. Santos, J.A. Roether, Electrospun polyhydroxybutyrate/poly(ε-caprolactone)/sol–gel-derived silica hybrid scaffolds with drug releasing function for bone tissue engineering applications, ACS Appl. Mater. Interfaces 10 (2018) 14540–14548, https://doi.org/10.1021/acsami.8b02656.
[18] G. Toskas, C. Cherif, R.-D. Hund, E. Laourine, B. Mahltig, A. Fahmi, C. Heinemann, T. Hanke, Chitosan(PEO)/silica hybrid nanofibers as a potential biomaterial for bone regeneration, Carbohydr. Polym. 94 (2013) 713–722, https://doi.org/10.1016/j.carbpol.2013.01.068.
[19] S.-H. Xia, S.-H. Teng, P. Wang, Synthesis of bioactive polyvinyl alcohol/silica hybrid fibers for bone regeneration, Mater. Lett. 213 (2018) 181–184, https://doi.org/10.1016/j.matlet.2017.11.084.
[20] C. Dhand, Y. Balakrishnan, S.T. Ong, N. Dwivedi, J.R. Venugopal, S. Harini, C. M. Leung, K.Z.W. Low, X.J. Loh, R.W. Beuerman, S. Ramakrishna, N.K. Verma,

R. Lakshminarayanan, Antimicrobial quaternary ammonium organosilane cross-linked nanofibrous collagen scaffolds for tissue engineering, Int. J. Nanomed. 13 (2018) 4473–4492, https://doi.org/10.2147/IJN.S159770.
[21] Y. Yang, M. Suzuki, H. Fukui, H. Shirai, K. Hanabusa, Preparation of helical mesoporous silica and hybrid silica nanofibers using hydrogelator, Chem. Mater. 18 (2006) 1324–1329, https://doi.org/10.1021/cm0519030.
[22] D. Liu, B. Li, Y. Guo, Y. Li, Y. Yang, Inner surface chirality of single-handed twisted carbonaceous tubular nanoribbons: helical carbonaceous tubular nanoribbons, Chirality 27 (2015) 809–815, https://doi.org/10.1002/chir.22496.
[23] J. Hu, Y. Yang, Single-handed helical polybissilsesquioxane nanotubes and mesoporous nanofibers prepared by an external templating approach using low-molecular-weight gelators, Gels 3 (2017) 2, https://doi.org/10.3390/gels3010002.
[24] M.A. Wahab, I. Imae, Y. Kawakami, I. Kim, C.-S. Ha, Functionalized periodic mesoporous organosilica fibers with longitudinal pore architectures under basic conditions, Microporous Mesoporous Mater. 92 (2006) 201–211, https://doi.org/10.1016/j.micromeso.2005.12.016.
[25] P. Yang, D. Zhao, B.F. Chmelka, G.D. Stucky, Triblock-copolymer-directed syntheses of large-pore mesoporous silica fibers, Chem. Mater. 10 (1998) 2033–2036, https://doi.org/10.1021/cm980201q.
[26] W. Yu, J. Shi, L. Wang, X. Chen, M. Min, L. Wang, Y. Liu, The structure and mechanical property of silane-grafted-polyethylene/SiO 2 nanocomposite fiber rope, Aquac. Fish. 2 (2017) 34–38, https://doi.org/10.1016/j.aaf.2017.01.003.
[27] H. He, J. Wang, X. Li, X. Zhang, W. Weng, G. Han, Silica nanofibers with controlled mesoporous structure via electrospinning: from random to orientated, Mater. Lett. 94 (2013) 100–103, https://doi.org/10.1016/j.matlet.2012.12.032.
[28] Y. Xie, C.A.S. Hill, Z. Xiao, H. Militz, C. Mai, Silane coupling agents used for natural fiber/polymer composites: a review, Compos. Part Appl. Sci. Manuf. 41 (2010) 806–819, https://doi.org/10.1016/j.compositesa.2010.03.005.
[29] A.C. Patel, S. Li, C. Wang, W. Zhang, Y. Wei, Electrospinning of porous silica nanofibers containing silver nanoparticles for catalytic applications, Chem. Mater. 19 (2007) 1231–1238, https://doi.org/10.1021/cm061331z.
[30] L.L. Xia, C.L. Li, Y. Wang, In-situ crosslinked PVA/organosilica hybrid membranes for pervaporation separations, J. Membr. Sci. 498 (2016) 263–275, https://doi.org/10.1016/j.memsci.2015.10.025.
[31] Y. Xu, Y. Wen, Y. Wu, C. Lin, G. Li, Hybrid nanofibrous mats with remarkable solvent and temperature resistance produced by electrospinning technique, Mater. Lett. 78 (2012) 139–142, https://doi.org/10.1016/j.matlet.2012.03.016.
[32] M. Xin, X. Zhang, J. Yang, M. Chen, X. Ma, J. Liu, Preparation and electrochemical sensing application of electrospun porous organosilica fibers, Electrochem. Commun. 48 (2014) 123–126, https://doi.org/10.1016/j.elecom.2014.09.001.
[33] S.-Q. Wang, J.-H. He, L. Xu, Non-ionic surfactants for enhancing electrospinability and for the preparation of electrospun nanofibers, Polym. Int. 57 (2008) 1079–1082, https://doi.org/10.1002/pi.2447.
[34] C.J. Brinker, G.W. Scherer, Sol-Gel Science: the Physics and Chemistry of Sol-Gel Processing, Elsevier Science, Saint Louis, 2014.
[35] J. Brus, M. Urbanová, A. Strachota, Epoxy networks reinforced with polyhedral oligomeric silsesquioxanes: structure and segmental dynamics as studied by solid-state NMR, Macromolecules 41 (2008) 372–386, https://doi.org/10.1021/ma702140g.
[36] F. Huang, B. Motealleh, W. Zheng, M.T. Janish, C.B. Carter, C.J. Cornelius, Electrospinning amorphous SiO2-TiO2 and TiO2 nanofibers using sol-gel chemistry and its thermal conversion into anatase and rutile, Ceram. Int. 44 (2018) 4577–4585, https://doi.org/10.1016/j.ceramint.2017.10.134.
[37] S. Sakka, K. Kamiya, The sol-gel transition in the hydrolysis of metal alkoxides in relation to the formation of glass fibers and films, J. Non-Cryst. Solids 48 (1982) 31–46, https://doi.org/10.1016/0022-3093(82)90244-7.
[38] Z. Ma, H. Ji, Y. Teng, G. Dong, J. Zhou, D. Tan, J. Qiu, Engineering and optimization of nano- and mesoporous silica fibers using sol–gel and electrospinning techniques for sorption of heavy metal ions, J. Colloid Interface Sci. 358 (2011) 547–553, https://doi.org/10.1016/j.jcis.2011.02.066.
[39] K. Iimura, T. Oi, M. Suzuki, M. Hirota, Preparation of silica fibers and non-woven cloth by electrospinning, Adv. Powder Technol. 21 (2010) 64–68, https://doi.org/10.1016/j.apt.2009.11.006.
[40] P. Innocenzi, Infrared spectroscopy of sol–gel derived silica-based films: a spectra-microstructure overview, J. Non-Cryst. Solids 316 (2003) 309–319, https://doi.org/10.1016/S0022-3093(02)01637-X.
[41] Z. Olejniczak, M. Łęczka, K. Cholewa-Kowalska, K. Wojtach, M. Rokita, W. Mozgawa, 29Si MAS NMR and FTIR study of inorganic–organic hybrid gels, J. Mol. Struct. 744–747 (2005) 465–471, https://doi.org/10.1016/j.molstruc.2004.11.069.
[42] R.M. Almeida, C.G. Pantano, Structural investigation of silica gel films by infrared spectroscopy, J. Appl. Phys. 68 (1990) 4225–4232, https://doi.org/10.1063/1.346213.
[43] R. Al-Oweini, H. El-Rassy, Synthesis and characterization by FTIR spectroscopy of silica aerogels prepared using several Si(OR)4 and R′′Si(OR')3 precursors, J. Mol. Struct. 919 (2009) 140–145, https://doi.org/10.1016/j.molstruc.2008.08.025.
[44] F. Huang, B. Motealleh, W. Zheng, M.T. Janish, C.B. Carter, C.J. Cornelius, Electrospinning amorphous SiO2-TiO2 and TiO2 nanofibers using sol-gel chemistry and its thermal conversion into anatase and rutile, Ceram. Int. 44 (2018) 4577–4585, https://doi.org/10.1016/j.ceramint.2017.10.134.
[45] J. Brus, Solid-state NMR study of phase separation and order of water molecules and silanol groups in polysiloxane networks, J. Sol. Gel Sci. Technol. 25 (2002) 17–28, https://doi.org/10.1023/A:1016032809131.
[46] J. Morell, M. Güngerich, G. Wolter, J. Jiao, M. Hunger, P.J. Klar, M. Fröba, Synthesis and characterization of highly ordered bifunctional aromatic periodic mesoporous organosilicas with different pore sizes, J. Mater. Chem. 16 (2006) 2809–2818, https://doi.org/10.1039/B603458F.
[47] G. Kickelbick, Hybrid Materials: Synthesis, Characterization, and Applications, WILEY-VCH, 2019. Place of publication not identified.
[48] V. Rebbin, R. Schmidt, M. Fröba, Spherical particles of phenylene-bridged periodic mesoporous organosilica for high-performance liquid chromatography, Angew. Chem. Int. Ed. 45 (2006) 5210–5214, https://doi.org/10.1002/anie.200504568.
[49] Y. Zhang, Y. Jin, H. Yu, P. Dai, Y. Ke, X. Liang, Pore expansion of highly monodisperse phenylene-bridged organosilica spheres for chromatographic application, Talanta 81 (2010) 824–830, https://doi.org/10.1016/j.talanta.2010.01.022.
[50] B. Rác, P. Hegyes, P. Forgo, Á. Molnár, Sulfonic acid-functionalized phenylene-bridged periodic mesoporous organosilicas as catalyst materials, Appl. Catal. Gen. 299 (2006) 193–201, https://doi.org/10.1016/j.apcata.2005.10.026.
[51] L. Sandbrink, T. Lazaridis, M. Rose, R. Palkovits, Ambient temperature gas phase sulfonation: a mild route towards acid functionalized ordered mesoporous organosilica, Microporous Mesoporous Mater. 267 (2018) 198–202, https://doi.org/10.1016/j.micromeso.2018.03.030.
[52] S. Inagaki, S. Guan, T. Ohsuna, O. Terasaki, An ordered mesoporous organosilica hybrid material with a crystal-like wall structure, Nature 416 (2002) 304–307, https://doi.org/10.1038/416304a.
[53] M. Aparicio, J. Mosa, F. Sánchez, A. Durán, Synthesis and characterization of proton-conducting sol–gel membranes produced from 1,4-bis(triethoxysilyl)benzene and (3-glycidoxypropyl)trimethoxysilane, J. Power Sources 151 (2005) 57–62, https://doi.org/10.1016/j.jpowsour.2005.03.042.
[54] Q. Wei, T. Becherer, S. Angioletti-Uberti, J. Dzubiella, C. Wischke, A.T. Neffe, A. Lendlein, M. Ballauff, R. Haag, Protein interactions with polymer coatings and biomaterials, Angew. Chem. Int. Ed. 53 (2014) 8004–8031, https://doi.org/10.1002/anie.201400546.
[55] C.D. Walkey, W.C.W. Chan, Understanding and controlling the interaction of nanomaterials with proteins in a physiological environment, Chem. Soc. Rev. 41 (2012) 2780–2799, https://doi.org/10.1039/C1CS15233E.

polymers

MDPI

Article

(1*S*,2*S*)-Cyclohexane-1,2-diamine-based Organosilane Fibres as a Powerful Tool Against Pathogenic Bacteria

Veronika Máková [1,*], Barbora Holubová [1], David Tetour [2], Jiří Brus [3], Michal Řezanka [1], Miroslava Rysová [4] and Jana Hodačová [2]

[1] Department of Nanomaterials in Natural Science, Institute for Nanomaterials, Advanced Technologies and Innovation, Technical University of Liberec, Studentská 1402/2, 461 17 Liberec, Czech Republic; barbora.holubova@tul.cz (B.H.); michal.rezanka@tul.cz (M.Ř.)

[2] Department of Organic Chemistry, University of Chemistry and Technology, Prague, Technická 5, 166 28 Prague, Czech Republic; davidtetour@seznam.cz (D.T.); jana.hodacova@vscht.cz (J.H.)

[3] Institute of Macromolecular Chemistry, Academy of Sciences of the Czech Republic, Heyrovsky Sq. 2, 162 06 Prague, Czech Republic; brus@imc.cas.cz (J.B.)

[4] Department of Nanomaterials and Informatics, Institute for Nanomaterials, Advanced Technologies and Innovation, Technical University of Liberec, Studentská 1402/2, 461 17 Liberec, Czech Republic; miroslava.rysova@tul.cz (M.R.)

* Correspondence: veronika.makova@tul.cz; Tel.: +420-485-353-863

Received: 14 December 2019; Accepted: 12 January 2020; Published: 14 January 2020

Abstract: An urgent need to find an effective solution to bacterial resistance is pushing worldwide research for highly effective means against this threat. Newly prepared hybrid organosilane fibres consisting of a (1*S*,2*S*)-cyclohexane-1,2-diamine derivative, interconnected in the fibre network via covalent bonds, were fully characterised via different techniques, including FTIR, TGA-FTIR, SEM-EDS, and solid-state NMR. Fibrous samples were successfully tested against two types of pathogenic bacterial strains, namely *Staphylococcus aureus*, and *Pseudomonas aeruginosa*. The obtained results, showing >99.9% inhibition against *Staphylococcus aureus* and *Pseudomonas aeruginosa* in direct contact compared to the control, may help particularly in case of infections, where there is an urgent need to treat the infection in direct contact. From this point of view, the above-mentioned fibrous material may find application in wound healing. Moreover, this new material has a positive impact on fibroblasts viability.

Keywords: organic-inorganic hybrids; organo-bridged silsesquioxane; sol-gel process; electrospinning; *Staphylococcus aureus*; *Pseudomonas aeruginosa*

1. Introduction

Pathogenic bacteria have become a worldwide problem. According to the World Health Organization (WHO) statistics, over 1.4 million people worldwide suffer from infections caused by pathogenic bacteria acquired in hospitals [1]. *Staphylococcus aureus* (*S. aureus*) and *Pseudomonas aeruginosa* (*P. aeruginosa*) are among the most problematic pathogenic bacteria closely connected with an extremely overgrowing resistance to antibiotics, which brings another major complication in the treatment [2,3]. The infections caused by *P. aeruginosa* are usually resistant to multiple antibiotics due to the bacterium's intrinsic resistance [4]. It is important to note that both bacterial strains are 1000 times more resistant in the form of a biofilm [5].

Due to the antibiotic resistance of these bacteria, great effort has been devoted to developing new antibiotics. One group of such compounds are, for example, *trans*-cyclohexane-1,2-diamine derivatives (DACHs). Previous studies have proved them to be very promising antibacterial

compounds against *P. aeruginosa* [6], Mycobacterium tuberculosis [7–9], and *S. aureus* [6,8]. Moreover, it was found that (1*S*,2*S*) enantiomers generally have lower minimum inhibitory concentrations compared to racemate [6].

Functional organosilica or organosilane-based hybrids for biomedicine applications are well known to the academic public and in various industrial applications [10–14]. In general, an ever-growing interest [13] lies not only in the mild synthesis conditions offered by the sol-gel process producing a broad range of end-products but also in the possibility of nanoscale tailoring of their chemical structure fulfilling the specific needs of biocompatibility and mechanical properties of targeted bio-applications [10–16].

Organosilica and organosilane materials with antibacterial properties are found particularly in the form of nanoparticles [17] or thin coatings [18] on various substrates. Surprisingly, the preparation of the hybrid fibres based on bridged organo-bis-silylated precursors is rarely reported [19,20]. Furthermore, in most cases, hybrid fibres are produced as a combination of silica alkoxides or organo-mono-silylated precursors mixed with organic polymers (poly(ε-caprolactone)/polyethylene terephthalate/polyvinylalcohol etc.) or biopolymers [16,18,21,22]. However, such materials are less degradable, and often inappropriate solvents, or precursors are employed. An example of such material is polyhydroxybutyrate/poly(ε-caprolactone)/silica hybrid nanofibrous scaffolds for bone tissue regeneration [23,24] or electrospun organosilane-loaded collagen nanofibrous scaffolds containing quaternary ammonium organosilane and octadecyldimethyl(3-trimethoxysilylpropyl)ammonium chloride with antibacterial activity [25].

To the best of our knowledge, a fibrous system combining the advantages of organosilane and cyclohexane-1,2-diamine derivatives has not been studied yet (or even prepared). This system may offer an answer to the urgent need for the development of new types of biomaterials, which may help to improve the problem of difficult-to-heal infections (wounds) caused by pathogenic bacteria in direct contact. This project deals with challenges in the preparation of antibacterial fibres with a pure organosilane composition based on a silylated (1*S*,2*S*)-cyclohexane-1,2-diamine precursor. No surfactants, low-molecular-weight polymeric gelators, or spinnable polymers were used during the subsequent electrospinning process, and the whole one-pot synthesis is based on a one solvent solution to minimise the toxicity of the formation of the fibres and their subsequent use.

2. Materials and Methods

Tetraethyl orthosilicate—TEOS (>99%, Merck, Prague Czech Republic), ethanol—EtOH (99.9%, Penta, Prague, Czech Republic), hydrochloric acid (35%, Prague, Czech Republic), deionised water (Milli-Q, Prague, Czech Republic). Aluminium foil thickness 12 μm (Rotilabo, Karlsruhe, Germany). (1*S*,2*S*)-1,2-Bis{*N*′-[3-(triethoxysilyl)propyl]ureido}cyclohexane (compound 1) was prepared according to the literature [26].

The standard procedure for the synthesis of a spinnable organosilane sol solution was as follows: Silica precursor composed of TEOS:compound 1 (in a molar ratio of 57:43), ethanol, deionised water, and HCl were added into a round bottom flask and stirred at 450 rpm/r.t./30 min (Table 1). The pH of the sols was adjusted to 2. Finally, the solution was heated to 90 °C in an oil bath at 450 rpm, refluxed for 4 h, and subsequently partially evaporated. The dynamic viscosity was measured before the electrospinning and appropriately adjusted. Hybrid fibres (marked as DACHsilane) were prepared via jet needle electrospinning (Table 1) and finally dried for 24 h in a desiccator for further use.

Inorganic silica dioxide nanofibres with an average diameter of 0.33 ± 0.08 μm, prepared according to the already-published procedure [27], were used as a standard material to assess antibacterial and cytotoxicity activity.

Table 1. Sols tested in electrospinning and conditions employed for the jet needle-electrospinning.

Sol-gel parameters		Parameters of needle-electrospinning				
Molar ratio r = [H_2O]/[silanes]	**Molar ratio Alc = [EtOH]/[silanes]**	**Viscosity [mPa·s]**	**Feeding rate [mL·h^{-1}]**	**Tip-to-collector distance [cm]**	**High Voltage [kV]**	**Temperature/relative humidity**
2.0	9.7	40–60	0.5–1	15–20	20–25	25 °C/30%

2.1. Characterisation Techniques

2.1.1. Scanning Electron Microscopy

The morphology of the hybrid DACHsilane fibres was studied by SEM (ZEISS Ultra Plus, Sigma Family, Jena, Germany). Samples were sputtered with a 2-nm platinum layer and were subsequently viewed as secondary electron images (1 kV). The fibre diameter was characterised using the NIS Elements software (LIM s.r.o., Liberec, Czech Republic) and was assessed from a total amount of 100 measurements per material, taken from five independent images. The results were evaluated in the form of the mean ± standard deviation.

Energy-dispersive X-ray spectroscopy (SEM-EDS, Oxford X-MAX 20, ZEISS Ultra Plus, Sigma Family, Jena, Germany) was used at 10 keV to evaluate the chemical composition of the prepared fibrous (DACHsilane) samples.

2.1.2. Fourier Transform Infrared Spectroscopy (FTIR)

FTIR spectrometry was used to assess the chemical structure of the prepared hybrid DACHsilane fibres. FTIR Spectrometer Nicolet iZ10 (Thermo Fisher Scientific, Waltham, MA, USA) with an attenuated total reflection (ATR) diamond crystal angle of 45°, and a spectral range of 4,000–700 cm^{-1} was used for the analysis. The number of sample scans: 16, number of background scans: 32, resolution: 4 cm^{-1}, gain: 4.0, apodisation: Happ–Genzel, correction: Atmospheric suppression, baseline.

2.1.3. ^{29}Si Cross Polarization Magic Angle Spinning Nuclear Magnetic Resonance (CP/MAS NMR) Spectroscopy

Solid state NMR analysis was used to evaluate the chemical structure of the prepared DACHsilane fibres. Spectra were measured at 11.7 T using a Bruker AVANCE III HD WB/US NMR spectrometer (Bruker, Ettlingen, Germany) in a double-resonance 4-mm probe head at spinning frequencies $\omega_r/2\pi$ = 7 and 10 kHz. In all cases, finely powdered dry samples were placed into 4-mm ZrO_2 rotors. All of the experiments were conducted at 303 K. The ^{29}Si CP/MAS NMR spectra were recorded at Magic Angle Spinning (MAS) of 7 kHz. The spectra were referenced to the external standard M8Q8 (−109.8 ppm). The number of scans was 0.5–5k depending on the amount of sample. For the quantitative analysis and deconvolution of ^{29}Si CP/MAS NMR spectra, the TopSpin 3.6 program package (Bruker) was used [28].

2.1.4. Thermogravimetric Analysis Fourier Transform Infrared Spectroscopy (TGA-FTIR)

The samples were analysed using a Q500 thermogravimetric analyser (TA Instruments, New Castle, PA, USA). Each sample was placed on a platinum pan and analysed in a non-reactive atmosphere of nitrogen with a flow rate of 60 mL/min. The samples were heated at 10 °C/min; the range was from 20 °C to 650 °C. The thermal decompose products were analysed by the Nicolet iS10 FTIR spectrometer (Thermo Fisher Scientific, Waltham, MA USA). Spectra were taken every 10 s with a resolution of 2 cm^{-1} in the spectral range of 4000–650 cm^{-1}.

2.2. Antibacterial Activity Assessments

All of the tested fibrous samples (round shape, the diameter 0.6 cm) were sterilised for 1 h at 120 °C before each bacterial experiment separately. Pure silica dioxide (SiO_2) fibres were used as standard comparison material in all experiments.

Antibacterial tests were performed using Gram-positive *Staphylococcus aureus* (CCM 3953) and Gram-negative *Pseudomonas aeruginosa* (CCM 3955) (ALE-G18, CSNI, collection of microorganisms, Masaryk University, Brno, Czech Republic). A Luria−Bertani (LB) broth medium was used to prepare the agar plates (Sigma-Aldrich, Merck, Czech Republic).

2.2.1. Qualitative Method

The Kirby–Bauer test was used to analyse the ability of both types of fibres (pure inorganic SiO_2 and hybrid DACHsilane) to inhibit the growth of *S. aureus* and *P. aeruginosa*. A total of 1 mL of both the bacterial inocula (initial optical cell density at 600 nm 0.15 ± 0.08 (McFarland standard concentration = 0.9×10^7 CFU/mL)), was spread over four LB agar plates separately using sterile swabs. The samples (round shape, the diameter 0.6 cm) were placed in the centre of the agar plate and incubated for 24 h at 37 °C. The bacterial growth-inhibiting effect was determined by the size of the inhibition zone around the samples.

2.2.2. Quantitative Method

The colony-forming unit (CFU) counting method was used to evaluate the antibacterial activities of the pure inorganic SiO_2 fibres (used as a standard comparison material) and newly prepared hybrid DACHsilane fibres against *S. aureus* and *P. aeruginosa* following the reported protocol [29].

The overnight cultures of bacteria (50 mL) in the Luria−Bertani (LB) broth were centrifuged for 5 min at 3780 rcf (relative centrifugal force) to remove supernatant, washed with hosphate-buffered saline (PBS) twice and then re-suspended in a sterile physiological saline solution (0.15 M NaCl, pH 7.0, 20 mM $NaHCO_3$) to an initial optical cell density at 600 nm (OD600) of 0.15 ± 0.08 (McFarland standard concentration = 0.9×10^7 CFU/mL)).

Fibrous samples with an approximate diameter of 0.6 mm were placed in sterile Fisher bottles (100 mL) with 20 mL of the prepared bacteria solution separately and were incubated for 5 h at 37 °C. Subsequently, the samples were taken out of the bacteria solution, put into sterile glass vials with 10 mL of physiological saline solution, and were gently shaken in a shaker (Heidolph Unimax 1010, Thermo Fisher Scientific, Pardubice, Czech Republic) for 7 min at 25 °C to remove the attached bacteria. The obtained suspensions were diluted 100 times, and 100 μL of each bacterial solution was taken to plate on (LB) agar plates. Each test was performed in triplicate. Viable colonies of microbes on the agar plate were counted, and the percentage of cell growth reduction (CGR, %) was calculated using the equation $CGR = (C_0 - C/C_0) \times 100\%$, where C_0 is the number of CFU of bacteria from the control sample and C is the number of CFU of bacteria from hybrid DACHsilane fibres [1,29].

2.2.3. Bacterial Adhesion

The bacterial adhesion of *S. aureus* and *P. aeruginosa* on the surface of each fibrous sample was evaluated according to the reported literature [29]. Several changes, appearing during the experiment, are mentioned below. The prepared samples were incubated in the bacterial solutions at the initial optical cell density (0.15 ± 0.08/600 nm) for 1 h at 37 °C. Subsequently, the samples were rinsed twice with distilled water, put on glass slides and covered with a Live/Dead Backlight, 1 Kit 30× diluted solution containing (1.67 mM of SYTO9—A and 18.3 mM propidium iodide—B, molar ratio 1:1). The samples were kept in the dark for 15 min and further analysed at 630 nm using the filters 44 fluorescein isothiocyanate (FITC) (green) and 43 cy3 (red). The live and dead bacteria (*S. aureus* and *P. aeruginosa*) attached to the surface of the samples were imaged using a fluorescent microscope (ZEISS Axio Imager 2, Jena, Germany).

2.3. Cytotoxicity Experiments

Cytocompatibility of the DACHsilane hybrid fibres was assessed using murine fibroblasts 3T3-A31. Prior to testing, the cells were maintained in a completed DMEM medium (4.5 g/L D-glucose, L-glutamine, sodium pyruvate, Sigma-Aldrich-Merck, CZ) supplemented with 5% foetal bovine serum (FBS, Biosera, CZ), 5% new-born calf serum (NBCS, Sigma-Aldrich-Merck, CZ), and a 1% penicillin-streptomycin (PS) antibiotic mixture. The cell viability assay was performed in compliance with the ISO 10993-5:2009 standard with minor modifications. Briefly, the 3T3-A31 fibroblasts were seeded into a 96-well plate (10,000 cells per well) and cultured for 24 h prior to the main experiment. The UV-C sterilised samples were extracted in a supplement-free media for 24 h (37 °C/100 rpm). After the extraction period, macroscopic residues were removed by sterile filtration. The obtained filtrates were supplemented by 5% FBS/5% NBCS/1% PS to final concentrations corresponding to 500 μg, 250 μg, and 125 μg fibres per 1 mL of complete medium. The cells were exposed to 100 μL of these extracts per well for 24 h under standard conditions (37 °C/5% CO_2). Each sample was tested six times and compared to the cell control (pristine complete medium), positive control (0.1% Triton x-100), and negative control (0.01% L-arginine). The inorganic silica dioxide nanofibres were used as a secondary control and went through the same elution process described above. After exposure for 24 h, the 3-(4,5-dimethyl-2-thiazolyl)-2,5-diphenyl-2*H*-tetrazolium bromide (MTT, Sigma-Aldrich-Merck, Prague, Czech Republic) viability assay was performed and evaluated by an absorbance reading at 570 nm. The final viability was calculated as a proportion of the cell control value. The results of the cell viability assay were supported by cell morphology evaluation, as described in Figure S6 in the Supplement.

3. Results and Discussion

A novel hybrid fibrous material marked as DACHsilane was prepared via electrospinning (Figure 1). Bis-silane precursors are known to behave as network builders during polymerisation and, hence, the resulting fibrous structures display unique material properties. The incorporation of compound **1** then leads to the formation of a hybrid material. This results in a rather weakly-branched, extended polysiloxane matrix required for the fibre-making process [20,30–32].

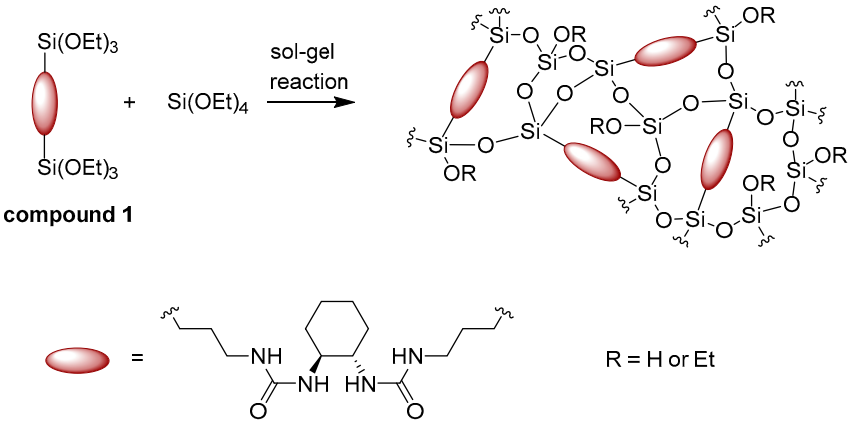

Figure 1. The sol-gel process of forming pure hybrid organosilane fibres based on compound **1**.

3.1. Characterisation of Pure Organosilane Fibres with DACH Functionality

Morphologically compact and homogeneous fibres with a diameter of 2.47 ± 0.91 μm (Figure 2a) were obtained via the needle electrospinning method. The prepared organosilane fibres are flexible and do not break during sample manipulation. Some of the fibres have a tendency to form in the helical structure, probably during the electrospinning procedure (inset image in Figure 2a).

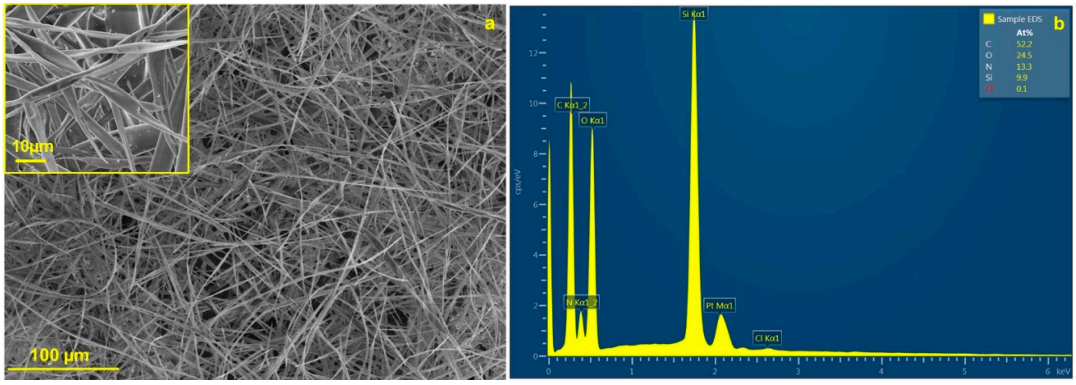

Figure 2. SEM image of the prepared hybrid fibres with an inset showing the helical structure of the parts of the fibres **a**); Energy Dispersive X-Ray Spectroscopy (EDS) spectra of the hybrid fibres **b**).

EDS analysis confirmed the presence of oxygen, carbon, nitrogen, and silicon in the fibrous structure (see Figure 2b). The visibility of nitrogen in the spectra is attributed to the urea functional groups. Moreover, this observation is in compliance with the FTIR result (Figure 3), which confirms the appearance of the characteristic vibrations corresponding to the urea NH-CO-NH and cyclic aliphatic hydrocarbon functionalities in the fingerprint area from 1700 to 1200 cm^{-1} (various stretching and bending vibrations). Primarily, the doublet at around 1630 and 1560 cm^{-1} (urea units; ν(CO) and δ(NH)) and the less intense peak at 1450 cm^{-1} (cyclic aliphatic hydrocarbon unit, $\delta(CH_2)$) provide strong evidence [33–35] that compound **1** is successfully preserved in the prepared organosilane fibrous material. Moreover, the area from 1200 to 400 cm^{-1} proves that no Si–C cleavage occurred in greater amounts, and the silica units progressed well towards the interconnected polysiloxane Si–O–Si network [33,36].

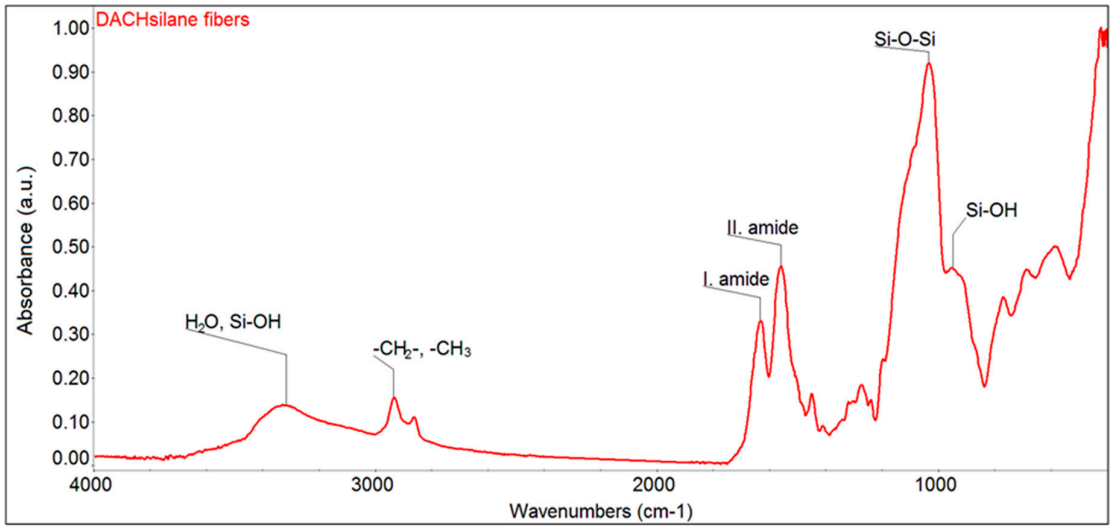

Figure 3. FTIR spectra of the prepared hybrid DACHsilane fibres made of compound 1.

Spectroscopic ^{29}Si CP/MAS NMR examinations further confirm the correct setting of sol-gel processing parameters in accordance with the above-mentioned research on the sol-gel processing of silica fibres [20,31,32]. The recorded ^{29}Si CP/MAS NMR spectrum of the studied organosilane mat (Figure 4) exhibits five clearly resolved resonances corresponding to the characteristic structure units of the siloxane network at different condensation reaction rates: two well-pronounced T^n signals (the organosilane bridged precursor; $C–Si(OSi)_n(OH)_{3-n}$) and three Q^n signals (the polysiloxane TEOS matrix; $Si(OSi)_n(OH)_{4-n}$) [31,33,34]. The overall composition of the siloxane fractions (Table 2) is

dominated by incompletely condensed T^2, Q^2, and Q^3 species together with a completely polymerised T^3 unit. These findings most probably indicate the formation of a ladder-like structure leading to a spinnable linear polymer (Figure 1), as fully-grown 3D Q^4 species would be rather unsuitable for electrospinning. As the organosilane (**1**) silicon prevails (compound **1**:tetraethoxysilane (TEOS) = 43:57 mol.%) in the composition formula, the T^n signals also dominate in the spectrum. The effect of the hydrolysis-polycondensation reaction inevitably leads to the copolymerisation between the structural units of TEOS and the organosilane modifier [31,37]. Hence, the successful formation of a Class II hybrid material [10] may be confirmed.

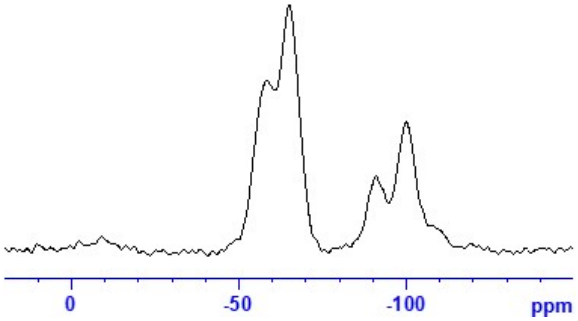

Figure 4. ^{29}Si CP/MAS NMR spectra of the hybrid DACHsilane fibres.

Table 2. Composition of the siloxane fraction defined as the total amount of individual T^n and Q^n structure units in molar %.

Relative amount of building units, %							RATIO Σ T^n:Q^n
T^1	T^2	T^3	Q^1	Q^2	Q^3	Q^4	
1	27	38	0	11	20	3	66:34

The thermogravimetric analysis coupled with FTIR spectroscopy (Figure S1) indicates that the prepared fibrous organosilane material is stable up to 200 °C, where a major weight loss begins and reaches a maximum at around 260 °C. This loss is attributed to the decomposition of the urea unit within the hybrid organosilane network. The TGA-FTIR analysis also confirms the presence of a small portion of water or solvent contained in the fibrous mat most probably originating from incomplete hydrolysis-polycondensation, as previously indicated in the ^{29}Si CP/MAS NMR spectroscopic evaluation.

3.2. Biomedical Applications

3.2.1. Assessment of the Inhibition Zone—Antibacterial Activity in Direct Contact

A qualitative test was performed to evaluate the antibacterial activity of the prepared hybrid DACHsilane fibres in direct contact (Figure S2). The prepared hybrid fibres exhibited a significant antibacterial effect, particularly against *S. aureus* in direct contact (Figure S2b in detail), rather than in the case of *P. aeruginosa*. Standard material, pure SiO_2 fibres, showed no antibacterial activity in direct contact for both of the tested bacterial strains after 24 h incubation (Figure S2a,c). Moreover, several bacterial colonies were observed directly under the standard samples in direct contact. All of the Petri dishes were densely populated by the bacterial colonies, except for very small areas around or under the samples made of hybrid DACHsilane fibres. The inhibition of bacteria for both strains was observed below the hybrid DACHsilane fibres (inset images Figure S2b,d) Moreover, the DACHsilane fibres showed a halo zone hint around the sample in the case of *S. aureus* (Figure S2b).

3.2.2. Assessment of Antibacterial Activity

The results related to the antibacterial activity in the solution were examined by calculating the bacterial cell growth reduction (CGR %) using Gram-positive bacteria *S. aureus* and Gram-negative

bacteria *P. aeruginosa*. Figure 5 shows visible differences between the purely inorganic and hybrid DACHsilane fibres. The examined hybrid fibrous samples seemed to show significant antibacterial activity compared to the control and standard inorganic fibrous samples (Table S1, Figures S3–S5 in the Supplement). The antibacterial activity of the purely SiO_2 fibrous material was significantly less compared to the tested hybrid fibrous material. Better results were observed against *S. aureus* with 91% antibacterial activity than against *P. aeruginosa,* where the antibacterial activity reached only 87%. When we compare these results to the control for cell bacterial growth (Figure S3), the inhibition activity for both bacterial strains is even higher than 99.9%, which is in close agreement with the recent literature [25]. The results obtained from this experiment (Figure 5) closely correspond to the bacterial adhesion test mentioned below, where *P. aeruginosa* has a higher tendency to adhere to the surface of the hybrid fibrous sample compared to *S. aureus*.

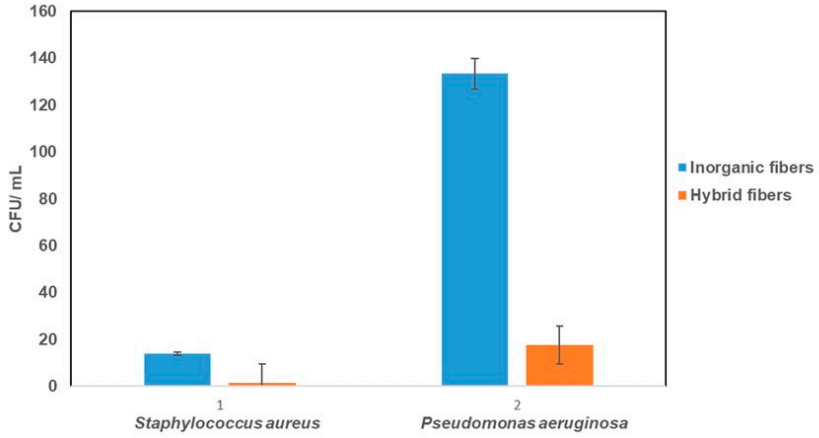

Figure 5. Comparison of the antibacterial activity for pure inorganic SiO_2 fibres and hybrid DACHsilane fibres against *S. aureus* and *P. aeruginosa*.

3.2.3. Bacterial Adhesion Activity

The bacterial adhesion to the surfaces of the fibrous samples against *S. aureus* and *P. aeruginosa*, was assessed by fluorescence imaging, see Figure 6. The green and red fluorescent spots indicate the live and dead bacteria, respectively. They were observed on the surface of the inorganic and hybrid fibres after 1 h incubation in the bacterial suspensions. The inorganic fibrous samples mostly exhibited green fluorescent spots scattered on the surface in both cases, suggesting live *S. aureus* and *P. aeruginosa* (Figure 6a,c). This fact indicates a lack of antibacterial properties of the tested standard SiO_2 fibres. Although the hybrid fibrous sample (DACHsilane) still shows a widespread attachment of both bacterial strains on its surface, it is important to note that most of them have a red fluorescence (Figure 6b,d), indicating a higher number of dead *S. aureus* and *P. aeruginosa* bacterial cells than viable (green) ones. Moreover, the bacterial adhesion to the surface of hybrid fibres is significantly weaker compared to the adhesion of the tested standard material for both bacterial strains. This observation is in agreement with the literature, where the antibacterial behaviour of similar molecule-based DACH derivatives was described [6]. The obtained results indicate that the activity of hybrid fibrous samples against *P. aeruginosa* is stronger in direct contact (Figure 6d).

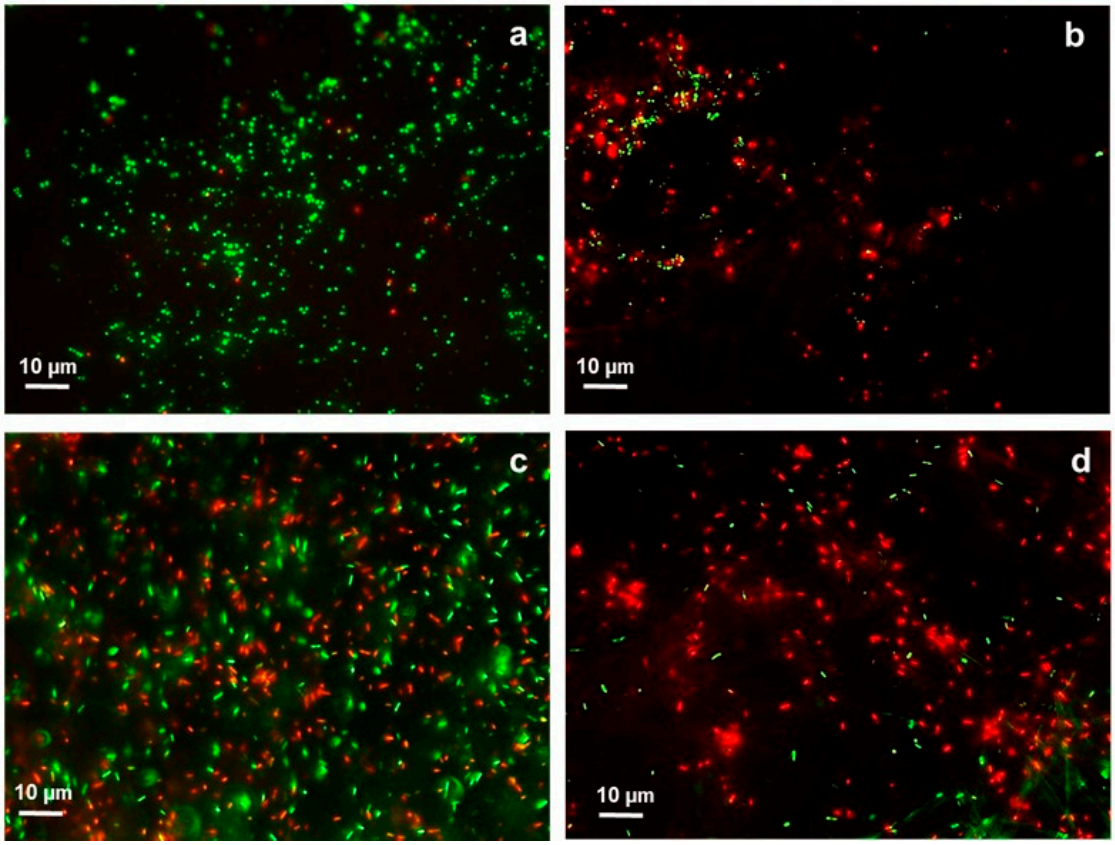

Figure 6. Fluorescence microscopy images of *S. aureus* on the surface of inorganic SiO_2 fibres (**a**) and on the surface of hybrid DACHsilane fibres (**b**). *P. aeruginosa* present on the surface of inorganic SiO_2 fibres (**c**) and on the surface of hybrid DACHsilane fibres (**d**). Green dots indicate live cells, while red dots dead cells.

3.3. Cytocompatibility Assessments

The cell viability assay performed on 3T3-A31 murine fibroblasts proved the cytocompatibility of the hybrid DACHsilane fibres in all three tested concentrations due to the viability highly exceeding the 70% CC level. As shown in Figure 7, exposure to the DACHsilane fibre extract led to increased cell viability in the case of the 500 µg/mL and 250 µg/mL extracts. The DACHsilane extracts had a concentration-dependent effect on cells as an increase in the extract concentration led to an increase in the cell viability from 97.2 ± 7.3% (125 µg/mL) up to 115.1 ± 4.9% (500 µg/mL). This led us to believe that the degradation products of the DACHsilane fibres are favouring cell proliferation. This effect was also observed with the inorganic silica dioxide nanofibres but in lower concentrations below 250 µg/mL (Figure 7). These findings were supported by a cell morphology analysis (see Figure S6 in the Supplement).

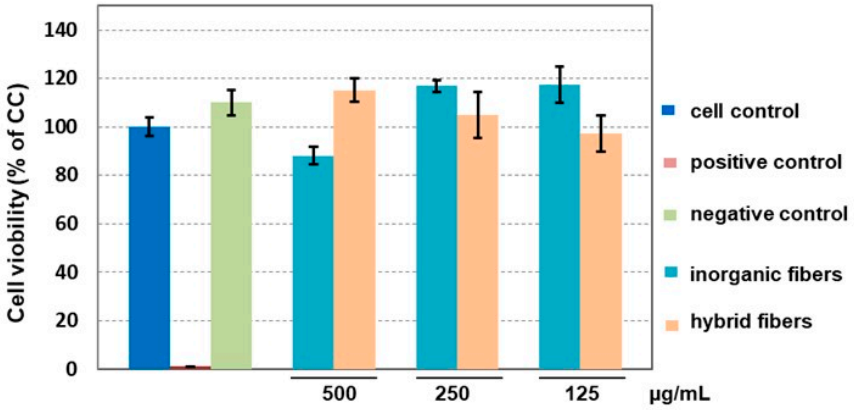

Figure 7. Comparison of the impact of hybrid DACHsilane nanofibres on the viability of 3T3-A31 cells compared to inorganic silica dioxide nanofibres as a control.

4. Conclusions

Homogeneous, purely organosilane fibres consisting of a (1*S*,2*S*)-cyclohexane-1,2-diamine bis-silane derivative in combination with TEOS were prepared for the first time in a one-pot sol-gel synthesis and electrospinning. The spinnable organosilane solution was acquired starting from a suitable choice of sol-gel processing parameters without the aid of electrospinning polymeric or surfactant easers. The resulting hybrid organosilane fibrous mat was confirmed to be uniform, thermally stable up to 200 °C, and sufficiently elastic. The prepared hybrid fibrous samples showed very promising antibacterial activity, particularly in direct contact with both of the tested pathogenic bacterial strains *S. aureus* and *P. aeruginosa*. These findings indicate that the organosilane fibres on the basis of (1*S*,2*S*)-cyclohexane-1,2-diamine may be a promising tool in the framework of the global issue of drug resistance caused by pathogenic bacteria. The assumptions made are also supported by the cytocompatibility study proving their biocompatibility and positive impact on fibroblasts viability, which may lead to a positive impact on wound healing.

Supplementary Materials: The following are available online at www.mdpi.com/xxx/s1, Figure S1: Thermogravimetric analysis of the prepared hybrid DACHsilane fibers coupled with FTIR spectroscopy; Figure S2: Qualitative test describing the inhibition zones for standard sample—pure SiO_2 fibers a) and hybrid DACHsilane fibers b) against *S. aureus*; pure SiO_2 fibers c) and hybrid DACHsilane fibers d) against *P. aeruginosa*. Scale bar 1cm; Figure S3: Control related to the bacterial cell growth of *Staphylococcus aureus* (S.A.) and *Pseudomonas aeruginosa* (P.A.). Both bacterial strains were diluted 100 times. Scale bar 1 cm; Figure S4: The bacterial cell growth of *Staphylococcus aureus* (S.A.) on the inorganic fiber sample a) and on the hybrid fiber sample b). Scale bar 1 cm; Figure S5: The bacterial cell growth of *Pseudomonas aeruginosa* (P.A.) on the inorganic fiber sample a) and on the hybrid fiber sample b). Scale bar 1 cm; Figure S6: The 3T3-A31 cells spindle-like morphology after 24 hours exposure to the DACHsilane fibres extracts (a) 0 µg/mL (CC), (b) 125 µg/mL, (c) 250 µg/mL and (d) 500 µg/mL Merge of modular contrast vizualization and nucleus staining (DAPI) (Leica DMi8, obj. 20×). Scale bar 100 µm; Table S1: Antibacterial activity of the tested fibrous samples against *Staphylococcus aureus* and *Pseudomonas aeruginosa*.

Author Contributions: conceptualization—V.M. and B.H.; methodology—J.H.; validation—J.H., M.Ř. and V.M.; formal analysis—J.B. and D.T.; investigation—B.H., V.M., D.T. and M.R.; resources—J.H. and M.Ř.; data curation—J.B.; writing—original draft preparation—V.M. and B.H.; writing—review and editing—M.Ř. and J.H.; visualization—V.M., B.H., M.R., J.B., M.Ř.; supervision—J.H. All authors have read and agreed to the published version of the manuscript.

Funding: This research was funded by the Project 18-09824S of the Czech Science Foundation (GA CR) and by the Ministry of Education, Youth and Sports of the Czech Republic, specific university research (MSMT No. 21-SVV/2019) and the European Union—European Structural and Investment Funds in the framework of the Operational Programme Research, Development, and Education project "Hybrid Materials for Hierarchical Structures (HyHi)", Reg. No. CZ.02.1.01/0.0/0.0/16_019/0000843.

Conflicts of Interest: The authors declare no conflict of interest.

References

1. Bogdanović, U.; Dimitrijević, S.; Škapin, S.D.; Popović, M.; Rakočević, Z.; Leskovac, A.; Petrović, S.; Stoiljković, M.; Vodnik, V. Copper-polyaniline nanocomposite: Role of physicochemical properties on the antimicrobial activity and genotoxicity evaluation. *Mater. Sci. Eng. C* **2018**, *93*, 49–60, doi:10.1016/j.msec.2018.07.067.
2. Nazir, A.; Kadri, S.M. An overview of hospital acquired infections and the role of the microbiology laboratory. *Int. J. Res. Med. Sci.* **2017**, *2*, 21–27.
3. Khan, H.A.; Baig, F.K.; Mehboob, R. Nosocomial infections: Epidemiology, prevention, control and surveillance. *Asian Pac. J. Trop. Biomed.* **2017**, *7*, 478–482, doi:10.1016/j.apjtb.2017.01.019.
4. Wang, Y.; Han, B.; Xie, Y.; Wang, H.; Wang, R.; Xia, W.; Li, H.; Sun, H. Combination of gallium(iii) with acetate for combating antibiotic resistant Pseudomonas aeruginosa. *Chem. Sci.* **2019**, *10*, 6099–6106, doi:10.1039/C9SC01480B.
5. Lichter, J.A.; Van Vliet, K.J.; Rubner, M.F. Design of Antibacterial Surfaces and Interfaces: Polyelectrolyte Multilayers as a Multifunctional Platform. *Macromolecules* **2009**, *42*, 8573–8586, doi:10.1021/ma901356s.
6. Sharma, M.; Joshi, P.; Kumar, N.; Joshi, S.; Rohilla, R.K.; Roy, N.; Rawat, D.S. Synthesis, antimicrobial activity and structure–activity relationship study of N,N-dibenzyl-cyclohexane-1,2-diamine derivatives. *Eur. J. Med. Chem.* **2011**, *46*, 480–487, doi:10.1016/j.ejmech.2010.11.027.
7. Beena, J.S.; Kumar, N.; Kidwai, S.; Singh, R.; Rawat, D.S. Synthesis and antitubercular activity evaluation of novel unsymmetrical cyclohexane-1,2-diamine derivatives. *Arch. Pharm. Weinh.* **2012**, *345*, 896–901, doi:10.1002/ardp.201200219.
8. Beena, J.S.; Kumar, D.; Kumbukgolla, W.; Jayaweera, S.; Bailey, M.; Alling, T.; Ollinger, J.; Parish, T.; Rawat, D.S. Antibacterial activity of adamantyl substituted cyclohexane diamine derivatives against methicillin resistant Staphylococcus aureus and Mycobacterium tuberculosis. *RSC Adv.* **2014**, *4*, 11962–11966, doi:10.1039/C4RA00224E.
9. Kumar, D.; Raj, K.K.; Bailey, M.; Alling, T.; Parish, T.; Rawat, D.S. Antimycobacterial activity evaluation, time-kill kinetic and 3D-QSAR study of C-(3-aminomethyl-cyclohexyl)-methylamine derivatives. *Bioorg. Med. Chem. Lett.* **2013**, *23*, 1365–1369, doi:10.1016/j.bmcl.2012.12.083.
10. *Hybrid Materials: Synthesis, Characterization, and Applications*; Kickelbick, G., Ed.; Wiley-VCH: Weinheim, Germany, 2007.
11. *Functional Hybrid Materials*; Gómez-Romero, P., Sanchez, C., Eds.; Wiley-VCH: Weinheim, Germany, 2004.
12. Sanchez, C.; Belleville, P.; Popall, M.; Nicole, L. Applications of advanced hybrid organic–inorganic nanomaterials: From laboratory to market. *Chem. Soc. Rev.* **2011**, *40*, 696, doi:10.1039/c0cs00136h.
13. Faustini, M.; Nicole, L.; Ruiz-Hitzky, E.; Sanchez, C. History of Organic-Inorganic Hybrid Materials: Prehistory, Art, Science, and Advanced Applications. *Adv. Funct. Mater.* **2018**, *28*, 1704158, doi:10.1002/adfm.201704158.
14. Sanchez, C.; Julián, B.; Belleville, P.; Popall, M. Applications of hybrid organic–inorganic nanocomposites. *J. Mater. Chem.* **2005**, *15*, 3559–3592, doi:10.1039/B509097K.
15. *Sol-Gel Nanocomposites*; Advances in Sol-Gel Derived Materials and Technologies; Gugliemli, M., Kickelbick, G., Martucci, A., Eds.; Springer: New York, NY, USA, 2013.
16. Kaur, S.; Gallei, M.; Ionescu, E. Polymer–Ceramic Nanohybrid Materials. In *Organic-Inorganic Hybrid Nanomaterials*; Kalia, S., Haldorai, Y., Eds.; Springer International Publishing: Cham, Switzerland, 2014; Volume 267, pp. 143–185.
17. Rai, R.V.; Bai, J.A. *Nanoparticles and Their Potential Application as Antimicrobials, Science against Microbial Pathogens: Communicating Current Research and Technological Advances*; Méndez-Vilas, A., Ed.; Formatex, Microbiology Series: Badajoz, Spain, 2011; Volume 1 (3), pp. 197–209.
18. Ciraldo, F.E.; Schnepf, K.; Goldmann, W.H.; Boccaccini, A.R. Development and Characterization of Bioactive Glass Containing Composite Coatings with Ion Releasing Function for Antibiotic-Free Antibacterial Surgical Sutures. *Materials* **2019**, *12*, 423, doi:10.3390/ma12030423.
19. Tao, S.; Li, G.; Yin, J. Fluorescent nanofibrous membranes for trace detection of TNT vapor. *J. Mater. Chem.* **2007**, *17*, 2730, doi:10.1039/b618122h.
20. Schramm, C.; Rinderer, B.; Tessadri, R. Synthesis and characterization of novel ultrathin polyimide fibres via sol-gel process and electrospinning. *J. Appl. Polym. Sci.* **2013**, *128*, 1274–1281, doi:10.1002/app.38543.

21. Gualandi, C.; Celli, A.; Zucchelli, A.; Focarete, M.L. Nanohybrid Materials by Electrospinning. In *Organic-Inorganic Hybrid Nanomaterials*; Kalia, S., Haldorai, Y., Eds.; Springer International Publishing: Cham, Switzerland, 2014; Volume 267, pp. 87–142.
22. Darder, M.; Aranda, P.; Ruiz-Hitzky, E. Bionanocomposites: A New Concept of Ecological, Bioinspired, and Functional Hybrid Materials. *Adv. Mater.* **2007**, *19*, 1309–1319, doi:10.1002/adma.200602328.
23. Ding, Y.; Li, W.; Correia, A.; Yang, Y.; Zheng, K.; Liu, D.; Schubert, D.W.; Boccaccini, A.R.; Santos, H.A.; Roether, J.A. Electrospun Polyhydroxybutyrate/Poly(ε-caprolactone)/Sol-Gel-Derived Silica Hybrid Scaffolds with Drug Releasing Function for Bone Tissue Engineering Applications. *ACS Appl Mater Interfaces* **2018**, *10*, 14540–14548, doi:10.1021/acsami.8b02656.
24. Ding, Y.; Yao, Q.; Li, W.; Schubert, D.W.; Boccaccini, A.R.; Roether, J.A. The evaluation of physical properties and in vitro cell behavior of PHB/PCL/sol–gel derived silica hybrid scaffolds and PHB/PCL/fumed silica composite scaffolds. *Colloids Surfaces B Biointerfaces* **2015**, *136*, 93–98, doi:10.1016/j.colsurfb.2015.08.023.
25. Dhand, C.; Balakrishnan, Y.; Ong, S.T.; Dwivedi, N.; Venugopal, J.R.; Harini, S.; Leung, C.M.; Low, K.Z.W.; Loh, X.J.; Beuerman, R.W.; et al. Antimicrobial quaternary ammonium organosilane cross-linked nanofibrous collagen scaffolds for tissue engineering. *IJN* **2018**, *13*, 4473–4492, doi:10.2147/IJN.S159770.
26. Moreau, J.J.E.; Vellutini, L.; Wong Chi Man, M.; Bied, C. Shape-Controlled Bridged Silsesquioxanes: Hollow Tubes and Spheres. *Chem. Eur. J.* **2003**, *9*, 1594–1599, doi:10.1002/chem.200390183.
27. Iimura, K.; Oi, T.; Suzuki, M.; Hirota, M. Preparation of silica fibres and non-woven cloth by electrospinning. *Adv. Powder Technol.* **2010**, *21*, 64–68, doi:10.1016/j.apt.2009.11.006.
28. Brus, J.; Urbanová, M.; Strachota, A. Epoxy Networks Reinforced with Polyhedral Oligomeric Silsesquioxanes: Structure and Segmental Dynamics as Studied by Solid-State NMR. *Macromolecules* **2008**, *41*, 372–386, doi:10.1021/ma702140g.
29. Liu, Z.; Qi, L.; An, X.; Liu, C.; Hu, Y. Surface Engineering of Thin Film Composite Polyamide Membranes with Silver Nanoparticles through Layer-by-Layer Interfacial Polymerization for Antibacterial Properties. *ACS Appl. Mater. Interfaces* **2017**, *9*, 40987–40997, doi:10.1021/acsami.7b12314.
30. Kickelbick, G. Introduction to Hybrid Materials. In *Hybrid Materials*; John Wiley & Sons, Ltd.: Hoboken, NJ, USA, 2007; pp. 1–48.
31. Brinker, C.J.; Scherer, G. *Sol-Gel Science: The Physics and Chemistry of Sol-Gel Processing*; Elsevier Inc.: Amsterdam, The Netherlands, 2013.
32. Sakka, S.; Kamiya, K. The sol-gel transition in the hydrolysis of metal alkoxides in relation to the formation of glass fibres and films. *J. Non-Cryst. Solids* **1982**, *48*, 31–46, doi:10.1016/0022-3093(82)90244-7.
33. Liu, F.; Fu, L.; Wang, J.; Meng, Q.; Li, H.; Guo, J.; Zhang, H. Luminescent film with terbium-complex-bridged polysilsesquioxanesElectronic supplementary information (ESI) available: IR, UV-Vis and excitation spectra and decay curves. See http://www.rsc.org/suppdata/nj/b2/b206815j/. *New J. Chem.* **2003**, *27*, 233–235, doi:10.1039/b206815j.
34. Liu, N.; Yu, K.; Smarsly, B.; Dunphy, D.R.; Jiang, Y.-B.; Brinker, C.J. Self-Directed Assembly of Photoactive Hybrid Silicates Derived from an Azobenzene-Bridged Silsesquioxane. *J. Am. Chem. Soc.* **2002**, *124*, 14540–14541, doi:10.1021/ja027991w.
35. Álvaro, M.; Benitez, M.; Das, D.; Ferrer, B.; García, H. Synthesis of Chiral Periodic Mesoporous Silicas (ChiMO) of MCM-41 Type with Binaphthyl and Cyclohexadiyl Groups Incorporated in the Framework and Direct Measurement of Their Optical Activity. *Chem. Mater.* **2004**, *16*, 2222–2228, doi:10.1021/cm0311630.
36. Innocenzi, P. Infrared spectroscopy of sol–gel derived silica-based films: A spectra-microstructure overview. *J. Non-Cryst. Solids* **2003**, *316*, 309–319, doi:10.1016/S0022-3093(02)01637-X.
37. Olejniczak, Z.; Łęczka, M.; Cholewa-Kowalska, K.; Wojtach, K.; Rokita, M.; Mozgawa, W. 29Si MAS NMR and FTIR study of inorganic–organic hybrid gels. *J. Mol. Struct.* **2005**, *744–747*, 465–471, doi:10.1016/j.molstruc.2004.11.069.

Polymer 228 (2021) 123862

Contents lists available at ScienceDirect

Polymer

journal homepage: www.elsevier.com/locate/polymer

Hybrid organosilane fibrous materials and their contribution to modern science

Veronika Máková *, Barbora Holubová, Ilona Krabicová, Johana Kulhánková, Michal Řezanka

Department of Nanochemistry, Institute for Nanomaterials, Advanced Technologies and Innovation, Technical University of Liberec, Studentská 1402/2, 461 17, Liberec, Czech Republic

ARTICLE INFO

Keywords:
Organic-inorganic hybrids
Organosilanes
Sol-gel
One-pot synthesis
Fibers

ABSTRACT

Nanomaterials together with nanotechnologies bring everyday challenges to modern material science and allow scientists worldwide to develop completely new types of unique materials having extraordinary properties. Although interest in hybrid organic-inorganic organosilane fibrous nanomaterials is rising, there is no review covering and completing the knowledge. Herein, organo-mono-silylated and organo-bis-silylated precursors were studied in detail, and synthetic strategies and outcomes were successfully applied for the formation of organosilane fibers using various different techniques such as self-assembly, drawing, and in particular electrospinning.

The presented findings are closely connected to the application potential, and show the promising prospects of these hybrid organosilane fibers in various fields of modern science and everyday life, covering optoelectronics, sensors, catalysis, energetics, filtration and medicine.

1. Introduction

The growing interest in inorganic-organic hybrid materials in both academic and industrial fields is due to the convergence of diverse expertise and is driven by the curiosity of open-minded scientists using a combination of different approaches [1]. This multilateralism of perspectives has led to one of the greatest advantages of hybrid materials – their "multifunctionality". However, as hybrid materials are always in competition with other materials, it is necessary to demonstrate their real added value. Therefore, the current development of modern hybrid materials is subjected to general rules taking into account the cost and efficiency of their production. The family of organosilanes is just the type of hybrid material to fulfil such demanding requirements [1,2].

Many hybrid organosilane materials in different forms (primarily coatings [3], particles [4] and composites [5]) have been successfully transferred to the market and further commercialized [1,6]. Moreover, the number of publications on such materials has continuously increased over the last 20 years (see Fig. 1a). Recently, excellent reviews related to this topic have been published [1,7,8]. Nevertheless, the primary scientific literature is surprisingly uninterested in the preparation of hybrid organosilane fibrous materials (see Fig. 1b) [9,10]. Yet, they are easily prepared from quite inexpensive precursors available on an industrial scale and, in addition, the way they are processed is compatible with proven industrial processes. Therefore, the newly prepared organosilane fibrous materials may offer a unique added value compared in particular to purely organic polymer fibers. Likewise, the environmental benefits should also be considered, as hybrid organosilane fibers may be prepared under the mild conditions of the sol-gel process with no harmful solvents or organic polymer additives, whereby avoiding the problems with nanoplastics [1,6,11–13].

In this context, research regarding the different ways of preparing organosilane (nano)fibers, their prospects and contribution to modern and currently growing scientific fields such as optoelectronics [14], sensors [15], catalysis [16], energetics [17], and medicine [18] among others should be highlighted. Herein, we present a comprehensive overview of the use of organosilane (nano)fibers prepared from organo-mono-silylated and organo-bis-silylated precursors. Firstly, the origins of organosilane fiber-making chemistry are briefly described in sub-section 1.1. Moreover, the historical overview together with important milestones related to this topic is given in Table 1. Then, there is an extensive discussion on the properties of organo-mono-silylated and organo-bis-silylated precursors, together with the related process leading to the preparation of convenient spinning solutions and the main fiber-making techniques. Finally, the contribution and potential of these

* Corresponding author.
E-mail addresses: veronika.makova@tul.cz (V. Máková), barbora.holubova@tul.cz (B. Holubová), ilona.krabicova@tul.cz (I. Krabicová), johana.kulhankova@tul.cz (J. Kulhánková), michal.rezanka@tul.cz (M. Řezanka).

https://doi.org/10.1016/j.polymer.2021.123862
Received 3 February 2021; Received in revised form 22 April 2021; Accepted 11 May 2021
Available online 1 June 2021

hybrid organosilane nanofibers are outlined, together with their benefits for modern science and different areas of human activity.

1.1. From silica gel to silica fibers and beyond

The beginnings of the silica, silicate, silane and organosilane chemistries belong to a period between the 17th century and the beginning of the 1940s. Between 1940 and 1980, mixed inorganic-organic materials were developed by various different weakly- or non-interacting scientific communities. In 1976 Yajima et al. [19] and later on, Ishikawa et al. [20] published studies describing polymeric networks, without siloxane bonds, based on polycarbosilanes and their conversion to ceramic fibers obtained by sintering an amorphous Si–Al–C–O fiber precursor at different temperatures. A similar study has also been published by Baldus et al., in 1999 [21], where the formation of ceramic fibers made of preceramic *N*-methylpolyborosilazane via the melt-spinning technique was described. All the above-mentioned types of ceramic fibers have found application in tough fiber-reinforced composites. The latter years were marked by the appearance of the first omnibus publications defining and establishing "the sol-gel community". A historical overview of the evolution of silica and its derivative chemistries is included in Table 1.

Probably given the difficulties of the low-temperature fiber-making process, it was not until the 1980s that silica fibers were prepared directly via sol-gel processing. Even though this decade was marked by the first appearance of organoalkoxysilane precursors [28,30,31], the first sol-gel derived fibers were purely inorganic, prepared from various metal alkoxides either by drawing directly from viscous sols at room temperature or by unidirectional freezing of gels [27]. Amorphous or polycrystalline, these first sol-gel fibers were structurally based not only on silica and silicates (SiO_2, SiO_2–TiO_2 (10–50%), SiO_2-AI_2O_3 (30%), SiO_2–ZrO_2 (7–48%), SiO_2–ZrO_2–Na_2O), but also on diverse aluminates, zirconates, titanates, nitrates and even cuprates or niobates [32]. However, as they displayed unsuitable microstructures for achieving ultrahigh purity and non-circular cross-sections, their potential applications were narrowed down to reinforcement, refractory textiles and high-temperature superconductors [11].

These first sol-gel silica fibers were prepared independently by the scientific groups of Sakka (Japan), W. C. LaCourse and H. G. Sowman (both USA) [32–36]. The group of Sakka et al. [27,32] was particularly interested in the course of sol-to-gel conversion and its influence on fiber-making potential. They were the first to describe the link between the presence of long-shaped particles in the sol and the spinnability, as will be discussed further in this review.

As these silica and silicate fibers are well known on both an academic and industrial scale [11,32], this review focuses on hybrid organosilane fibers that have still managed to evade the eye principal hybrid material reviewers [1,6,12]. It was not until the late 2000s that hybrid organosilane fiber-manufacturing came to the forefront of scientific interest (Fig. 1b). Its methods and strategies will be described further in the present review.

2. The hybrid nature of organosilane precursors

It is essential to understand the hybrid nature of organosilane precursors in order to tailor the structure of the resulting fibrous materials on a molecular level. Generally, hybrid materials are defined as multicomponent materials having at least one of their organic and/or inorganic components blended on the nanometer scale. Commonly, one of these components is inorganic and the other is organic [1,2,12]. The properties of such hybrid materials are then achieved due to the strong synergy of these organic and inorganic components depending on the presence of a large hybrid interface [37].

Therefore, the nature of the interactions, energy, and linkability of the interfacial boundaries plays an important role in the modulating of the properties of the final material. From this point of view, hybrid materials can be divided into two main classes: Class I where the organic and inorganic components interact via weak bonds, e.g. van der Waals, hydrogen bonds, or electrostatic bonds; and Class II where the organic and inorganic components are linked by rather strong chemical interactions as covalent or iono-covalent bonds [5]. In addition, there is still no clear borderline between inorganic-organic hybrid materials and inorganic-organic nanocomposites as large molecular building blocks of hybrid materials can already be of nanometer length scale [12]. Common knowledge states that there is a gradual transition between both of them. Nanocomposites come with discrete structural units ranging from 1 to 100 nm (nanoparticles/rods/tubes usually incorporated in organic polymers), while hybrid materials are more often defined by the use of inorganic or organic units formed in situ by molecular precursors (e.g. the sol-gel process) [12]. Organosilane fibrous materials belong mostly to the Class II hybrid materials and they are often used to prepare a wide range of hybrid (nano) composites. The organosilane hybrid structure is well assured by a strong covalent Si–C bond stable enough to provide a homogeneous material in which the organic moieties bound to two $SiO_{1.5}$ units are uniformly distributed as elementary building blocks [12,38].

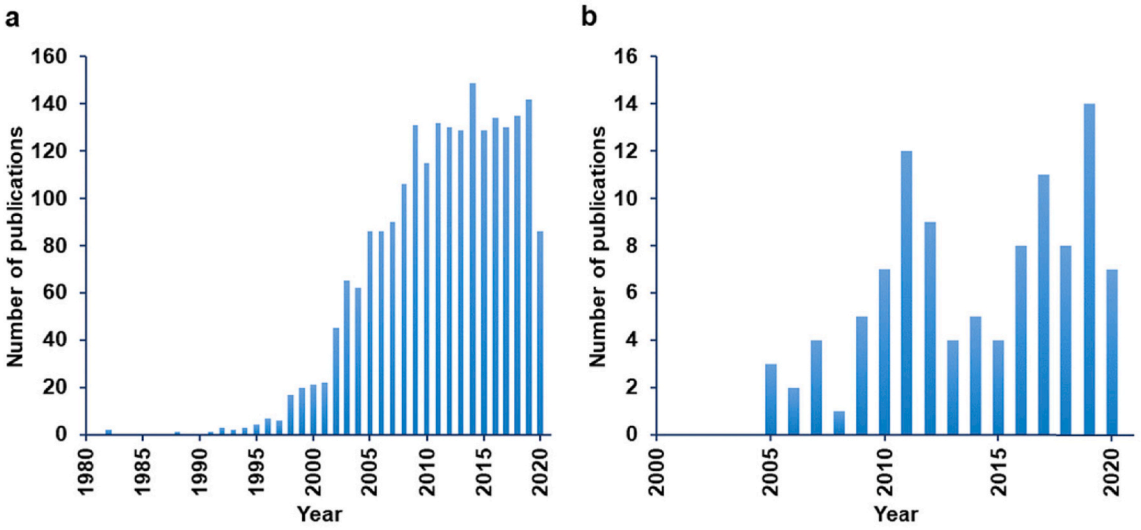

Fig. 1. Development in the number of publications related to hybrid organo-alkoxysilane materials (left – **a**; keywords hybrid AND organo*sil*) and nanofibrous materials containing organo-alkoxysilanes (right – **b**; keywords nanofib* AND organo*sil*). (Data source: WoS, up to August 2020).

The chemistry related to organo-alkoxysilanes has been well described and there is a wide range of commercially available organosilane precursors. The properties and the synthesis of molecules having the formula $Si(OR')_x$-R_{4-x} (x = 1–3) containing stable Si-R groups (R = alkyl, aryl, acryl, epoxy, amino group etc.) and hydrolysable alkoxy Si-OR′ units have also been widely described. These kinds of organosilane precursors are known as organo-mono-silylated precursors, while organo-bridged trialkoxysilanes [$(R'O)_3$Si-R-Si$(OR')_3$] may be referred to as organo-bis-silylated precursors having the same well explored background [39]. The R group is, as in the case of organo-mono-silylated precursors, an organic unit, but in this case directly linked to two Si atoms through Si–C covalent bonds. Arylenes, alkylenes, cyclams, crown ethers, porphyrins, polymers, and many others have been used as the organic component. This diversity of organic moieties enables variation of porosity, thermal stability, optical clarity, refractive index, chemical resistance, hydrophobicity, and dielectric constant [37,40].

Hydrolysis and the subsequent condensation of such silylated organo-trialkoxides (T) (see Fig. 2) result in a formation having the above-mentioned basic repeating unit [$RSiO_{1.5}$]. Moreover, as the number of various alkoxy groups on Si determinates the potential for forming multiple bonds with other silica atoms, the resulting level of crosslinking may differ drastically from the structure of silsesquioxanes. The final hybrid material may be controlled using a whole variety of functional organo-alkoxysilanes from difunctional dialkoxysilanes (D) forming linear oligo or polysiloxane structures to monofunctional trialkoxysilanes (T) or tetraalkoxysilanes (Q) having a tendency to form highly crosslinked polymers depending on a number of sol-gel parameters. In addition, as the organosilane precursors may possess many different geometries (aryl rigid rod spacers, alkylic flexible spacers), they may be used to precisely control the parameters that govern the structures of the targeted hybrid materials [38].

Furthermore, it is necessary to take into consideration that the organo-bis-silylated precursors have a higher ability for self-organization than organo-mono-silylated precursors. This property is a great advantage in the formation of highly organized structures such as crystal-like structures in non-mesoporous organosilane materials [38]. In the silicon-based sol-gel process, the network behavior of organo-trialkoxysilanes (T) with various types of attachment of the organic moiety to silicon may manifest itself in three networking ways (Fig. 3).

Bridged bis-silylated organosilane precursors are referred to as "network builders" – their co-polycondensation with or without a tetraalkoxysilane precursor leads to the creation of materials in which the organic segment is an integral part of the hybrid network. By contrast, mono-silylated organosilane precursors act in the final structure as so-called "network modifiers" ultimately modifying a discrete area of the homogeneous silica network. In addition, if the organic moiety is intended to undergo further chemical reaction (as a sort of surface anchor), then organo-trialkoxysilane (e.g.: amino-functionalized silanes) serves as a so-called "network functionalizer" [12].

As may be seen, concise use of mono-silylated or bis-silylated organo-alkoxysilanes in sol–gel processing is a fascinating bottom-up approach to fabricating new functional hybrid materials with numerous applications.

2.1. Sol-gel process of organo-trialkoxysilanes leading to fiber formation

Generally, the thermal stability of fragile organics is limited to a high temperature, meaning that high temperatures cannot be used during the hybrid formation process. Thanks to soft sol–gel processes, it is possible to overcome this limitation during the preparation of hybrid organosilane materials. These types of materials have undergone tremendous development over the past few years and even fiber-making research has benefited greatly from mild sol-gel processing [1,5,6,15,16,37,41].

However, the sol-gel process of organo-trialkoxysilanes leading to fiber formation is more demanding in terms of a suitable set of sol-gel processing parameters. Mentioned parameters, including the detailed equations describing the whole sol-gel process from the beginning until the end, are clearly described and can be found in many literature sources, most recently in the review written by Catauro et al. [42], which has been published this year. As already stated in the 1980s by Sakka et al. [32,35] for silica fibers based on tetraethoxysilane (TEOS) and tetramethoxysilane (TMOS) in general, the most crucial issue is the spinnability of the sol, whose occurrence is essential for fiber formation. According to their research, a sol should be spinnable when hydrolysis is suppressed. As a result, the condensation rate and extent of branching are low enough to increase the concentration and viscosity of organo-siloxane polymers without premature gelation. Hence, the spinnability should usually be achieved as a combination of acid-catalyzed sol-gel conditions with a r = water/silane ratio of less

Table 1
A historical overview of the developments leading to hybrid organosilane materials.

Year	Scientist(s)	Discovery	References
1640	J. B. van Helmont (Belgium)	The first contribution regarding silicon chemistry.	[1]
1779	T. Berman (Sweden)	Description of the first silica "gel" formation.	
1824	J. J. Berzelius (Sweden)	New molecular silicon and organosilicon precursors	
1843	J. J. Berzelius (Sweden)	Synthesis of $SiCl_4$	
1844	J. J. Ebelmen (France)	"Grandfather of sol-gel chemistry". Description of the formation of silicic ethers	
1857	Friedrich Wöhler (Germany)	Silicon tetrahydride (SiH_4) Hypothesis regarding the existence of an alternative organic chemistry based on silicon	
1863	C. Friedel (France) and J. M. Crafts (USA)	Synthesis of the first organosilicon compound, tetraethylsilane (TEOS)	
1871	A. Ladenburg (Germany)	Hydrolysis of Et_3SiOEt to form triethylsilanol (Et_3SiOH), the first "silanol"	
1904	F. S. Kipping (United Kingdom)	Application of the newly discovered Grignard's reagents to synthetize a wide range of new organo- and chlorosilanes starting from $SiCl_4$	[22]
1952	H. J. Deuel (Germany)	The first organic derivatives of silicates formed through covalent bonds of organic groups and the silicate network	[23]
1964	A. N. Lentz (Germany)	Firstly reported preparation of organic derivatives of silicates	[24]
1978	K. Andrianov (Russia)	The first syntheses of organoalkoxysilanes containing the Si–C covalent bond.	[25]
1980	W. Mahler & M. F. Bechtold (USA)	The first freeze-formed silica fibers	[26]
1980s	Sakka S. (Japan); W. C. LaCourse, H. G. Sowman (USA)	The first preparation of silica and silicate fibers by drawing directly from viscous sols at room temperature	[27]
1985	H. Schmidt (Germany)	Silicon allows a large variety of organic functionalization thanks to the stability of the Si–C bond	[28]
1990	C. J. Brinker and G. Scherer (USA)	Publication of the book "Sol-Gel Science".	[29]
1992	K. Shea (United Kingdom); R. Corriu (France)	Several simultaneously developed molecular-level hybrids by hydrolysis and condensation of new polyfunctional alkoxysilane containing groups acting as aryl or acyclic, rigid or flexible spacers	[30,31]
Late 2000s	Various research groups	Preparation of hybrid organosilane fibers on the basis of sol-gel processing	Further in this review

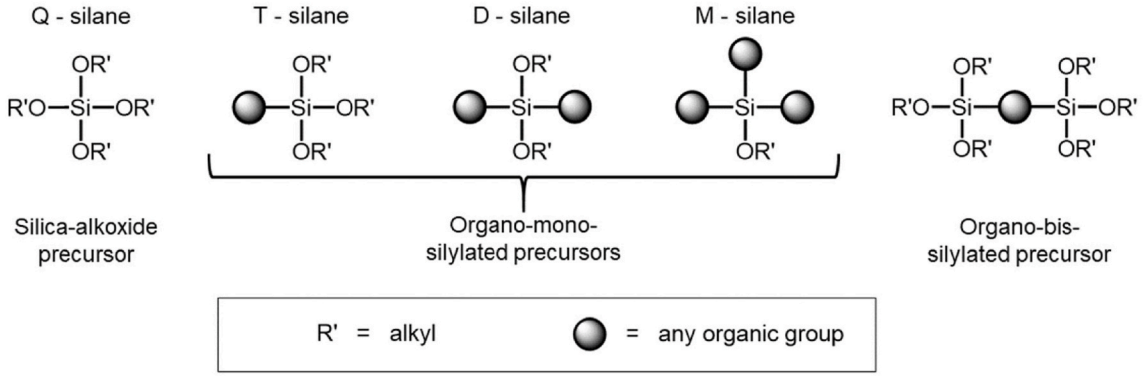

Fig. 2. Scheme showing the different types of organosilanes.

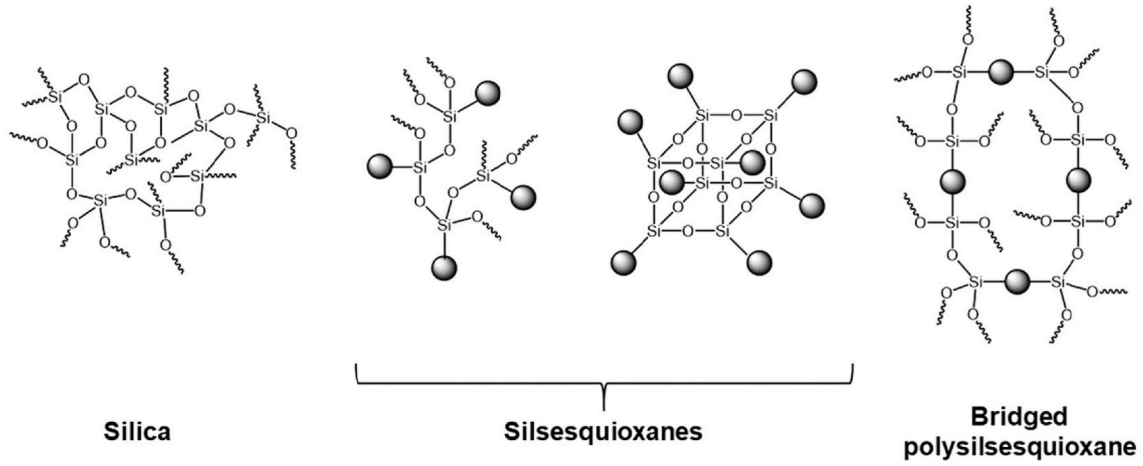

Fig. 3. Selected organosilane precursors transforming into nets during polycondensation processes. Pure silica is included for comparison.

than 2. The subsequent hydrolysis and polycondensation reactions should result in the development of a ladder-like crosslinking between the linear polymer siloxane chains [32,35].

Therefore, a structurally convenient polymerization in an acidic medium is the most important factor influencing the preparation of spinnable sols. In a classic (and already extensively studied) sol-gel reaction [11], the alkoxy groups Si-OR′ hydrolyze into silanol Si–OH groups (sol), which subsequently condensate to a 3D polysiloxane (-Si-O-Si-) polymeric network that is filled with a solvent (gel). In an acidic medium, the alkoxide and silanol are first protonated in a fast step. The silicon atom then becomes more electrophilic and susceptible to backside attack by water or neutral silanol in hydrolysis and condensation reaction steps, respectively. As a result, the protonated silanol preferentially condensates with the least acidic silanol end groups, which leads to less branched clusters desirable for fiber manufacturing [43–46].

Although acidic conditions accelerate the hydrolysis and enhance the silanol entities stability at the beginning of the process, the same conditions slow down the rate of the self-condensation reactions, as can be seen from in situ ^{1}H and ^{13}C NMR [47]. That is why the water/silane ratio should be kept low in order to suppress the process to further reduce the branching. Likewise, the sol-gel reaction rate of organo-trialkoxysilanes and its outcomes are strongly affected by steric and inductive effects. It should be taken into consideration that the hydrolysis will be rather enhanced with polar and electron-providing organic moiety, due to the improvement of the solubility in the water by the formation of hydrogen bonds and the stabilization of the positively charged intermediates of the sol-gel reactions. On the other hand, the steric hindrance of the organic species generally significantly slows down the hydrolysis rates [11,43–46,48–50].

To summarize, the basic factors strongly influencing not only fiber formation on the basis of organo-trialkoxysilane precursors, but sol-gel processing in general, may be divided into two main groups: Among the primary factors belong the types of catalysts, water/silane ratio, pH, and organo-functional groups, which strongly influence the polymerization outcomes, while the secondary factors, such as temperature, solvent, ionic strength, leaving group, and silane concentration, influence the reaction rates [43]. In addition, the viscosity of spinnable sols should be minutely observed throughout the process of hydrolysis-polycondensation as a concentration dependence is characteristic for the presence of linear (organo) siloxane polymers. Hence, the conditions suitable for various fiber formation techniques may be determined [9,10,32,51].

Nevertheless, the primary academic literature struggles with the above-described suitable polymerization of organosilanes in long spinnable polymeric chains. Therefore, most research groups enhance the sol formulas with various types of surfactants, low-molecular-weight polymeric gelators or spinnable polymers in order to facilitate the fiber making process. However, with a concise choice of sol-gel processing parameters, spinnable sols and fibers purely on the basis of organo-mono-silylated and/or organo-bis-silylated analogues can be obtained (Fig. 4) via sol-gel “one-pot synthesis” [9,10].

2.2. *Common fiber-making techniques - their prospects and consequences*

Fibers have been a fundamental part of human life since the dawn of civilization [52]. A huge number of papers have reported the preparation, characterization and applications of different types of nanofibers

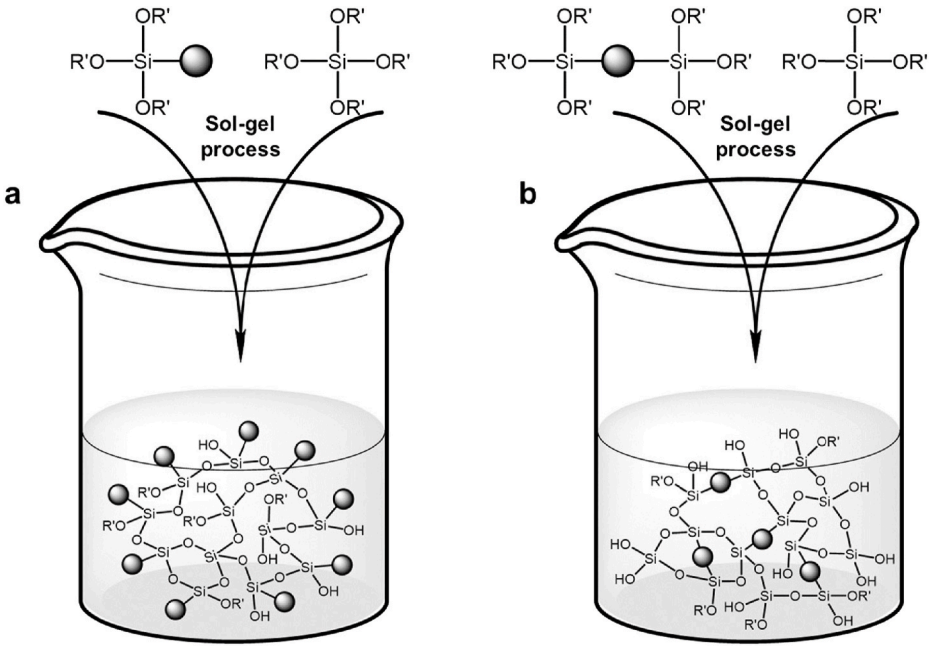

Fig. 4. Scheme describing the polycondensation processes of organo-mono-silylated **a**) and organo-bis-silylated precursors **b**).

via various techniques (Fig. 5) mainly allowing the inclusion of electrospinning, drawing and self-assembly [53,54].

2.2.1. *Electrospinning*

Electrospinning is known as a versatile and viable technique for generating ultrathin fibers made of polymeric, metal oxide materials, as well as their combination. Remarkable progress has been made with regard to the development of electrospinning methods and engineering of electrospun nanofibers to suit or enable various applications [52,55]. According to the data released by "Research and Markets", the global market for nanofibers can reach 1 billion USA dollars by the end of 2021 [52]. Although electrospun nanofibers have unique applications, they still encounter several challenges in the production stage: (i) large volume processing, (ii) reproducibility; and (iii) safety [53].

The electrospinning equipment consists of four major components: a high-voltage power supply, a syringe pump, a spinneret, and a collector. The main principle is based on a small amount of viscoelastic fluid, which is pumped out through the spinneret and has a tendency to form a spherical droplet as a result of the confinement of surface tension. Thanks to the interconnection of the droplet with a high-voltage power supply, its surface is quickly covered by charges of the same sign. The repulsion among these charges counteracts the surface tension and destabilize the spherical shape. If the repulsion is strong enough to overcome the surface tension, the droplet is deformed into a conical shape and a jet emanates from the apex of the cone. As a result, is the formation of the fibers together with the evaporation of the solvent [52].

The electrospinning process is influenced by various different factors and parameters, which are essential for the successful formation of fibers [56]: (i) environmental parameters, such as solution temperature, humidity and air velocity in the electrospinning chamber; (ii) solution properties, such as elasticity, viscosity, conductivity and surface tension; and (iii) governing variables, such as distance between the tip and counter electrode, electrical potential, flow rate, the molecular weight of the selected polymers, and the geometry of the collector [55].

The viscosity of the spinning solution is one of the critical aspects of the fiber-forming technology, which can be determined by varying the concentration of the polymer solution. Solutions with an optimum viscosity only yield the respective fibers in micro to nanoscale diameters

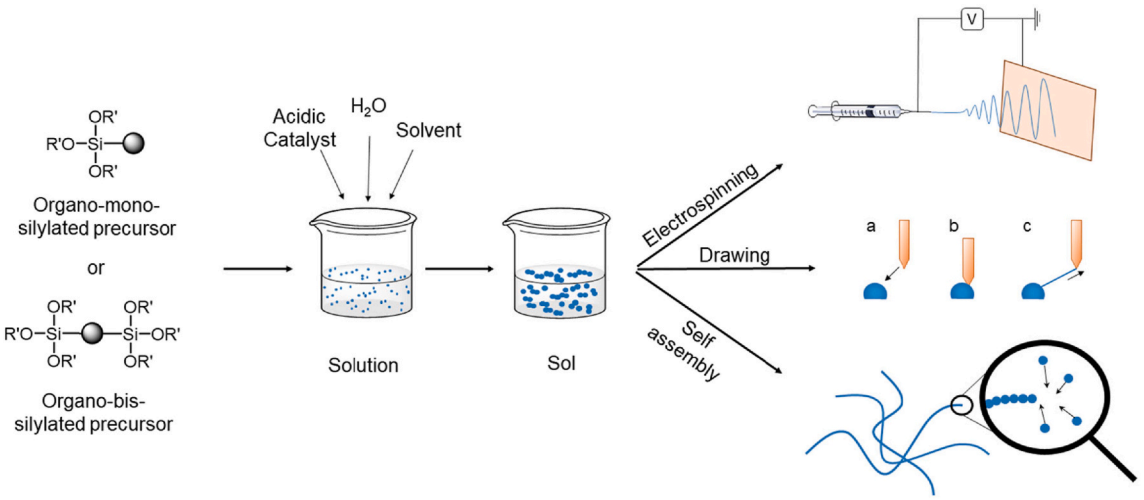

Fig. 5. Preparation of nanofibers from organo-mono-silylated and/or organo-bis-silylated precursors using various fiber making techniques.

[9]. During the electrospinning process, the applied voltage needs to be high enough to overcome the surface tension of the spinning solution to produce fibers. Yang et al. [57] reported that by reducing the surface tension of the solution without changing the concentration, beaded fibers may be converted into smooth fibers. Likewise, the conductivity of the solution may play a key role in the fiber formation process [56]. Similarly, the diameter and shape of the gauge may change the diameter and morphology of the fiber, respectively. The distance from the tip of the needle to the collector gives an ample opportunity for the solvent to evaporate. A lesser distance results in thicker/beaded fibers being formed, whereas a greater distance results in discontinuous fibers [52]. The alignment/orientation of the fibers primarily depends on the type of collector used, such as pin, plate, cross bar, rotating rods or wheels, drum, liquid bath and disk etc. In general, the fiber diameter and the pore diameter increase with an increase in the polymer concentration and flow rate. The geometry of the collector influences the arrangement of the fibers [53]. Through optimization of the above-mentioned parameters, fibers can be obtained randomly or in an ordered way. The choice of determining parameters is made on the basis of the polymer solution and the applicability of the formed fibers.

2.2.2. Drawing

The first attempt to draw a fiber was described in the 19th century. The experiment involved shooting an arrow from a droplet of a melted polymer using a crossbow [58]. In 1998, Ondarcuhu and Joachim published a drawing experiment, whereby a single fiber was formed from a droplet of a polymer solution using the tip of a scanning tunneling microscope (STM) [59]. Nowadays, the mechanical drawing of fibers is divided into two main categories: drawing from a solution [57,60] or from a melt [61]. Drawing as a method is particularly used for the production of fibers for optical devices [62,63], optical sensing or nanophotonic fibers [57,61,64,65].

The principle of the drawing method is based on the mechanical pulling of a polymer solution out of its base droplet, resulting in evaporation of the solvent and fiber solidification at real-time [58]. Polymeric micro or nanofibers can be fabricated using two different ways of drawing, through glass micro-pipettes and/or with help of atomic force microscope (AFM) or scanning tunneling microscope (STM) probe tips. This method is suitable for the formation of fibers having determined geometrical characteristics [66].

Drawing has several drawbacks compared to the other methods used for nanofiber formation [67]. These include process control, a limited-time of the process influenced by polymer droplet solidification, changes in the viscosity of the droplet with time, and speed of the solvent evaporation from the deposited droplet [60]. On the other hand, one of the greatest advantages of the drawing process is the ability to prepare oriented fibers at the range from nanometers to micrometers, compared to electrospun fibers, which are randomly oriented at similar scales [68].

The literature focused on the preparation of fibers made of organosilane precursors includes a publication from 1998 describing the preparation of mesoporous silica fibers by drawing [69]. However, the overwhelming majority of papers dealing with this method are focused on drawing from purely organic polymers [58,60,64].

2.2.3. Self-assembly

The principle of the self-assembly technique may be described as the spontaneous and reversible process in which a disordered system of pre-existing components (molecules, polymers, colloids, or macroscopic particles) are organized into ordered and/or functional structures or patterns via non-covalent interactions without external direction [70].

In general, these are spontaneous processes tending towards an equilibrium resulting in various shapes and forms [71]. In chemistry, self-assembly is typically associated with energy minimization processes and thermodynamic equilibrium [72]. Whitesides and Grzybowski divide self-assembly into two categories: static and dynamic. Static self-assembly corresponds to “molecular self-assembly”, while dynamic self-assembly corresponds more to “self-organization” [73]. In polymer chemistry, Yamaguchi et al. consider self-assembly and dissipative structures as equilibrium and none-equilibrium forms of pattern formation, regarding them as two complementary manifestations of self-organization [71,74].

Despite the firm attention of academic literature [75–81] organosilane fibers prepared in the way and the technique itself have a number of disadvantages including the stability of self-assembly solutions, fiber length usually being only 100–200 nm, and fiber fragility with low mechanical resistance [76,77,82]. In most cases, self-assembled organosilane fibers have a tendency to be formed into short helical structures with a highly rough surface. Moreover, compared to electrospun fibers, manipulation is very demanding as they are not able to form a continuous layer within a solution.

Numerous studies have been devoted to the self-organization of organo-mono-silylated and organo-bis-silylated precursors and mesoporous materials made of them obtained via supramolecular self-assembly [38]. A wide range of literature regarding the self-assembly organization of organo-mono-silylated and organo-bis-silylated precursors into different shapes including nanofibers already exists and will be described further in this review.

3. Hybrid organosilane fibers based on organo-mono-silylated precursors

In the moderate literature dealing with the preparation of hybrid organosilane fibrous materials based on organo-mono-silylated precursors, three principal strategies emerge in relation to their preparation. Firstly and most easily, a wide range of organo-mono-silylated precursors are mixed together with various organic polymers functioning as a spinnable mediator. Likewise, organo-mono-silylated precursors may also be used in the second step to functionalize the prepared inorganic silica or organic polymer fibers. In both cases, the used spinnable mediator (organic polymer) may not bring any added value or may even be toxic in later use. Finally, organo-mono-silylated precursors either on their own or in a mixture with tetraalkoxysilanes may be combined to form a spinnable sol resulting in a purely organosilane composition of fibers. Therefore, the organic moiety is linked to inorganics entirely through Si–C bonds.

Either way, after sufficient networking these organo-mono-silylated mixtures undergo the above-mentioned fiber-making methods (electrospinning, drawing) or directly self-assemble into fibrous forms. Whichever method is used, the resulting fibrous materials should be a Class II organosilane hybrid displaying Si–C bonds in its structure. Nevertheless, depending on the other components, the structural variety may show a complex of hybrid links oscillating between Class I and II hybrids and even nanocomposites. The following chapter is dedicated to hybrid fibers based on organo-mono-silylated precursors, demonstrates the variety of synthetic approaches, and presents some of the most intriguing applications.

3.1. Hybrid organosilane fibers containing organic polymers

As already outlined, the spinnability of organo-alkoxysilanes appears to be the biggest obstacle in the subsequent electrospinning and drawing processes of organosilane fiber manufacturing. The difficult search for suitable sol-gel parameters achieving ladder-like spinnable organosiloxane polymer chains may be avoided by using a wide selection of surfactants, low-molecular-weight polymeric gelators or spinnable polymers. Organic polymers used as a so-called “spinnability carrier” in combination with organo-alkoxysilanes or alkoxysilanes seem to be a prolific source of hybrid organosilane or silica/polymer fibers. The most commonly-used organic polymers are poly(methylmethacrylate) (PMMA), polyvinylpyrrolidone (PVP), polycaprolactone (PCL), polyvinylalcohol (PVA), polystyrene (PS), and polyacrylonitrile (PAN).

Electrospinning is the most widely-used technique for fiber-manufacturing of organo-alkoxysilane and organic polymer solution mixtures. Nevertheless, mixtures of organic polymers with tetraalkoxysilanes (TEOS at most) prevail and are also commonly referred to as organosilane hybrid fibers. However, the resulting structure does not contain Si–C bonds, but Si–O–C links connecting the inorganics with organic polymers (which is not quite in the scope of this review). There are many examples, such as the research of Li, J. et al. [83] who studied the tensile performance of TEOS/PMMA fibrous mats or the preparation of polyhydroxybutyrate (PHB)/PCL/TEOS fibrous scaffolds with a drug releasing function [84] to support bone tissue recovery. Organic polymers are often combined with tetraalkoxysilanes to create pore-forming (structure-directing) agents and subsequently are fired out to leave pure mesoporous silica fibers as a result [85].

Nevertheless, such examples of hybrid organosilane fibers from organo-mono-silylated precursors and organic polymers are not numerous. Ma et al. [86] reported the formation of superhydrophobic fibers (Fig. 6) by the electrospinning of poly(styrene-*b*-dimethylsiloxane) block copolymers blended with 23.4 wt% homopolymer polystyrene - polydimethylsiloxane - polystyrene (PS-PDMS/PS) from a solution in a mixed solvent of tetrahydrofuran (THF) and dimethylformamide (DMF). The resulting fibrous mats (fiber diameters ranging from 150 to 400 nm) showed a water contact angle of 163° attributed to the combined effect of surface enrichment with PDMS and increased surface roughness.

Another PDMS hybrid was prepared by Wei, Z. et al. [87] together with polyethylene oxide (PEO). The organic polymer was used only as an electrospinning carrier in a small ratio of approximately 0.3–0.5 wt% together with silica sol. Interestingly, the resulting hydrophobic silica/PDMS/PEO hybrid fibrous mats displayed good thermal stability (>600 °C) promising in related applications. Likewise, the hydrophobicity of PVA fibers was enhanced by Mustafa H. Ugur et al. [88] by adding a whole range of organo-mono-silylated precursors to an electrospinning PVA solution. Cross-linked PVA/organosilica electrospun mats (Fig. 7) with reticulated structures (average fiber diameter of approximately 70 nm) were obtained with varying percentages of organosilane sol produced through the acetic acid catalyzed reaction of dimethyldimethoxysilane (DMDMOS), methyltrimethoxysilane (MTMS), tridecafluoro-1,1,2,2-tetrahydrooctyltriethoxysilane (FAS1313; Dynasylan® F 8261) and phenyltrimethoxysilane (PTMS; Dynasylan® 9165) in an isopropyl alcohol (IPA)–water mixture.

Likewise, Arslan et al. [89] used the –OH groups available on the cellulose acetate (CA) structure to proceed with basic sol−gel reactions initiated by a mixture with reactive fluoro-alkoxysilane (FS) (Dynasilan F8261; FS). Perfluoro groups consequently modified the hydrophilic CA nanofibers (NF) to display superhydrophobic properties. Therefore, FS/CA-NF may be quite practical for future application in oil-water separators, as well as self-cleaning or water resistant nanofibrous structures [89].

Finally, an interesting combined method of in situ reduction and sol–gel processing was used to prepare novel fibrous membranes made of Ag@gelatin–silica hybrid nanofibers from gelatin, 3-glycidoxypropyltrimethoxysilane, and Ag@gelatin nanoparticles (NPs) [90]. The resulting fibrous mats showed strong photo-catalytic and antibacterial activity and may be easily recycled with a high recovery efficiency making them ideal adepts for removal of both organic pollutants and microbial contaminants from wastewater.

In rare cases, drawing and self-assembly techniques use a combination of organo-mono-silylated precursors with organic polymers. Drawing process have been used to fabricate vinyltrimethoxysilane (VTMS) grafted polyethylene (PE)/SiO_2 nanocomposite fiber ropes [91]. The VTMS-*g*-PE/SiO_2 fibrous hybrid displayed remarkably improved breaking load and breaking strength compared to pure PE fiber ropes and decreased elongation at break. Mixtures of organic polymers with organo-alkoxysilanes are not commonly used in self-assembly techniques.

3.2. Hybrid organosilane fibers via functionalization

The functionalization of previously prepared fibers is a commonly used method mainly due to its ease. Typically, inorganic or organic fibers are simply dip-coated in a sol based on an organosilane precursor often in combination with TEOS or TMOS. In any case, the resulting material is layered as the first fiber becomes the core and the dipped organosilane makes an external topcoat (a method referred to as "functionalizing"), which may be even multiplied.

The core fiber can be any kind of hydrolysable inorganic, organic or composite material, so the principle of sol-gel processing may be applied. Hence, this procedure is well known in industrial conditions and the functionalization with various organosilanes is securely

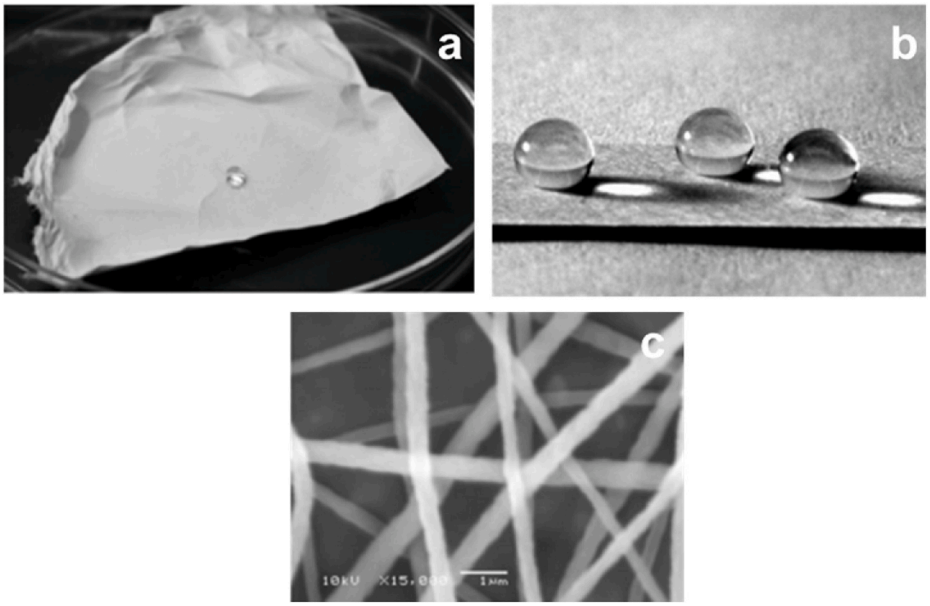

Fig. 6. Free-standing mat composed of PS-PDMS/PS electrospun fibers **a**); several 20 μL water droplets on the mat, showing a superhydrophobic surface **b**); SEM image of the prepared fibers at 6000x magnification (scale bar = 2 μm) **c**); [86].

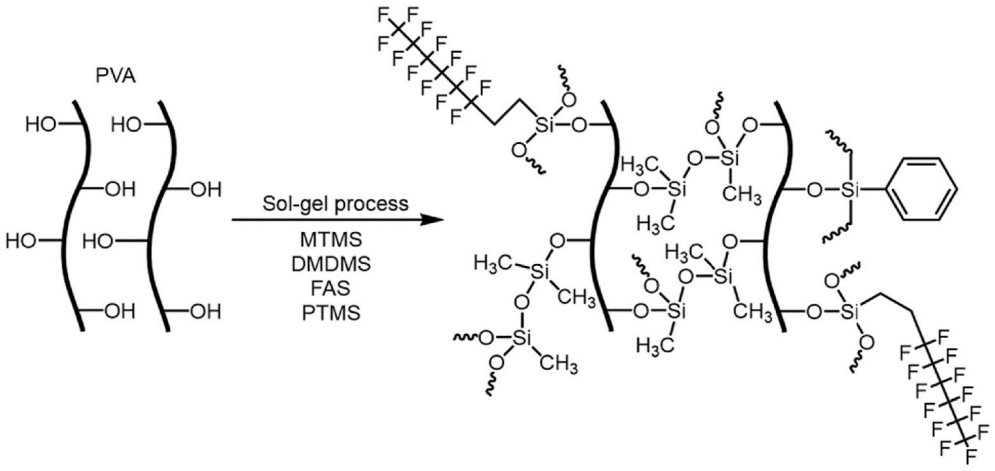

Fig. 7. Scheme of PVA/silica nanofibrous mats, adapted according to reference [88].

performed on glass or silica fibers (SiO_2) modified via 3-mercaptopropyltrimethoxysilane (MPTMS) (Fig. 8) marked as –SH and silver nanoparticles [92–94], various organic polymers [95–97], cellulose acetate [89,98,99] or even wool [100] and composite materials [101,102]. Nevertheless, there are also very specific strategies of silanization for more demanding materials, such as (nano) cellulose fibers representing so called "never-dried" materials. Beaumont et al. [103] proposed a two-step silanization protocol for nanostructured celluloses under aqueous conditions using catalytic amounts of hydrogen chloride and then sodium hydroxide. The developed protocol enables the incorporation of vinyl, thiol, and azido groups onto cellulose fibers and cellulose nanofibrils without curing or solvent-exchange. Hence, the functionalized celluloses remain never-dried, and no agglomeration or hornification occurs in the process.

The most commonly used organo-mono-silylated precursors include fluoro-alkoxysilanes often in combination with TEOS, employed to increase the hydrophobicity of the core fibers [89,95,97,99]. Likewise, the popularity of 3-aminopropyltriethoxysilane (APTES), 3-glycidyloxypropyltrimethoxysilane (GPTMS) and 3-mercaptopropyltrimethoxysilane (MPTMS) will be illustrated in the following section dedicated to applications using fibers based on organo-mono-silylated precursors.

3.3. Purely organosilane fibers

Probably due to the above-mentioned difficulty in achieving spinnable solutions, there are only a few research groups investigating organosilane fibers based purely on organo-mono-silanes (with or without tetraalkoxysilanes).

Groups led by Schramm [51] and Aytan [104] prepared polyimide-silane fibers (Fig. 9) as new kinds of conductive electrolytes. Even if the starting sol-gel solution was based on organo-mono-silylated precursors, the first step consisted in the synthesis of a silylated polyamic acid precursor (sil-PAA). The silanization proceeded with the help of GPTMS or APTES, and in order to enhance the final properties of the resulting fibers, the sol-gel process was subsequently enriched [104] by other alkoxysilanes (PDMS, 3-(trimethoxysilyl)propyl methacrylate (TMSPMA), 3-(triethoxysilyl)propyl isocyanate (ICPTMS)). The water-soluble electrospun fibers were then subjected to a thermal imidization treatment at various temperatures. As a result, these water-insoluble organosilane materials with a nanoscale fibrous structure were stable at relatively high temperatures and showed electrolyte absorption and sufficient conductivity at room temperature [51,104,105].

Another research group of McDowell [106] synthesized the starting organosilane precursor. In this case, high molecular weight polyferrocenylmethylvinylsilane (PFMVS) was synthesized by anionic ring-opening polymerization and further functionalized through Pt-catalyzed hydrosilylation using ethoxysilane to afford a polyferrocenylsilane (PFS) precursor. Electrospun electroactive microfibers from this gelable PFS cross-linkable alkoxysilane displayed interesting strain-induced buckling behavior on electroactuation at low voltages and, hence, could potentially rival existing bilayer actuators. See Fig. 10 [106].

The simplest synthesis in terms of the starting sol-gel solution may be found in the research of He et al. [107]. They prepared a range of electrospun mesoporous (organo)silica nanofibers. The silica sols with the surfactant Pluronic F127 were prepared with the addition of a MPTMS precursor and its influence on the fiber internal structure was

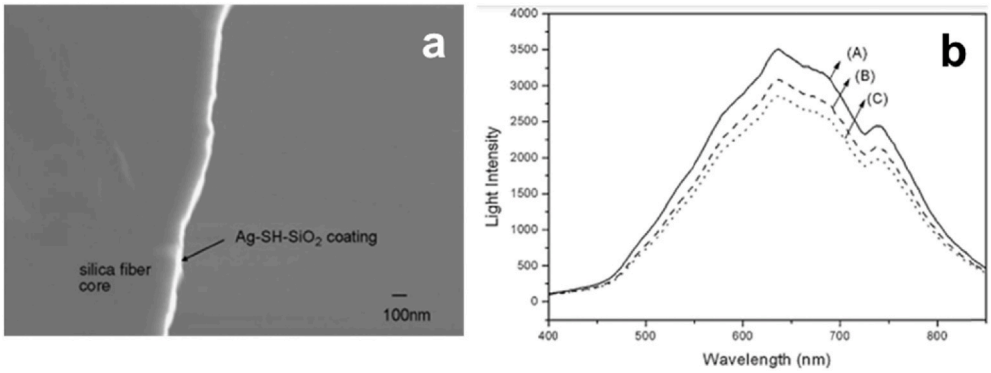

Fig. 8. A SEM image of the cross-section of an optical fiber coated via MPTMS containing Ag nanoparticles and its changes in light intensity guided through the coated fiber probe [92].

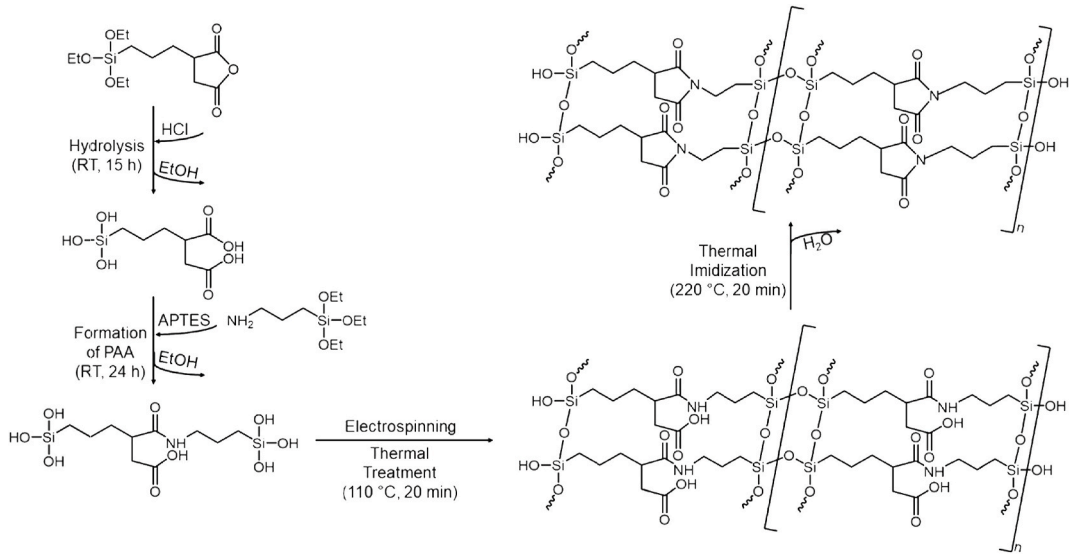

Fig. 9. Schematic representation of the preparation of polyimide-silane fibers, adapted according to reference [105].

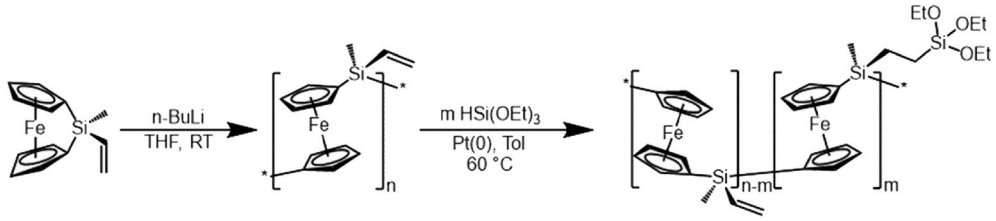

Fig. 10. Scheme showing the formation of an organo-mono-silylated precursor, adapted according to reference [106].

evaluated. With the reduced F127/TEOS mass ratio, the diameter of the (organo)silica nanofibers decreased, but the size and the orientation of the internal mesopores were remarkably regulated (Fig. 11). Such a fibrous hierarchical hybrid material may be of great interest for modern optical and biomedical applications [107].

4. Hybrid fibrous materials based on organo-bis-silylated precursors

The development of sophisticated organized hybrid materials, made of organo-bis-silylated precursors, exhibiting enhanced properties, plays an important role in tacking the challenging topics of the current scientific domains [108,109]. The first bridged organo-bis-silylated

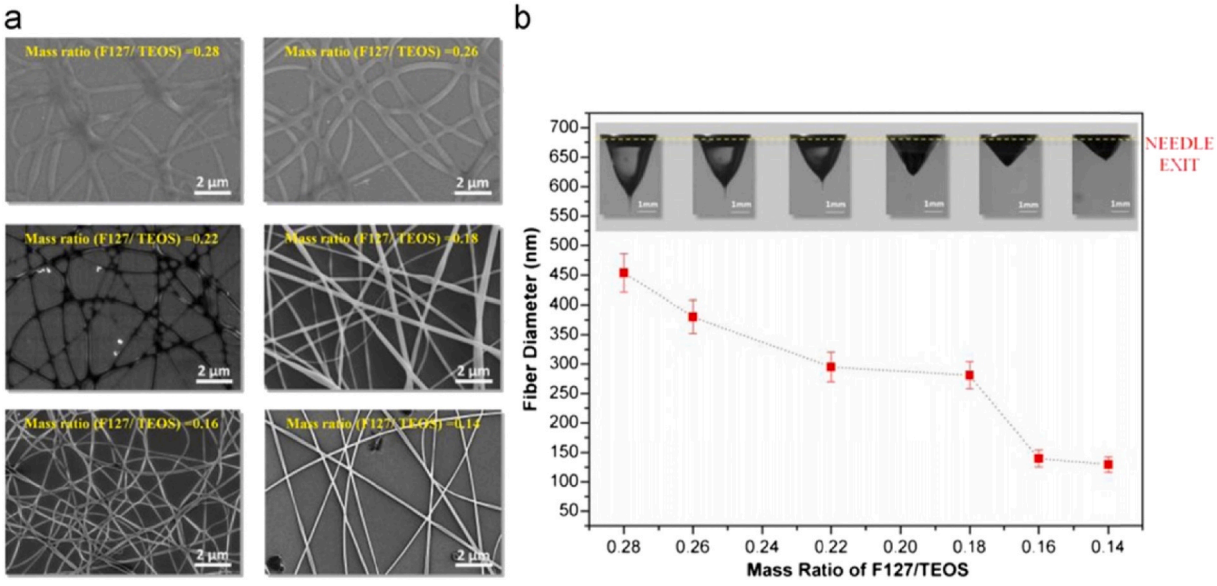

Fig. 11. SEM images of silica nanofibers prepared using sols with different F127/TEOS mass ratios **a**); and the relationship between the fiber diameter and the F127/TEOS mass ratios **b**); [107].

monomers, having arylene and acetylene bridging groups, were firstly used for sol-gel polymerization to form bridged polysilsesquioxanes coatings deposited on glass in the 1950s [39]. However, it was not until the start of the 1990s that bis(trimethoxysilyl)organometallic precursors with different structural features were first synthesized [30].

Nowadays, the number of organo-bis-silylated precursors with a wide variety of organic molecules is continuously increasing and they can be finally incorporated into the targeted materials [108,110,111].

4.1. Hybrid organo-bis-silylated materials: powders prevail over fibers

Several synthetic approaches leading to the preparation of monomers for bridged polysilsesquioxanes currently exist, these include e.g. metalation; hydrosilylation, and organotrialkoxysilane functionalization [39]. From the "fiber-formation" point of view, a very promising class of organo-bis-silylated precursors is shown in Fig. 12. These precursors are well described in the synthesis and formation of periodic mesoporous organosilica (PMO) materials [112]. Shea et al. reported the process of sol-gel synthesis regarding monolithic bridged silsesquioxane using 15 different alkane-, alkene-, alkyne-, aromatic-, functionalized- and organometallic-bridged precursors [39,110].

Many bridged polysilsesquioxanes exhibit excellent thermal stability in inert atmospheres and in air. Phenylene-bridged polysilsesquioxanes are stable up to 500 °C. Alkylene-bridged polysilsesquioxanes are stable to over 400 °C. However, there is a lack of experiments describing the mechanical properties of bridged polysilsesquioxanes [39]. The most distinguishing features of arylene bridged polysilsesquioxanes are that they are porous and have extremely high surface areas, which may also be observed in the case of the fibrous form, which has promising potential for filtration, catalysis or adsorption [9]. Although conventional silica-based materials are generally regarded as biocompatible and suitable for *in vivo* use, the bio-safety of organo-bridged materials is still not entirely clear because of the lack of extensive and detailed *in vitro* and *in vivo* research and evaluations [113].

Interestingly, in the research or review literature, there are very few research papers focused on the preparation of purely organosilane fibrous materials using organo-bis-silylated precursors [9,10,105,114]. The greatest obstacles seem to lay in the supposed difficulty of the polymerization process of organo-bridged silanes, their conversion into a spinnable polymeric solution and the choice of suitable electrospinning technique.

Until 2020, only two solitary research papers regarding these types of nanofibers were published [105,114]. Tao et al. [114] dealt with the fabrication of purely organosilane electrospun nanofibrous mats containing porphyrin unit bridged organosilanes; however, the final material contained a very low amount of these organo-bridged silanes (10^{-4} mol %) compared to TEOS (i.e. the result was mainly silica fibers). The second group [105] used the co-polycondensation process of two organosilanes combined with the sol-gel process and electrospinning to form ultra-thin polyimide fibers, also called as poly(amic)acid (PAA) fibers. Mentioned fibers are made of combination (3-triethoxysilylpropyl)succinic anhydride (TESP-SA) with either TEOS or methyltriethoxysilane (MTEOS) which were hydrolyzed and reacted subsequently with APTES, leading to the formation of an electrospinnable PAA solution. However, the solution had to be adjusted before electrospinning with a non-ionic surfactant Triton X-100 to improve the spinnability, but this reagent inevitably remained in the hybrid structure [105,115].

Nevertheless, the proof that all of the above-mentioned sol-gel parameters may be effectively linked to obtain spinnable sols can be found in the following research papers [9,10]. Both papers describe the one-pot synthesis of purely organosilane fibers without the addition of any kinds of surfactants, low-molecular-weight polymeric gelators or spinnable polymers (Figs. 13 and 14), which were successfully produced on an industrial electrospinning device, paving the way for possible fabrication on a large scale. Moreover, the use of mono and bis-silylated model benzene functionalized organoalkoxysilanes [9] or a custom-made bis-silylated 1,2-diaminocyclohexane derivative [10] proves the possibility of designing a molecularly engineered material tailored to specific applications such as reusable catalysts, adsorption agents, conducting membranes or as novel types of biomaterials with additional properties.

If organo-bis-silylated precursors are not used in fiber-making via electrospinning and drawing techniques, the self-assembly procedure counterweights this lack of interest. Helical hybrid nanofibers have attracted the attention of many research groups due to their potential application for chiral catalysis and separations [76,77,116]. Although many approaches to the preparation of helical mesoporous silica nanofibers have been developed, those for the preparation of helical organic–inorganic mesoporous hybrid organosilane nanofibers are rare [77]. They may be prepared using chiral low-molecular weight amphiphiles [117] or mixtures of a cationic and fluorinated surfactant. Moreover, the reduction of surface free energy was proposed as the driving force of helix formation in the fiber structure [77].

A wide range of helical fibers has been prepared using various synthetic methods including self-assembled bridged silsesquioxane helical fibers formed through hydrogen bonds promoted by the urea groups within the organic bridged fragment [118]; periodic mesoporous ethene-1,2-diyl-silica nanorods (Fig. 15) prepared using cetyltrimethylammonium bromide (CTAB) in concentrated aqueous

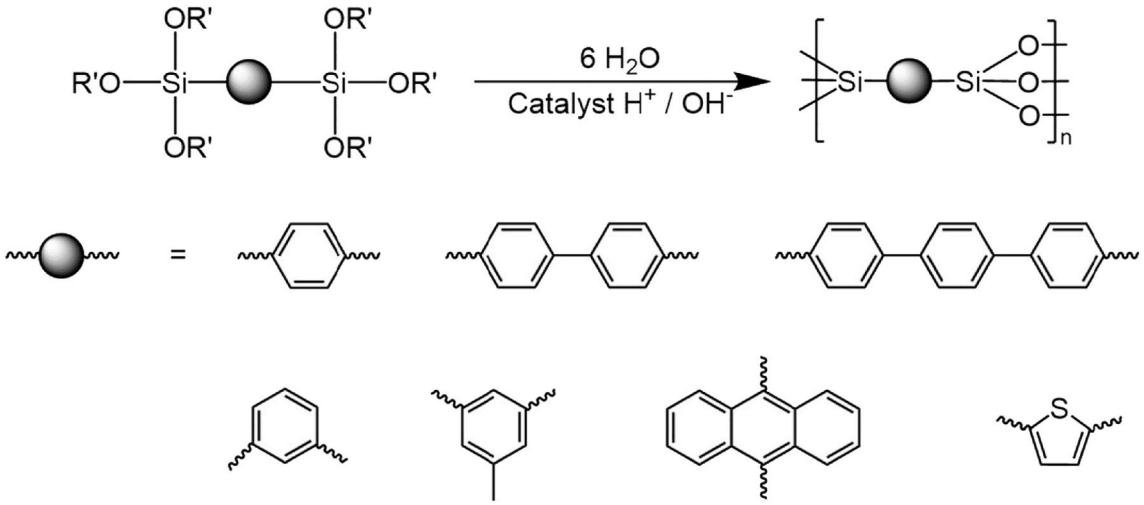

Fig. 12. Representatives of arylene bridged polysilsesquioxanes.

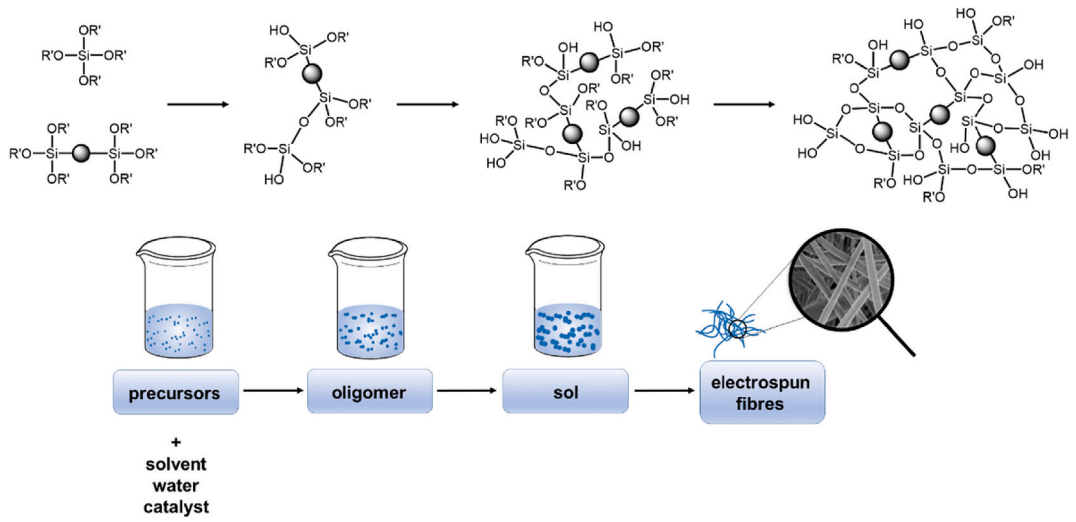

Fig. 13. General scheme of the use of any organo-bis-silylated precursor leading to the formation of organosilane fibers.

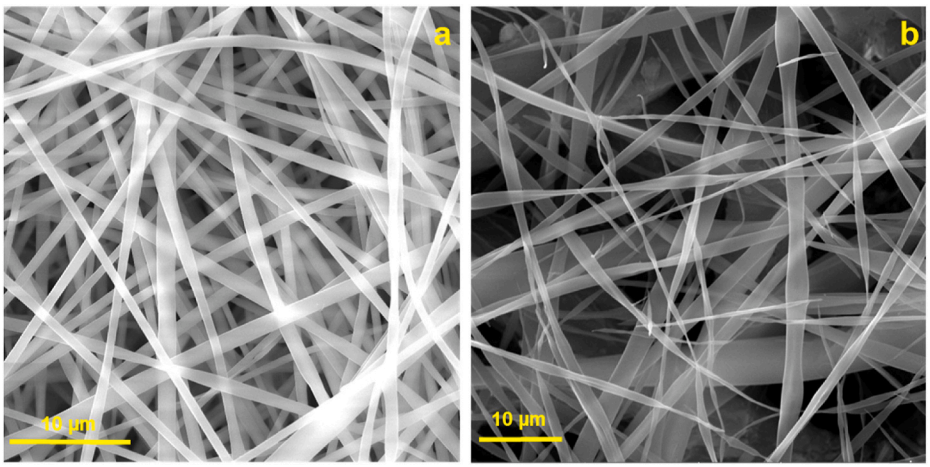

Fig. 14. Electron microscopy images showing organosilane nanofibers prepared from a combination of 1,4-Bis(triethoxysilyl)benzene with TEOS - sample **a**), and nanofibers prepared from a (1*S*,2*S*)-cyclohexane-1,2-diamine – bis – silylated precursor in combination with TEOS - sample **b**).

ammonia solutions, applicable in fields such as chiral separation and catalysis [116]; mesoporous silica nanofibers using co-structure-directing agents e.g. chiral anionic surfactants [119,120]; screw-like hierarchical chiral fibers constructed by co-templating two building blocks, DNA and porphyrin with using cationic organosilane precursor as a formation support [121]; single-handed helical mesoporous poly-bis-silsesquioxane (methylene, ethane-1,2-diyl, ethene-1,2-diyl, benzene-1,4-diyl, biphenyl-4,4′-diyl bridged) nanofibers prepared by sol–gel polymerization using chiral cationic low molecular weight gelators (LMWGs) and different types of catalysts e.g. HCl, NaOH, and ammonium hydroxide [122]; organosilane fibers obtained from acidic catalyzed syntheses using either TEOS or tetra(isopropoxy) silane (TPOS) in the presence of various oils [75]; mesoporous hybrid silica nanofibers made of 1,4-bis(trimethoxysilyl) benzene with a high surface area [76,80]; mesoporous ethane-1,2-diyl–silica nanofibers prepared using CTAB and (*S*)-2-methyl-1-butanol (MB) as a co-structure-directing agent, whose helical pitch is controllable by changing the MB/CTAB 0.5–10 M ratio [78,123]; and mesoporous methylene, ethane-1,2-diyl, ethene-1,2-diyl, benzene-1,4-diyl silica nanofibers prepared using CTAB and (*S*)-β-citronellol as a co-structure-directing agent under basic pH with a range of 0.2–2.0 μm in length and 100–200 nm in diameter with helical pitches of approximately 1.0 μm [77,81].

Hierarchically organized functionalized periodic mesoporous organosilica (PMO) fibers with longitudinal pore architectures have been prepared via a simple one-pot synthesis procedure from the co-condensation of 1,2-bis(triethoxysilyl)ethane with either ICPTMS or 1-[3-(trimethoxysilyl)propyl] urea in basic pH. The diameters of the fibers range from 50 to 300 nm, and the lengths are up to 7 μm [124]. Single-handed helical benzene-1,4-diyl bridged polysilsesquioxane nanofibers have been prepared through a different supramolecular templating approach [79,125].

Helical mesoporous silica, methylene, ethane-1,2-diyl, ethene-1,2-diyl, benzene-1,4-diyl, octane-1,8-diyl nanofibers have been prepared by sol−gel polymerization using a chiral cationic gelator under a shear flow. The morphologies of the silica nanofibers were sensitive to preparation conditions. In acidic conditions, right-handed helical nanofibers were observed (Fig. 16), and in basic conditions, rod-like mesoporous nanofibers were formed [80].

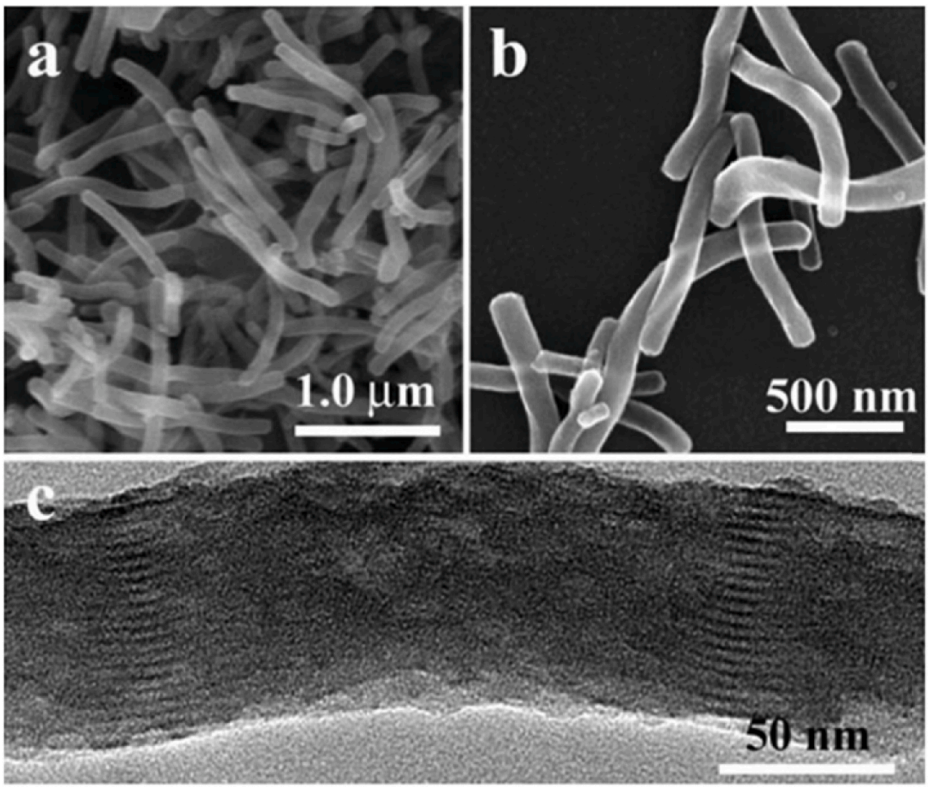

Fig. 15. Electron microscopy images of the formation of mesoporous ethane-1,2-diyl – silica nanorods via the self-assembly process. FESEM microscopy (**a,b**) and TEM microscopy (**c**) [116].

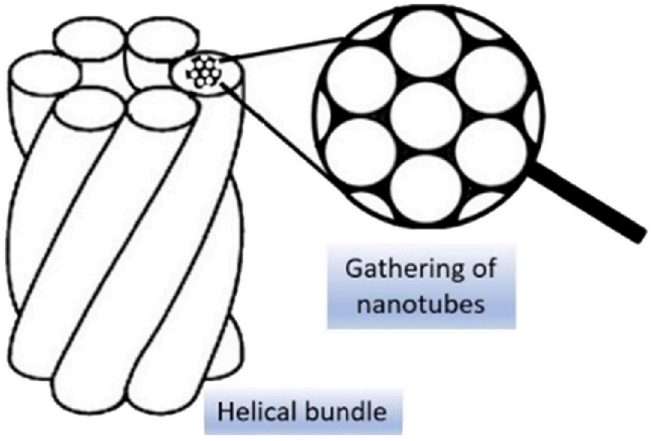

Fig. 16. Schematic representation of right-handed helical nanofibers.

5. Application potential and prospective of the reviewed fibrous materials

5.1. (Nano)fibers prepared from organo-mono-silylated precursors and their perspective

Taking account of the availability of raw materials, easy maneuverability, and outstanding chemical, physical, optical and mechanical properties, organo-alkoxysilanes in the form of fibers may find a wide range of potential applications in various different fields of current interest [101,102,126,127]. Examples include ternary nanofibers having remarkable solvent and temperature resistance (e.g. in DMF at 200 °C) [100] and nanofibrous PVA/PAA/SiO_2 mats having unique malleability and high breaking elongation [82]. This versatility is typical for all of the discussed materials; nevertheless, others will be discussed in the appropriate sections according to their target design, i.e. optoelectronics and sensors, energetics, filtration and adsorption, catalysis and biomedicine.

5.1.1. Optoelectronics and sensors

Organo-mono-silylated precursors are especially useful in optoelectronic devices and sensor applications due to their wide range of functional groups, which can be selected to facilitate the covalent attachment of indicator molecules directly to the targeted areas. These precursors may be used various different forms e.g. organo-alkoxysilane coatings deposited on organic fibers, directly prepared organic-inorganic fibers from convenient organo-mono-silylated precursors, inorganic fibers modified with the above-mentioned precursors, and many other possibilities bringing additional properties to these fibrous materials [94]. According to the literature, APTES is one of the most frequently used organo-mono-silylated precursors and is known as a coupling agent for sensors. It is usually used to bond organic probe molecules to glass, silica sol-gel surfaces, optical glass fibers and other types of organic, inorganic and or hybrid organic-inorganic fibers [94,128,129]. Some of the newest environmentally-friendly and low-cost applications for optoelectronic devices include two types of high-performance polyimide (PI) fibers, which are modified with APTES (KH-550) and applied in light-weight composite devices possessing a high strength modulus, higher temperature resistance and lower density [130].

Typical representatives of hybrid organic-inorganic fibers are organically modified silica (ORMOSIL) fibers used in microchip couplers for optoelectronic applications [93], or electroactive electrospun PFS fibers functionalized by pendant alkoxysilane groups, which have been successfully incorporated into miniature electrochemical cells containing lithium triflate/γ-butyrolactone electrolyte [106]. Other examples include optical fibers coated with different types of organo-monosilylated precursors such as APTES, GPTMS, PDMS with or

without TEOS used for sensor applications [94], optical fibers coated with an Ag-doped silica nanocomposite used as sensors for trace ammonia in gas samples [92], or optical PMMA fibers coated with a mixture of TEOS and methyltriethoxysilane (MTES) or phenyltriethoxysilane (PTES) doped with bromophenol blue, which have been successfully applied as low-cost pH sensors for monitoring biological fluids for the diagnosis and evaluation of therapies in wound healing applications [96].

5.1.2. Energetics

Nano-structured fibrous materials consisting of organic and inorganic components are an interesting alternative to the pure polymeric materials used in energetics. The new types of hybrid fibrous materials offer higher mechanical, chemical and physical resistance, which is necessary for stable performance in all modern energetics devices such as new types of fuel cells and/or lithium-ion batteries [131–133].

Hybrid organic-inorganic electrospun fibrous membranes made of (2-(4-(chlorosulfonyl)phenyl)ethyl)trichlorosilane (CSPTC) with TEOS, polyvinylidenefluoride-hexafluoropropylene (PVDF-HFP) in DMF are typical representatives of hybrid power devices used for proton exchange membrane fuel cells working at a high temperature. The inorganic parts allow the more effective transport of protons and the water management and organic materials bring softness, tightness, processability to the overall system [134]. Other examples include hybrid 1, 4-bis(triethoxysilyl)benzene/GPTMS fibrous membranes with sulfonated aromatic rings providing proton conductivity [131].

Electrospun fibers based on a combination of GPTMS modified polyamic acid and alkoxysilane functional poly(dimethylsiloxane), subsequently soaked with 0.5 M $LiFP_6$ solution, and used as a hybrid gel electrolyte for lithium-ion batteries are an example of the newest research work in this area [104], as well as reinforced nanofiber composites prepared with a combination of PVA and nanosilica modified with mercaptopropionic acid and MPTMS [135]. Mullite fibers (MF) functionalized via APTES used as a filament in wound epoxy nanocomposites [136] or aramid fibers functionalized with APTES [137,138] also show promising potential in energetics.

5.1.3. Filtration and adsorption

Hybrid fibrous membranes used in water [139] or air filtration systems, which are made of or modified via organo-mono-silylated precursors, offer additional properties such as durability, good tensile properties, chemical stability, catalytic properties, sufficient porosity compared to the conventional systems already used [140,141].

Most of the currently used filtration membranes are made of organic polymers, which are subsequently functionalized via different types of organo-mono-silylated precursors. These include electrospun cellulose acetate nanofibers (CA-NF) modified with perfluoro alkoxysilanes (FS/CA-NF) for oil–water separation purposes [89], omniphobic fibrous cellulose acetate membranes containing silica nanoparticles modified via APTES used for desalinating the wastewaters with low-surface-tension contaminants [99], other types of organic fibrous membranes modified via APTES [142–144], composite PVA/TEOS/APTES fiber membranes, used to remove cadmium from aqueous solution [145], or polyacrylonitrile fibers functionalized via APTES in PDMS membranes used for air filtration systems [146].

Surprisingly, when we focus on the literature related to the preparation of purely organoalkoxysilane fibrous membranes, we find that most of the filtration systems are based on the combination of organic fibrous membranes modified via organo-alkoxysilane nanoparticles and nanocoatings. There are only a few solitary research papers describing the preparation of purely organosilane fibrous membranes used in filtration applications [105,114].

The first of them Tao et al. [114] describe the preparation of porphyrin-doped nanocomposite fibers in the form of nanofibrous membranes, which were prepared thanks to the combination of sol–gel chemistry and the electrospinning technique, without the addition or help of organic polymers. The membrane was successfully tested as a novel fluorescence-based chemosensor for the rapid detection of trace vapor (10 ppb) of explosive, particularly it has exhibited remarkable sensitivity to trace (2,4,6-trinitrotoluene) TNT vapor.

The second group of Schramm et al. [105] prepared ultra-thin polyimide fibers, which were thermally treated at 220 °C. This temperature supports the rise of the formation of polyimide (PI) groups in the final polysiloxane network and fibers, thus prepared, have a ladder-like structure. Moreover, the authors use the incorporation of various organo-trialkoxysilanes with different functional groups enabling the production of ultra-fine fiber mats with tailor-made properties. Prepared fibers may be applied in the filtration, sensor systems or drug release processes.

5.1.4. Catalysis

According to a literature search of the application of organo-mono-silylated precursors strictly in the form of (nano)fibers in catalysis, there is only a very small number of research papers compared to the same precursors used in the form of nanoparticles or nanocoatings on different substrates [16,147]. Most of the published literature describes organic fibers functionalized via different types of alkoxides, or organo-mono-silylated precursors. Specific examples of fibrous systems used for catalytic applications include linear poly(ethylene imine) (PEI) fibrous aggregates modified via TEOS or TMOS, which are able to reduce $PtCl_4^{2-}$ [148], or nanoporous silica fibers functionalized with MPTMS used for solid-phase microextraction (SPME) of phenolic compounds [149], mesoporous silica nanofibers made of a combination of TEOS and MPTMS, whose mesostructure corresponds to MCM-41 NPs systems [150].

5.1.5. Medicine and biomaterials

Hybrid fibrous materials made of organo-mono-silylated precursors find their widest application in the field of medicine, and particularly in various types of scaffolds applicable in cell growth, and/or wound care. They are typically used in a combination of organic polymers, alkoxides and organo-mono-silylated precursors [54] e.g. mixtures of poly(γ-glutamic acid) (γ-PGA)/TEOS and GPTMS providing an excellent extracellular matrix in bone tissue regeneration [151], silica/poly(L-lactic acid) (PLLA) for skeletal defect regeneration [152], protein-encapsulated fiber mats using a combination of poly(γ-glutamate) (PGA)/(GPTMS) offering an effective method of encapsulating bioactive molecules (Fig. 17) while maintaining their structure and function [153], drug delivery systems based on PCL/PLA) with Halloysite nanotubes (HNT) [154], regenerated cellulose nanofibers (RC-NF) with PCL, modified via APTES with the aim of increasing the mechanical properties of the prepared scaffolds [155], APTES functionalized electrospun poly(*N*-vinyl-2-pyrrolidone) fibers (NH_2-PVP) capping gold nanoparticles for drug delivery systems working at different pH (5.0, 6.0, 7.4) supporting cell growth [156,157], or fibrous materials used in wound-healing applications with antibacterial effects composed of mesoporous silica nanoparticles in PVP nanofiber mats [158,159].

5.2. Hybrid materials made of organo-bis-silylated precursors and their promising applications

Hybrid organosilane materials based on organo-bis-silylated precursors in various different forms (mainly nanoparticles) seem to be a very promising class of materials having an extraordinary properties applicable in separation methods, e.g. chromatographies [160]. Earlier, ethane-1,2-diyl and benzene-1,4-diyl bridged polysilsesquioxanes functionalized with amino and thiol groups in the form of nanoparticles have been used as adsorbents of volatile organic compounds (*n*-hexane, *n*-heptane, cyclohexane, benzene, triethanolamine, acetonitrile) from gas phase chromatography [161]. Another application of these materials may be found in catalysis [110,162–166] and/or in optics [109,110,167,168]. Another example in this field is carbon/silica superstructures

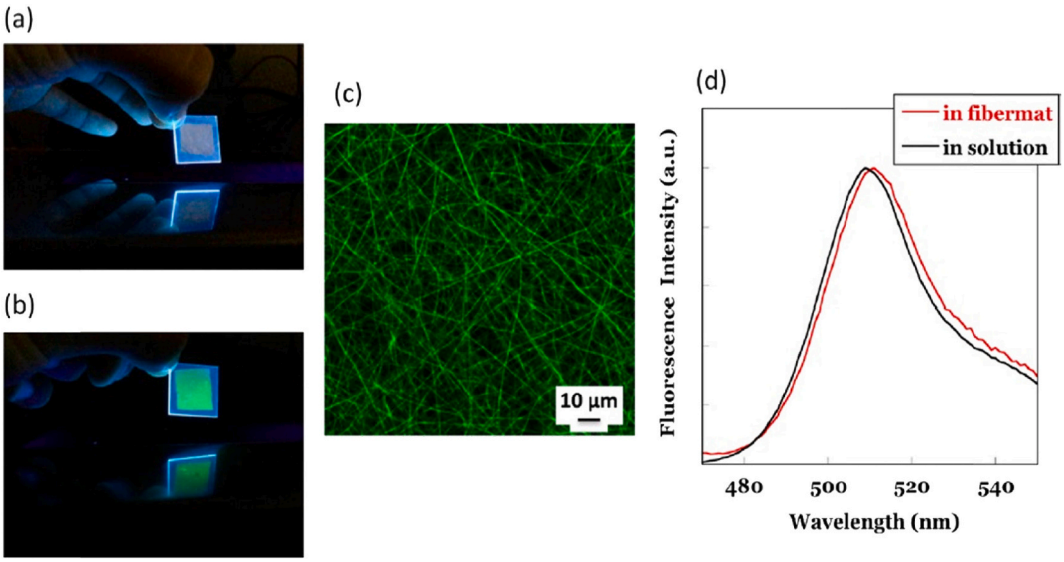

Fig. 17. Fluorescence emission (excited at 312 nm) of silica/PGA fiber mats without encapsulated green fluorescent protein (GFP) wetted with a 20 mM phosphate buffer (pH 7) **a**); fluorescence emission (excited at 312 nm) of silica/PGA fiber mats with encapsulated GFP wetted with a 20 mM phosphate buffer (pH 7) **b**); fluorescence image of GFP-encapsulated silica/PGA fiber mats wetted with a 20 mM phosphate buffer (pH 7) using a laser scanning confocal microscope (excited at 405 nm) **c**); fluorescence spectra (excited at 460 nm) of GFP encapsulated in a silica/PGA fiber mat (red line) or in a 20 mM phosphate buffer (pH 7, black line) **d**); [153]. (For interpretation of the references to colour in this figure legend, the reader is referred to the Web version of this article.)

made of perylenediimide-bridged silsesquioxane (PDBS) with controllable morphologies (tubes, fibers or spheres), sizes and excellent electrical properties, which are very promising candidates for optoelectronics and sensing devices [169]. In general, organosilanes with various different forms containing aromatic rings (Fig. 18) have a significant potential for use in modern batteries [111].

The above-mentioned findings prove that novel hybrid pure organosilane materials based on bridged alkoxysilane precursors and on top of that in a fibrous form belong to a promising class of materials offering additional value and aiming at a wide range of end-applications [9,10] particularly catalysis, separations [76,77,116] and/or modern biomaterials having additional value [121].

6. Conclusion and outlook

This review humbly reflects on the past and current research regarding the preparation of hybrid organosilane fibrous materials and their contribution to modern science. The present study concerns organo-mono-silylated and organo-bis-silylated precursors stressing the consequent synthetic strategies and outcomes from the point of view of fiber formation. Likewise, the presented findings are complemented with a subsequent survey of their applications highlighting the promising prospects of such hybrid organosilane fibers in the various different fields of modern science.

From the origins of silica and (organo)silane fiber-making chemistry to the successful preparation of pure organosilane fibers via a one-pot synthesis, this review theoretically covers the basics of sol-gel processing for the preparation of spinnable sols and maps the most common

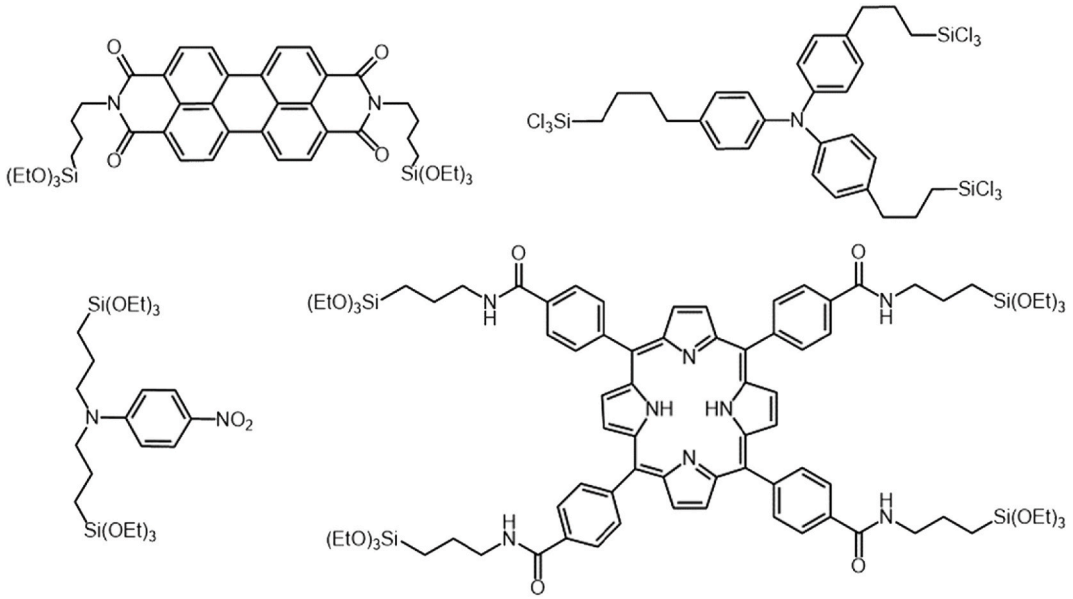

Fig. 18. Examples of bridged polysilsesquioxanes with chromophore bridging groups, adapted according to reference [39].

fiber-making techniques. Hybrid organosilane fibrous materials based on organo mono- or bis-silylated precursors respectively are examined based on their preparation with or without the use of surfactants, polymeric or low-molecular additives.

The various classes of hybrid organosilane (nano)fibers provide additional value compared to the conventional fibrous systems already in use and may be applied to many fields of modern science including optoelectronics, energetics, filtration, catalysis and medicine. Many of presented hybrid organosilane fibrous materials seem to have a strong potential to open up completely new directions in hybrid material chemistry with an emphasis on the non-toxicity, environmental friendliness and efficiency of their performance.

Funding

This work was supported by the Czech Science Foundation (GA CR) [project number 18-09824S]; the Ministry of Education, Youth and Sports of the Czech Republic and the European Union - European Structural and Investment Funds [project registration number CZ.02.1.01/0.0/0.0/16_025/0007293].

Declaration of competing interest

The authors declare that they have no known competing financial interests or personal relationships that could have appeared to influence the work reported in this paper.

References

[1] M. Faustini, L. Nicole, E. Ruiz-Hitzky, C. Sanchez, History of organic–inorganic hybrid materials: prehistory, art, science, and advanced applications, Adv. Funct. Mater. 28 (2018) 1704158, https://doi.org/10.1002/adfm.201704158.
[2] CRC concise encyclopedia of Nanotechnology, CRC press (n.d.), https://www.routledge.com/CRC-Concise-Encyclopedia-of-Nanotechnology/Kharisov-Kharissova-Ortiz-Mendez/p/book/9781466580343. (Accessed 6 May 2020).
[3] R.B. Figueira, Hybrid sol–gel coatings for corrosion mitigation: a critical review, Polymers 12 (2020) 689, https://doi.org/10.3390/polym12030689.
[4] A. Bouibed, R. Doufnoune, Synthesis and characterization of hybrid materials based on graphene oxide and silica nanoparticles and their effect on the corrosion protection properties of epoxy resin coatings, J. Adhes. Sci. Technol. 33 (2019) 834–860, https://doi.org/10.1080/01694243.2019.1571660.
[5] C. Sanchez, B. Julián, P. Belleville, M. Popall, Applications of hybrid organic–inorganic nanocomposites, J. Mater. Chem. 15 (2005) 3559–3592, https://doi.org/10.1039/B509097K.
[6] C. Sanchez, P. Belleville, M. Popall, L. Nicole, Applications of advanced hybrid organic–inorganic nanomaterials: from laboratory to market, Chem. Soc. Rev. 40 (2011) 696–753, https://doi.org/10.1039/C0CS00136H.
[7] V.P. Ananikov, Organic–inorganic hybrid nanomaterials, Nanomaterials (Basel) 9 (2019), https://doi.org/10.3390/nano9091197.
[8] R.S. Andre, R.C. Sanfelice, A. Pavinatto, L.H.C. Mattoso, D.S. Correa, Hybrid nanomaterials designed for volatile organic compounds sensors: a review, Mater. Des. 156 (2018) 154–166, https://doi.org/10.1016/j.matdes.2018.06.041.
[9] B. Holubova, V. Makova, J. Mullerova, J. Brus, K. Havlickova, V. Jencova, A. Michalcova, J. Kulhankova, M. Rezanka, Novel chapter in hybrid materials: one-pot synthesis of purely organosilane fibers, Polymer 190 (2020) 122234, https://doi.org/10.1016/j.polymer.2020.122234.
[10] V. Máková, B. Holubová, D. Tetour, J. Brus, M. Řezanka, M. Rysová, J. Hodačová, (1*S*,2*S*)-Cyclohexane-1,2-diamine-based organosilane fibres as a powerful tool against pathogenic bacteria, Polymers 12 (2020) 206, https://doi.org/10.3390/polym12010206.
[11] C.J. Brinker, G.W. Scherer, Sol-Gel Science: the Physics and Chemistry of Sol-Gel Processing, Elsevier Inc., 2013, https://doi.org/10.1016/C2009-0-22386-5.
[12] G. Kickelbick, Hybrid Materials: Synthesis, Characterization, and Applications, John Wiley & Sons, 2007.
[13] G. Schottner, Hybrid Sol−Gel-derived Polymers: applications of multifunctional materials, Chem. Mater. 13 (2001) 3422–3435, https://doi.org/10.1021/cm011060m.
[14] A. Godet, T. Sylvestre, V. Pecheur, J. Chretien, J.-C. Beugnot, K.P. Huy, Nonlinear elasticity of silica nanofiber, APL Photonics 4 (2019), 080804, https://doi.org/10.1063/1.5103239.
[15] M. Barczak, C. McDonagh, D. Wencel, Micro- and nanostructured sol-gel-based materials for optical chemical sensing, Microchim. Acta. 183 (2016) 2085–2109, https://doi.org/10.1007/s00604-016-1863-y, 2005-2015.
[16] U. Díaz, D. Brunel, A. Corma, Catalysis using multifunctional organosiliceous hybrid materials, Chem. Soc. Rev. 42 (2013) 4083–4097, https://doi.org/10.1039/C2CS35385G.
[17] S. Karamikamkar, H.E. Naguib, C.B. Park, Advances in precursor system for silica-based aerogel production toward improved mechanical properties, customized morphology, and multifunctionality: a review, Adv. Colloid Interface Sci. 276 (2020) 102101, https://doi.org/10.1016/j.cis.2020.102101.
[18] T. Linhares, M.T. Pessoa de Amorim, L. Duraes, Silica aerogel composites with embedded fibres: a review on their preparation, properties and applications, J. Mater. Chem. A. 7 (2019) 22768–22802, https://doi.org/10.1039/c9ta04811a.
[19] S. Yajima, J. Hayashi, M. Omori, K. Okamura, Development of a silicon carbide fibre with high tensile strength, Nature 261 (1976) 683–685, https://doi.org/10.1038/261683a0.
[20] T. Ishikawa, Y. Kohtoku, K. Kumagawa, T. Yamamura, T. Nagasawa, High-strength alkali-resistant sintered SiC fibre stable to 2,200 °C, Nature 391 (1998) 773–775, https://doi.org/10.1038/35820.
[21] P. Baldus, M. Jansen, D. Sporn, Ceramic fibers for matrix composites in high-temperature engine applications, Science 285 (1999) 699–703, https://doi.org/10.1126/science.285.5428.699.
[22] N.R. Thomas, Frederic stanley kipping—pioneer in silicon chemistry: his life & legacy, Siliconindia 2 (2010) 187–193, https://doi.org/10.1007/s12633-010-9051-x.
[23] H. Deuel, Organic derivatives of clay minerals*, Clay Miner. Bull. 1 (1952) 205–214, https://doi.org/10.1180/claymin.1952.001.7.04.
[24] C.W. Lentz, Silicate minerals as sources of trimethylsilyl silicates and silicate structure analysis of sodium silicate solutions, Inorg. Chem. 3 (1964) 574–579, https://doi.org/10.1021/ic50014a029.
[25] K.A. Andrianov, A.A. Zhdanov, V.Y. Levin, Some physical properties of organosilicon ladder polymers, Annu. Rev. Mater. Sci. 8 (1978) 313–326, https://doi.org/10.1146/annurev.ms.08.080178.001525.
[26] W. Mahler, M.F. Bechtold, Freeze-formed silica fibres, Nature 285 (1980) 27–28, https://doi.org/10.1038/285027a0.
[27] S. Sakka, K. Kamiya, The sol-gel transition in the hydrolysis of metal alkoxides in relation to the formation of glass fibers and films, J. Non-Cryst. Solids 48 (1982) 31–46, https://doi.org/10.1016/0022-3093(82)90244-7.
[28] H.K. Schmidt, New Type of Non-crystalline Solids between Inorganic and Organic Materials, 1985, https://doi.org/10.22028/D291-24311.
[29] Sol-Gel Science, Elsevier, 1990, https://doi.org/10.1016/C2009-0-22386-5.
[30] R.J.P. Corriu, J.J.E. Moreau, P. Thepot, M.W.C. Man, New mixed organic-inorganic polymers: hydrolysis and polycondensation of bis(trimethoxysilyl) organometallic precursors, Chem. Mater. 4 (1992) 1217–1224, https://doi.org/10.1021/cm00024a020.
[31] K.J. Shea, D.A. Loy, O. Webster, Arylsilsesquioxane gels and related materials. New hybrids of organic and inorganic networks, J. Am. Chem. Soc. 114 (1992) 6700–6710, https://doi.org/10.1021/ja00043a014.
[32] S. Sakka, T. Yoko, Fibers from gels, J. Non-Cryst. Solids 147–148 (1992) 394–403, https://doi.org/10.1016/S0022-3093(05)80650-7.
[33] A.E. Comyns, Sol-gel technology for thin films, fibers, preforms, electronics, and specialty shapes Edited by Lisa C. Klein; Noyes Publications, Park Ridge, New Jersey, 1988. pp. xxi + 407, price $72.00 (USA), Br. Polym. J. 21 (1989) 361–362, https://doi.org/10.1002/pi.4980210420. ISBN 0-8155-1154-X.
[34] C.T. Ho, W.C. LaCourse, R.A. Condrate, A. Jillavenkatesa, A Raman spectral investigation of structural variations in thin silicate glass fibers, Mater. Lett. 23 (1995) 237–240, https://doi.org/10.1016/0167-577X(95)00037-2.
[35] H. Kozuka, H. Kuroki, S. Sakka, The change of flow characteristics of Si(OC2H5)4 solutions in the course of sol-to-gel conversion, J. Non-Cryst. Solids 101 (1988) 120–122, https://doi.org/10.1016/0022-3093(88)90377-8.
[36] J. Geltmeyer, J. De Roo, F. Van den Broeck, J.C. Martins, K. De Buysser, K. De Clerck, The influence of tetraethoxysilane sol preparation on the electrospinning of silica nanofibers, J. Sol. Gel Sci. Technol. 77 (2016) 453–462, https://doi.org/10.1007/s10971-015-3875-1.
[37] P. Judeinstein, C. Sanchez, Hybrid organic–inorganic materials: a land of multidisciplinarity, J. Mater. Chem. 6 (1996) 511–525, https://doi.org/10.1039/JM9960600511.
[38] S. Fujita, S. Inagaki, Self-organization of organosilica solids with molecular-scale and mesoscale periodicities, Chem. Mater. 20 (2008) 891–908, https://doi.org/10.1021/cm702271v.
[39] K.J. Shea, D.A. Loy, Bridged polysilsesquioxanes. Molecular-engineered hybrid Organic−Inorganic materials, Chem. Mater. 13 (2001) 3306–3319, https://doi.org/10.1021/cm011074s.
[40] S. Fujita, M.P. Kapoor, S. Inagaki, Organic-inorganic hybrid mesoporous silica, in: A. Muramatsu, T. Miyashita (Eds.), Nanohybridization of Organic-Inorganic Materials, Springer, Berlin, Heidelberg, 2009, pp. 141–169, https://doi.org/10.1007/978-3-540-92233-9_7.
[41] Y. Tang, Z. Tao, F.V. Bright, Sol hydrolysis and condensation reaction time influence the sensitivity of class II xerogel-based sensing materials, J. Sol. Gel Sci. Technol. 42 (2007) 127–133, https://doi.org/10.1007/s10971-007-1532-z.
[42] M. Catauro, S.V. Ciprioti, Characterization of hybrid materials prepared by sol-gel method for biomedical implementations. A critical review, Materials (Basel) 14 (2021), https://doi.org/10.3390/ma14071788.
[43] A.A. Issa, A.S. Luyt, Kinetics of alkoxysilanes and organoalkoxysilanes polymerization: a review, Polymers 11 (2019) 537, https://doi.org/10.3390/polym11030537.
[44] G.J. McIntosh, Theoretical investigations into the nucleation of silica growth in basic solution part II – derivation and benchmarking of a first principles kinetic model of solution chemistry, Phys. Chem. Chem. Phys. 15 (2013) 17496–17509, https://doi.org/10.1039/C3CP53223B.

[45] S. Okumoto, N. Fujita, S. Yamabe, Theoretical study of hydrolysis and condensation of silicon alkoxides, J. Phys. Chem. 102 (1998) 3991–3998, https://doi.org/10.1021/jp980705b.

[46] T.W. Zerda, I. Artaki, J. Jonas, Study of polymerization processes in acid and base catalyzed silica sol-gels, J. Non-Cryst. Solids 81 (1986) 365–379, https://doi.org/10.1016/0022-3093(86)90503-X.

[47] M.-C. Brochier Salon, P.-A. Bayle, M. Abdelmouleh, S. Boufi, M.N. Belgacem, Kinetics of hydrolysis and self condensation reactions of silanes by NMR spectroscopy, Colloid. Surface. Physicochem. Eng. Aspect. 312 (2008) 83–91, https://doi.org/10.1016/j.colsurfa.2007.06.028.

[48] G. Jia, Q.-H. Wan, Separation and identification of oligomeric vinylmethoxysiloxanes by gradient elution chromatography coupled with electrospray ionization mass spectrometry, J. Chromatogr. A 1395 (2015) 129–135, https://doi.org/10.1016/j.chroma.2015.03.079.

[49] Y. Jiang, Q.-H. Wan, Separation and identification of oligomeric phenylethoxysiloxanols by liquid chromatography-electrospray ionization mass spectrometry, J. Chromatogr. A 1394 (2015) 95–102, https://doi.org/10.1016/j.chroma.2015.03.043.

[50] A.S. Lee, S.-S. Choi, K.-Y. Baek, S.S. Hwang, Hydrolysis kinetics of a sol-gel equilibrium yielding ladder-like polysilsesquioxanes, Inorg. Chem. Commun. 73 (2016) 7–11, https://doi.org/10.1016/j.inoche.2016.09.004.

[51] C. Schramm, B. Rinderer, R. Tessadri, Synthesis and characterization of novel ultrathin polyimide fibers via sol–gel process and electrospinning, J. Appl. Polym. Sci. 128 (2013) 1274–1281, https://doi.org/10.1002/app.38543.

[52] J. Xue, T. Wu, Y. Dai, Y. Xia, Electrospinning and electrospun nanofibers: methods, materials, and applications, Chem. Rev. (2019), https://doi.org/10.1021/acs.chemrev.8b00593.

[53] S. Thenmozhi, N. Dharmaraj, K. Kadirvelu, H.Y. Kim, Electrospun nanofibers: new generation materials for advanced applications, Mater. Sci. Eng., B 217 (2017) 36–48, https://doi.org/10.1016/j.mseb.2017.01.001.

[54] R. Sahay, P.S. Kumar, R. Sridhar, J. Sundaramurthy, J. Venugopal, S. G. Mhaisalkar, S. Ramakrishna, Electrospun composite nanofibers and their multifaceted applications, J. Mater. Chem. 22 (2012) 12953–12971, https://doi.org/10.1039/C2JM30966A.

[55] D.I. Braghirolli, D. Steffens, P. Pranke, Electrospinning for regenerative medicine: a review of the main topics, Drug Discov. Today 19 (2014) 743–753, https://doi.org/10.1016/j.drudis.2014.03.024.

[56] D. Lukáš, A. Sarkar, L. Martinová, K. Vodseď álková, D. Lubasová, J. Chaloupek, P. Pokorný, P. Mikeš, J. Chvojka, M. Komárek, Physical principles of electrospinning (Electrospinning as a nano-scale technology of the twenty-first century), Textil. Prog. 41 (2009) 59–140, https://doi.org/10.1080/00405160902904641.

[57] Q. Yang, X. Jiang, F. Gu, Z. Ma, J. Zhang, L. Tong, Polymer micro or nanofibers for optical device applications, J. Appl. Polym. Sci. 110 (2008) 1080–1084, https://doi.org/10.1002/app.28716.

[58] K. Strnadová, L. Stanislav, I. Krabicová, F. Sabol, J. Lukášek, M. Řezanka, D. Lukáš, V. Jenčová, Drawn aligned polymer microfibres for tissue engineering, J. Ind. Textil. (2019), https://doi.org/10.1177/1528083718825318, 1528083718825318.

[59] T. Ondarçuhu, C. Joachim, Drawing a single nanofibre over hundreds of microns, Europhys. Lett. 42 (1998) 215, https://doi.org/10.1209/epl/i1998-00233-9.

[60] A.S. Nain, J.C. Wong, C. Amon, M. Sitti, Drawing suspended polymer micro-/nanofibers using glass micropipettes, Appl. Phys. Lett. 89 (2006) 183105, https://doi.org/10.1063/1.2372694.

[61] X. Xing, Y. Wang, B. Li, Nanofiber drawing and nanodevice assembly in poly (trimethylene terephthalate), Opt. Express, OE. 16 (2008) 10815–10822, https://doi.org/10.1364/OE.16.010815.

[62] D. Liu, J. Li, W. Huang, S. Yang, Progress in polymer complex fibers, Acta Polym. Sin. (2018) 445–455, https://doi.org/10.11777/j.issn1000-3304.2017.17285.

[63] Z. Wang, N. Li, W. Lu, W. Chen, Highly-efficient fabrication and crystallinity and orientation of polyacrylonitrile nanofibers, Acta Polym. Sin. (2018) 755–764, https://doi.org/10.11777/j.issn1000-3304.2017.17226.

[64] C. Meng, Y. Xiao, P. Wang, L. Zhang, Y. Liu, L. Tong, Quantum-dot-doped polymer nanofibers for optical sensing, Adv. Mater. Weinheim. 23 (2011) 3770–3774, https://doi.org/10.1002/adma.201101392.

[65] A.C.A. Wan, M.F. Leong, J.K.C. Toh, Y. Zheng, J.Y. Ying, Multicomponent fibers by multi-interfacial polyelectrolyte complexation, Advanced Healthcare Materials 1 (2012) 101–105, https://doi.org/10.1002/adhm.201100020.

[66] A.S. Nain, C. Amon, M. Sitti, Proximal probes based nanorobotic drawing of polymer micro/nanofibers, IEEE Trans. Nanotechnol. 5 (2006) 499–510, https://doi.org/10.1109/TNANO.2006.880453.

[67] S.A. Harfenist, S.D. Cambron, E.W. Nelson, S.M. Berry, A.W. Isham, M.M. Crain, K.M. Walsh, R.S. Keynton, R.W. Cohn, Direct drawing of suspended filamentary micro- and nanostructures from liquid polymers, Nano Lett. 4 (2004) 1931–1937, https://doi.org/10.1021/nl048919u.

[68] Z. Xie, H. Niu, T. Lin, Continuous polyacrylonitrile nanofiber yarns: preparation and dry-drawing treatment for carbon nanofiber production, RSC Adv. 5 (2015) 15147–15153, https://doi.org/10.1039/c4ra16247a.

[69] P. Yang, D. Zhao, B.F. Chmelka, G.D. Stucky, Triblock-copolymer-directed syntheses of large-pore mesoporous silica fibers, Chem. Mater. 10 (1998) 2033–2036, https://doi.org/10.1021/cm980201q.

[70] K.S. Mali, S. De Feyter, Principles of molecular assemblies leading to molecular nanostructures, Phil. Trans. Math. Phys. Eng. Sci. 371 (2013), https://doi.org/10.1098/rsta.2012.0304, 20120304.

[71] J.D. Halley, D.A. Winkler, Consistent concepts of self-organization and self-assembly, Complexity 14 (2008) 10–17, https://doi.org/10.1002/cplx.20235.

[72] K.F. Bohringer, U. Srinivasan, R.T. Howe, Modeling of capillary forces and binding sites for fluidic self-assembly, Technical Digest. MEMS, in: 14th IEEE International Conference on Micro Electro Mechanical Systems (Cat. No.01CH37090), 2001, https://doi.org/10.1109/MEMSYS.2001.906555, 2001.

[73] G.M. Whitesides, B. Grzybowski, Self-assembly at all scales, Science 295 (2002) 2418–2421, https://doi.org/10.1126/science.1070821.

[74] T. Yamaguchi, N. Suematsu, H. Mahara, Self-organization of hierarchy: dissipative-structure assisted self-assembly of metal nanoparticles in polymer matrices, Nonlinear Dynamics in Polymeric Systems (2004) 16–27.

[75] F. Kleitz, F. Marlow, G.D. Stucky, F. Schüth, Mesoporous silica Fibers: synthesis, internal structure, and growth kinetics, Chem. Mater. 13 (2001) 3587–3595, https://doi.org/10.1021/cm0110324.

[76] H. Li, B. Li, Y. Chen, X. Wu, J. Zhang, Y. Li, K. Hanabusa, Y. Yang, Transfer helix and chirality to 1,4-phenylene silica nanostructures, Mater. Chem. Phys. 118 (2009) 135–141, https://doi.org/10.1016/j.matchemphys.2009.07.018.

[77] Y. Li, L. Bi, S. Wang, Y. Chen, B. Li, X. Zhu, Yonggang Yang, Preparation of helical mesoporous ethylene-silica nanofibers with lamellar mesopores on the surfaces, Chem. Commun. 46 (2010) 2680–2682, https://doi.org/10.1039/b926593g.

[78] S. Wang, B. Li, L. Bi, M. Zhang, Y. Chen, Y. Li, Yonggang Yang, Preparation of helical mesoporous ethylene-silica nanofibers using CTAB and (S)-2-methyl-1-butanol, Mater. Lett. 65 (2011) 2261–2264, https://doi.org/10.1016/j.matlet.2011.04.079.

[79] Z. Xiao, Y. Guo, B. Li, Yi Li, Preparation and characterization of single-handed helical carbonaceous nanofibers using 1,4-phenylene bridged polybissilsesquioxanes, J. Wuhan Univ. Technol.-Materials Sci. Ed. 31 (2016) 1149–1154, https://doi.org/10.1007/s11595-016-1504-7.

[80] Y. Yang, M. Suzuki, H. Fukui, H. Shirai, Kenji Hanabusa, Preparation of helical mesoporous silica and hybrid silica nanofibers using hydrogelator, Chem. Mater. 18 (2006) 1324–1329, https://doi.org/10.1021/cm0519030.

[81] M. Zhang, Y. Li, L. Bi, W. Zhuang, S. Wang, Y. Chen, B. Li, Yonggang Yang, Preparation of helical mesoporous ethenylene-silica nanofibers with lamellar mesopores on their surface, Chin. J. Chem. 29 (2011) 933–941, https://doi.org/10.1002/cjoc.201190191.

[82] D. Liu, B. Li, Y. Guo, Y. Li, Y. Yang, Inner surface chirality of single-handed twisted carbonaceous tubular nanoribbons, Chirality 27 (2015) 809–815, https://doi.org/10.1002/chir.22496.

[83] J. Li, C. Nie, B. Duan, X. Zhao, H. Lu, W. Yin, Y. Li, X. He, Tensile performance of silica-based electrospun fibrous mats, J. Non-Cryst. Solids 470 (2017) 184–188, https://doi.org/10.1016/j.jnoncrysol.2017.05.016.

[84] Y. Ding, W. Li, A. Correia, Y. Yang, K. Zheng, D. Liu, D.W. Schubert, A. R. Boccaccini, H.A. Santos, J.A. Roether, Electrospun polyhydroxybutyrate/poly (epsilon-caprolactone)/sol-gel-derived silica hybrid scaffolds with drug releasing function for bone tissue engineering applications, ACS Appl. Mater. Interfaces 10 (2018) 14540–14548, https://doi.org/10.1021/acsami.8b02656.

[85] C. Wu, W. Yuan, S.S. Al-Deyab, K.-Q. Zhang, Tuning porous silica nanofibers by colloid electrospinning for dye adsorption, Appl. Surf. Sci. 313 (2014) 389–395, https://doi.org/10.1016/j.apsusc.2014.06.002.

[86] M. Ma, R.M. Hill, J.L. Lowery, S.V. Fridrikh, G.C. Rutledge, Electrospun poly (styrene- *block* -dimethylsiloxane) block copolymer fibers exhibiting superhydrophobicity, Langmuir 21 (2005) 5549–5554, https://doi.org/10.1021/la047064y.

[87] Z. Wei, J. Li, C. Wang, J. Cao, Y. Yao, H. Lu, Y. Li, X. He, Thermally stable hydrophobicity in electrospun silica/polydimethylsiloxane hybrid fibers, Appl. Surf. Sci. 392 (2017) 260–267, https://doi.org/10.1016/j.apsusc.2016.09.057.

[88] M.H. Ugur, B. Oktay, A. Gungor, N. Kayaman-Apohan, Highly thermally resistant, hydrophobic poly(vinyl alcohol)-silica hybrid nanofibers, J. Serb. Chem. Soc. 83 (2018) 885–897, https://doi.org/10.2298/JSC171121032H.

[89] O. Arslan, Z. Aytac, T. Uyar, Superhydrophobic, hybrid, electrospun cellulose acetate nanofibrous mats for oil/water separation by tailored surface modification, ACS Appl. Mater. Interfaces 8 (2016), https://doi.org/10.1021/acsami.6b05429, 19747–19754.

[90] Y. Yao, L. Shen, A. Wei, T. Wang, S. Chen, Facile synthesis, microstructure, photocatalytic activity, and anti-bacterial property of the novel Ag@gelatin-silica hybrid nanofiber membranes, J. Sol. Gel Sci. Technol. 89 (2019) 651–662, https://doi.org/10.1007/s10971-018-04914-z.

[91] W. Yu, J. Shi, L. Wang, X. Chen, M. Min, L. Wang, Y. Liu, The structure and mechanical property of silane-grafted-polyethylene/SiO 2 nanocomposite fiber rope, Aquaculture and Fisheries 2 (2017) 34–38, https://doi.org/10.1016/j.aaf.2017.01.003.

[92] H. Guo, S. Tao, Silver nanoparticles doped silica nanocomposites coated on an optical fiber for ammonia sensing, Sensor. Actuator. B Chem. 123 (2007) 578–582, https://doi.org/10.1016/j.snb.2006.09.055.

[93] K.W.K. Li, E.J. Salley, P. Melman, M.J. Tabasky, J. Zhao, C.Y. Li, Self-aligned ormosil waveguide devices, in: L.G. HubertPfalzgraf, S.I. Najafi (Eds.), Organic-Inorganic Hybrid Materials for Photonics, Spie-Int Soc Optical Engineering, Bellingham, 1998, pp. 58–64, https://doi.org/10.1117/12.312920.

[94] D.A. Nivens, Y.K. Zhang, S.M. Angel, A fiber-optic pH sensor prepared using a base-catalyzed organo-silica sol-gel, Anal. Chim. Acta 376 (1998) 235–245, https://doi.org/10.1016/S0003-2670(98)00505-4.

[95] M. Ma, R.M. Hill, G.C. Rutledge, A review of recent results on superhydrophobic materials based on micro- and nanofibers, J. Adhes. Sci. Technol. 22 (2008) 1799–1817, https://doi.org/10.1163/156856108X319980.

[96] B. Schyrr, S. Pasche, E. Scolan, R. Ischer, D. Ferrario, J.-A. Porchet, G. Voirin, Development of a polymer optical fiber pH sensor for on-body monitoring application, Sensor. Actuator. B Chem. 194 (2014) 238–248, https://doi.org/10.1016/j.snb.2013.12.032.

[97] N.E. Zander, Hierarchically structured electrospun fibers, Polymers 5 (2013) 19–44, https://doi.org/10.3390/polym5010019.
[98] R. Bel-Hassen, S. Boufi, M.-C.B. Salon, M. Abdelmouleh, M.N. Belgacem, Adsorption of silane onto cellulose fibers. II. The effect of pH on silane hydrolysis, condensation, and adsorption behavior, J. Appl. Polym. Sci. 108 (2008) 1958–1968, https://doi.org/10.1002/app.27488.
[99] D. Hou, C. Ding, C. Fu, D. Wang, C. Zhao, J. Wang, Electrospun nanofibrous omniphobic membrane for anti-surfactant-wetting membrane distillation desalination, Desalination 468 (2019), https://doi.org/10.1016/j.desal.2019.07.008. UNSP 114068.
[100] X.M. He, K.L. Xie, Dyeing properties of chitosan-sulfamic acid solution treated wool with silane coupling agent, AMR (Adv. Magn. Reson.) 331 (2011) 377–381. https://doi.org/10.4028/www.scientific.net/AMR.331.377.
[101] B. Sharma, R. Chhibber, R. Mehta, Seawater ageing of glass fiber reinforced epoxy nanocomposites based on silylated clays, Polym. Degrad. Stabil. 147 (2018) 103–114, https://doi.org/10.1016/j.polymdegradstab.2017.11.017.
[102] B. Sharma, R. Chhibber, R. Mehta, Curing studies and mechanical properties of glass fiber reinforced composites based on silanized clay minerals, Appl. Clay Sci. 138 (2017) 89–99, https://doi.org/10.1016/j.clay.2016.12.038.
[103] M. Beaumont, M. Bacher, M. Opietnik, W. Gindl-Altmutter, A. Potthast, T. Rosenau, A general aqueous silanization protocol to introduce vinyl, mercapto or azido functionalities onto cellulose fibers and nanocelluloses, Molecules 23 (2018) 1427, https://doi.org/10.3390/molecules23061427.
[104] E. Aytan, M.H. Ugur, N. Kayaman-Apohan, Synthesis, characterization, and ionic conductivity of electrospun organic-inorganic hybrid gel electrolytes, Polym. Eng. Sci. 60 (2020) 619–629, https://doi.org/10.1002/pen.25320.
[105] C. Schramm, B. Rinderer, R. Tessadri, Synthesis and characterization of hydrophobic, ultra-fine fibres based on an organic–inorganic nanocomposite containing a polyimide functionality, Polym. Polym. Compos. 27 (2019) 268–278, https://doi.org/10.1177/0967391119832408.
[106] J.J. McDowell, N.S. Zacharia, D. Puzzo, I. Manners, G.A. Ozin, Electroactuation of alkoxysilane-functionalized polyferrocenylsilane microfibers, J. Am. Chem. Soc. 132 (2010) 3236, https://doi.org/10.1021/ja9089236.
[107] H. He, J. Wang, X. Li, X. Zhang, W. Weng, G. Han, Silica nanofibers with controlled mesoporous structure via electrospinning: from random to orientated, Mater. Lett. 94 (2013) 100–103, https://doi.org/10.1016/j.matlet.2012.12.032.
[108] S.C. Nunes, V. deZeaBermudez, Structuring of amide cross-linked non-bridged and bridged alkyl-based silsesquioxanes, Chem. Rec. 18 (2018) 724–736, https://doi.org/10.1002/tcr.201700096.
[109] S.S. Park, M. Santha Moorthy, C.-S. Ha, Periodic mesoporous organosilicas for advanced applications, NPG Asia Mater. 6 (2014) e96, https://doi.org/10.1038/am.2014.13, e96.
[110] A. Noureddine, C.J. Brinker, Pendant/bridged/mesoporous silsesquioxane nanoparticles: versatile and biocompatible platforms for smart delivery of therapeutics, Chem. Eng. J. 340 (2018) 125–147, https://doi.org/10.1016/j.cej.2018.01.086.
[111] M. Weinberger, P.-H. Su, H. Peterlik, M. Linden, M. Wohlfahrt-Mehrens, Biphenyl-bridged organosilica as a precursor for mesoporous silicon oxycarbide and its application in lithium and sodium ion batteries, Nanomaterials 9 (2019) 754, https://doi.org/10.3390/nano9050754.
[112] J. Morell, M. Güngerich, G. Wolter, J. Jiao, M. Hunger, P.J. Klar, M. Fröba, Synthesis and characterization of highly ordered bifunctional aromatic periodic mesoporous organosilicas with different pore sizes, J. Mater. Chem. 16 (2006) 2809–2818, https://doi.org/10.1039/B603458F.
[113] X. Du, X. Li, L. Xiong, X. Zhang, F. Kleitz, S.Z. Qiao, Mesoporous silica nanoparticles with organo-bridged silsesquioxane framework as innovative platforms for bioimaging and therapeutic agent delivery, Biomaterials 91 (2016) 90–127, https://doi.org/10.1016/j.biomaterials.2016.03.019.
[114] S. Tao, G. Li, J. Yin, Fluorescent nanofibrous membranes for trace detection of TNT vapor, J. Mater. Chem. 17 (2007) 2730–2736, https://doi.org/10.1039/B618122H.
[115] S.-Q. Wang, J.-H. He, L. Xu, Non-ionic surfactants for enhancing electrospinability and for the preparation of electrospun nanofibers, Polym. Int. 57 (2008) 1079–1082, https://doi.org/10.1002/pi.2447.
[116] L. Bi, Y. Li, S. Wang, Z. Zhu, Y. Chen, Y. Chen, B. Li, Yonggang Yang, Preparation and characterization of twisted periodic mesoporous ethenylene-silica nanorods, J. Sol. Gel Sci. Technol. 53 (2010) 619–625, https://doi.org/10.1007/s10971-009-2140-x.
[117] Y. Yang, M. Suzuki, S. Owa, H. Shirai, K. Hanabusa, Control of mesoporous silica nanostructures and pore-architectures using a thickener and a gelator, J. Am. Chem. Soc. 129 (2007) 581–587, https://doi.org/10.1021/ja064240b.
[118] J.J.E. Moreau, B.P. Pichon, M.W.C. Man, C. Bied, H. Pritzkow, J.-L. Bantignies, P. Dieudonné, J.-L. Sauvajol, A better understanding of the self-structuration of bridged silsesquioxanes, Angew. Chem. Int. Ed. 43 (2004) 203–206, https://doi.org/10.1002/anie.200352485.
[119] H. Jin, L. Wang, N. Bing, Mesoporous silica helical ribbon and nanotube-within-a-nanotube synthesized by sol-gel self-assembly, Mater. Lett. 65 (2011) 233–235, https://doi.org/10.1016/j.matlet.2010.09.051.
[120] Y. Zhao, C. Beuchat, Y. Domoto, J. Gajewy, A. Wilson, J. Mareda, N. Sakai, S. Matile, Anion−π catalysis, J. Am. Chem. Soc. 136 (2014) 2101–2111, https://doi.org/10.1021/ja412290r.
[121] Y. Cao, Y. Duan, L. Han, S. Che, Hierarchical chirality transfer in the formation of chiral silica fibres with DNA-porphyrin co-templates, Chem. Commun. 53 (2017) 5641–5644, https://doi.org/10.1039/c7cc02382k.
[122] J. Hu, Y. Yang, Single-handed helical polybissilsesquioxane nanotubes and mesoporous nanofibers prepared by an external templating approach using low-molecular-weight gelators, Gels 3 (2017) 2, https://doi.org/10.3390/gels3010002.
[123] W. Zhu, B. Li, L. Bi, S. Wang, W. Zhuang, Y. Li, Yonggang Yang, Preparation of mesoporous 1,4-phenylene-silica nanorings through a dual-templating approach, Chin. J. Chem. 30 (2012) 144–150, https://doi.org/10.1002/cjoc.201180464.
[124] M.A. Wahab, I. Imae, Y. Kawakami, I. Kim, C.-S. Ha, Functionalized periodic mesoporous organosilica fibers with longitudinal pore architectures under basic conditions, Microporous Mesoporous Mater. 92 (2006) 201–211, https://doi.org/10.1016/j.micromeso.2005.12.016.
[125] W. Zhuang, L. Bi, M. Zhang, S. Wang, Y. Li, B. Li, Yonggang Yang, Structural control of mesoporous 1,4-phenylene-silica using the mixture of CTAB/SDS, Chin. J. Chem. 29 (2011) 883–887, https://doi.org/10.1002/cjoc.201190183.
[126] J. Muthu, J. Priscilla, A. Odeshi, N. Kuppen, Characterisation of coir fibre hybrid composites reinforced with clay particles and glass spheres, J. Compos. Mater. 52 (2018) 593–607, https://doi.org/10.1177/0021998317712568.
[127] J. Park, R. Subramanian, Interfacial shear-strength and durability improvement by monomeric and polymeric silanes in basalt fiber epoxy single-filament composite specimens, J. Adhes. Sci. Technol. 5 (1991) 459–477, https://doi.org/10.1163/156856191X00602.
[128] M. Jimenez, J. Gonzalez-Benito, A.J. Aznar, J. Baselga, Hydrolytic degradation of polysiloxanic coatings on glass fibers, Bol. Soc. Esp. Ceram. Vidr. 39 (2000) 425–430, https://doi.org/10.3989/cyv.2000.v39.i4.791.
[129] X.-C. Zhang, X. Xiong, J. Yu, Z.-X. Guo, Amine-functionalized thermoplastic polyurethane electrospun fibers prepared by co-electrospinning with 3-amino-propyltriethoxysilane and preparation of conductive fiber mats, Polymer 53 (2012) 5190–5196, https://doi.org/10.1016/j.polymer.2012.09.015.
[130] J. Zhou, F. Liu, X. Dai, L. Jiao, H. Yao, Z. Du, H. Wang, X. Qiu, Surface modification of high-performance polyimide fibres by using a silane coupling agent, Compos. Interfac. 26 (2019) 687–698, https://doi.org/10.1080/09276440.2018.1526607.
[131] M. Aparicio, J. Mosa, F. Sánchez, A. Durán, Synthesis and characterization of proton-conducting sol–gel membranes produced from 1,4-bis(triethoxysilyl)benzene and (3-glycidoxypropyl)trimethoxysilane, J. Power Sources 151 (2005) 57–62, https://doi.org/10.1016/j.jpowsour.2005.03.042.
[132] F. Si, N. Zhao, L. Chen, J. Xu, Q. Tao, J. Li, C. Ran, A superhydrophobic surface with high performance derived from STA-APTES organic-inorganic molecular hybrid, J. Colloid Interface Sci. 407 (2013) 482–487, https://doi.org/10.1016/j.jcis.2013.06.068.
[133] Y. Zheng, X. Kong, I. Usman, X. Xie, S. Liang, G. Cao, A. Pan, Rational design of the pea-pod structure of SiOx/C nanofibers as a high-performance anode for lithium ion batteries, Inorg. Chem. Front. 7 (2020) 1762–1769, https://doi.org/10.1039/D0QI00069H.
[134] V. Maneeratana, J.D. Bass, T. Azais, A. Patissier, K. Valle, M. Marechal, G. Gebel, C. Laberty-Robert, C. Sanchez, Fractal inorganic-organic interfaces in hybrid membranes for efficient proton transport, Adv. Funct. Mater. 23 (2013) 2872–2880, https://doi.org/10.1002/adfm.201202701.
[135] B. Oktay, E. Basturk, M.V. Kahraman, N.K. Apohan, Thiol-yne photo-clickable electrospun phase change materials for thermal energy storage, React. Funct. Polym. 127 (2018) 10–19, https://doi.org/10.1016/j.reactfunctpolym.2018.03.018.
[136] D. Dhanapal, A. Muthukaruppan, A.K. Srinivasan, Tetraglycidyl epoxy reinforced with surface functionalized mullite fiber for substantial enhancement in thermal and mechanical properties of epoxy nanocomposites, Siliconindia 10 (2018) 585–594, https://doi.org/10.1007/s12633-016-9496-7.
[137] C. Jia, R. Zhang, C. Yuan, Z. Ma, Y. Du, L. Liu, Y. Huang, Surface modification of aramid fibers by amino functionalized silane grafting to improve interfacial property of aramid fibers reinforced composite, Polym. Compos. 41 (2020), https://doi.org/10.1002/pc.25519, 2046–2053.
[138] X. Zhang, G. Wu, Grafting halloysite nanotubes with amino or carboxyl groups onto carbon fiber surface for excellent interfacial properties of silicone resin composites, Polymers 10 (2018) 1171, https://doi.org/10.3390/polym10101171.
[139] F. Yalcinkaya, A review on advanced nanofiber technology for membrane distillation, Journal of Engineered Fibers and Fabrics 14 (2019), https://doi.org/10.1177/1558925018824901, 1558925018824901.
[140] R. Rajan, E. Rainosalo, S.P. Thomas, S.K. Ramamoorthy, J. Zavasnik, J. Vuorinen, M. Skrifvars, Modification of epoxy resin by silane-coupling agent to improve tensile properties of viscose fabric composites, Polym. Bull. 75 (2018) 167–195, https://doi.org/10.1007/s00289-017-2022-2.
[141] A.V. Rajulu, L.G. Devi, R.R. Devi, Effect of orientation of fibers and coupling agent on tensile properties of phenolic/silica composites, J. Reinforc. Plast. Compos. 27 (2008) 599–603, https://doi.org/10.1177/0731684407079092.
[142] T.A. Otitoju, B.S. Ooi, A.L. Ahmad, Synthesis of 3-aminopropyltriethoxysilane-silica modified polyethersulfone hollow fiber membrane for oil-in-water emulsion separation, React. Funct. Polym. 136 (2019) 107–121, https://doi.org/10.1016/j.reactfunctpolym.2018.12.018.
[143] Z. Yu, X. Min, F. Li, Q. Chen, Synthesis of Ag-SiO2-APTES nanocomposites by blending poly(vinylidene fluoride) membrane with potential applications on dye wastewater treatment, Nano 13 (2018), https://doi.org/10.1142/S1793292018500340, 1850034.
[144] Y. Zhao, J. Qiu, H. Feng, M. Zhang, The interfacial modification of rice straw fiber reinforced poly(butylene succinate) composites: effect of aminosilane with different alkoxy groups, J. Appl. Polym. Sci. 125 (2012) 3211–3220, https://doi.org/10.1002/app.36502.
[145] M. Irani, A.R. Keshtkar, M.A. Moosavian, Removal of cadmium from aqueous solution using mesoporous PVA/TEOS/APTES composite nanofiber prepared by

sol–gel/electrospinning, Chem. Eng. J. 200–202 (2012) 192–201, https://doi.org/10.1016/j.cej.2012.06.054.
[146] L. Hu, J. Cheng, Y. Li, J. Litt, J. Zhou, K. Cen, Amino-functionalized surface modification of polyacrylonitrile hollow fiber-supported polydimethylsiloxane membranes, Appl. Surf. Sci. 413 (2017) 27–34, https://doi.org/10.1016/j.apsusc.2017.04.006.
[147] S.S. Park, C.-S. Ha, Organic–inorganic hybrid mesoporous silicas: functionalization, pore size, and morphology control, Chem. Rec. 6 (2006) 32–42, https://doi.org/10.1002/tcr.20070.
[148] J.-J. Yuan, P.-X. Zhu, N. Fukazawa, R.-H. Jin, Synthesis of nanofiber-based silica networks mediated by organized poly(ethylene imine): structure, properties, and mechanism, Adv. Funct. Mater. 16 (2006) 2205–2212, https://doi.org/10.1002/adfm.200500886.
[149] M. Shamizadeh, M.B. Gholivand, M. Shamsipur, P. Hashemi, Mercaptopropyl-functionalized nanoporous silica as a novel coating for solid-phase microextraction fibers, Anal. Methods. 7 (2015) 2505–2513, https://doi.org/10.1039/c4ay02826k.
[150] Synthesis of novel mesoporous silica twist nanofibers through Co-condensation Method–《Chemical journal of Chinese Universities》2012年08期 (n.d.), http://en.cnki.com.cn/Article_en/CJFDTotal-GDXH201208001.htm. (Accessed 24 April 2020).
[151] C. Gao, S. Ito, A. Obata, T. Mizuno, J.R. Jones, T. Kasuga, Fabrication and in vitro characterization of electrospun poly (gamma-glutamic acid)-silica hybrid scaffolds for bone regeneration, Polymer 91 (2016) 106–117, https://doi.org/10.1016/j.polymer.2016.03.056.
[152] G. Poologasundarampillai, B. Yu, J.R. Jones, T. Kasuga, Electrospun silica/PLLA hybrid materials for skeletal regeneration, Soft Matter 7 (2011) 10241–10251, https://doi.org/10.1039/c1sm06171b.
[153] S. Koeda, K. Ichiki, N. Iwanaga, K. Mizuno, M. Shibata, A. Obata, T. Kasuga, T. Mizuno, Construction and characterization of protein-encapsulated electrospun fibermats prepared from a silica/poly(gamma-glutamate) hybrid, Langmuir 32 (2016) 221–229, https://doi.org/10.1021/acs.langmuir.5b02862.
[154] H.J. Haroosh, Y. Dong, D.S. Chaudhary, G.D. Ingram, S. Yusa, P.L.A. Electrospun, PCL composites embedded with unmodified and 3-aminopropyltriethoxysilane (ASP) modified halloysite nanotubes (HNT), Appl. Phys. Mater. Sci. Process 110 (2013) 433–442, https://doi.org/10.1007/s00339-012-7233-7.
[155] S. Inukai, N. Kurokawa, A. Hotta, Mechanical properties of poly(epsilon-caprolactone) composites with electrospun cellulose nanofibers surface modified by 3-aminopropyltriethoxysilane, J. Appl. Polym. Sci. 137 (2020) 48599, https://doi.org/10.1002/app.48599.
[156] A. Kurniawan, F. Gunawan, A.T. Nugraha, S. Ismadji, M.-J. Wang, Biocompatibility and drug release behavior of curcumin conjugated gold nanoparticles from aminosilane-functionalized electrospun poly (N-vinyl-2-pyrrolidone) fibers, Int. J. Pharm. 516 (2017) 158–169, https://doi.org/10.1016/j.ijpharm.2016.10.067.
[157] S. Taokaew, M. Phisalaphong, B.Z. Newby, Modification of bacterial cellulose with organosilanes to improve attachment and spreading of human fibroblasts, Cellulose 22 (2015) 2311–2324, https://doi.org/10.1007/s10570-015-0651-x.
[158] D. Li, W. Nie, L. Chen, Y. Miao, X. Zhang, F. Chen, B. Yu, R. Ao, B. Yu, C. He, Fabrication of curcumin-loaded mesoporous silica incorporated polyvinyl pyrrolidone nanofibers for rapid hemostasis and antibacterial treatment, RSC Adv. 7 (2017) 7973–7982, https://doi.org/10.1039/c6ra27319j.
[159] Y. Liu, Q. Li, H. Liu, H. Cheng, J. Yu, Z. Guo, Antibacterial thermoplastic polyurethane electrospun fiber mats prepared by 3-aminopropyltriethoxysilane-assisted adsorption of Ag nanoparticles, Chin. J. Polym. Sci. 35 (2017) 713–720, https://doi.org/10.1007/s10118-017-1928-3.
[160] Y. Zhang, Y. Jin, H. Yu, P. Dai, Y. Ke, X. Liang, Pore expansion of highly monodisperse phenylene-bridged organosilica spheres for chromatographic application, Talanta 81 (2010) 824–830, https://doi.org/10.1016/j.talanta.2010.01.022.
[161] A. Dabrowski, M. Barczak, Bridged polysilsesquioxanes as a promising class of adsorbents. A concise review, Croat. Chem. Acta 80 (2007) 367–380.
[162] E. Doustkhah, H. Mohtasham, M. Hasani, Y. Ide, S. Rostamnia, N. Tsunoji, M. Hussein N. Assadi, Merging periodic mesoporous organosilica (PMO) with mesoporous aluminosilica (Al/Si-PMO): a catalyst for green oxidation, Molecular Catalysis 482 (2020) 110676, https://doi.org/10.1016/j.mcat.2019.110676.
[163] null Iamamoto, null Sacco, null Biazzotto, null Ciuffi, null Serra, Porphyrinosilica and metalloporphyrinosilica: hybrid organic-inorganic materials prepared by sol-gel processing, An. Acad. Bras. Cienc. 72 (2000) 59–66, https://doi.org/10.1590/s0001-37652000000100008.
[164] D. Jiang, Q. Yang, H. Wang, G. Zhu, J. Yang, C. Li, Periodic mesoporous organosilicas with trans-(1R,2R)-diaminocyclohexane in the framework: a potential catalytic material for asymmetric reactions, J. Catal. 239 (2006) 65–73, https://doi.org/10.1016/j.jcat.2006.01.018.
[165] W. Liu, H. Wei, H. Li, Y. Wang, L. Wu, B. Li, Y. Li, Y. Yang, Structurally coloured organic–inorganic hybrid silica films with a chiral nematic structure prepared through a self-templating approach, Liquid Crystals, 0, 1-5, https://doi.org/10.1080/02678292.2020.1791984, 2020.
[166] S. Shylesh, P.P. Samuel, S. Sisodiya, A.P. Singh, Periodic mesoporous silicas and organosilicas: an overview towards catalysis, Catal. Surv. Asia 12 (2008) 266, https://doi.org/10.1007/s10563-008-9056-2.
[167] L. Brigo, V. Auzelyte, K.A. Lister, J. Brugger, G. Brusatin, Phenyl-bridged polysilsesquioxane positive and negative resist for electron beam lithography, Nanotechnology 23 (2012) 325302, https://doi.org/10.1088/0957-4484/23/32/325302.
[168] D.A. Loy, K.J. Shea, Bridged polysilsesquioxanes. Highly porous hybrid organic-inorganic materials, Chem. Rev. 95 (1995) 1431–1442, https://doi.org/10.1021/cr00037a013.
[169] H. Peng, Y. Zhu, D.E. Peterson, Y. Lu, Nanolayered carbon/silica superstructures via organosilane assembly, Adv. Mater. 20 (2008) 1199, https://doi.org/10.1002/adma.200701303. -+.

Dr. Veronika MÁKOVÁ (born ZAJÍCOVÁ) **Born:** 14.9.1984 in Turnov, citizenship CZ

Jobs and academic functions:

• 2011 – PhD in Material Engineering, Technical University of Liberec

• Since 2011 – Junior Researcher at Institute for Nanomaterials, Advanced Technologies and Innovation, Technical University of Liberec.

• 2014–2015 Junior Researcher at Institut de Science et d'Ingénierie

Supramoléculaires (ISIS), Université de StrasbourgPublications

and patents:

• 17 Scientific original papers; h – index 6 (WOS 1/2/2021)

• 4 National patents and 1 patent application

• 2 International patents

Scientific interests:

• inorganic–organic materials and their properties; sol-gel method; nanofibres and their formation; nanomaterials based on organoalkoxysilanes their synthesis and functionalization

Dr. Barbora HOLUBOVÁ

Born: 8.7.1989 in Pardubice, citizenship CZ

Jobs and academic functions:

• 2019 – PhD in Chemistry and Technology of Materials, University of Chemistry and Technology, Prague

• Since 2018 – Junior Researcher at Institute for Nanomaterials, Advanced Technologies and Innovation, Technical University of Liberec

• Various student or work internships under the programme Erasmus+ (France, Germany) or Athens (France)

Publications and patents:

• 5 Scientific original papers; h – index 1 (WOS 1/2/2021)

• 1 National standardized methodology

Scientific interests:

• hybrid organoalkoxysilane materials and their characterization via FTIR, Raman spectroscopy and solid state NMR; sol-gel chemistry; various electrospinning techniques

Ilona KRABICOVÁ

Born: 17. 6. 1993 in Litoměřice, citizenship CZ

Jobs and academic functions:

• Since 2017 – PhD candidate in Nanotechnology, Technical University of Liberec

• Since 2018 – Junior Researcher at Institute for Nanomaterials, Advanced Technologies and Innovation, Technical University of Liberec

• 2020 – Internship within the group of Prof. Francesco Trotta University of Turin, Italy

Publications and patents:

• 4 Scientific original papers; h – index 2 (WOS 1/2/2021)

Scientific interests:

• cyclodextrin polymers; nanomaterials their synthesis and functionalization; nanomaterials with medical applications

Johana KULHÁNKOVÁ

Born: 13.11.1994 in Liberec, citizenship CZ

Jobs and academic functions:

• 2019 – Master degree at University of Chemistry and Technology Prague; Faculty of Chemical Technology

• Since 2019 – PhD candidate in Nanotechnology, Technical University of Liberec (Institute for Nanomaterials, Advanced Technologies and Innovation)

• 2020–2021 Internship within the group of Prof. Aldo R. Boccaccini at Friedrich-Alexander-Universität Erlangen-Nürnberg, Germany

Publications and patents:

• 1 Scientific original paper

Scientific interests:

• silicon chemistry; hybrid biomaterials and biocomposites based on silica; sol-gel method; hybrid nanofibres and their characterization via electron microscopies

Dr. Michal ŘEZANKA

Born: 17. 2. 1983 in Prague, citizenship CZ

Jobs and academic functions:

• 2012 – PhD PhD in the field of organic chemistry from Charles University, Prague

• 2013–2014 Internship within the group of Prof. P. D. Beer at University of Oxford (GB)

• 2014–2017 Junior Researcher at Institute for Nanomaterials, Advanced Technologies and Innovation, Technical University of Liberec

• Since 2017 the Head of the Nanochemistry Department at Technical University of Liberec (CZ)

Publications and patents:

• 28 Scientific original papers; h – index 11 (WOS 1/2/2021)

• 1 National Patent

Scientific interests:

• organic synthesis; synthesis and functionalization of cyclodextrins and their derivatives; functionalization of various types of inorganic and organic nanomaterials; solid state and liquid state NMR

ÚŘAD PRŮMYSLOVÉHO VLASTNICTVÍ
Antonína Čermáka 2a 160 68 Praha 6

WWW.UPV.CZ

Tel.: 220 383 111 Fax: 224 324 718 E-mail: posta@upv.cz Datová schránka: ix6aa38

PŘIHLÁŠKA VYNÁLEZU
se žádostí o udělení patentu

Pořadové číslo: D21032294
(Vyplní Úřad)

Spisová značka přihlášky: PV 2021-160

Potvrzení o přijetí vydáno dne:	**31.03.2021 10:46:34**
MPT	
Vyřizuje	.....
Kód	.....

DRUH PŘIHLÁŠKY

Typ přihlášky	národní
Druh přihlášky	Nová přihláška vynálezu

NÁZEV VYNÁLEZU

Způsob přípravy solu pro přípravu hybridních organosilanových vláken elektrostatickým zvlákňováním, tímto způsobem připravený sol a hybridní organosilanová vlákna připravená elektrostatickým zvlákňováním tohoto solu

PŘIHLAŠOVATEL

1 Právnická osoba: Technická univerzita v Liberci, Studentská 1402/2, 46001 Liberec, Liberec I-Staré Město, Česká republika

Další identifikační údaje
IČ: 46747885

Přihlašovatel je i původcem Ne

PŮVODCE

1 Mgr. Máková Veronika, Ph.D., Poděbradova 1300, 51251 Lomnice nad Popelkou, Česká republika

Pokud si původce **nepřeje být zveřejněn** - vyplňte "ANO" Ne

2 Ing. Mgr. Holubová Barbora, Ph.D., K Zámečku 295, 53003 Pardubice, Pardubičky, Česká republika

Pokud si původce **nepřeje být zveřejněn** - vyplňte "ANO" Ne

3 Ing. Kulhánková Johana, Balbínova 96/26, 46001 Liberec, Liberec XII-Staré Pavlovice, Česká republika

Pokud si původce **nepřeje být zveřejněn** - vyplňte "ANO" Ne

ZÁSTUPCE

1 Fyzická osoba: Ing. Dobroslav Musil, patentová kancelář, Ing. Musil Dobroslav, Zábrdovická 801/11, 61500 Brno, Zábrdovice, Česká republika
Tel. :545424915, Fax: 545211483, Email: bendova@patent-musil.cz

Další identifikační údaje
IČ: 64281582, Dat.nar.: 25.11.1950, Č.j.zástupce: PS4427CZ, Ev.č. KPZ ČR: 99

Plná moc již byla u Úřadu uložena jako prezidiální

Číslo prezidiální plné moci 13543

Počet patentových nároků 16

PODNIKOVÝ VYNÁLEZ

Jedná se o PODNIKOVÝ VYNÁLEZ Ano

NABÍDKA LICENCE

Ne

SEZNAM PŘÍLOH

Typ přílohy	Soubor
Obrázek k anotaci	PS4427CZ - obrázek k anotaci.pdf
otisk přílohy (sha1): c056042a94fc645bfe4fca56f9a62faa4d862bd3	
Výkresy	PS4427CZ - výkresy.pdf
otisk přílohy (sha1): eb5c31c3e1ff5c4cb817072acf4e24ee3a87bdef	
Anotace	PS4427CZ - anotace.docx
otisk přílohy (sha1): c74c43b70e36c2c7670b8f0b2b849960a2325bcd	
Patentové nároky	PS4427CZ - patentové nároky.docx
otisk přílohy (sha1): da3864ef9e8307f2fb3339b11c7ce37b552c84b8	
Popis vynálezu	PS4427CZ - popis vynálezu.docx
otisk přílohy (sha1): b9075cef0328db11cec110361f3eefffc2c50db3	
Plná moc	TUL - prezidiální plná moc 13543.pdf
otisk přílohy (sha1): 30f2bc99271547b89e8da047c7418fbb437bc262	

ŽÁDOST O ÚPLNÝ PRŮZKUM

ŽÁDÁM O PROVEDENÍ ÚPLNÉHO PRŮZKUMU u této přihlášky vynálezu podle zákona č. 527/1990 Sb., o vynálezech

Ano

O úplný průzkum lze požádat buď při podání přihlášky (výběrem ANO/NE ve formuláři) nebo formou samostatné žádosti kdykoli během následujících 36 měsíců.

SOUHLAS S PŘEDÁNÍM VÝSLEDKŮ REŠERŠE pro účely Pravidla 141 EPC přímo

Ano

Vysvětlivky (poznámka):

V případě, že budete z této přihlášky nárokovat právo přednosti v následné evropské patentové přihlášce a máte zájem, aby požadavek podle Pravidla 141 EPC, tj. předložení výsledků rešerše Evropskému patentovému úřadu (EPÚ) provedl přímo náš Úřad, pak vyberte volbu "ANO". Jinak musíte požadavku z Pravidla 141 EPC vyhovět sami.

INFORMACE O VÝŠI SPRÁVNÍHO POPLATKU

Správní poplatek za podání přihlášky vynálezu přihlašovatelem je stanoven na 1 200,- Kč.
Správní poplatek za podání přihlášky vynálezu přihlašovatelem, který je současně i původcem, je stanoven na 600,-

Způsob platby Převodem z účtu *

Poznámka: Správní poplatek se platí při podání přihlášky.
Kolky lze platit pouze pro platby do 5 000,- Kč (včetně).
*) Číslo účtu správních poplatků ÚPV: 3711-21526001/0710
**) Ostatní informace jsou uvedeny v nápovědě.

místo pro nalepení kolku

Potvrzuji pravdivost a úplnost shora uvedených údajů a žádám o udělení patentu.

Přihlášku podává zástupce.

Datum 31.03.2021
Email bendova@patent-musil.cz

Jméno a příjmení Dobroslav Musil

Podpis
(U právnické osoby případně i razítko)

VAROVÁNÍ PŘED AKTIVITOU PODVODNÝCH SUBJEKTŮ

Podvodné faktury vyzývající k zaplacení poplatků | Rejstříky, které nesouvisí s oficiálními rejstříky průmyslových práv Úřadu průmyslového vlastnictví

Úřad průmyslového vlastnictví upozorňuje přihlašovatele a vlastníky průmyslových práv a jejich zástupce, že mohou být písemně nebo elektronicky osloveni některými soukromými společnostmi s kontaktními údaji na území ČR nebo jiných států.

Nabízejí za různé poplatky v různých měnách zveřejnění, registraci či evidenci průmyslových práv v jejich rejstřících nebo databázích vedených na Internetu.

Úřad průmyslového vlastnictví opětovně varuje, že takovéto služby nikterak nesouvisí ani s úředními rejstříky či databázemi vedenými Úřadem průmyslového vlastnictví ani s právní ochranou poskytovanou podle příslušných právních předpisů. Nevyužití nabízených služeb nemá žádné právní účinky týkající se platnosti průmyslových práv.

Klamavé výzvy můžete zasílat na adresu: fraud@upv.cz
více na www.upv.cz

Europäisches Patentamt
European Patent Office
Office européen des brevets

Acknowledgement of receipt

We hereby acknowledge receipt of your request for grant of a European patent as follows:

Submission number	9773826
Application number	EP21172710.2
File No. to be used for priority declarations	EP21172710
Date of receipt	07 May 2021
Your reference	PS4427EP
Applicant	Technicka univerzita v Liberci
Country	CZ
Title	Method for the preparation of a sol for the preparation of hybrid organosilane fibers by electrostatic spinning, the sol prepared by this method and hybrid organosilane fibers prepared by the electrostatic spinning of this sol
Documents submitted	package-data.xml application-body.xml DRAWNONEPO.pdf\PS4427EP - drawings in Czech.pdf (12 p.) f1002-1.pdf (1 p.)
	ep-request.xml ep-request.pdf (5 p.) SPECNONEPO.pdf\PS4427EP - patent application in Czech.pdf (37 p.)
Submitted by	CN=Dobroslav Musil 18855
Method of submission	Online
Date and time receipt generated	07 May 2021, 12:06 (CEST)
Message Digest	7F:CC:FD:E5:D7:19:7F:97:99:17:E1:81:CA:CC:01:B9:EF:BE:40:81

/European Patent Office/

DAS access code
The access code generated for this application and used to retrieve the priority documents from WIPO's Digital Access Service (DAS) is indicated in the document appended to this acknowledgement of receipt. Please note that the appended document is non-public and will not be published.

/European Patent Office/

Europäisches Patentamt
European Patent Office
Office européen des brevets

DAS access code

To access and retrieve the priority document from WIPO's Digital Access Service (DAS) in respect of

Application number	EP21172710.2
Applicant	Technicka univerzita v Liberci

the European Patent Office has generated the following code:

DAS access code	9A53

For further information, see OJ EPO 03/2019.

Date and time receipt generated	07 May 2021, 12:06 (CEST)

This unique access code allows the applicant to authorise participating intellectual property offices to retrieve a certified copy of the present application (as priority document) via WIPO DAS.
The code will only be valid if the requirements for according a date of filing are met (see OJ EPO 03/2019).